Dissecting Thermosensory Suppression of Immunity in *Arabidopsis*

Catherine Helen Gardener

John Innes Centre

Thesis for the degree of Doctor of Philosophy (PhD)

Submitted for examination to the University of East Anglia in February 2019

Final version including minor corrections submitted in June 2019

Abstract

As sessile organisms, plants must modify growth and development to suit their environment and ensure reproductive success. Moderate increases in temperature accelerate plant growth whilst compromising immunity. As yet, the precise mechanism through which plants sense and integrate temperature information and coordinate signalling networks influencing growth and immunity are not fully explored. In this thesis, ambient temperature increases of just 2.5˚C were found to strongly influence pathogen resistance. These increases compromised both Pattern-Triggered Immunity (PTI) as well as Effector-Triggered Immunity (ETI), resulting in overall attenuation of immune outputs. Importantly, modulation of immunity was found to be a reliable thermosensory output. Using *PATHOGENESIS RELATED1* (*PR1*) as a marker, a novel mutant *resilient 1* (*res1*) with temperature-resilient immunity was isolated from a *PR1-LUC* based forward genetic screen. *res1* displays robust and temperature resilient immunity, alongside generally perturbed thermosensory responses, suggesting that RES1 is part of a key thermosensory pathway. RES1 was mapped to the gene encoding the cyclic nucleotide gated calcium channel, *CNGC2*. A missense mutation in *res1* resulted in an amino acid substitution (A457T) in CNGC2. This mutation also led to the generation of a novel splice variant of this channel, with an in-frame deletion of 14 amino acids. This novel variant appears to impede function of CNGC2 and affect downstream signalling. These findings implicated CNGC2 and therefore changes in calcium dynamics as coordinating ambient temperature signalling. Despite its temperature-resilient maintenance of SA-Triggered Immunity (SATI), *res1* has compromised early PTI responses. This response was found to be common to other mutants with perturbed SATI. The existence of negative feedback between this layer of immunity and early PTI signalling was thus identified as a general phenomenon. Knowledge generated from this study both of the nature of TSI and its underlying molecular control will have many potential implications, including devising strategies for climate-resilient disease resistance in crops.

Contents

Acknowledgements

I would like to extend my deepest gratitude to Dr. Vinod Kumar and all the previous members of the Kumar lab for their help, guidance and collaboration over the years. Being a part of this lab has enabled me to grow and develop as a scientist. In particular, I would like to thank Dr. Sreeram Gangappa and Dr. Souha Berriri for teaching me the tricks of the trade when it comes to working with plants and their pathogens. Also, to Dr. Fran Robson, Laura Hebberecht-Lopez and James Russel for their help with implementing the large-scale pathogen experiments and for their amazing seed sorting skills.

My greatest thanks go to Vinod, whose supervision has enabled me to cultivate a love of plant science, genetics and molecular biology throughout the course of my PhD which and whose guidance has helped me develop a skills base indispensable for whichever direction my future career in science takes. The *resilient1* project has been an exciting journey and I am grateful for being allowed to play a part in its progression. I have not had the best luck with my health over the past few years. In addition to his excellent scientific support, Vinod has remained encouraging and understanding through difficult times. Without this I don't think I would have been able to finish my studies. I would also like to thank him for his many helpful comments and suggestions over the course of writing this thesis.

My sincere thanks also go to my co-supervisors, Prof. Richard Morris and Prof. Lars Østergaard for their roles in my progress and development. Also, to my industrial CASE partner, PBL and in particular to Dr. Jan Chojecki for sitting on my supervisory committee and organising such an interesting and enlightening placement. In addition, to everybody at Leaf Expression Systems, for allowing me to contribute to the development of a new, exciting company and providing me with invaluable work experience and skills development whilst on placement with you.

I would also like to thank all the members of the Feng, Coen, Sablowski, Dean and Bevan labs on the top floor of CDB for their friendship, collaboration and endless willingness to put the world to rights over a cup of tea. In particular, to Billy for his

support over the years but especially over the past few months, where he has been amazing! Also, to Cathy and Eleri for their support and friendship.

My gratitude also goes to all members of the horticultural services and media kitchen teams. In particular to Lesley Phillips and Tim Wells for looking after endless rounds of transgenics. Also, to Grant Calder for his help getting me going on the microscope and to Andy Davis and Phil Robinson for the fantastic job they have done with all the beautiful plant photos in my thesis. I would also like to thank the members of the GSO for their support, to the John Innes Hardship Fund for supporting me financially during my unexpectedly long write-up period, and to BBSRC for funding this PhD.

I also want to say a special thank you to my wonderful mother, Suzanne for her unwavering kindness and support, throughout the last four years and beyond. Likewise, to Martin, for being such a calm and helpful partner, especially over the past months. Lastly, to my dad, the previous Dr. Gardener, I am thankful for your introducing me to the world of science at a young age. I hope to do your name justice since you are no longer here to own it.

Work by others

Part of the study reported in Chapter 2 has been done jointly with Souha Berriri and Sreeramaiah Gangappa. Data arising from joint work has been appropriately attributed.

The work detailed in Chapter 3 is furtherance of an MSc project work by Prawpun (Nad) Kasemthongsri (UEA – 2012).

Abbreviations

ΔMAF	Change in mutant allele frequency
◦C	degrees Celsius
ABA	Abscisic acid
ACD6	ACCELERATED CELL DEATH 6
ANOVA	Analysis of variance
AO1	AMINE OXIDASE 1
APG5	AUTOPHAGY 5
ARP6	ACTIN RELATED PROTEIN 6
ARR	Age-related resistance
ATP	Adenosine triphosphate
AUX	Auxin
AVR	Avirulence
BAK1	BRI1-ASSOCIATED RECEPTOR KINASE 1
BaR	Basta resistance
BC3F2	Backcross 3, second generation
BG1	BIG GRAIN 1
bHLH	basic helix-loop-helix
BIK1	BOTRYTIS INDUCED KINASE 1
BON1	BONZAI 1
BR	Brassinosteroids
Bt	Bacillus thuringensis
BZR1	BRASSINAZOLE-RESISTANT 1
CaM	Calmodulin
CaMBD	Calmodulin-binding domain
cAMP	cyclic adenosine monophosphate
CaMV	Cauliflower mosaic virus
CAPS	Cleaved, Amplified Polymorphic Sequences
CBP60G	Calmodulin binding protein 60-like G
cDNA	complementary DNA
CDPK	Calcium-dependent protein kinase
CER	Controlled Environment Room
CFU	Colony forming units
cGMP	cyclic guanine monophosphate
CIM	Constitutive immunity
CIR	Constitutively induced resistance
CK	Cytokinins

cm	centimetres
CNBD	Cyclic nucleotide-binding domain
CNGC2	CYCLIC NUCLEOTIDE-GATED CHANNEL 2
CNGC4	CYCLIC NUCLEOTIDE-GATED CHANNEL 4
cNMPs	cyclic nucleotide monophosphates
Col-0	Columbia-0
COP1	CONSTITUTIVELY PHOTOMORPHOGENIC 1
CPR1	CONSTITUTIVE EXPRESSOR OF PR1
Ct	Cycle threshold
DET1	DE-ETIOLATED 1
dH_2O	distilled water
DND1	DEFENCE, NO DEATH 1
DPI	Days post inoculation
EDS1	ENHANCED DISEASE SUSCEPTIBILITY 1
EF1α	ELONGATION FACTOR 1α
EMS	Ethyl methanesulfonate
ER	Endoplasmic reticulum
ET	Ethylene
ETI	Effector-triggered immunity
EtOH	Ethanol
ETS	Effector-triggered susceptibility
F1	First filial generation
F2	Second filial generation
F3	Third filial generation
FAB2	FATTY ACID BIOSYNTHESIS 2
FIR	flg22-induced resistance
FLC	FLOWERING LOCUS C
flg22	Conserved 22 amino acide peptide from bacterial flagellin
FLM	FLOWERING LOCUS M
FLS2	FLAGELLIN SENSITIVE 2
FRET	Förster resonance energy transfer
FRK1	FLG22-INDUCED RECEPTOR-LIKE KINASE 1
FSQ6	FRUCTOSE-SENSING QUANTITATIVE TRAIT LOCUS 6
FT	FLOWERING LOCUS T
fw	fresh weight
GA	gibberellins/gibberellic acid
GAUT14	GALACTURONOSYLTRANSFERASE 14
gDNA	genomic DNA

GFP	Green fluorescent protein
GM	Growth medium
GWB	Gateway binary
h	hours
H2A.Z	Histone 2A variant Z
HPAT3	HYDROXYPROLINE O-ARABINOSYLTRANSFERASE
HPI	Hours post induction
HR	hypersensitive response
HRP	Horseradish peroxidase
HSP	Heat shock protein
HTA11	HISTONE 2A 11
HTA9	HISTONE 2A 9
HY5	ELONGATED HYPOCOTYL 5
INA	2, 6-dichloro-isonicotinic acid
JA	Jasmonic Acid
km	kilometers
LD	Long days
LUC-	Low *LUCIFERASE*
LUC+	High *LUCIFERASE*
M1	First generation after mutagenic treatment
M2	Second generation after mutagenic treatment
M3	Third generation after mutagenic treatment
M4	Fourth generation after mutagenic treatment
MAPK	Mitogen Activated Protein Kinase
mg	milligrams
min	minutes
MIP2	MAG2-INTERACTING PROTEIN 2
MIRO1	MIRO-RELATED GTPASE 1
ml	millilitres
MLK1	MUT9P-LIKE KINASE 1
mM	millimoles/ millimolar
mM	micromoles/ micromolar
MNU2	MITOCHONDRIAL NUCLEASE 2
MPK3	MITOGEN ACTIVATED KINASE 3
MPK4	MITOGEN ACTIVATED KINASE 4
MPK6	MITOGEN ACTIVATED KINASE 6
MS	Murashige and Skoog
MYB43	MYB-DOMAIN PROTEIN 43

N	Normal concentration
NBLRR	Nucleotide binding, leucine rich repeat
NLR	Nucleotide binding, leucine rich repeat
nM	nanomoles/ nanomolar
NPR1	NONEXPRESSOR OF PATHOGENESIS RELATED 1
OAP	Odd Area Profile
OD_{600}	Optical density of a sample measured at a wavelength of 600 nm
OE	Overexpressor
PAD4	PHYTOALEXIN DEFICIENT 4
PAMP	Pathogen-associated molecular pattern
PCR	Polymerase chain reaction
Pfr	Active Phytochrome B
PhyB	Phytochrome B
PIE1	photoperiod independent early flowering
PIF4	PHYTOCHROME-INTERACTING FACTOR 4
pifq	phytochrome-interacting factor quadruple mutant of pif1, pif3, pif4, pif5
PPK2	PHOTOREGULATORY PROTEIN KINASE 2
Pr	Inactive Phytochrome B
PR	PATHOGENESIS-RELATED
PR1	PATHOGENESIS-RELATED 1
PR1-LUC	PATHOGENESIS-RELATED 1 - LUCIFERASE
PR5	PATHOGENESIS-RELATED 5
PRA1.B6	PRENYLATED RAB ACCEPTOR 1.B6
PRC2	Polycomb Repressive Complex 2
PRR	pattern recognition receptor
PTI	pattern (PAMP)triggered immunity
Pto	Pseudomonas syringae pathover tomato
Pto DC3000	Pseudomonas syringae pathovar tomato DC3000
Pto DC3000 (AvrRps4)	Pseudomonas syringae pathovar tomato DC3000 expressing bacterial effector AvrRps4
Pto DC3000 lux	Pseudomonas syringae pathovar tomato DC3000 expressing the luxCDABE operon from *Photorhabdus luminescens*
Pv	Pathovar
qPCR	quantitative polymerase chain reaction
qRT-PCR	quantitative, reverse transcription polymerase chain reaction
QTL	quantitative trait locus
R	Resistance
RBOHD	Respiratory burst oxidase homologue D

res1	resilient1
RLCK	Receptor like cytoplasmic kinase
RLK	Receptor-like kinase
RLU	Relative luminescence units
RNA-seq	RNA sequencing
RNAi	RNA interference
ROS	Reactive oxygen species
RRC1	REDUCED RED LIGHT RESPONSES IN cry1, cry2 BACKGROUND
s	seconds
SA	Salicylic acid
SAR	Systemic acquired resistance
SARD1	SAR-DEFICIENT 1
SATI	Salicylic acid triggered immunity
SD	Short days
sec	seconds
SEF	SERRATED LEAVES AND EARLY FLOWERING
SIL	Single insertion line
SNC1	Suppressor of nonexpressor of PR1, constitutive1
SNP	single nucleotide polymorphism
SOC1	SUPPRESSOR OF OVEREXPRESSION OF CO 1
SUMO	Small ubiquitin-like modifier
SV1	Splice variant 1
SV2	Splice variant 2
SVP	SHORT VEGETATIVE PHASE
SWC6	SWR1 COMPLEX 6
T	Temperature
TBF1	TL1-BINDING TRANSCRIPTION FACTOR 1
TBS	Tris-buffered saline
TBST	Tris-buffered saline plus Tween-20
TF	Transcription factor
TMG	Thermomorphogenesis
TPR1	TOPLESS-RELATED 1
TSI	Thermosensory suppression of immunity
TT1	THERMOTOLERANT 1
TTSS	Type three secretion system
UPR	Unfolded protein response
V	Volts
VIN3	VERNALISATION-INSENSITIVE 3

VLG	VACUOLELESS GAMETOPHYTES
WT	Wild type
XTR7	XYLOGLUCAN ENDOTRANSGLUCOSYLASE 7
YUC8	YUCCA 8
αpTpY	α phosphoThreonine, phosphoTyrosine
µM	micromoles/ micromolar

1 Introduction

Plants are able to sense and respond to environmental signals which fluctuate diurnally and seasonally throughout their life cycle as well as over evolutionary time. Precise regulation of responses to these signals and adaptation to their environment is crucial to plant survival and reproductive success. External signals such as temperature, photoperiod and biotic interactions strongly influence plant processes such as growth, development and immune activation through networks of hormone-mediated signalling and changes in gene expression [1-3].

Environmental cues modulate development as well as priming plants to potentially detrimental stressful conditions [4]. As sessile organisms, plants must tailor their responses to the specific stress and combinations of stresses experienced in order to tolerate these external challenges [5,6]. The inbuilt ability to anticipate and adapt to environmental conditions is ubiquitous in biology, and plants are highly adaptable over both their lifetime and evolutionary time [7,8]. Plant species have adapted to external extremes such as ~50°C range of temperatures [9] high salinity [10] or other chemical stresses [11] as well as a huge diversity of positive and negative biotic interactions [12]. However, the accelerated abiotic and biotic changes which are predicted as a result of climate change will impose strong constraints on plant survival, particularly to crop species which have reduced levels of genetic diversity due to millennia of selective breeding [13-17]. To date, the effects of climate change have already influenced plant flowering, growth and development, distribution and species interactions [18,19], effects which will be exaggerated in the future. Climate change therefore poses a significant threat to food security, in part due to increases in abiotic stress, but additionally due to the impacts of altered ambient temperature conditions on growth and development as well as interactions with their biotic environment.

Increases in ambient temperature below those considered stressful simultaneously affect plant growth and defence [20], resulting in increases in elongation-growth and acceleration of flowering which go hand-in-hand with decreases in resistance to a wide range of crop pathogens [1,20]. This strong influence of the environment on plant

immunity has long been known; as far back as 370-286 BC, the Greek scholar Theophrastus observed how cereals grown at higher altitude and wind exposure experienced lower incidence of disease compared with plants grown closer to sea level [21]. This resistance however is accompanied by fitness costs which can inhibit plant growth and reproduction [20].

More recently, the effects of climate change on range and severity of disease outbreaks has been highlighted through studies and modelling of important crops and their pathogens such as wheat stripe rust (Puccinia striiformis) and Phoma stem canker (Leptosphaeria maculans) in oilseed rape [22,23]. Hundreds of plant pathogens and pests have already exhibited a poleward shift of around 2.7 km/year on average since 1960 [24] and crop losses as a result of climate change have been predicted to increase by more than £50M in 2050 [25,26].

Direct effects of moderate increases in ambient temperature can be observed on plant immunity as well as pathogen virulence [1,27] however the molecular mechanisms and signal hierarchy underpinning these processes in plants are not yet fully understood. In particular, many important aspects of the mechanisms by which plants sense and integrate changes in ambient temperature still remain elusive. Understanding of how moderate increases in temperature bring about the suppression of immunity alongside promotion of thermosensory growth responses is not yet complete.

Current climate change protocol aims to limit a global temperature increase to 1.5℃ above pre-industrial levels in order to reduce the impacts of climate change [28], but local increases in excess of this are expected, alongside changes in other abiotic factors [8]. Understanding the mechanism through which plants sense moderate increases in temperature and use this cue to modulate their phenotypic responses is therefore crucial to understand in the context of climate change. In addition, the apparent active attenuation of immunity under elevated ambient temperature conditions is an important and insufficiently understood biological phenomenon which is important commercially to ensure future food security and has potential to provide a novel insight into plant thermosensory mechanisms in general.

Understanding both thermosensory growth and immune suppression responses can provide crucial information towards understanding plant mechanisms of sensing and integrating important environmental cues such as temperature. Through an integrated approach, expanding understanding of these important processes with a view to the production of climate resilient crops is becoming increasingly important in order to counteract the negative effects of environmental changes on crop production [29].

1.1 Plant immune systems

Interactions with surrounding biota have shaped the evolution of both plants and their associated microbial communities, as well as that of insect pests and herbivores [30-32]. As a result, plants possess multi-faceted mechanisms to appropriately respond to a diverse range of biotic encounters, including pathogenic, epiphytic or symbiotic interactions as well as to adapt to changes in biotic interactions over evolutionary time [33]. Of particular significance is the immunity mechanism which enables rapid reactions to pathogenic microbes. The first layer of plant immunity involves the recognition of highly conserved molecular patterns shed by pathogens during interactions with the plant. Fungal chitin and bacterial flagellin, quorum sensing molecules and elongation factor Tu are some well-known examples of pathogen-associated molecular patterns (PAMPs) which are recognised by pattern recognition receptors (PRRs) on the surface of plant cell membranes [33-36]. Recognition of these conserved molecular signatures triggers anti-pathogenic strategies such stomatal closure, production of chitinase against fungal cell walls or callose production as a physical barrier and mechanism to reduce intercellular flux in a process known as pattern triggered immunity (PTI) [35,37,38]. In response to this process, pathogens have evolved mechanisms of evading or suppressing PTI initiation or signalling through secretion of a vast diversity of interfering molecules called effectors, in a process termed effector triggered susceptibility (ETS) [33]. These compounds are encoded by pathogenic *AVIRULENCE* (*AVR*) genes and are typically delivered into host cytoplasm through the use of bacterial type III secretion systems [33]. In turn, plants have evolved molecular mechanisms of effector recognition which trigger further rapid, robust and longstanding resistance which is specific towards the pathogen encountered, known

as effector-triggered immunity (ETI) [39](Figure 1-1). Further evolution or horizontal gene transfer can enable pathogens to target ETI mechanisms within the plant and in turn plants can recognise this process in a continuous, rapid arms race with their pathogens [33]. This plant-pathogen contest constantly drives selection both for resistance in plants and virulence in pathogens [35]. Recognition of pathogenic effectors typically occurs through highly polymorphic resistance (*R*) genes encoding nucleotide binding, leucine rich repeat (NB-LRR, NLR) proteins. *NLR* genes are often found in clusters as a result of local genome rearrangements and provide opportunities for recognition of pathogenic modifications or evolution due to the high sequence variation and domain shuffling which can rapidly create divergent haplotypes [20].

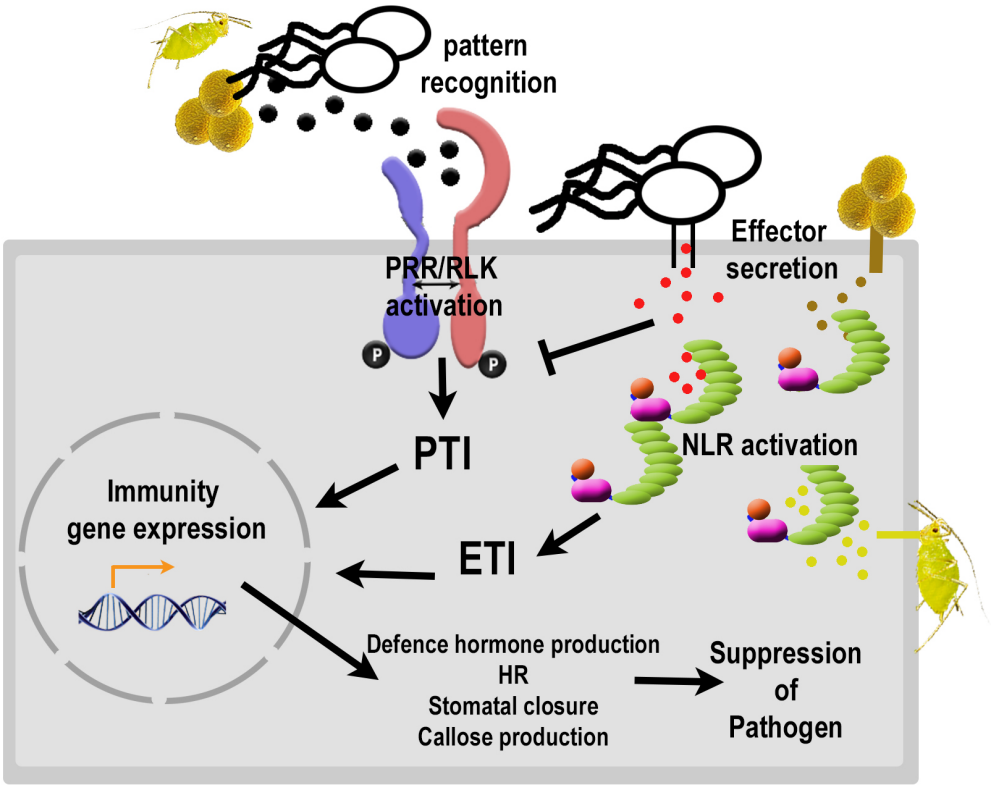

Figure 1-1 Plant immunity - Apoplastic pathogen associated molecular patterns are recognised by cell surface receptors (PRRs) and associated with receptor like kinases in order to initiate downstream signalling, genetic reprogramming and induction of defence hormones and their associated pathways to enable techniques to suppress pathogen growth. Pathogenic bacteria, fungi and aphids are examples of important pathogens which deliver cytoplasmic effectors through the use of secretion systems such as bacterial TTSSs, fungal haustoria or aphid stylets. These effectors are recognised by plant NLR proteins and trigger ETI, which further strengthens defence responses.

PTI and ETI have therefore evolved to recognise distinct molecular patterns and initiate downstream pathways in order to suppress pathogen growth and colonisation. Initiation of PTI is brought about through extracellular receptor-like kinases (RLKs) and initiates signal transduction through interaction with receptor-like cytoplasmic kinases (RLCKs), activation of mitogen activated protein kinase (MAPK) cascades, transient bursts of reactive oxygen species (ROS) production and calcium signalling in order to activate diverse mechanisms to restrict pathogen growth [37]. ETI involves intracellular recognition of AVR proteins, initiation of ROS and calcium signalling mechanisms and production of defence hormones such as salicylic acid (SA), jasmonic acid (JA) and ethylene (ET), depending on the nature of the pathogen encountered [39]. In PTI responses, the activation of MAPK and ROS signalling cascades leads to activation of the hypersensitive response, a generalised response mechanism thought to restrict colonisation and proliferation of pathogens [40]. Similarly, recognition of NLR proteins during ETI can also trigger this process [41]. Transient production of ethylene can also be observed following activation of MAPK cascades in plants as well as following ETI induction. The production of master transcription factors such as SARD1 and CBP60G are thought to coordinate central immune signalling processes common to both PTI and ETI and initiate upregulation of defence gene expression and hormone production [42].

Historically, PTI and ETI have been categorised as distinct processes but recently the differences between these processes has been narrowed down [43]. Classically, processes such as HR SAR were attributed to ETI [33] however, studies have also shown PAMP perception has been shown to trigger SAR in Arabidopsis [43,44].

In general, components of plant immune responses including PTI and ETI are coordinated by a network of interconnected hormones which can act antagonistically or synergistically, depending on the nature of the pathogen encountered. Three classes of plant associated pathogenic bacteria exist, resistance to which facilitated by appropriate hormonal responses coordinated through a central network of regulatory molecules. Biotrophs invade or establish close contacts with the host cells without compromising the plant's health. Necrotrophs actively parasitise the plant

until it dies then feed off its remains [45]. Hemibiotrophs are parasites that often have a biotrophic stage, but gradually lead to the demise of the plant [46,47].

In response to these pathogens, SA, JA and ET act as primary signals governing immune responses along with abscisic acid (ABA), auxins (AUX), giberrellins (GA), cytokinins (CK) and brassinosteroids (BR) [48]. SA is a phenolic molecule which is known to control biotrophic pathogen responses as well as initial resistance to some phloem-feeding insects as well as affecting many plant processes including growth, development, senescence, and stress responses[49,50]. JA is an organic compound which primarily acts alongside ET, a volatile signalling molecule, to induce resistance to herbivorous pests and necrotrophic pathogens (Figure 1-2) [51,52]. Other hormones such as ABA, AUX, GA, CK and BR which have been well characterised for their roles in growth are now known to play roles in coordination of responses to specific pathogens [53].

Typically, SA and JA are thought to act antagonistically and, in some cases, synergistically to coordinate resistance to pathogens with different life strategies [52] (Figure 1-2). These hormones once produced mediate the initiation of downstream signalling which, through action of key transcription factors, activate gene expression as appropriate for the nature of the pathogenic challenge [54](Figure 1-2).

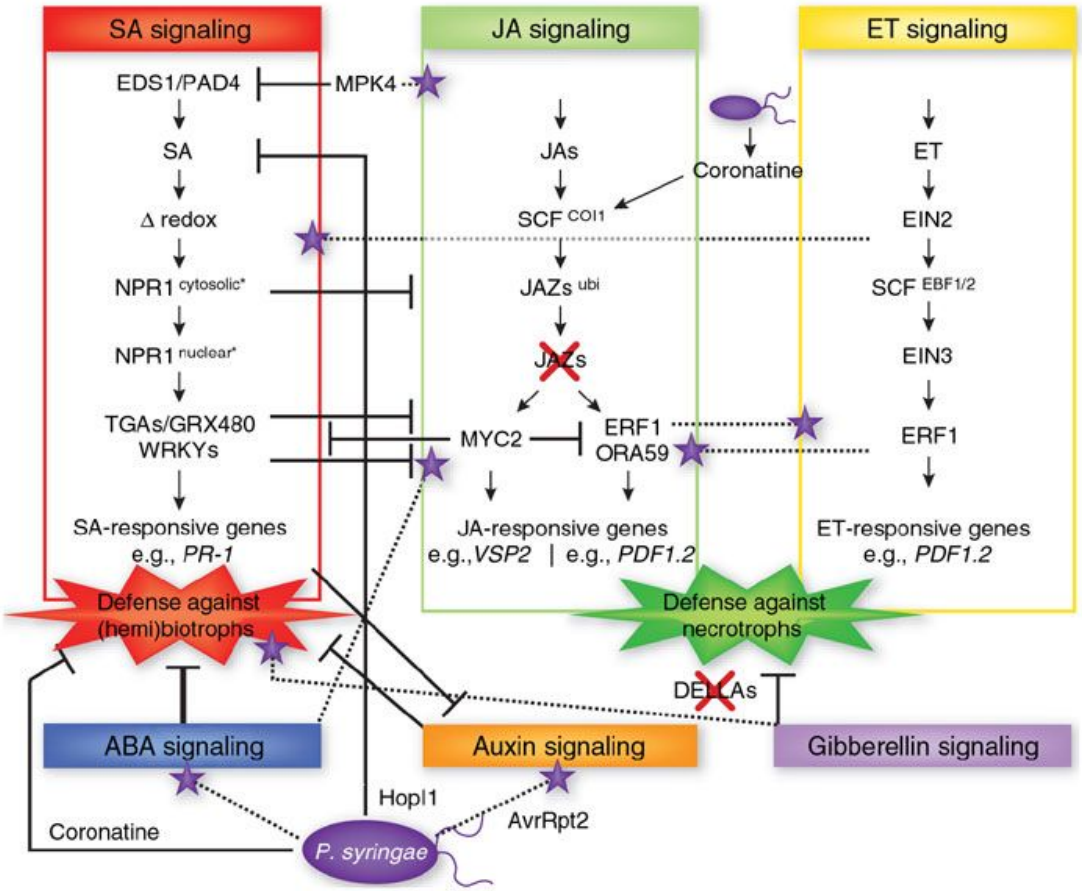

Figure 1-2 Network of plant hormones in immune response – SA, JA and ET act to initiate signalling pathways which interact with other factors such as ABA, AUX and GA to mediate gene expression and downstream responses to hemibiotrophic, biotrophic or necrotrophic pathogens. Figure presented with permission from Pieterse *et al* (2009) [54].

Both PTI and ETI activation are known to initiate local resistance reactions and SA production which then triggers broad spectrum, systemic resistance known as systemic acquired resistance (SAR) and primes plants to subsequent pathogen challenge [55-57]. Both systems of immunity lead to activation of key signalling processes and increases in defence gene expression. Components such as ENHANCED DISEASE SUSCEPTIBILITY1 (EDS1) and PHYTOALEXIN DEFICIENT4 (PAD4) were identified as essential signalling components for NLR initiation of SA biosynthesis [58] but have now been implicated as having wider roles in SA-related resistance programs (Figure 1-2). *eds1-2* mutants lack SA-dependent as well as independent immune processes and are therefore unable to mount effective resistance to biotrophic pathogens such as *Pto* DC3000 [59,60,61]. SA-independent regulation of SA-responsive genes by these factors confers resilience of these

pathways to pathogenic perturbations as well as SA conferring recovery for loss of EDS1/PAD4 immune signalling [60,61]. Strong buffering capabilities such as this can be observed across plant immune networks in order to maintain resistance in the face of effector targeting of any particular sector along with other positive and negative regulatory systems which exist to ensure optimisation of biotic interactions [62,63]. At a subcellular level, many different organelles contribute towards plant immunity. Signalling and communication between the nucleus [64,65] chloroplasts [66-68] and ER [69] are all essential to initiate and propagate signals, thus making them further targets for pathogen effectors and important aspects to understand with regards to coordination of plant immunity.

In addition to optimising responses to pathogens, these organellar and subcellular pathways enable simultaneous detection and integration of environmental stimuli in order to conserve resources and modulate their physiology in the most beneficial way to ensure survival and reproduction. The high energetic and resource cost of plant immunity has led to an antagonism developing between growth and defence, two highly resource-hungry processes.

1.2 Growth vs defence trade off in plants

Maintenance of plant resistance under all conditions is not possible for plants due to energy restrictions as well as the hormonal antagonisms existing between resistance mechanisms to different pathogens [70]. Plants must constantly optimise their metabolic processes and prioritise environmental cues, resulting in an observable tradeoff between growth and defence. Increasing resistance reduces overall fitness of plants in areas with lower pathogen burden, but is beneficial when pathogenic pressure is high.

Originally, this tradeoff was identified and characterised as an output of JA-mediated defences against herbivory. Resistance to herbivores such as aphids requires allocation of resources to chemical and structural defences such as production of toxic or distasteful compounds [71]. These processes must receive resource priority when under attack but be suppressed when environmental conditions favour growth, in order to maximise plant fitness and reproductive success [72]. Production of

metabolites and sugars are highly controlled and directed where most needed throughout the plant, making the identification of a cost of resistance on plant growth within the SA-mediated sector of immunity equally predictable [2]. Induction of this sector of defence typically results in compromised growth, and conversely, attenuating it results in plants with increased growth [73]. In terms of JA-mediated resistance, the direct fitness costs of defence activation are easily observable in terms of both growth and reproduction [74]. Artificial induction of this sector in cases such as transgenic crops expressing the widely used Cry toxins from *Bacillus thuringensis* (Bt) have shown a reduction in resistance to non-target herbivores [75]. In parallel, artificial introduction of R gene-mediated resistance in wheat and barley has shown a 9-21% yield penalty [76], thus highlighting the detrimental effects of these tradeoffs on food production and necessity to conduct cost/benefit analyses on future crop breeding processes, with respect to both biotic and abiotic challenges.

The observed fitness costs upon activating responses to the multiple pathogen types encountered have supported evidence for a direct tradeoff between growth and defence in plants. There are many theories as to the nature and molecular basis for this tradeoff, which exists at all levels of plant immunity. Initially, closing of stomata is one of the most important responses to PAMP perception but may incidentally reduce the uptake of CO_2 and thus limit photosynthetic capability of the plant. Stomatal aperture is regulated by abscisic acid (ABA), a plant hormone which acts antagonistically with SA in response to abiotic stress and is thus considered a negative regulator of plant resistance [77,78], thus providing another challenge for plants to overcome when simultaneously exposed to multiple environmental triggers.

Pathogens such as *Pseudomonas syringae* Pv. tomato DC3000 (*Pto* DC3000), a hemi-biotrophic pathogen, can further harness this antagonism through production of virulence effectors such as coronatine which act to regulate or induce JA signalling at the expense of SA, leading to stomatal opening, thus promoting its colonisation [79,80] (Figure 1-2).

Plants must therefore balance these tradeoffs through alterations in gene expression, a process which is both modulated by and results in production of appropriate hormones governing growth and immunity [2,48] (Figure 1-3).

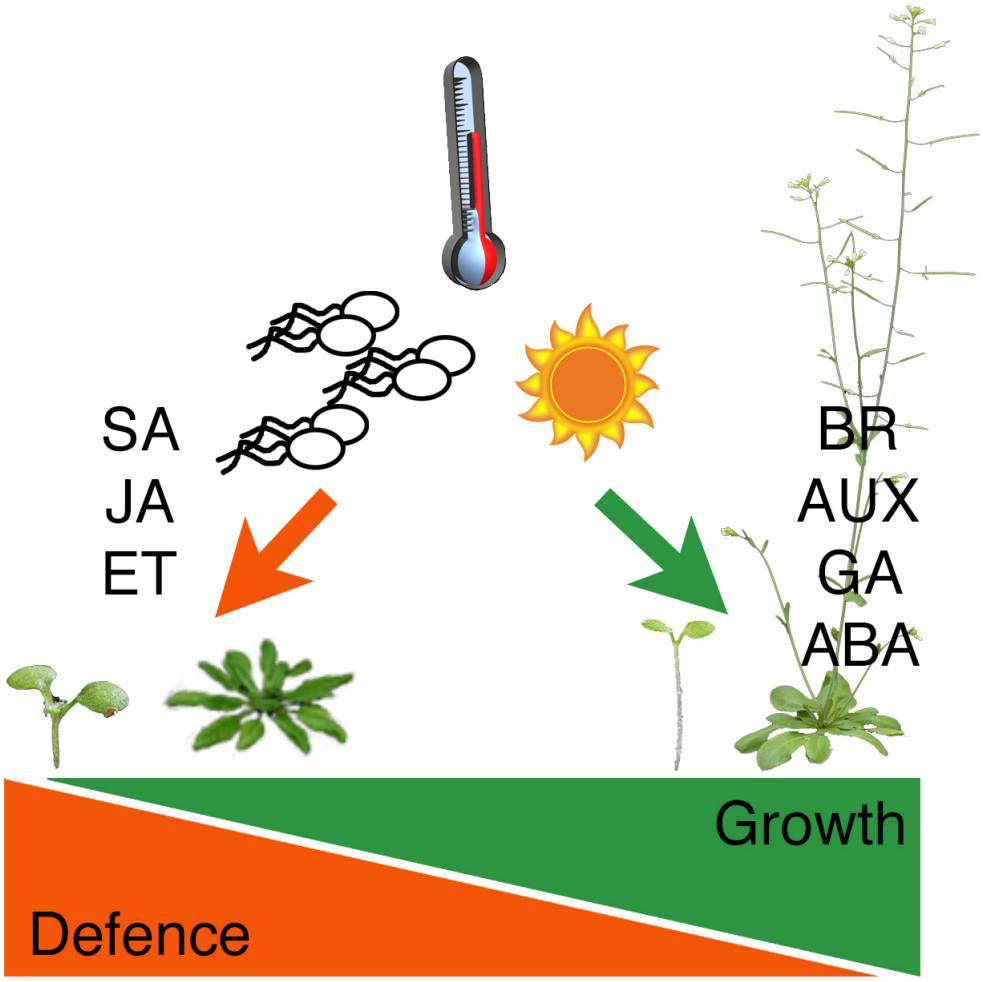

Figure 1-3 The growth vs defence tradeoff in plants – Depending on external environmental conditions and biotic interactions, plants allocate photosynthetic and nutrient resources towards growth or defence processes, which are both energetically costly. Low temperatures favour high immunity in order to combat pathogens, in processes primarily mediated by SA, JA and et (Orange), whereas at high temperatures, growth and acceleration of flowering are favoured (Green) at the expense of defence processes. In addition, photoperiod further modulates these processes.

The growth/ defence tradeoff in plants is modulated by several important environmental signals such as temperature, humidity and photoperiod [1,81](Figure 1-3). Low temperatures tend to favour defensive procedures, whereas high temperatures favour growth and reproduction[2]. Additionally, low and high temperatures are thought to differentially affect different components of immunity. It is currently thought that low temperatures favour ETI, whilst at high temperatures, PTI is preferentially strengthened [82]. This is thought to be as a result of lower

temperatures favouring effector secretion, with higher temperatures favouring bacterial multiplication and therefore presence of more PAMPs [82]. Previous study of this differential effect of elevated ambient temperature on both PTI and ETI did not allow for sufficient temperature acclimation to unquestionably establish their observations as an ambient temperature response however [82], so this response remains to be verified.

Downstream to environmental cues, several key genes and transcription factors are known to act positively or negatively to regulate growth and defence. For example, the SAR-inducible *PATHOGENESIS RELATED (PR)* genes are known to strongly associate with SA mediated resistance whilst compromising growth [83] furthermore, they act antagonistically with mediated growth genes such as auxins, brassinosteroids and gibberellic acid (GA) [2,20,84] (Figure 1-3). Transcription factors such as the heat shock factor-like TL1-binding transcription factor 1 (TBF1) and phytochrome interacting factors (PIFs) by modulation of growth and defence gene expression [85,86]. In addition, other regulatory factors such as cytokines can enhance defence activation by SA dependent and independent processes as well as inducing shoot growth [87]. Many upstream factors are thus thought to regulate growth and defence on a wider scale, resulting in activation of these pathways. Factors such as SA accumulation are both a measurable output of this process as well as having their own direct impact on balancing growth and immunity [87,88]. SA is also known to play a crucial role in age-related resistance (ARR), where plants become less susceptible to virulent pathogens as they mature [89,90], highlighting its regulation over the course of development as well as in balance with growth responses. Furthermore, An *Arabidopsis* calmodulin binding transcription factor, *Arabidopsis thaliana* signal responsive *At*sr1 was shown to be involved in regulation of R-gene mediated defences, mutants of which show elevated resistance to both avirulent and virulent pathovars of *Pseudomonas syringae* [91].

1.2.1 Plant thermosensory mechanisms

Temperature is a highly influential environmental cue, in part because of the effects of very small changes in temperature to modulate plant phenology [92] but particularly

through its direct thermodynamic effects on protein structure and stability [93-95], which make this cue perceivable through processes such as the unfolded protein response (UPR) [96]. This is in contrast to other environmental inputs, which tend to influence a key subset of plant components in order to bring about appropriate changes. Crucially, temperature is able to modulate responses to a wide range of environmental or seasonal signals [1,81,97] giving it a strong power over plant phenotypic responses.

Direct effects of temperature increase on subcellular compartments have begun to be unpicked. One of the most noticeable effects of temperature on subcellular composition is direct changes to the structure and fluidity of the plasma membrane [98-100] (Figure 1-4). Small increases or decreases in temperature correlate with fluidity and thus affect the ability of plasma membrane proteins to move freely around the outside of the cell [97,100]. Once temperatures begin to reach stressful levels, plants can modify the structure of their membranes in order to tolerate these changes [101].

Plasma membranes are comprised of phospholipids with a large degree of structural diversity and whose fluidity is altered by compositional alterations [102] as well as external parameters such as temperature [103]. Temperature changes affect fluidity through modulating rigidity of the fatty acid tails of the phospholipids [104], thus altering properties or movement of membrane-bound proteins and changing the permeability of the cell [101]. Mechanisms are in place to ensure adjustment of membrane physical characteristics and to minimise disturbances of function [105]. Detection of changes in membrane characteristics can even act directly as a stress transduction signalling mechanism [98,106]. The plasma membrane is similarly responsible for maintenance of an apoplastic-cytoplasmic calcium gradient, which, by controlling the entry of calcium into the cytosol through channels embedded in it, as well as associated bursts of ROS govern signalling in response to environmental stimuli [107-109](Figure 1-4). Dynamic changes in plasma membrane fluidity are thought to directly affect calcium channels or their interactions with other subcellular components [99,110] which then regulate downstream signalling to a wide range of biotic and abiotic signals [111-113]. It remains to be seen whether plants are able to

detect absolute temperature, or whether it is perceived changes in temperature on plant processes which are important.

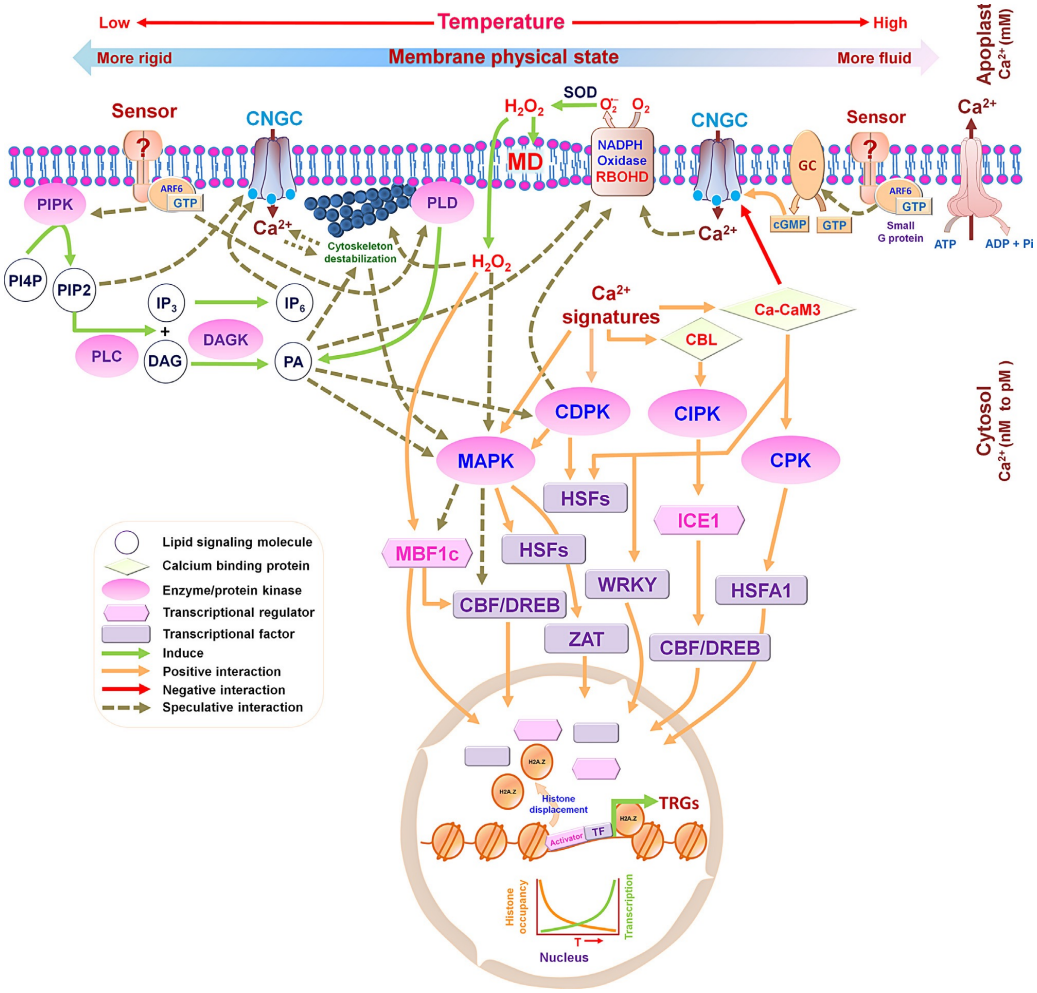

Figure 1-4 Plant thermosensory mechanisms – Some of the key known factors of plant thermoperception. Changes in temperature alter plasma membrane physical state, thus affecting plasma membrane bound components of plant signalling responses. Downstream, phosphorylation cascades are facilitated by other signals such as Ca^{2+} influxes. Within the nucleus, transcription factors such as PIF4 and H2A.Z histone deposition regulate expression of temperature regulated genes. Figure presented with permission from Bahuguna and Jagadish (2014) [97].

Direct effects of temperature on protein stability such as denaturation or conformational change can also be perceived through the Unfolded Protein Response (UPR) [114], which is typically triggered in plants to prevent aberrant protein accumulation [115]. This process is governed through pathways within the endoplasmic reticulum (ER) [116] and acts to initiate appropriate activation of stress response genes in the nucleus [96] such as production of heat shock proteins (HSPs) which function as molecular chaperones to protect proteins from further denaturation or aggregation

[100] as well as playing roles in regulation of other important processes such as immune responses[85] as previously mentioned. Monitors of unfolded proteins can be considered as thermosensors although they are not thought directly thermoresponsive and are nonspecifically initiated in response to internal or external stresses rather than high ambient temperature [114,115]. Two putative UP sensors have recently been characterised which result in the production of heat shock proteins and attenuation of global protein translation in response to stressful temperatures [114]. In addition, in a recent study, a quantitative trait locus (QTL), *Thermo-tolerance 1, TT1* was found to underpin thermotolerance in African rice (*Oryza glabberima*) [117]. *O. glabberima* represents a highly heat tolerant variety of rice which was domesticated separately to other Asian varieties [117,118]. TT1 was mapped to the α2 subunit of the 26s proteasome required for degradation of cytotoxic denatured proteins [117]. This finding highlighted the importance of perception and degradation of denatured proteins for thermotolerance and adaptation of crop species to warmer climates [118].

Other pathways of thermotolerance for important crop species include modulation of flowering time, which plants must ensure occurs at the right time in order to reproduce successfully. Flowering is one of the most notable responses to elevated temperature and depends on several key factors, most notably the transcriptional regulator, FLOWERING LOCUS C (FLC). FLC acts through binding and repression of two flowering promotion genes, *FLOWERING LOCUS T* (*FT*) and *SUPPRESSOR OF OVEREXPRESSION OF CONSTANS1* (*SOC1*) [119]. *FLC* downregulation under cold temperatures is required for vernalisation in order to derepress flowering. Regulation of this repressor is coordinated by two thermosensitive pathways [120]. One pathway downregulates the transcription of *FLC* in the cold [121,122] , and the second requires the action of Polycomb Repressive Complex 2(PRC2) and VERNALISATION INSENSITIVE3 (VIN3) to epigenetically silence *FLC* and maintain inactivation of this gene in the spring [120,121]. A recent study showed the temperature-dependent regulation of FLC was not specific to any node within the FLC network, suggesting that thermosensing may be distributed amongst signalling networks [120].

In addition to regulation by FLC, PIF4 and the FLOWERING LOCUS M (FLM)-SHORT VEGETATIVE PHASE (SVP) complex act to activate or de-repress FT [123]. FLM is an important factor contributing to thermosensitivity of flowering and is regulated in a temperature-dependent way by alternative splicing coupled with nonsense-mediated mRNA decay[123]. Identification of alternative splicing in FLM highlighted nonsense-mediated decay as a crucial mechanism for modulation of environmental responses in plants [123].

In addition to these known effects of temperature on subcellular processes, several key players have recently been identified which act primarily under ambient temperatures to sense and integrate temperature with other key environmental signals. Phytochrome B (PhyB) and its regulation of PIF4 is a process which were initially recognised as important components of the shade avoidance response in plants but more recently this process has been shown as equally key to temperature responses [124 125-128].

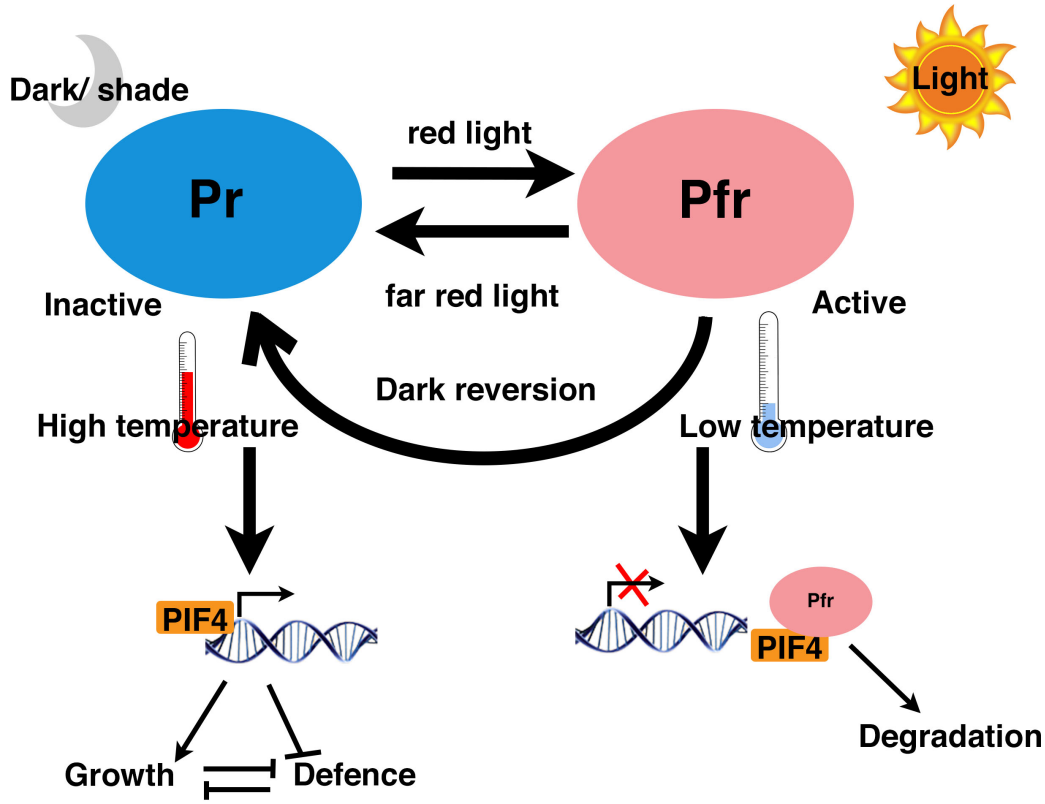

Figure 1-5 Thermoregulation of PhyB and PIF4-mediated gene expression – Phytochrome B in its inactive state (Pr) is activated by red light, resulting in conformational change to the active form, Pfr. Activation causes Pfr to localise to the nucleus, binding to PIF4 and targeting it for degradation by the 26s proteasome [129]. High temperature or dark reverts PhyB back to its inactive, Pr form, allowing PIF4 to bind to growth gene promoters

and facilitate growth genes [127,129]. Additionally this bHLH transcription factor represses the activation of defence genes [127].

Phytochromes are light absorbing photoreceptors which undergo an activating, reversible conformational change depending on enrichment of light colour which in the case of PhyB result in translocation of these proteins and thus interaction with the downstream basic helix-loop-helix (bHLH) transcription factor, PIF4 to positively regulate reallocation of resources to elongation growth responses in order to reach higher quality sunlight [124,130] (Figure 1-5). Recently, these components have been highlighted in regulation of the similar thermosensory elongation growth responses [126]. In particular, PhyB's conformational changes were shown as temperature sensitive [131,132] (Figure 1-5) as well as PIF4 shown as able of modulating the temperature sensitivity of *snc1* gain of function (GOF) mutant plants [127].

Photoperiod along with circadian clock regulation are similarly known to play crucial roles in the activation and timing of immune responses[81,133]. In particular, integration of these processes with circadian clock components such as DEETIOLATED1(DET1) [134] has been shown. DET1 was discovered through its role in repression of photomorphogenesis and is important for degradation of key transcription factors which promote this process such as ELONGATED HYPOCOTYL 5 (HY5) [135], but now with its partner CONSTITUTIVELY PHOTOMORPHOGENIC1 (COP1) has been shown to modulate coordination of growth and immunity in response to photoperiod and temperature changes [81,136]. Another level of regulation of these processes was recently shown through studies involving the SMALL UBIQUITIN-LIKE MODIFIER (SUMO) E3 ligase protein, SIZ1. In combination with COP1, this protein acts to amplify thermomorphogenic responses upstream to PIF4 and regulates SNC1 at the protein and transcript level as well as other parallel processes [137-139]. Altogether, Phyb/PIF4 represent an important regulatory hub of plant thermosensory responses which act at the centre of a central network coordinating growth and defence. Whilst important, these factors likely represent one of several important regulatory hubs of plant thermosensory responses. Furthermore, the details of the molecular mechanisms of temperature sensing and signal transduction

are still unknown. It will therefore be necessary for future studies to elucidate the complete pathway of sensing and signal transduction governing temperature responses in plants.

As I have already detailed, ambient temperature changes affect both immunity as well as growth and development. In fact, TSI could be considered one of the most notable outputs of plant thermosensory responses in general. This response is robust and easily quantified through study of key immune gene activation, accumulation of defence hormones terms of downstream outputs of signalling networks by the ability to restrict pathogen growth. Whilst the existence of this phenomenon is well established, many of the specifics of this process itself along with its initiation mechanisms and regulatory procedures required for such plant-wide drastic changes are yet to be determined.

1.2.2 Autoimmunity and the growth-defence trade-off

Regulatory mechanisms governing SA-mediated resistance and its associated tradeoff with growth have been identified through studies involving autoimmune mutants with constitutively elevated SA levels as well as plants lacking crucial components of defence pathways such as *NahG* transgenic lines expressing the bacterial salicylate hydroxylase which have been shown to increase growth and seed yield [73]. Autoimmunity in plants leads to constitutive resistance to pathogens at the cost of growth and development and can occur through mis-regulation of a wide variety of immune components [140]. Naturally occurring autoimmune loci such as *Accelerated Cell Death6* (*ACD6*) enhance adaptation to pathogen pressure over evolutionary time, with maintenance of a hyperactive *ACD6* allele in a population beneficial on long-term fitness when selective pathogen pressures vary in spite of its mild deleterious consequences on growth and development [17].

Gain of function mutations in NB-LRR proteins underlie the phenotypes of a large proportion of autoimmune mutants and highlight the strong association of SA increases with growth defects [140]. Of these mutants, one of the most characterised

as a result of its wide-ranging properties and strong effects on plant phenotype is *suppressor of npr1-1, constitutive1* (*snc1*), which was isolated in a screen for suppressors of the SAR regulatory mutant, *non-expressor of PR1-1* (*npr1-1*) [141]. *snc1-1* is a gain-of-function allele which displays constitutive activation of both SA dependent and independent immunity modulated by the *RPP4/ 5* resistance gene cluster, resulting in constitutive activation of an NB-LRR protein and consequent severe dwarfism [141,142]. These processes are independent of *NPR1* and subject to PAD4/EDS1 function [141,142]. Several subsequently identified autoimmune mutants such as *constitutive expressor of PR1-1* (*cpr1-1*) and *bonzai1* (*bon1-1*) were later revealed as negative regulators of *SNC1,* showing constitutively high levels of this gene at moderate ambient temperature [143], highlighting the strong participation and tight regulation of this R protein with regards to growth and defence in plants. Recent studies have also shown that tighter translational control over this pathway results in maintenance of resistance in the field without a noticeable fitness cost [144], however resistance conferred by gain of function of this gene is still strongly dependent on growth temperature [143,145]. In addition, recently the stability of R proteins has been shown as dependent on temperature, with low temperatures favouring their accumulation [91,146].

1.2.3 Temperature modulation of the growth-defence trade-off

Typically, it has been shown how both addition of NLR-mediated immunity to specific pathogens to crop species, and the constitutive immunity displayed by autoimmune mutants show strong attenuation of this resistance under moderately elevated ambient temperature conditions [143,147,20]. Autoimmune mutants caused by gain of function of *SNC1* or attenuation of its regulators *CPR1* and *BON1* show strong thermal reversion of both growth and immune phenotypes [143]. Conversely, downstream to these components a gain-of-function mutation in Arabidopsis R gene *RPP4* causes temperature deregulation of this protein, causing plants to become more sensitive to low temperatures [148].

This temperature regulation of R-gene or SA-mediated immunity is a widespread and robust phenomenon. With the exception of occasional documented cases such as

the hemibiotrophic rice blast and stripe rust fungi [149,150] and antiviral RNA silencing mechanisms [151-154], moderate increases in ambient temperature reduce resistance to a wide range of plant pathogens [1].

In parallel, plants undergo a process of morphological and architectural changes known as thermomorphogenesis upon perception of increases in ambient temperature within the non-stressful range to allow them to adapt to otherwise detrimental conditions [155]. Thermosensory suppression of immunity (TSI) and thermomorphogenesis (TMG) are both robust, plant-wide reactions to increases in ambient temperature which can be quantified through changes in physiology and gene expression. Up to this point, the primary mechanism of dissecting plant thermosensory responses has been through thermomorphogenic adaptations which can be easily quantified through measures such as hypocotyl and petiole elongation, petiole hyponastic growth and acceleration of flowering transition [155]. Through studies on growth and development, many important aspects of plant thermosensory mechanisms have been identified. To understand how TSI and TMG are brought about as outputs of plant thermosensory responses, it is first necessary to establish the mechanisms through which plants sense and respond to changes in ambient temperature.

1.3 Thermosensory suppression of immunity

Whilst there remain many unanswered questions as to the mechanisms governing immunity and growth processes at elevated ambient temperatures, several important moderators of these processes have been identified. Regulation by small RNAs [156], transcription factors [85,127,136] and incorporation of the variant histone, H2A.Z [157,158] is needed to coordinate downstream elements of this global transcriptional reprogramming [159] resulting in immune activation and repression of growth genes [160].

Of these, H2A.Z is known to play important roles in regulation of both thermosensory growth [157] and immunity [158,161]. Through alterations in chromatin accessibility [162], incorporation of this histone variant prevents aberrant activation of thermosensory response genes at low ambient temperature as well as preventing repression of low

temperature-specific genes [157] (Figure 1-6). As a result, mutants lacking effective incorporation of H2A.Z into nucleosomes phenocopy plants grown at elevated ambient temperatures [157] and therefore provide another route through which to dissect thermosensory responses. In addition, eviction of this histone have been shown as crucial for activation of the warm ambient temperature transcriptome through factors such as HSFA1 [163].

Deposition of H2A.Z depends on the SWR1 chromatin remodeling complex [164]. Studies carried out in mutants lacking key components of SWR1, as well as H2A.Z-deficient mutants, allow for in-depth investigation of the contribution of these components to TSI as well as the central coordination of thermosensory processes in general. A mutation in *ACTIN RELATED PROTEIN6* (*ARP6*), a subunit of this complex responsible for insertion of these histone variants, results in plants which phenocopy those grown at warm temperatures in both their physiology and defence phenotypes[157]. Constitutive activation of heat-inducible genes in mutants such as *arp6* caused by their lack of H2A.Z incorporations means transcription of elevated temperature – related genes can occur at lower temperatures. These mutants display constitutive, high temperature responses such as elongation growth, in a manner dependent on PIF4 [128,165]. Furthermore, their constitutive high ambient temperature transcriptome makes them a useful resource for studying thermosensory responses.

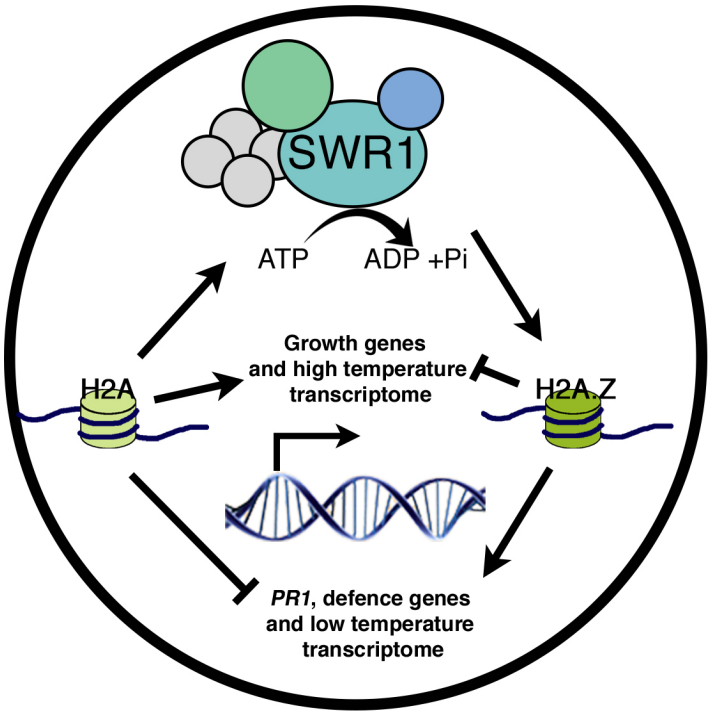

Figure 1-6 SWR1-mediated H2A.Z deposition is required for repression of high ambient temperature transcriptome - including suppression of immunity-associated genes and promotion of those associated with thermosensory growth. This process is dependent on the ATP-dependent chromatin remodeling complex, SWR1.

It is not known whether this tradeoff and TSI confers any selective advantage [166] or whether it is a direct metabolic consequence of resource allocation, which has not yet been selected against since plants have slowly adapted their thermosensory capabilities ("thermostats") over evolutionary time. Regardless of its evolutionary cause, this thermosensory response of immune suppression is remarkably robust. In autoimmune mutants which have constitutively elevated defences at a cost to their growth, this response appears to be maintained and leads to reversion of their phenotypes upon growth at moderately elevated temperatures [140,143]. Many thermosensitive autoimmune mutants have been documented, such as those with constitutive *PR1* activation/ SAR identified in *constitutively induced resistance (cir), constitutive expressor of PR1* (*cpr*) and *constitutive immunity* (*cim*) mutant screens [1,167,168], in addition to *snc1-1* as I have previously mentioned. *snc1-1* gain of function shows a particularly strong thermosensory response, resulting in both loss of this robust immunity and a reversion of its dwarf phenotype [145,143]. Recent progress has identified the abilities of intragenic mutations or modifications of *SNC1* sequence/ SNC1 protein as well as perturbations in PIF4/ BZR1 function to render SNC1-

mediated immunity insensitive to temperature [166,169,139,127]. This mutant still maintains thermosensory loss of *PR1* expression in some cases in spite of displaying reversion of its growth and other defence phenotypes. These studies have shown the importance of post translational modification and interactions in governing plant environmental responses [170,171], however the precise mechanisms via which plants sense temperature and bring about these global immune changes is not yet known.

1.4 Thesis objectives

With this thesis, my key objective is to establish a novel mechanism of temperature sensing though dissection of TSI in plants. To achieve this, I will begin by verifying the effects of temperature on key stages of plant immunity and its associated signalling pathways. Following this, using TSI as an output of plant thermosensory responses, my aims are to identify and characterise an important thermosensory component with wider roles in coordination of growth and immunity. Through gaining a greater understanding as to the nature of the mechanism required to suppress immunity at warmer ambient temperatures in *Arabidopsis,* I therefore aim to gain a greater understanding of plant thermoperception and crucial signalling mechanisms governing both growth and immunity in plants.

Dissection of the upstream mechanisms by which plants sense and respond to temperature will therefore facilitate further characterisation of TSI along with TMG and progress understanding as to plant thermosensory signalling networks. Better understanding of plant thermosensory mechanisms will facilitate understanding of the potential effects of climate change on food security alongside development of potential mitigation strategies for these effects.

2 Thermosensory Suppression of Immunity

2.1 Introduction

2.1.1 Ambient temperature changes oppositely affect plant growth and immunity

Temperature is one of the most influential environmental cues that modulate plant phenology. Non-stressful elevations in ambient temperature result in changes to growth and development whilst altering both basal and inducible immune processes [20]. These increases promote elongation growth and reproductive transition whilst reducing immune activation to a wide range of pathogens [20]. For example, resistance to the hemibiotrophic pathogen, *Pseudomonas syringae, pv.* tomato, DC3000 (*Pto* DC3000) in *Arabidopsis* is significantly reduced between 22 and 28℃ [147]. Concurrently, small increases in temperature result in elongation growth of plant organs and acceleration of flowering [126,172]. As previously discussed, a direct trade-off between growth and defence is necessitated by the high energy and resource costs of both processes[173,174,175]. In a similar manner, elevated temperature simultaneously promotes growth whilst inhibiting plant immune responses. As a result, Thermosensory Suppression of Immunity (TSI) represents a valuable resource via which to understand how plants sense and adequately respond to temperature. Unlike plant growth responses which are relatively easy to characterise, the complex nature of plant immune systems requires a more in-depth understanding of TSI in order to cement this process as a readout of thermosensory responses. Thermomorphogenic responses have been recently characterised comprehensively for a range of ambient temperatures [92] however the sensitivity of plant immunity to smaller changes in temperature (≤ 5℃) has not been characterised. Understanding the degree of sensitivity of plant immune systems to temperature, and whether this process occurs as a programmed genetic response or as a result of a catastrophic breakdown beyond a critical threshold, have yet to be determined.

2.1.2 Plant thermosensory mechanisms

Many important aspects of plant temperature sensing are currently known. Key factors such as PhytochromeB (PhyB) and PHYTOCHROME INTERACTING FACTOR4

(PIF4) which were initially identified as components of the shade avoidance response have recently been implicated in sensing and transduction of temperature signals [126,131,132]. Furthermore, deposition of the histone variant, H2A.Z is known to play a key role in global transcriptional reprogramming and regulation of temperature responses, mediated by the chromatin remodeling complex, SWR1c [157]. Whilst significant progress has been made in understanding thermosensory regulation of growth and development [155,176], the effects of temperature on TSI remain to be fully characterised. Previous work has identified differential effects of temperature on PTI and ETI With a few exceptions, the direct effects of temperature on signalling mechanisms as well as upstream regulators of thermosensory processes are not yet known [1,20].

Plants and infectious microbial communities exist in a constant arms race with one another. Recognition of small, conserved molecular motifs of pathogens by cell surface receptors (pattern recognition receptors, PRRs) initiates defence mechanisms in a process known as pattern-triggered immunity (PTI) in order to suppress pathogen colonisation and multiplication [33,177]. Successful pathogen recognition triggers plant responses such as stomatal closure, secretion of antimicrobial compounds, callose deposition and restriction of nutrient transfer [37]. Bacteria in response secrete effectors to suppress immune activation [33]. During avirulent plant-pathogen interactions, plants successfully recognise and respond to bacterial effectors in order to successfully mount effector triggered immunity (ETI), a stronger and more prolonged response to bacterial challenge.

Whilst PTI and ETI share several common outputs and are not always distinguishable *in vivo*[43], each process requires distinct recognition and early signalling machinery. Extracellular PRRs are required for PTI activation, whereas cytoplasmic NB-LRR proteins govern effector recognition, neutralisation and signalling (in ETI).

Although it is difficult to differentiate between PTI and ETI, it is possible to trigger both processes in isolation and thus to identify their respective downstream responses. Induction of PTI in isolation can be brought about through treatment of plants with purified elicitors such as flg22, a 22-amino acid peptide that corresponds

to bacterial flagellin, as well as by the use of non-pathogenic strains such as *Pto* DC3000 (hrpA/*hrcC-)* which lack bacterial type three secretion systems necessary for cytoplasmic delivery of effectors [178]. ETI can be triggered specifically through the introduction of non-native effectors to these bacteria [179]. Through studies using these methods of plant defence induction, it is possible to specifically dissect the effects of temperature on PTI and ETI.

Changes in temperature can simultaneously and differentially affect resistance to different pathogens [1]. It has previously been hypothesised how, in line with variations in pathogen virulence patterns, different temperature regimes favour PTI or ETI [82], rather than ambient temperature universally suppressing pathogen response processes. One of the most studied aspects of plant immunity with respect to temperature is suppression of NLR (R-gene) mediated immunity (ETI) and SA production in the context of resistance to the hemibiotrophic pathogen, *Pto* DC3000.

In this chapter I have further expanded the knowledge of TSI where it has previously been lacking, as well as determined the specific effects of temperature on each layer of plant immunity. In particular, effects of temperature on PTI was an area particularly lacking validation which I aimed to address. An overall increase in understanding the nature of TSI will enable future dissection of the molecular mechanisms underpinning this process. This will then strengthen the foundations upon which to build further knowledge of plant thermosensory processes through study of TSI.

2.2 Results

2.2.1 Elevated temperature suppresses immunity

Whilst the effects of increasing ambient temperature on plant immunity have long been known, recent advances have allowed the characterisation of this phenomenon in detail. For example, Wang *et al* (2009) [147] showed how a moderate upshift in the ambient temperature range reduced plants resistance to virulent pathogens. Since then, this interaction has been used as a model system to investigate plant-pathogen responses in many different environmental contexts [27,81,89,180]. Furthermore, it has been hypothesised how elevated ambient temperatures co-ordinately decrease ETI and increase PTI responses [82]. However, too short a temperature treatment was used in these experiments to realistically mimic ambient temperature increases. Optimising assay conditions is necessary so as to realistically assess the effect of temperature on immunity without the confounding effects of temperature on growth and development. Validating a set of growth conditions to this effect is therefore essential before attempting to broaden understanding of the effect of elevated temperature on immunity.

To validate previous findings and to trial biologically relevant growth conditions to use throughout this study, I assessed resistance of wild-type (WT) Col-0 and *eds1-2* mutant plants to virulent *Pto* DC3000 under two moderate, non-stressful temperature regimes. Following 3 days stratification at 4℃, plants were grown for 4 weeks at 22℃ under short photoperiod conditions (SD). To ensure homogeneity of plant growth and minimise the effects of temperature on growth and elongation responses, all plants were initially grown at 22℃ before being shifted to 27℃ for 3 days or further maintained at the lower temperature as in Gangappa *et al* (2017) [127]. Three days post-temperature shift, plants were spray inoculated with *Pto* DC3000 (OD_{600} = 0.02) in 0.01% Silwet until runoff, then maintained at their respective temperature (22/ 27℃) for a further three days. Following this, bacterial colony forming units (CFU) per cm^2 leaf area were quantified from 4-6 plants per temperature. *eds1-2* (hereafter *eds1*) mutant plants were included alongside WT as

a susceptible control. Since differences in resistance to *Pseudomonas syringae* in Arabidopsis can be seen for different rosette leaves [89], I used three leaves of a similar age from each plant from which to measure bacterial titre (colony forming units (CFU)) at 3 days post inoculation (DPI).

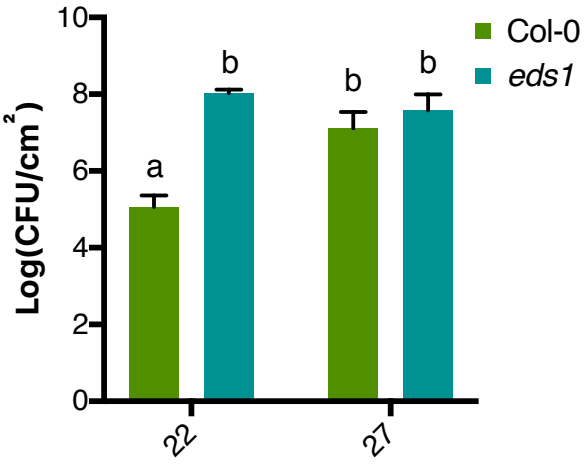

Figure 2-1 EDS1-dependent immunity to *Pto* DC3000 in *Arabidopsis* decreases with increasing temperature - Resistance of 5-week-old, 22/ 27°C-acclimated Col-0/ *eds1* plants to virulent PtoDC3000 was measured through bacterial CFU per cm² at 3 dpi. Statistical analysis of bacterial growth between temperature and genotype was conducted through two-way Analysis of Variance (ANOVA) followed by Tukey's multiple comparisons test carried out, n=6 plants per genotype/ treatment. One representative example is shown here of 4 biological replicates.

In spite of its virulence on *Arabidopsis* Col-0, from Figure 2-1 it can be seen that WT plants are still able to restrict *Pto* DC3000 growth at 22°C. Consistent with previous studies, 27°C grown plants displayed a decrease in resistance to *Pto* DC3000. No difference was observed between temperatures in *eds1* plants, suggesting that elevated ambient temperature suppress EDS1- mediated resistance.

Simultaneously with compromising defence, increases in ambient temperature result in elongation-growth and consequent architectural changes as previously established [181,127]. Though short, the duration of growth at 27°C for the pathogen assay consequently was sufficient to observe plant growth increases in line with increases in severity of disease symptoms as shown (Figure 2-2).

Figure 2-2 Phenotypic responses of plants to elevated temperature - 5-week old Col-0 plants pictured following 3 days elevated temperature acclimation followed by three days of pathogen challenge. Scale bar = 1 cm

At 22°C, plants remain relatively compact and show early signs of infection such as yellowing (chlorosis). In comparison, plants grown at 27°C display notably elongated petioles and increase in overall rosette size, along with an increase in chlorosis and wilting because of increased bacterial colonisation.

2.2.2 Modest changes in temperature suppress immunity

As shown above, a "modest" increase of 5°C has significantly compromised resistance to *Pto* DC3000 (Figure 2-2). In fact, this temperature differential is sufficient to completely alter plant physiology. Whilst shifts of this magnitude have previously been considered "modest" or "moderate", two qualitative terms dependent on interpretation, an increase of this amount could in fact be considered significant in relative terms through its effects on plant responses. Plants can sense and respond to temperature changes of as little as 1°C in order to respond appropriately to environmental changes [182]. The degree of sensitivity of plants to temperature is significant since, according to even the most conservative estimates, average global temperatures are set to increase 2-3°C. Such increases are predicted to affect plant life in the wild as well as the field, thus simultaneously affecting biodiversity and food security [23,183]. It is therefore important to assess the impact of smaller changes in temperature on important plant processes, such as immunity, in order to mitigate these problems in the future.

Currently, relatively little is understood for temperature upshifts ≤5°C on plant phenology. Studies on thermomorphogenesis [92] and resistance, particularly in the context of hybrid necrosis [184], have begun to unravel the coordination of elevated

temperature responses in plants grown under a smaller temperature gradient. The precise nature of TSI following smaller changes in temperature however has not been previously characterised. Whether plants gradually lose immunity as part of a controlled, deliberate process or whether this breakdown happens drastically at a specific threshold unique to the species or ecotype used is yet to be determined.

To understand changes in immunity over a narrower range of temperature conditions, I grew Col-0 and *eds1* plants as before for 4 weeks at 22°C SD before moving plants up or down a temperature gradient and spray inoculating with *Pto* DC3000. A total temperature range of 10°C was investigated, in 2.5°C intervals.

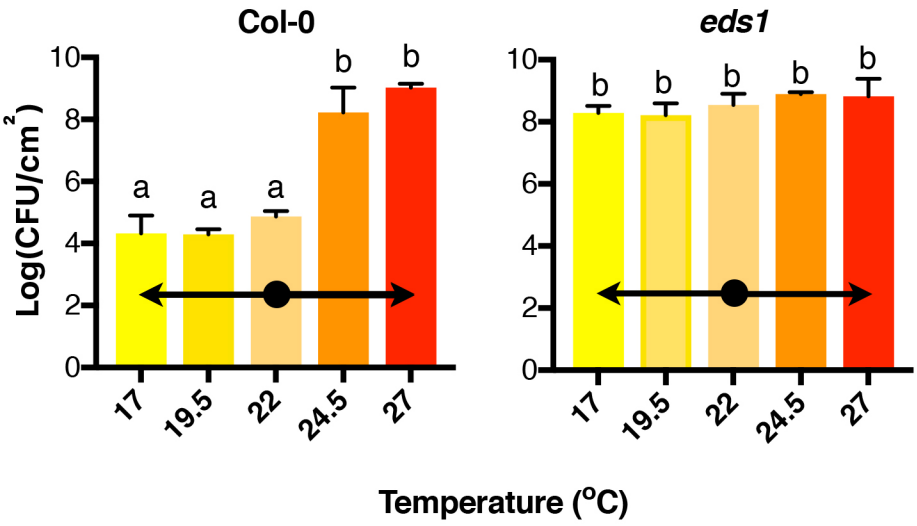

Figure 2-3 The effect of moderate increases in temperature on resistance to *Pto* DC3000 - Plants grown at 22°C before being shifted up or down temperature in 2.5°C temperature increments were infected with *Pto* DC3000 and bacterial CFU quantified at 3 dpi. Statistical analysis of bacterial growth between temperature and genotype was conducted through two-way ANOVA followed by Tukey's multiple comparisons test carried out, n=6 plants per genotype/ treatment, individual genotypic graphs are displayed side by side with common statistical analyses included. The arrows across the bars indicate the temperature shift from the initial growth temperature. One biological replicate in adult plants only is shown here. Further replicates were carried out in seedlings.

One can see here how a smaller increase in temperature from 22°C than previously tested remains effective in eliciting TSI in *Arabidopsis*. Upshifting WT plants 2.5°C was sufficient to significantly decrease resistance to *Pto* DC3000, resulting in infection levels in line with 27°C- grown plants. From this experiment, a drastic breakdown of defences at high temperature rather than a gradual response is apparent.

In addition to this, no beneficial effect on immunity was detected by further decreasing temperature from 22°C in WT plants (Figure 2-3). *eds1* plants were more

susceptible than WT regardless of temperature conditions, indicating no effect of temperature in resistance of this mutant or equally, bacterial growth rate.

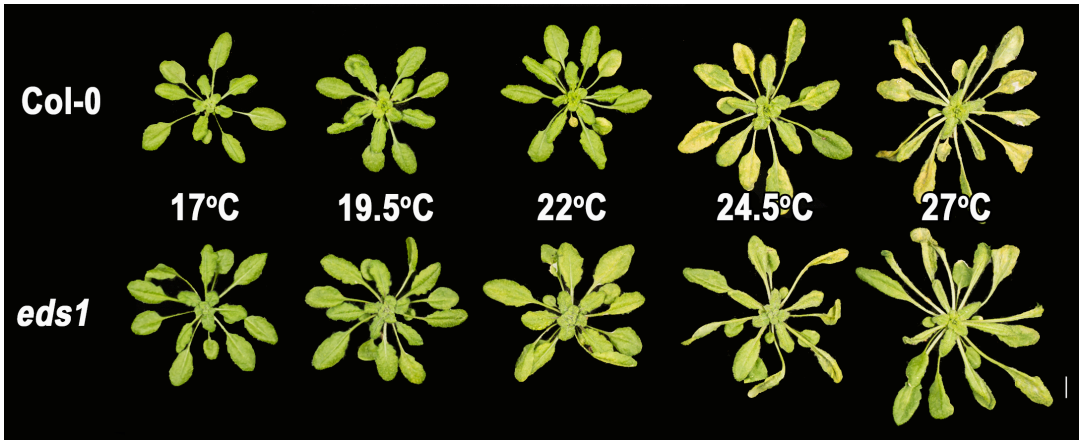

Figure 2-4 Graduated temperature changes affect disease symptom severity and thermosensory growth – Four-week-old plants acclimated to 22°C followed by growth at 17, 19.5, 22, 24.5 or 27°C for three days and infection with *Pto* DC3000 for a further 3 days at their respective temperatures. Representative plants were chosen for each temperature based on observation and bacterial CFU subsequently quantified. Scale bar = 1cm.

In line with the immune responses observed in Figure 2-3, WT plants shifted to 24.5°C show much more severe symptoms of infection than those grown at 22°C alongside signs of thermosensory elongation growth (Figure 4). Plants grown at 27°C appear to show further progression of thermomorphogenesis but are almost comparable to their 24.5°C - grown counterparts in terms of infection severity. Relatively little difference can be observed between plants grown at 17 – 22°C here, further substantiating observed CFU measurements. Coordinated increases in growth and suppression of immunity can thus be seen as tightly interlinked as a result of a growth/defence trade-off, with a 2.5°C increase sufficing to initiate modulation of this process by temperature.

EDS1 and PAD4 are well-established coordinators of SA-mediated immunity [59,61]. WT plants grown at elevated temperatures under these conditions phenocopy *eds1* mutants, thus highlighting the loss of SA-mediated immunity in these plants, as reported earlier. Clearly, EDS1 plays a key role in resistance at ambient temperatures ≤22°C and small increases than previously documented are sufficient to affect the function of this pathway. Interestingly here, despite the demonstrably similar levels of bacteria present on leaves (Figure 2-3), there is a lack of apparent disease

symptom severity at lower temperatures in *eds1* plants. This may suggest an effect of temperature on symptom development such as pathogen-induced leaf chlorosis, independent of EDS1-mediated immunity.

Chlorosis caused by nutritional deficiency or pathogen infection has long been recognised [185], but the precise physiological causes of this symptom under different stresses are not yet understood. The visible differences between infected *eds1* plants could represent a pathogenic transition from a biotrophic, asymptomatic growth to a necrotrophic, higher effector-secreting stage of this hemibiotrophic pathogen [367]. Effector production and pathogen virulence has recently been demonstrated as increasing in line with temperature [27], in contrast to previous studies [186]. In bacterial strains lacking production of the Jasmonate-mimicking effector coronatine (*Pto* DC3118), a reduction in pathogen-associated leaf chlorosis was also observed at 28°C compared to *Pto* DC3000 despite similar levels of pathogen load as a result of TSI [27]. Plants inoculated with *Pto* DC3000 strains lacking type three secretion systems lack disease symptoms [27]. Artificial attenuation of SA-mediated immunity by coronatine is clearly an effective strategy for a biotrophic pathogen, however any direct effect of this molecule on chlorosis is not yet known. The response observed in Figure 2-4 must therefore represent similar increases in production or delivery of any number of other effectors in *Pseudomonas syringae*. The chlorosis observed in WT plants may not be directly representative of increased bacterial load, showing the need to quantify infection level in addition to describing observed infection symptoms.

This study has demonstrated a high degree of sensitivity of plant immunity to temperature changes and further revealed the potential for catastrophic, pathogen-induced drop in crop health and thus yield in the future. Whether the responses observed occur as a result of directionality and magnitude of shift or as a result of detection of specific temperature threshold cues remains to be seen, and may be established further through a better understanding as to the molecular mechanism of thermosensory signaling.

2.2.3 Thermosensory suppression of immunity is independent of developmental stage

In addition to responses to changes in temperature, plant immunity and growth patterns depend strongly on developmental stage [187]. It is well known that development and resistance reciprocally influence each other, most commonly an increase in resistance can be observed in more mature plants [90,188] although seedling-specific immunity can also be observed [189-191]. To determine whether the pattern observed for TSI in adult plants is growth stage-specific, I next characterised TSI in seedlings. Having previously observed no difference between the lower temperatures, I modified the previous temperature regime to exclusively investigate the effect of increasing temperature on pathogen resistance.

To minimize the confounding effect of temperature influences on plant growth, seedlings for each temperature regime were initially grown together at the lowest temperature tested (17℃). Following stratification at 4℃, seedlings were grown for 8 days at 17℃ before being shifted upwards 5, 7.5 or 10℃ to 22, 24.5 or 27℃ for three days acclimation before spray inoculation. To enable additional visualization of pathogen growth on seedlings, *Pto* DC3000 expressing the luminescent *Photorhabdus luminescens* luxCDABE operon (*Pto* DC3000-lux hereafter) was used [192] to infect plants and luminescence was visualised at 3 dpi.

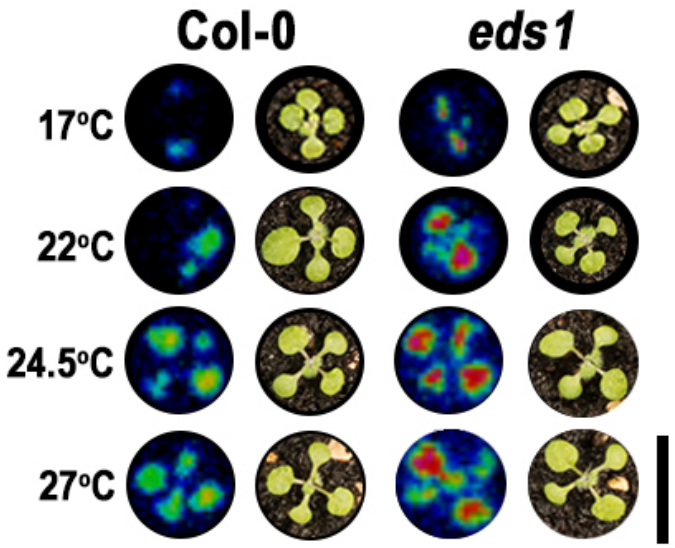

Figure 2-5 *Pto* DC3000-LUX infection of Col-0 and *eds1-2* seedlings at 17-27℃ - Representative seedlings from each temperature tested showing degree of colonisation of luminescent Pto DC3000-lux. Scale bar = 1 cm, for photographed seedlings only, luminescence images are approximately to-scale of the same seedlings.

In a similar manner to that observed for adult plants, an increase in bacterial growth followed increases in temperature, as evident from luminescence of bacteria on seedling cotyledons (Figure 2-5). Unlike their adult counterparts, *eds1* seedlings showed a weak response to temperature between 17 and 22℃ but were all clearly more heavily infected than WT at each temperature tested. This suggests that increases in temperature affect EDS1-independent as well as dependent pathways, which appears to be particularly apparent in seedlings in comparison with adult plants.

Following the imaging of bacterial load on these seedlings, I subsequently quantified bacterial CFU per mg fresh weight (fw).

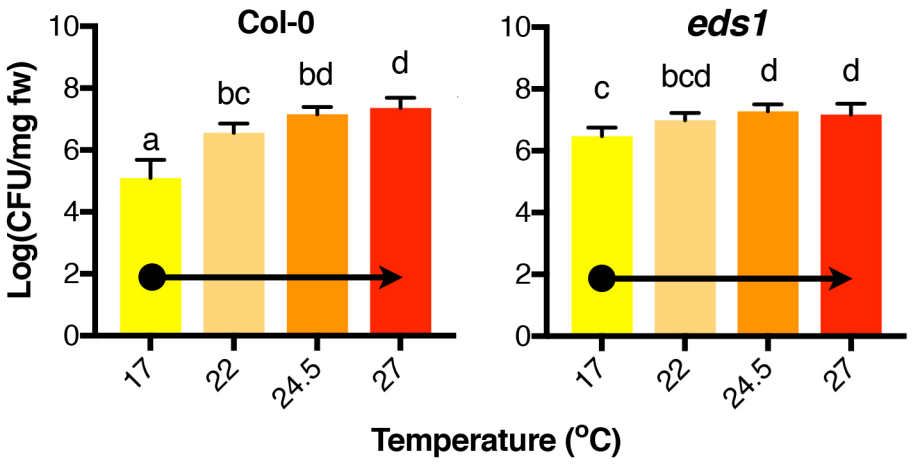

Figure 2-6 Moderate increases in temperature affect resistance to *Pto* DC3000 in seedlings - Bacterial CFU/ mg fresh weight in 14-day-old Arabidopsis seedlings acclimated to 17°C before being shifted 5-10°C upwards and infected with *Pto* DC3000. Statistical analysis of bacterial growth between temperature and genotype was conducted through one-way ANOVA followed by Tukey's multiple comparisons test and displayed as before (n=6). The arrow across the bars indicate the temperature shift. Data presented here is a representative example of 3 biological replicates.

I previously observed how resistance to *Pto* DC3000 decrease with incremental increases in temperature in 4-5-week-old *Arabidopsis* plants. The same response is clearly observable in younger plants (Figure 2-6). From this data we can see the importance of initial acclimation/ growth temperature followed by relative increase. Pre-growth of seedlings at 17°C ensured the effect of temperature increases only were measured. As a result, seedlings displayed a gradual loss of immunity as temperature was increased where before no difference between 17 and 22°C could be detected. This may suggest that degree of change of temperature rather than absolute perceived temperature plays a role in TSI. Also, - in the *eds1* seedlings, slight differences could be observed between temperatures. This suggests the existence of non-*EDS1*-dependent immune processes active in seedlings which are both temperature-sensitive and deactivated as plants age. A recent study highlighted the likely existence of pathways acting in parallel with EDS1, such as EXA1-mediated modulation of NLR-based resistance which was also shown to be partially independent from SNC1-mediated resistance [193]. Similar mechanisms could therefore play a moderate role in seedling immunity, resulting in the differences observed in Figure 2-6 in comparison with WT plants. As a control, *eds1* plants still

displayed a higher level of infection than WT and showed no temperature sensitivity at temperatures ≤22°C, further supporting the observation that elevated ambient temperature compromises EDS1-mediated immunity.

Taken together with the adult plant phenotypes, these data show that TSI is a robust process, independent of growth stage. Further to this, direction and amplitude of change rather than specific perceived temperature appear important for this process. In order to enable further in-depth dissection of TSI, a 22-27°C temperature upshift remains a robust differential for use in future experiments.

2.2.4 Thermosensory suppression of Effector-Triggered Immunity

As a whole, the effects of temperature on plant immunity are easily visible through the effects on pathogen growth suppression by the plant. These responses occur as a result of highly complex layers of plant immune signalling resulting in appropriate activation of defences. Detection of microbial signatures (PAMPs or effectors) associated with plant pathogens result in downstream activation of defences such as increasing defence hormone levels and gene expression. These systems in turn bring about the appropriate pathogen-suppression mechanisms necessary to address the specific biotic challenge presented.

Whilst the downstream outputs of these processes show temperature sensitivity, relatively little is currently known as to the specific effects of temperature on the mechanistic processes involved. Previous studies have demonstrated the differential effects of temperature on PAMP- and effector-triggered immunity, in particular the thermosensitivity of R gene-mediated immunity is well known. The NLR protein SNC1 is known to positively regulate plant immunity impacting plant growth and represents one of the most extensively studied and influential examples of a thermosensitive R protein. Both gene expression and protein function of SNC1 are tightly regulated and its function is strongly impeded by growth at increased ambient temperatures [194,166]. In *Arabidopsis*, the bacterial effector, AvrRps4, which typically acts by increasing bacterial growth in susceptible hosts [195], triggers ETI responses via two interacting NB-LRR proteins RPS4/RRS1 [196,197]. Studies using *Pto* DC3000 expressing this effector have indicated a strong sensitivity of RPS4- mediated ETI to

elevated temperature in *Arabidopsis thaliana*, a resistant host [82]. In addition, other effectors such as HopZ1a and AvrRpt2 have been shown to bring about the hypersensitive response (HR) in a thermoresponsive manner although the results gained from this study suggested plants were still able to impede bacterial growth at high temperature in an ecotype-dependent manner [198]. Many of the findings of this study could be due to confounding effects of unusual growth conditions. To validate thermosensory suppression of ETI, I investigated this effect under a set of more consistent environmental conditions as described earlier.

I grew plants for 4 weeks at 22°C before shifting them to 27°C or maintaining them at 22 for three days and spray inoculating with *Pseudomonas syringae pv.* DC3000 expressing the virulence effector a*vrRPS4* (*Pto* DC3000 (AvrRps4)) (OD_{600} = 0.02) and growing on for a further three days at their respective temperatures. I then measured bacterial CFU/cm^2 as above.

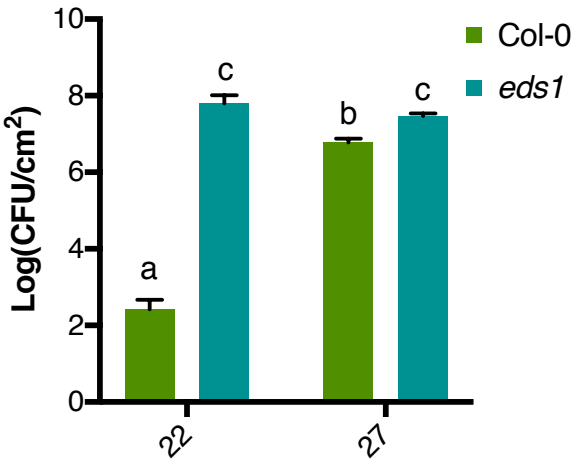

Figure 2-7 Resistance to avirulent *Pto* DC3000 (AvrRps4) in *Arabidopsis* decreases with increasing temperature - Resistance of 5-week-old Col-0/ *eds1-2* to this bacterial strain following 3 days acclimation at 27°C in shifted plants plus 3 days of pathogen growth at their respective temperatures. Statistical analysis of bacterial growth between temperature and genotype was conducted through two-way Analysis of Variance (ANOVA) followed by Tukey's multiple comparisons test carried out, n=5-6 plants per genotype/ treatment. One representative example of 3 biological replicates is displayed here.

As a result of robust ETI, triggered through AvrRps4 expression by *Pto* DC3000, strong resistance can be observed at 22°C, in an EDS1-dependent manner. Upon growth at elevated temperature however, resistance is reverted almost to the level of *eds1*. In comparison with the virulent interaction previously observed, where increasing

temperature by 5℃ resulted in a ~1000-fold difference in bacterial colonisation, the presence of AvrRps4 resulted in a ~1,000,000–fold difference in bacterial colony forming units between 22 and 27℃. These results are in line with the majority of studies as to the effect of increases in ambient temperature on ETI [1,82]. More detailed studies in the future would be helpful in order to further dissect thermosensory suppression of this layer of immunity.

2.2.5 Thermosensory suppression of Pattern-Triggered Immunity

The results above clearly show that plant immunity is sensitive to elevated temperature. One of the earliest steps in the plant-microbe interaction is the recognition of the microbes by the host. As described earlier, conserved motifs released by colonising microorganisms are recognised by pattern recognition receptors on plant cell membranes in order to initiate a signalling cascade resulting in the initial immune responses associated with PTI.

Given the strong sensitivity of plant immunity to elevated temperature, it is logical that PTI could be modulated by temperature in a similar manner. In line with decreases in ETI which I have successfully validated, previous work has found PTI responses to increase with temperature [82], in a process which was hypothesised to be coordinated with bacterial life history changes such as increased production or shedding of PAMPS at elevated temperature. Since it is not possible to validate PTI in isolation through direct pathogen infection, I aimed to validate these results by investigating pre-treatment with flg22 on priming plants to subsequent pathogen challenge at 22 and 27℃. This flg22-induced resistance (FIR) has previously been validated as a robust method through which to quantify PTI responses [199].

It has been shown that under our experimental conditions, elevated temperature compromises PTI in Arabidopsis as assayed by the sensitivity of flg22-induced resistance (Berriri, Gangappa, Gardener et al. (Unpublished)). In brief, five plants each of Col-0 and *fls2* lines were grown for four weeks at 22℃ before being shifted to 27℃ for three days or maintained at 22℃ and sprayed with 100 nM flg22 for 24

hours prior to spray inoculation with *Pto* DC3000. Plants were grown for a further 3 days at their respective temperatures following infection, after which bacterial CFU/cm^2 was measured.

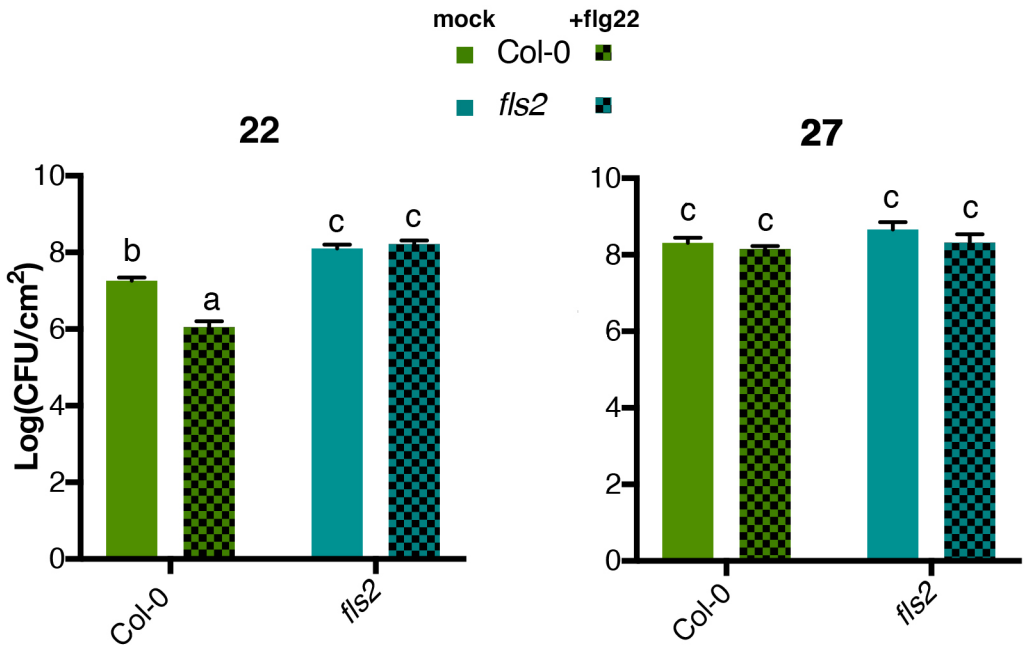

Figure 2-8 flg22-induced resistance to *Pto* DC3000 in Col-0 plants at 22 and 27℃ - 5-week-old plants pretreated with 100 nM flg22 or mock solutions were infected with *Pto* DC3000 and CFU quantified at 3 dpi. Statistical analysis conducted – 2-way ANOVA followed by Tukey's post hoc multiple comparisons test (n=5). This experiment was performed by Sreeram Gangappa.

Data presented here represent the difference between basal immunity to this pathogen (mock) and basal immunity plus the effects of initiating PTI responses (+flg22) and thus a useful measure of PTI activation. *fls2* was included as a mutant lacking flg22 perception and thus an insensitive control. Whilst mock treated Col-0 plants still show some level of PTI activation in comparison with *fls2*, pre-treatment with flg22 further enhanced this effect at 22℃ (Figure 2-8). This is indicative of effective PTI responses at 22℃ in WT, a process which appears to be strongly abolished at 27℃. These results seem to suggest that PTI responses, like their ETI counterparts, are inhibited through growth at elevated temperature, in contrast with previous observations [82]. These data were consequently sufficient to prompt a more comprehensive dissection of thermosensory suppression of PTI.

2.2.6 Differential effects of temperature on PTI outputs

One of the earliest detectable signs of PTI activation is the production of reactive oxygen species (ROS). ROS production was initially characterised as a mechanism of direct inhibition of pathogen growth [200], but more recently its crucial roles in cell-cell communication and plant-wide PTI signalling as well as systemic responses to a wide variety of abiotic stresses have been characterised [201,202]. In the early stages of pattern recognition signalling, influxes of Ca^{2+} activate Calcium-Dependent Protein Kinases (CDPKs) and BOTRYTIS INDUCED KINASE1 (BIK1) is activated by phosphorylation. Both factors can subsequently phosphorylate and activate the NADPH oxidase, RBOHD, thus activating initial PTI signal transduction [203,204].

Production of ROS species occurs in two phases– an initial, transient burst as part of PTI signalling, followed by a prolonged increase thought to coincide with the activation of ETI [205]. Tightly controlled activation of ROS signalling facilitates subsequent responses to pathogens as well as other abiotic stresses or environmental signals [203]. Despite understanding the role of ROS in signaling mechanisms, the effect of elevated temperature specifically on PAMP-induced ROS burst remains unknown. I therefore assessed PTI-associated ROS production in *Arabidopsis* directly following flg22 treatment.

I grew 6 plants per temperature condition for 4 weeks at 22℃ before being shifted to 27℃ or maintained at 22 for a further three days. 3 mm leaf discs were excised from plants and incubated overnight in 96 well plates with 200 µl sterile dH2O at their respective temperatures. Water was removed and leaf discs were then treated with 100 nM flg22, luminol and peroxidase before Relative Light Units (RLU) emitted as a result of ROS production were measured over a 40-minute period.

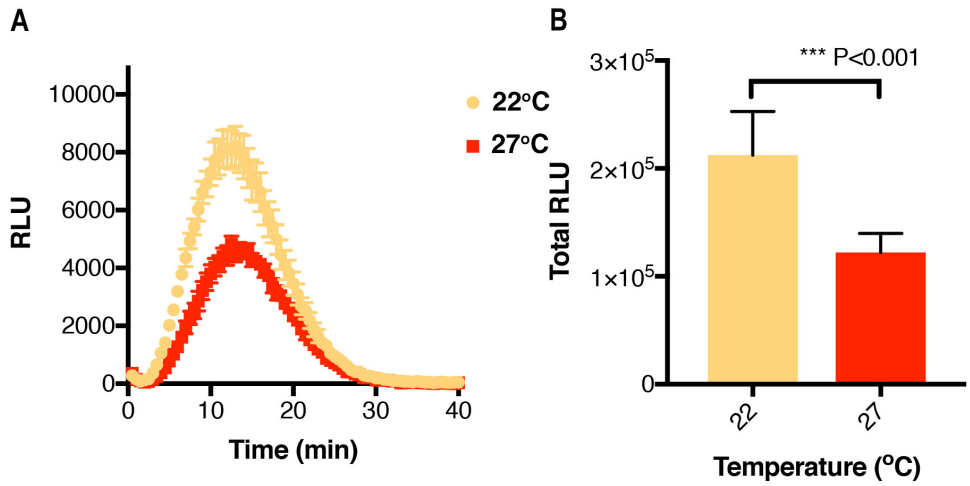

Figure 2-9 Flg22-induced ROS burst in Col-0 plants at 22 or 27℃ - Average RLU for 3 disks/leaves per plant quantified for 40 minutes post-induction with 100 nM flg22, n=6 plants per temperature, (A) or in total, per plant (B). Data from same experiment presented in both panels. (A) shows pattern of ROS production, (B) data from (A) complied into average total ROS produced for each sample of 3 leaf discs per plant. Statistical analysis: unpaired t-test of total ROS. One representative example of 3 biological replicates is displayed here.

A burst of ROS production can be seen to be initiated in WT plants following flg22 treatment at 22℃. This ROS burst is dampened in the plants grown at 27℃ (Figure 2-9 A). When I consolidated data from each time point into total RLU (Figure 2-9 B) plants grown at 27℃ displayed a decrease in total ROS production of almost 50% compared to their 22℃ grown counterparts. This goes to show a direct effect of temperature on this signalling mechanism, which is likely to at least partially underpin a decrease in PTI output at elevated temperatures.

Following increases in ROS production, in early PTI signalling is the activation of Mitogen Activated Protein Kinase (MAPK) cascades. Upon initiation of PTI, sequential phosphorylation of MAPKs in the cytosol acts to transmit signals in at least two different pathways in a process which is necessary to initiate the complete transcriptional reprogramming of defence activation [33,37,206]. The underlying mechanism through which PRRs activate MAPK cascades remains unclear however [207] A summary of known aspects of early PTI signalling can be seen in Figure 2-10.

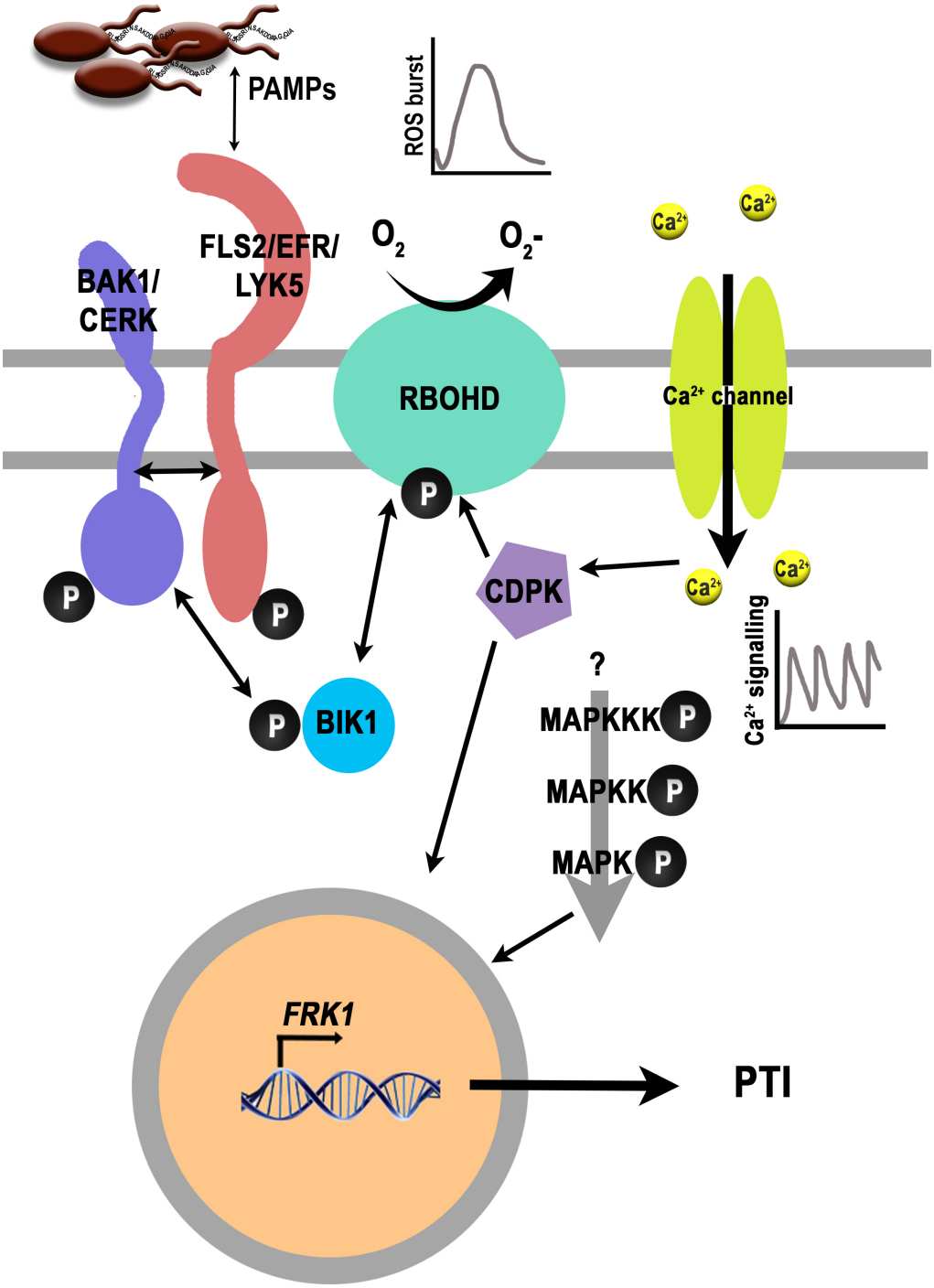

Figure 2-10 Current mechanistic model of PTI signalling – PAMPs (eg. flg22, EF-tu, chitin) are recognised by specific PRRs (FLS2, EFR, LYK5, respectively) on plasma membrane surfaces and interact with coreceptors (BAK1/ CERK) in order to initiate downstream signalling. Phosphorylation of BIK1 and activation of CDPKs through Calcium binding upon PAMP-triggered influx of calcium both act to activate RBOHD and thus ROS burst. MAPK cascades are activated through phosphorylation and act alongside Ca^{2+}/ ROS associated pathways to bring about activation of PTI associated genes and thus activate plant-wide PTI responses.

To assess the effect of increasing ambient temperature on MAPK signalling, I used an anti- Phospho-p44/42 MAPK (Erk1/2)(Thr202/Tyr204) HRP conjugate antibody (anti phosphoThreonine, phosphoTyrosine - αpTpY) to detect levels of phosphorylated MAPK 3, 4 and 6 specifically. These three kinases in particular are known for their importance in modulation of PTI signal transduction and thus functionality of this crucial pathway in plants [208,209].

Following stratification for 3 days at 4°C, I grew seedlings on ½ MS + 1% glucose for 7 days at 22°C SD before shifting them to 27°C or maintaining them at 22°C for a further three days. After a total of 10 days growth, seedlings were induced with 100 nM flg22 in 0.01% Silwet or mock (0.01% Silwet) solutions and tissue harvested 15 minutes post-induction. Total seedling protein was extracted and run on SDS-PAGE gels to separate proteins by molecular weight. HRP Conjugated anti phospho-p44/42 MAPK (Erk1/2; Thr202/Tyr204) rabbit monoclonal antibodies (Cell Signaling) were used to detect the level of MAP kinase phosphorylation.

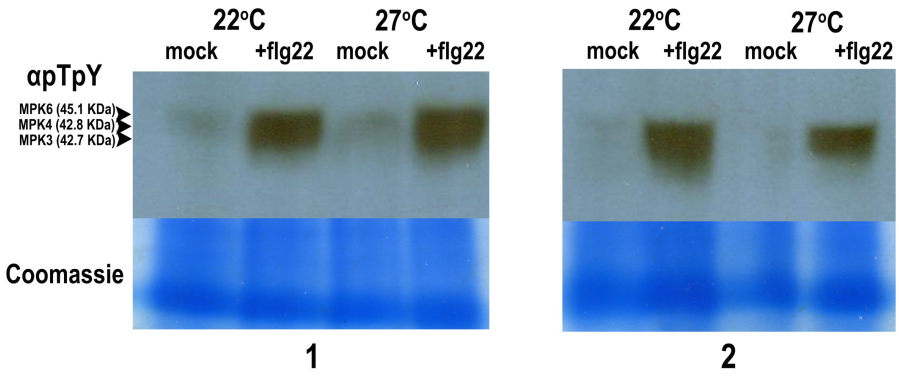

Figure 2-11 MAPK activation in Col-0 seedlings at normal vs elevated ambient temperature - Mock(-) and 100nm flg22 (+) treated seedlings grown at 22 or 27°C and protein extracted. MAPK 3, 4 and 6 activation were quantified using SDS-PAGE followed western blot with αpTpY antibody. Ponceau staining for protein loading quantification was imaged on SDS-PAGE gel (bottom panel) two representative repeats are displayed.

Interestingly, unlike FIR and ROS burst activation, there appears to be little or no difference in MAPK activation at 22 and 27°C (Figure 2-11). Robust MAPK activation upon flg22 treatment is observed in flg22-treated relative to mock treated seedlings at both 22 and 27°C. This seems to suggest that while the physiological outputs of PTI are compromised, early events in pathogen recognition and signalling such as

MAPK cascade shown here remain robust at elevated ambient temperature. This is not entirely unexpected, since MAPK activation and ROS burst appear to function independently in PTI [177]. Altogether I have now confirmed how, in contrast to what has previously been hypothesised, PTI outputs decrease with increases in ambient temperature. This may occur wholly or in part because of dampened ROS signalling, yet independent of MAPK activation. In addition to direct activation of PTI signalling, following pathogen perception plants are thought to trigger upregulation of PAMP machinery in order to maintain and reinforce PTI outputs [178]. I therefore set out to characterise key aspects of PTI machinery to determine whether expression levels increase with PAMP treatment, and whether elevated ambient temperature affects this response.

2.2.7 Temperature modulates reinforcement of PTI machinery

The earliest sign of thermosensitivity of PTI I have observed so far is attenuation of PAMP-induced ROS burst, by RBOHD activation. To assay the potential of a PTI-specific positive feed-forward mechanism on this process I next looked at induction of *RBOHD* and its associated kinase *BIK1* at 22 and 27℃.

I grew Col-0 seedlings on soil at 22℃ SD for one week following stratification before shifting them to 27℃ or maintaining them at 22℃ for 3 days. Following this, seedlings were treated either with 100 nM flg22 in 0.01% Silwet or mock (0.01% Silwet) solutions. I harvested tissue from groups of above-soil parts of seedlings at 3 hours-post-induction (hpi) and extracted RNA from samples to prepare cDNA for qPCR.

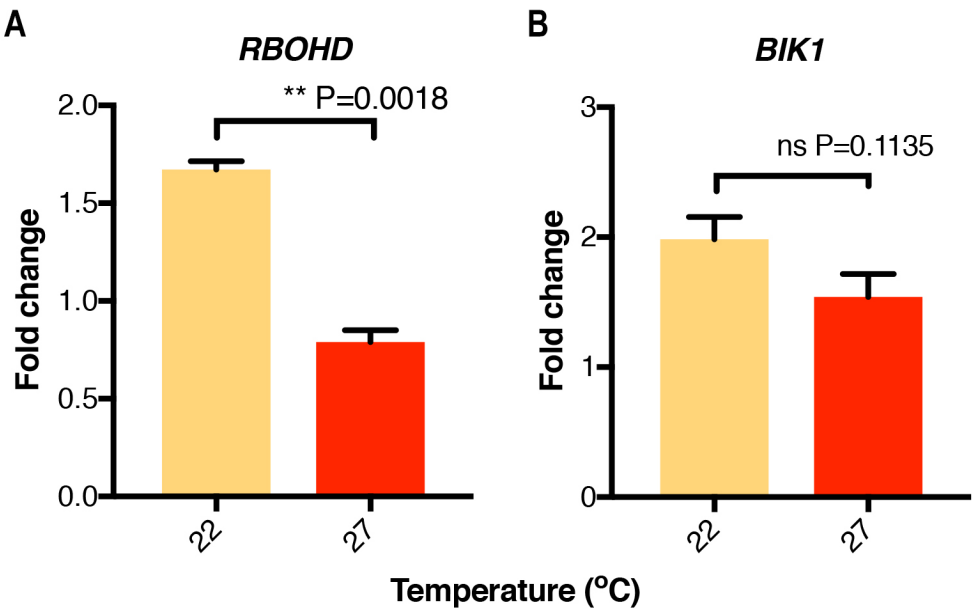

Figure 2-12 *RBOHD* and *BIK1* induction in Col-0 seedlings at 22 and 27℃ - Seedlings grown at constant 22°C or shifted to 27°C for three days and induced with flg22 for 3 hours before tissue being harvested for gene expression. Data are shown as fold change from mock-treated seedlings for each temperature and are normalized to *EF1α* expression. Statistical analysis carried out: unpaired t-tests. n=6-8 biological/ technical replicates.

As previously hypothesised, activation of PTI in these seedlings leads to feed-forward upregulation of *RBOHD* expression. This may act to strengthen or strongly maintain PTI-induced ROS burst upon subsequent or continued pathogen challenge. A noticeable decrease in induction of this gene can be seen in seedlings grown at 27°C (Figure 2-12 A) which suggests this process can act as a measurable readout of thermosensory suppression of PTI. Induction of *RBOHD* could also act as a pre-emptive mechanism for strengthening subsequent ETI responses, where RBOHs are known to play a role [210]. Although it can be clearly seen to be upregulated by PAMP treatment, *BIK1* induction is not affected by an increase in ambient temperature (Figure 2-12 B).

To verify the decrease in fold change in response to temperature induction rather than basal levels of these genes I collected tissue from untreated seedlings subjected to the same temperature conditions to obtain T0 gene expression.

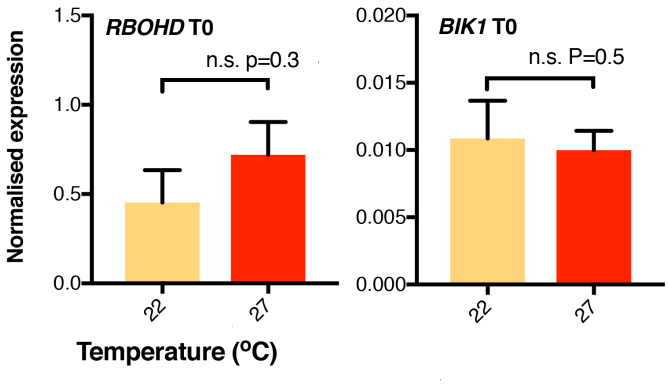

Figure 2-13 Basal levels of *RBOHD* and *BIK1* are not affected by temperature - Seedlings were grown at constant 22°C or shifted to 27°C for three days before tissue being harvested for gene expression. Data are shown as normalized to *EF1α* expression. Statistical analysis carried out: unpaired t-test (*RBOHD*) or Mann-Whitney U test (*BIK1*). n=6-8 biological/ technical replicates.

No difference in basal expression of *RBOHD* or *BIK1* could be detected with increasing temperature (Figure 2-13). This led me to conclude PTI induction of these genes specifically is lost through growth at 27°C.

Further upstream to RBOHD/BIK1, the leucine rich repeat receptor like kinase, FLS2, is responsible for recognition of the N-terminus of flg22 [37,211]. Along with its coreceptor BAK1, recognition of flg22 is facilitated leading to calcium-dependent membrane depolarisation and RBOHD activation.

To further investigate potential thermosensory feed-forward PTI effects on these components, I investigated gene expression changes at 22 and 27°C. Using cDNA isolated from seedlings in Figure 2-12 I used qRT-PCR to amplify and quantify expression of *FLS2* and *BAK1* and data prepared as previously.

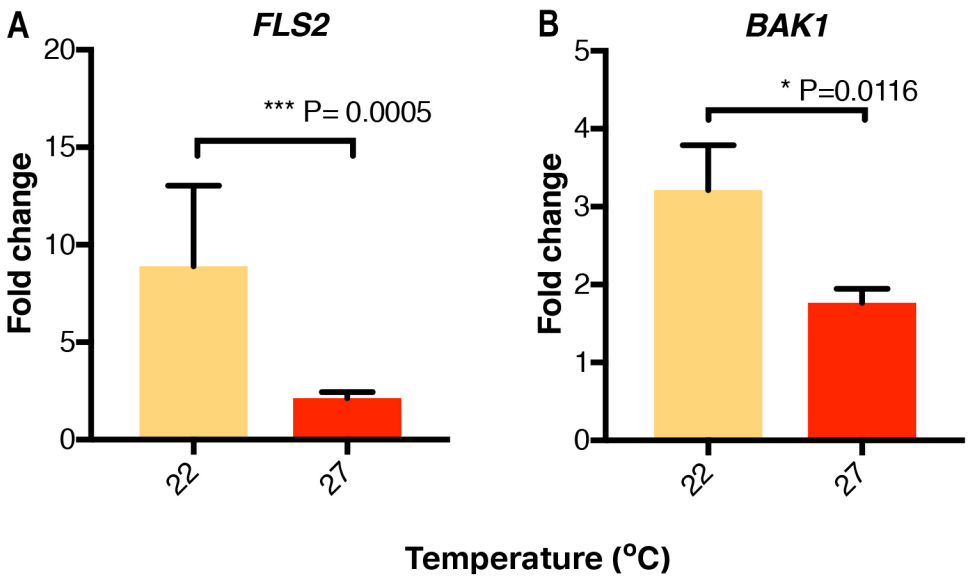

Figure 2-14 PAMP-triggered induction of *FLS2* and *BAK1* at 22 and 27℃ - Fold change of FLS2 compared to mock treated seedlings at both temperatures, all data first normalized to *EF1α*. Mann-Whitney test used to analyze difference in median value of n=6-8 biological/ technical replicates.

In line with what I observed for *RBOHD*, *FLS2* expression is strongly induced upon PTI activation. This induction is highly attenuated by growth at 27℃ (Figure 2-14 A). In addition, I found that the coreceptor *BAK1* is induced in response to flg22 treatment, in a temperature-dependent manner (Figure 2-14 B). The strong upregulation of this machinery shows the potential for reinforcement of PTI responses and thus sensitivity to further pathogen challenge at 22℃ in plants. This response is abolished when ambient temperature is increased.

To verify this response as a result of attenuation of PTI induction of these genes as before, I investigated levels of basal expression of these genes in mock-treated seedlings separately.

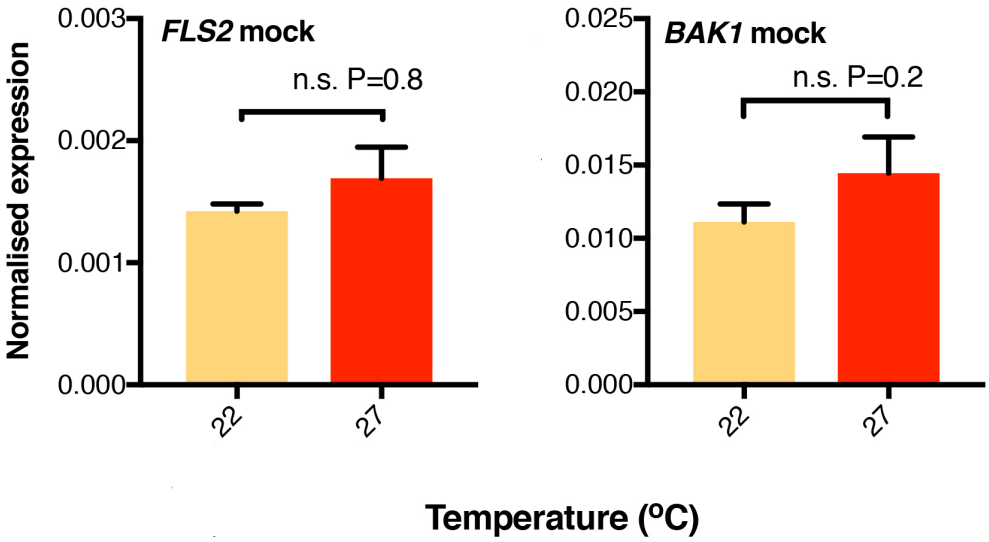

Figure 2-15 Basal levels of *FLS2* and *BAK1* are not affected by temperature - Seedlings were grown at constant 22°C or shifted to 27°C for three days before being treated with mock (0.01% Silwet) solution for 3 hours and being harvested for gene expression. Data are shown as normalized to *EF1α* expression. Statistical analysis carried out: unpaired t-test (*BAK1*) or Mann-Whitney U test (*FLS2*). n=6-8 biological/ technical replicates.

As for *BIK1* and *RBOHD*, whose uninduced levels of expression do not change with changes in temperature, levels of *FLS2* and *BAK1* do not change with increasing temperature to 27°C (Figure 2-15). This observation verifies the temperature responses detected in Figure 2-14 as specific to PTI induction rather than basal expression changes.

The fortification of machinery in this manner is likely part of a global transcriptomic response to PAMP perception. I therefore next aimed to understand further global changes in gene expression in response to flg22 at 22 vs 27°C.

2.2.8 Elevated ambient temperature suppresses PAMP-triggered gene expression

In light of the finding that PAMP-triggered immunity signalling as well its fortification is compromised at elevated temperature, I sought to study this response in detail. In order to further dissect this process, I began characterisation of thermosensory PTI outputs through measurement of the expression pattern of key PTI-associated genes, starting with *FLG22-INDUCED RECEPTOR LIKE KINASE1 (FRK1).*

FRK1 was identified as a marker for PTI from a library of flg22-responsive genes rapidly and robustly activated at early time points following elicitor treatment [212,213]. It is most strongly expressed 2-4 hours post induction, however upregulation is already detectable 30 minutes post-induction [212].

To investigate how *FRK1* expression levels alter with changing temperatures I grew WT seedlings on soil for 7 days at 22°C before shifting to 27°C for 3 days or maintaining at the lower temperature. I then sprayed plants with 100 nM flg22 in 0.01% Silwet or a mock (0.01% Silwet) solution for three hours and collected above-ground tissue for RNA extraction and cDNA synthesis. In addition, I collected untreated (T0) samples as before to assess basal levels of this gene. I then measured *FRK1* expression levels using qPCR to assess basal level and inducibility of this gene at both temperatures. FRK1 expression was normalized to the expression of housekeeping gene EF1α [214] for each biological replicate. FRK1 inducibility was calculated by comparing the normalized expression of flg22-induced samples with that of the mock treated seedlings for each temperature respectively, to yield fold change in expression upon 3 hours flg22 treatment. Four technical repeats were compared for two or three biological replicates for each treatment condition.

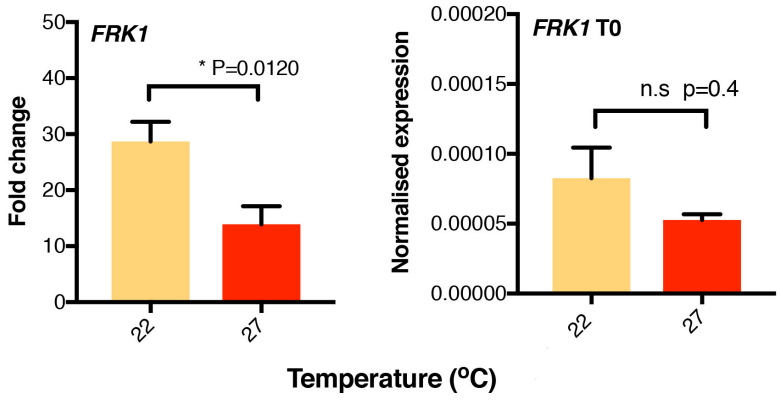

Figure 2-16 Flg22-triggered induction and basal *FRK1* at 22 and 27°C - Expression of *FRK1* in flg22-trested seedling as a factor of basal (mock) expression levels, first normalized to the housekeeping gene, EF1α. *FRK1* basal (untreated) levels (T0) normalised to EF1α. Mann-Whitney test for difference between medians. n=6-8 biological/ technical replicates.

Whilst a strong induction of this gene can be observed at 22°C, these data clearly show a decrease in expression at 27°C in these WT plants (Figure 2-16). In agreement with the data gathered for flg22-induced resistance shown above, elevated

temperature appears to suppress PAMP-triggered induction of gene expression. No difference in basal (T0) levels of this gene could be observed (Figure 2-16) This result shows that the increased susceptibility to Pto DC3000 at elevated temperature is at least in part due to the failure to mount early defence responses upon recognition of microbial signals. This is in contrast to an earlier study, where Cheng *et al.* (2013) [82] showed how a total of 20-60 minutes of temperature acclimation resulted in elevated levels of PTI with increasing temperature, and the optimal temperature for *FRK1* expression to be 28°C [82], a temperature at which I have now observed strong attenuation of this gene. It is likely that this amount of acclimation time used in this earlier study is not sufficient to represent a stable temperature increase since for a 3-day acclimation period and the observed output could represent heat shock rather than ambient temperature responses. Heat shock has previously been shown to induce transient, moderate increases in SA [215] which could explain the discrepancies observed.

To further substantiate the observed *FRK1* expression pattern following PAMP recognition at elevated temperature, I next used an *FRK1* promoter-luciferase fusion line [216] to monitor *FRK1-LUCIFERASE* (*FRK1-LUC*) expression at a wider range of temperatures. I grew FRK1-luc seedlings on soil for 7 days at 17°C shifting them up 5, 7.5 or 10°C for 3 days and inducing with 1 μM flg22 for 3 h. This increased concentration of flg22 was necessary to visually quantify expression of *FRK1-LUC* here. Luminescence was visualized using Photek imaging following addition of luciferin substrate.

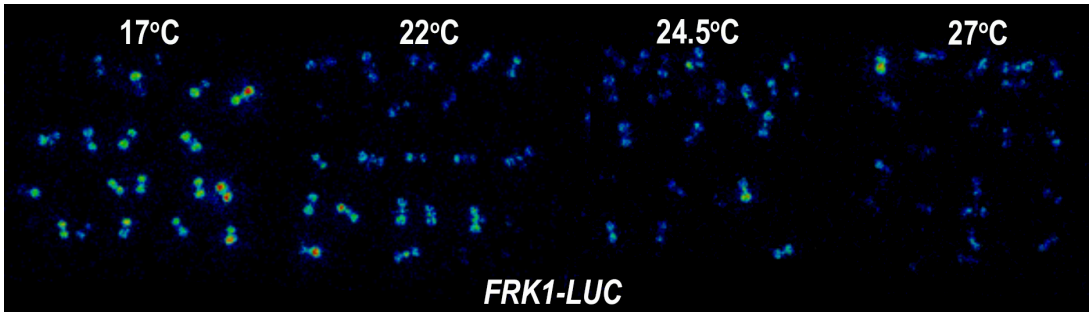

Figure 2-17 flg22-induced *FRK1-LUC* expression in seedlings – 10-day old plants were imaged following 3 days of alternative temperature treatment and induced with 1 μM flg22 for 3 hours. Luminescence was imaged following luciferin addition using a Photek HRPCS-3 PSU photon counting apparatus.

In agreement with the gene expression data already collected, these plants show strong flg22-induced *FRK1* expression at 17°C, which appears to decrease incrementally with increasing temperature.

To quantify this response, I measured individual seedling luminescence in Relative Light Units (RLU) for 41-49 seedlings per temperature following temperature shift and induction as per Figure 2-17.

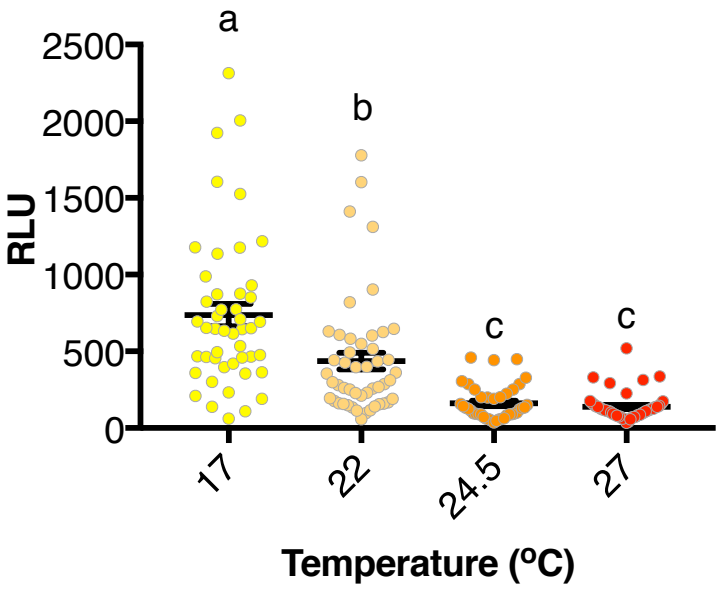

Figure 2-18 *FRK1-LUC* expression as measured in Relative Light Units per seedling at 17 – 27°C - RLU per seedling for 7-day-old seedlings grown at 17°C followed by 17, 22, 24.5 or 27°C for 3 days before being induced for 3 hours with 1 μM flg22. Bars represent mean + SEM. D'Agostino & Pearson normality test failed by all temperatures, so nonparametric Kruskal-Wallis test for multiple comparisons was used followed by Dunn's multiple comparison test.

Robust induction of *FRK1-LUC* can be observed at 17 or 22°C, which is strongly attenuated at elevated temperatures, further highlighting the response I have previously observed for endogenous levels of this gene (Figure 2-18). There was no noticeable difference in the level of induction between the two highest temperatures measured, suggesting that a moderate growth temperature of 24.5°C was sufficient to completely suppress flg22 induction of *FRK1*. This is in line with what I have observed for resistance to *Pto* DC3000 previously and suggests that temperature simultaneously affects both PTI and ETI. Whether this is coordinated by a central process or is as a result of differential, simultaneous changes in the machinery

associated with detection and transmission of responses initiated by PAMPs/ effectors, is yet to be determined. To determine whether, in line with *FRK1* expression, global PTI-associated gene expression changes are regulated by temperature, I investigated overall changes in gene expression in response to PAMP induction between 22 and 27°C.

2.2.9 Global PTI-associated transcription is suppressed at high temperature

To characterise thermosensory effects on global PTI changes, RNA-seq was carried out (Berriri, Gangappa, Gardener et al., (unpublished)) on seedlings induced with 100 nM flg22 for 3 hours following growth at 22°C for 7 days followed by 27°C as before. I analysed RNA-seq data to investigate global transcriptional regulation patterns for PTI at 22 and 27°C. I selected genes either ≥2-fold up or downregulated in flg22-treated seedlings relative to mock at 22°C, and subsequently compared the same subset of genes from 27°C grown seedlings.

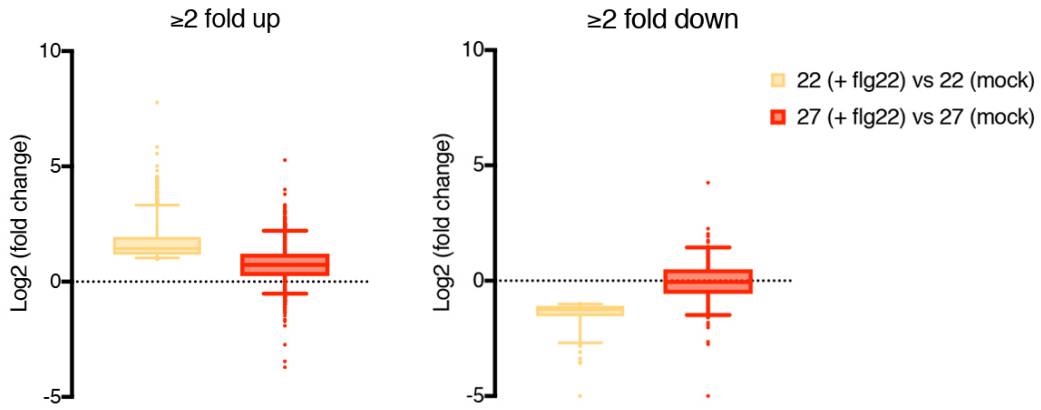

Figure 2-19 Global transcriptional PTI response at 22 and 27°C - Seedlings were grown at 22°C for 7 days followed by 3 days at either 22 or 27°C before being induced with 100nm flg22 or mock treated with 0.01% Silwet and tissue collected. Data was analysed to identify genes ≥2 fold up or downregulated at 22°C in flg22-treated seedlings. The same genes are displayed for plants grown in parallel at 27°C and show both up and down-regulated genes are attenuated compared to 22°C. RNA-seq data obtained from samples collected by Souha Berriri

Many of the genes which are ≥2-fold upregulated in 22°C grown plants are attenuated by growth at 27°C (Figure 2-19). Similarly, for genes ≥2 fold downregulated at 22°C, most do not show any induction at 27°C (Figure 2-19).

Overall this goes to show how elevated temperature attenuates both transcriptional activation and repression in response to microbial signatures.

Global transcriptional reprogramming in response to PAMP recognition on this scale is likely to be due to the effects of temperature on major transcriptional regulatory components. Chromatin remodelling has been shown to be a key regulator of global gene regulation [217]. ATP-dependent chromatin remodelling has been shown to be key for large-scale regulation of gene expression in eukaryotes, through modulation of chromatin accessibility to transcriptional machinery at different loci [218]. Global transcriptional responses to elevated temperature have been shown to be controlled by the variant histone H2A.Z-containing nucleosome dynamics [157]. H2A.Z is incorporated in to nucleosomes by the SWR1 ATP-dependent chromatin remodelling complex (SWR1c) [158]. H2A.Z underlies responses to developmental and environmental cues [219] and plants lacking the ability to incorporate this histone phenocopy plants grown at elevated ambient temperature [157,163]. In parallel, H2A.Z incorporation plays an important role in defence responses. Gene expression profiling of plants lacking *HTA9/ HTA11*, two of the three functional H2A.Z genes, uncovered SA-dependent immune function as underlying a major portion of mis-regulated genes [158,161].

H2A.Z, therefore, acts as a central reprogramming hub in response to environmental changes. H2A.Z dynamics underpin the coordination of transcriptomic changes of both growth and defence at elevated temperature. I have shown how, in a similar manner to SA-mediated immunity, PTI responsive genes are suppressed by elevated temperature. I therefore set out to determine whether H2A.Z deposition underpins this response. Substitution of H2A for H2A.Z in nucleosomes depends on the ATP-dependent, multi-subunit SWR1c chromatin remodelling complex [161]. Several components of SWR1c have been shown to play collaborative as well as independent roles in TSI [158,220]. Mutations in two subunits, PHOTOPERIOD-DEPENDENT EARLY FLOWERING1 (PIE1), and SERRATED LEAVES AND EARLY FLOWERING/ SWR1 COMPLEX 6 (SEF/ SWC6), have highlighted roles in deposition of H2A.Z, and global gene regulation. Mutants in these subunits show a reduction in defences in line with those of the *hta9, hta11* double mutant [158] and were therefore selected for further

study of the role of H2A.Z in moderating PTI responses and thermosensory suppression.

2.2.10 H2A.Z-deficient mutants are compromised in PTI

To determine if outputs of PTI are attenuated in SWR1/ H2A.Z-deficient mutants, flg22-induced resistance of these plants was investigated (Gangappa, Gardener et al. (unpublished)). Five plants per genotype were grown for 5 weeks at 22°C before being treated with 100 nM flg22 in 0.01% Silwet or mock (0.01% Silwet) solutions for 24h. Following this, plants were spray inoculated with *Pto* DC3000 and bacterial CFU measured at 3 dpi. Alongside *pie1*, *swc6* and *hta9, hta11*, flg22-sensing deficient *fls2* mutants were included as an insensitive control [211].

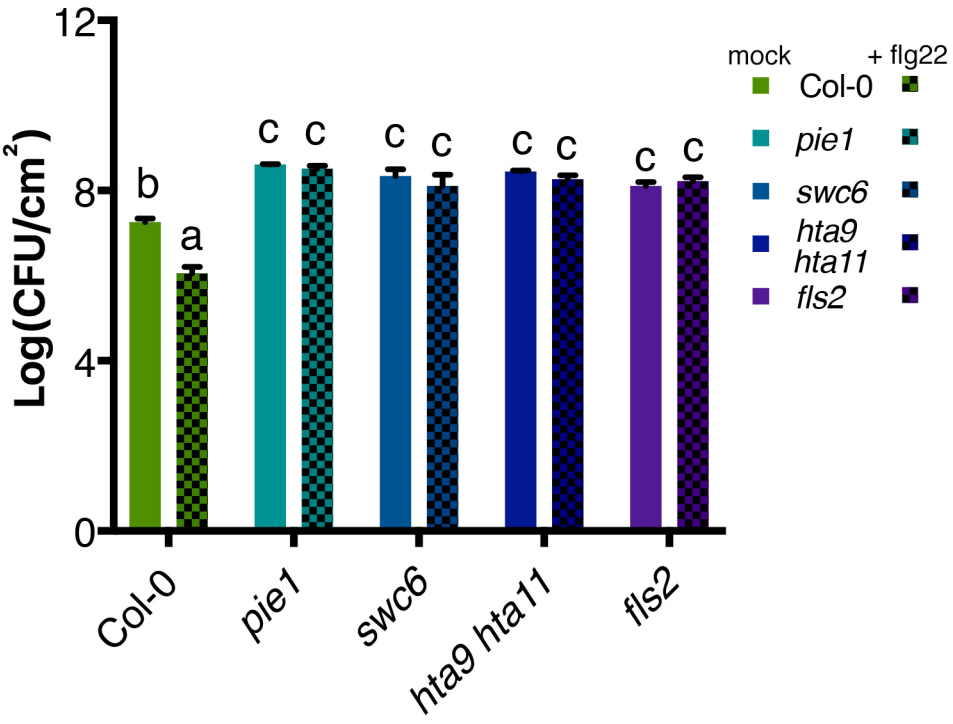

Figure 2-20 Flg22-induced resistance to *Pto* DC3000 in SWR1/ H2A.Z-deficient mutants – 5-week-old Col-0, *pie1, swc6*, *hta9 hta11* and *fls2* plants were treated with 100 nM flg22 and infected with *Pto* DC3000 (experiment conducted by Gangappa). Plain colours represent mock-treated plants, full colours represent flg22-pretreated plants. Statistical analysis conducted – 2-way-anova followed by Tukey's post hoc multiple comparisons test, n=5.

These mutants show higher levels of susceptibility to this pathogen even at 22°C. In comparison with WT plants, which show enhanced resistance to *Pto* DC3000 after priming with flg22, all three mutants showed no effect of flg22-pretreatment on resistance (Figure 2-20). Levels of susceptibility in these mutants were comparable with those of *fls2* which is not capable of flg22-triggered PTI. This data suggests that,

similarly to plants grown at elevated temperatures and levels of SA-mediated immunity in H2A.Z-deficient plants, these mutants lack effective PTI responses. Since H2A.Z/ SWR1-deficient mutants phenocopy high temperature-grown plants, the lack of basal resistance to *Pto* DC3000 here is expected and in line with the hypothesis of a role for H2A.Z dynamics in thermosensory suppression of PTI.

2.2.11 PTI responses are underpinned by SWR1-mediated deposition of H2A.Z

The lack of immune priming shown above demonstrates that mutants with defective incorporation of H2A.Z into their chromatin are compromised in PTI responses. Lack of response here therefore demonstrates how H2A.Z plays a key role in mediating thermosensory suppression of PTI. To further dissect PTI in these mutants, I determined the effect of H2A.Z deficiency on *FRK1* induction as well as basal expression levels of PTI machinery previously characterised in high-ambient temperature-grown plants. To investigate the role of H2A.Z dynamics and the SWR1c complex in PTI-induced gene expression changes, I grew Col-0, *pie1*, *swc6, hta9 hta11* double mutant and *fls2* plants for 10 days on soil at 22℃ SD. Seedlings were then induced with 100 nM flg22 in 0.01% Silwet or mock solutions for 3 hours, above-soil tissue harvested and cDNA made. To compare *FRK1* in these mutants to WT plants at 22℃, I quantified levels of this gene through qPCR.

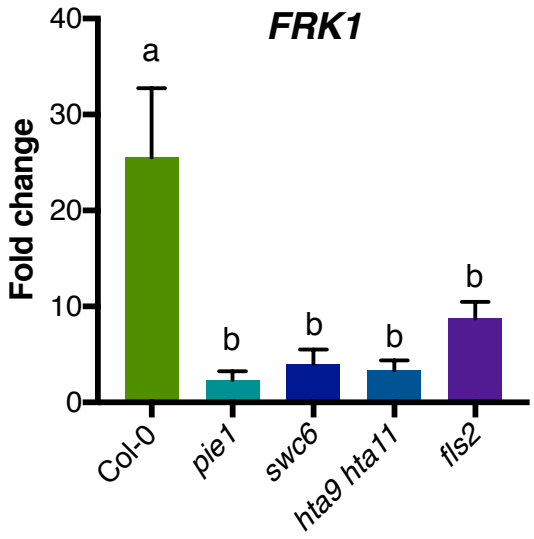

Figure 2-21 *FRK1* expression in H2A.Z deposition deficient mutants and the flagellin-insensitive mutant, *fls2* - Seedlings harvested following growth at 22℃ SD for 10 days and 3 hours induction with 100 nM flg22. *fls2* seedlings were included as a control. Statistical analysis conducted: One-way ANOVA followed by Tukey's multiple comparison test. n=9 (3 biological + 3 technical replicates).

In accordance with the earlier results, *FRK1* was strongly induced by PAMP treatment in WT plants. This response was strongly abolished in each of the mutants tested. In fact, the level of *FRK1* induction in SWR1 mutants was comparable to the *fls2* mutant. This seems to support the response observed for FIR in these mutants and suggests constitutive lack of PTI activation capability in H2A.Z-deficient mutants and thus H2A.Z dynamics as underpinning effective PTI responses in plants.

To determine whether this strong abolition of gene expression was underpinned by a downregulation in flg22-sensing machinery and thus lack of sensitivity to PAMPs, in a manner similar to the *fls2* mutant. I measured basal levels of *FLS2/ BAK1* expression in these mutants. Seedlings were grown as before at 22℃ SD for 10 days. Tissue was harvested without treatment to obtain basal gene expression level through qPCR.

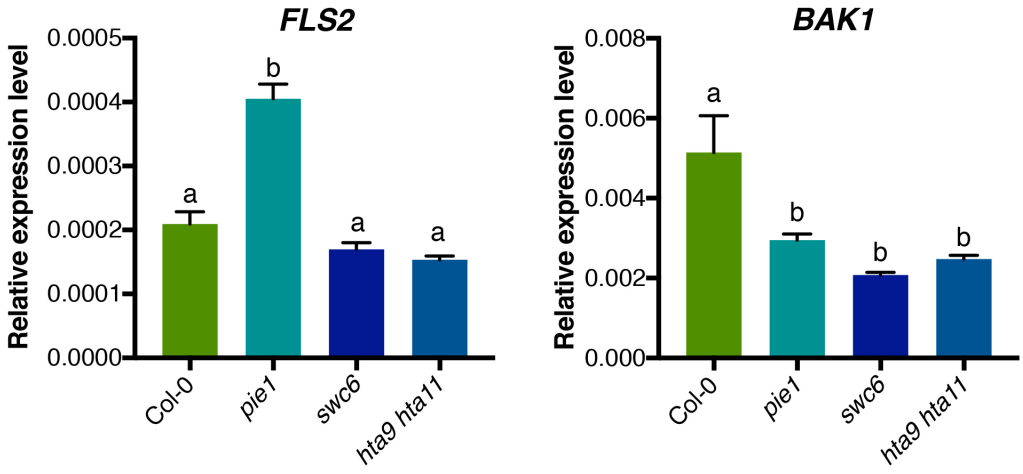

Figure 2-22 *FLS2* and *BAK1* expression in H2A.Z-deficient mutants - Expression assayed through qRT-PCR in T0 (untreated) 10-day old seedlings. Absolute values normalized to EF1α. Statistical analysis conducted - One-way ANOVA followed by Tukey's multiple comparisons test. n=9 (3 biological + 3 technical replicates).

No reduction in basal FLS2 expression was observed in either *hta9 hta11* or *swc6* mutants compared to WT. *pie1* mutants however showed a much higher level of expression (Figure 2-22). As previously observed, downstream outputs of PTI in *pie1* are analogous to those of *swc6* and *hta9 hta11,* yet other studies have shown PIE1 as playing a distinct role in SA-mediated immunity compared to other SWR1 mutants

[158]. Unlike *FLS2*, *BAK1* expression is noticeably decreased in all of the mutants tested. Lack of adequate expression of *BAK1* may at least in part underpin the dampened PTI responses in these mutants through its effects on FLS2-mediated signal transduction. The difference in *pie1* mutants may be reflective of the pleiotropic roles of PIE1 in gene regulation, which requires further studies.

Using mutants lacking key components of the ATP-dependent chromatin remodelling complex SWR1 and thus adequate H2A.Z deposition, I have shown a crucial role H2A.Z plays in modulating PTI responses in plants. Further to this, I have shown how SWR1 components play distinct as well as collaborative roles in this process in addition to ETI processes as previously shown [158].

2.3 Conclusions

2.3.1 Moderate changes in temperature negatively affect both PTI and SA-mediated immunity in plants

In this chapter I have shown how plant defence responses are highly sensitive to small changes in ambient temperature. Where previously, 5°C temperature upshifts have been known to co-ordinately affect plant immunity as well as growth, a narrower window of temperature change can now be seen to simultaneously decrease SA-mediated defences and resistance to pathogens, as well as attenuating expression of the PTI-associated marker gene, *FRK1*. Just 2.5°C increase can therefore be said to be sufficient to initiate plant thermosensory responses and likely reflects a more sensitive "thermostat" in plants than previously hypothesised. This sensitivity, as previously demonstrated for other environmental responses in rice [182] highlights the potentially damaging effects of the moderate increases expected as a result of climate change [28]. For future experiments I have also confirmed a 5°C upshift as an effective procedure to dissect the molecular mechanisms underpinning plant thermosensory responses regardless of vegetative developmental stage. Whilst a robust response can be observed between these temperatures, it will be important to consider more comprehensive temperature ranges for future studies on TSI, especially with regard to the growth-defence trade-off. Here I have also gathered novel information regarding the specific changes brought about by temperature on PTI and showed how temperature increases specifically negatively affect this process.

2.3.2 H2A.Z mediates temperature-induced modulation of PTI

H2A.Z deposition has previously been shown crucial for numerous environmental responses [157,158,161,163]. This histone variant is known to regulate gene expression through its effects on chromatin accessibility at different temperatures [157,219] and bring about coordinated changes in development, growth [157,221] and immunity [158,161]. Previously however, its role in coordination of PTI responses was not known.

At low temperatures, H2A.Z nucleosomes typically show higher occupancy, thus preventing activation of the elevated temperature transcriptome [158]. Plants lacking H2A.Z deposition machinery therefore phenocopy warm-grown plants. In further confirmation of what I have observed for plants grown at high ambient temperature, mutants lacking efficient deposition of H2A.Z lack adequate PTI activation (Figure 2-23). As previously [158], I have demonstrated how different components of the SWR1 chromatin remodeling complex may differentially affect gene expression outputs.

Particularly in the context of the novel effect of elevated ambient temperature on PTI, the data I have collected in this study has begun to establish the role of SWR1 and H2A.Z deposition in coordinating transcriptomic responses to PAMP perception in the plant, both through PTI detection machinery and *FRK1* expression.

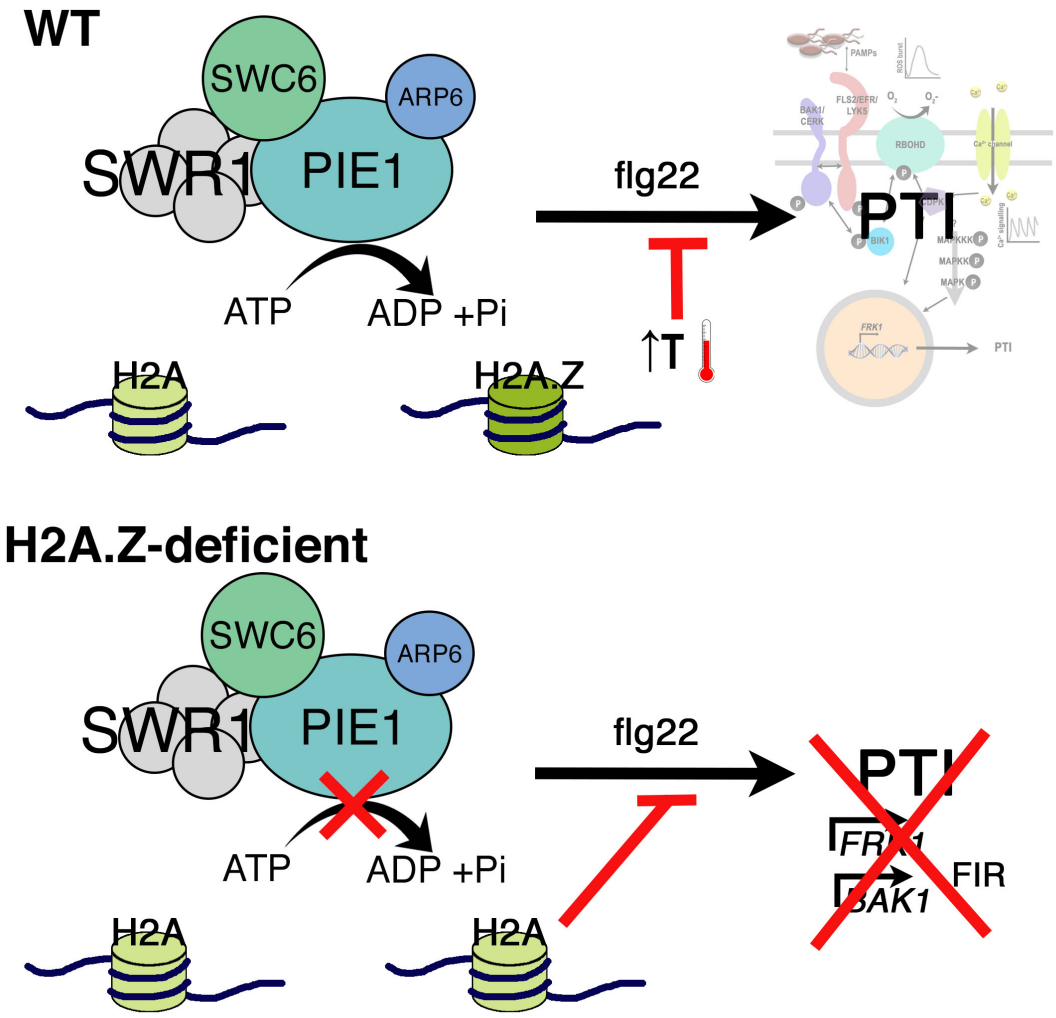

Figure 2-23 PTI activation in plants is dependent on H2A.Z deposition – At low ambient temperature (22°C), deposition of H2A.Z allows normal activation of PTI upon elicitor challenge. Increasing temperature or artificially preventing incorporation of this alternative histone prevents PTI activation, reinforcement of PAMP-sensing machinery and reactionary gene expression.

Altogether, PTI has now begun to be established as an output of plant thermosensory responses, despite its relatively weak, transient governance of plant immunity compared with ETI [222]. Both PTI and ETI are known to result in downstream accumulation of SA and its associated robust defence responses. It remains to be determined whether these pathways are simultaneously regulated by a central thermosensory mechanism or whether temperature affects each aspect of plant immunity simultaneously, yet individually. To understand TSI as a whole therefore, it is necessary to study both individual and common outputs of this process. An overall understanding of TSI and the mechanisms regulating it will provide novel ways to understand and dissect plant thermosensory mechanisms.

3 *resilient1* – A Window into Plant Thermosensing

3.1 Introduction

3.1.1 Plant thermosensors

A suite of thermosensory modules and networks are thought to be necessary for coordination of diverse changes in plant physiology brought about by ambient temperature increases. In order to modulate growth and developmental transitions, plants must integrate noisy temperature signals and bring about appropriate responses on a daily basis. This requires mechanisms to sense both absolute and relative temperature over time to ensure maintenance of fitness and reproduction. Such integration was recently shown to initiate *FLC*-dependent transition to flowering, where plants were able to react to temperature patterns over time to judge seasonal progress [223,121]. Understanding the mechanisms by which plants sense and respond to these seasonal and diurnal temperature changes holds particular importance in the context of food security since minor perturbations could severely affect plant temperature responses and thus crop yields in the face of climate change.

Over recent years, several molecular components of thermosensory signalling and response have been identified [97], in addition to identification of central hubs of environmental signal integration. Both SWR1-mediated chromatin remodelling [157] and the interaction and function of PhytochromeB (PhyB) with the bHLH transcription factor, PIF4 have been shown as hubs coordinating thermosensory responses such as elongation growth, flowering time and TSI [128,136,224], with PhyB having been shown as directly affected by temperature [131,132]. However, the precise mechanisms through which cellular components sense temperature signals and integrate them into physiological outputs remain elusive.

As I have now demonstrated, suppression of immunity under moderately increased ambient temperature conditions (TSI) is a measurable output of plant thermosensory responses. Most importantly, with the progress made towards understanding this phenomenon in Chapter 2, I have now cemented this process as a potential standpoint from which to study plant thermosensory mechanisms. Improved knowledge of how plants bring about TSI following ambient temperature upshifts

would enable further progress to be made towards an understanding of plant thermosensing as well as the contribution of specific molecules to plant environmental perception and responses.

3.1.2 A novel mutant screen

In my previous chapter, I showed how increases in ambient temperature negatively affect plant immune processes. Furthermore, the immediate responses of plants upon recognition of pathogens such as PAMP-induced ROS burst and activation of pattern triggered immunity (PTI)-associated gene expression are lost at increased temperatures. Thermosensory suppression of PTI can thus be taken as a robust output of thermosensory responses.

Whilst there is a clear effect on PTI, ambient temperature changes are known to equally affect SA-mediated immunity. Multiple defence signalling pathways including PTI culminate in SA expression and its associated downstream responses[33]. Currently, it is not known whether temperature influences these pathways through a single, universal mechanism or whether individual nodes of immunity are directly affected or modulated by temperature changes. Since SA and its associated responses represent a unified output of a wider molecular signalling network of immunity, it can thus can act as a measurable output of the combined effects of temperature on immunity. SA accumulation within plant cells leads to activation of *Pathogenesis Related* (*PR*) genes, which are required for systemic acquired resistance (SAR) [225]. Plants lacking SA-mediated defences show reduced expression of *PR* genes and are not able to establish resistance to biotrophic pathogens [167]. Of these genes, *PR1* is known to be strongly upregulated following exposure to pathogens and induced following SA accumulation [226]. Expression of this gene and its association with long-standing resistance to a broad spectrum of pathogens has been well established [78]. Previous genetic screens have successfully used this gene as the basis for a luciferase reporter-based selection to identify *constitutive induced resistance* (*cir)* and *constitutive expression of PR1 (cpr)* mutants with altered SA-mediated immunity under normal ambient temperature conditions[167,168,227].

The use of these transgenic *PR1-LUCIFERASE* expressing plants (*PR1-LUC*) here paved the way towards understanding of SA-mediated plant immunity through identification of key players such as NPR1, JAR1 and EIN2 [83,167,227]. In addition, *PR1*-based studies provided the basis for the identification of key components of TSI components such as SNC1 and SIZ1, mutants of which show constitutive expression of this gene along with SA-mediated immunity at normal ambient temperatures [139,145,166]. *PR1*, just as SA is strongly attenuated through growth at high ambient temperatures [82,139], and even in previously identified mutants such as those described above as constitutively expressing this gene, expression is strongly attenuated by growth at high ambient temperatures[139,143].

It is therefore possible to use this gene both as a measurable molecular output of immune activation throughout the plant, but also as a robust marker for thermosensory suppression of SA-mediated immunity. For my purposes here, the use of the previously described *PR1-LUC* reporter line presents as an important resource with which to study TSI, through its capability to provide rapid visualisation of SA mediated immunity as an output of combined immune activation [167].

In this chapter, using reporter-based selection for perturbed *PR1* output of a mutagenised population I was able to harness TSI as a fundamental output of plant thermosensory responses and build upon work carried out by Prawpun Kasemthongsri (2012) in her master's thesis [228] in order to identify and characterise an important coordinator of ambient temperature responses in plants.

3.2 Results

3.2.1 *PR1* - a robust marker for TSI

Numerous previous studies have demonstrated the thermosensory suppression of *PR1* [82,139] in addition to confirming the ability of *PR1-LUC* to mirror endogenous levels of this gene [227]. To assess the effects of increasing ambient temperature on expression of this gene under my experimental conditions, I first aimed to characterise expression levels in Col-0 seedlings through qPCR analysis. Following induction with flg22, I aimed to characterise endogenous *PR1* expression both at 22°C where this gene is typically strongly induced [167] and 27°C, where SA triggered immune suppression is reflected in low levels of this gene [1,82,147].

To begin with I stratified WT (Col-0) seedlings on soil and grew at 22°C SD conditions for 7 days before shifting half of the seedlings to 27°C SD for three days and maintaining the other half at 22°C. Following this, seedlings were treated with 100 nM flg22 in 0.01% Silwet until leaf runoff (~5 ml per 770 cm^2 tray) for 18 hours and tissue collected for RNA extraction, cDNA synthesis and qPCR. Measurement of *PR1* expression was taken for three biological and three technical replicates and normalised to levels of the housekeeping gene, EF1α.

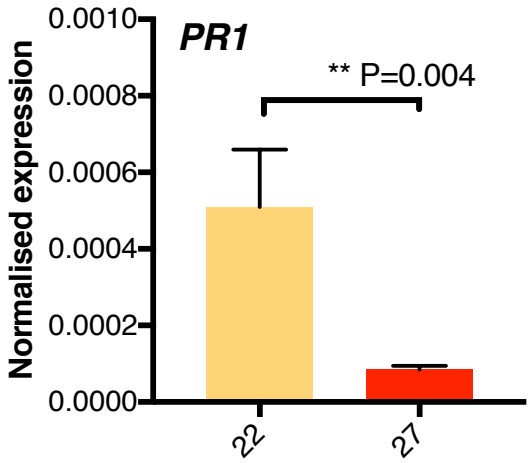

Figure 3-1 Endogenous *PR1* expression of WT plants at both normal (22°C) and elevated (27°C) ambient temperatures - Eleven-day old seedlings under moderate or elevated ambient temperature regimes were assessed for *PR1* expression in comparison to levels of the housekeeping gene, EF1α. Where *PR1* expression is high in WT plants induced with flg22 at 22°C, expression is strongly attenuated at 27°C. Statistical analysis carried out – Mann-Whitney U test.

Here, it is clear to see how expression of *PR1* in flg22-treated seedlings is strong at 22℃ (Figure 3-1). Expression of this gene is strongly attenuated in seedlings grown at 27℃ (Figure 3-1). These data support previous characterisation of expression patterns of *PR1* and its attenuation at high ambient temperatures [82,139]. Furthermore, since *PR1* expression is known as a marker for SA immune activity [229], this study validates the use of this marker gene as a marker for thermosensory suppression of immunity in seedlings grown under my experimental conditions.

As a robust marker for SA and SAR, expression of *PR1* in the transgenic luciferase-based reporter construct line, *PR1-LUC* has been shown to recapitulate that of endogenous gene expression [167,227], but so far the ability of this reporter to mimic endogenous levels under different temperature regimes has not been characterised. To determine whether expression of *PR1-LUC* mimics endogenous expression of this gene following pathogen challenge at high temperature, I grew *PR1-LUCIFERASE* expressing (henceforth *PR1-LUC*) seedlings as before at 22℃ for 7 days, followed by a temperature shift to 27℃ or maintenance at 22℃ for a further three days. I then induced seedlings with 100 nm flg22 in 0.01% Silwet and quantified *PR1-LUC* expression at 18 hours post-induction (hpi). To quantify expression of this gene, as previously I treated seedlings with 1 mM luciferin in 0.01 % Triton X-100 and visualised luminescence with the Photek HRPCS-3 photon counting camera.

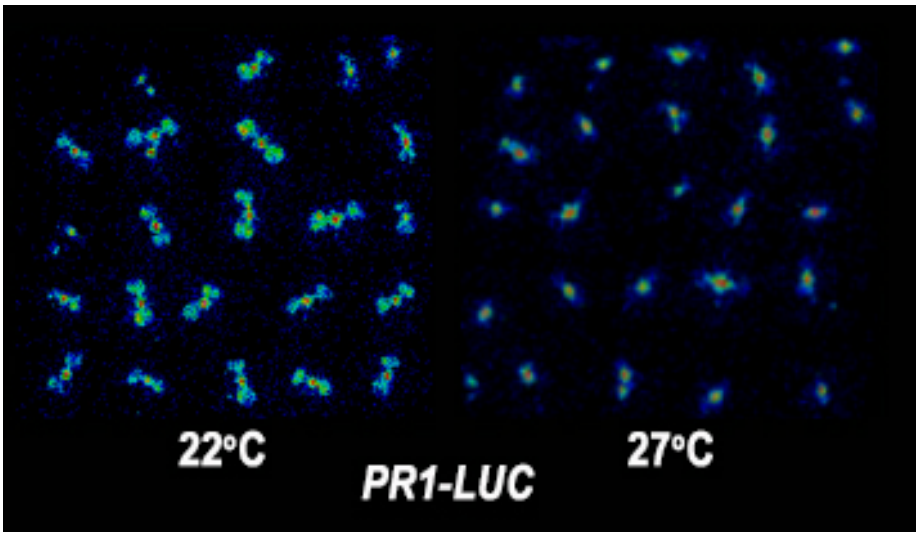

Figure 3-2 flg22-induced *PR1-LUC* expression in WT seedlings at 22 and 27℃ - Seven-day old seedlings grown at 22°C were shifted to 27°C or maintained at constant temperature for three days and induced with flg22 for 18 hours. *PR1-LUC* expression displayed as luminescence can be seen as strongly induced at 22°C in seedlings, and attenuated at 27°C.

As expected, high expression of this reporter gene can be observed in seedlings grown at 22℃. Whilst luminescence is detectable in the central meristematic region of seedlings grown at 27℃, any cotyledonous expression is strongly suppressed at 27℃. These data corroborate the utility of *PR1-LUC* as a marker line for *PR1* expression and further support the evidence previously obtained to show abolition of *PR1* expression at high temperature.

3.2.2 Identification and isolation of the *resilient* mutants

Ethyl methane sulfonate (EMS) mutagenesis was carried out on seeds from the *PR1-LUC* reporter line [167]. >1000 M1 seedlings were grown and seeds from each M1 plant collected separately, constituting >1000 M2 families. Seeds from these segregating M2 lines were grown on soil and assessed for *PR1-LUC* expression at 27℃ under the screen conditions developed by Kasemthongsri (2012) [228]. Seedlings from each M2 line were grown for 7 – 10 days at 22℃ SD before being shifted to 27℃ for 3 days and induced with 100 nm flg22 in 0.01 % Silwet. Imaging was carried out 18-24 hpi as before (Figure 3-3). Putative mutants maintaining robust *PR1-LUC* expression at 27℃ were selected and carried forward for further characterisation. M3 seedlings from individual lines were collected and luciferase activity via luminescence quantification was characterised at both 22 and 27℃ as before to confirm uniformity of high expression and homozygosity of mutants to take forward to the M4 generation [228].

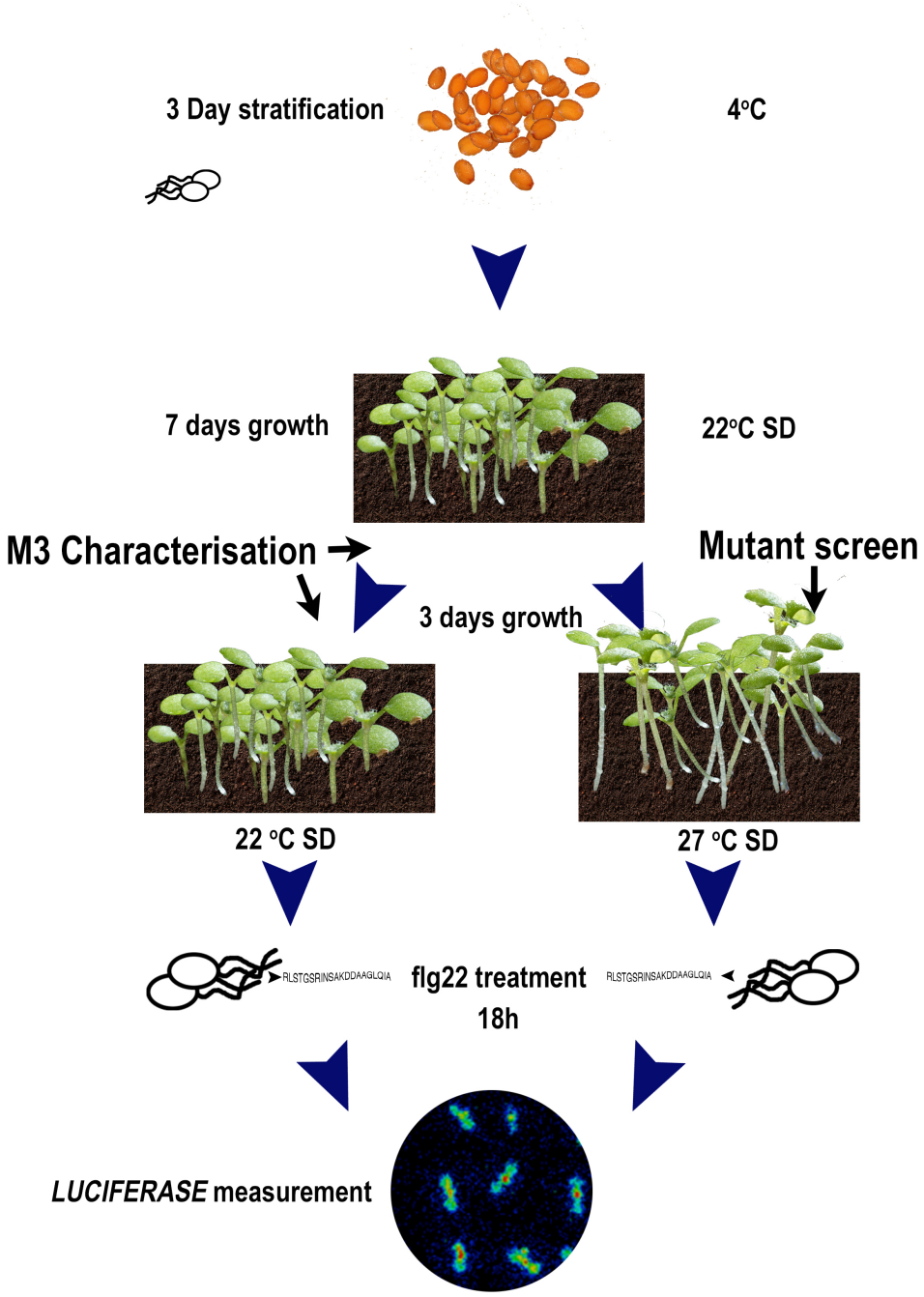

Figure 3-3 *resilient* mutant screen (27℃) and *LUC* expression characterisation (22 + 27℃) – Mutagenised *Arabidopsis* seedlings were grown under short day conditions for 10 days at either constant 22°C or for 7 days at 22°C followed by three days at 27°C or maintenance at 22°C and induced with 100 nM flg22. *PR1-LUC* expression 18hpi was measured through addition of luciferase substrate – 1 µM luciferin in 0.01% Triton X-100 – and measured using the Photek HRPCS-3 PSU. 717 high *PR1-LUC*-expressing lines from this screen were taken forward for further characterisation following confirmation of robust expression of this gene both at 22°C and 27°C. This work was carried out by Nad Kasemthongsri (2012) [228].

From a total of >10000 M2 families, ~2000 were screened and 717 putative mutants were identified based on robust *PR1-LUCIFERASE* expression at 27°C [228] (Figure 3-4). Following confirmation of their strong *PR1-LUC* induction in the third generation (M3), these novel mutants with robust, thermostable expression of *PR1-LUC* reporter were subsequently called the ***res**ilient* (*res*) mutants. These mutants show high levels of reporter gene expression which is maintained even with the 5°C temperature upshift normally associated with TSI. Examples of several of these mutants is presented in Figure 3-4.

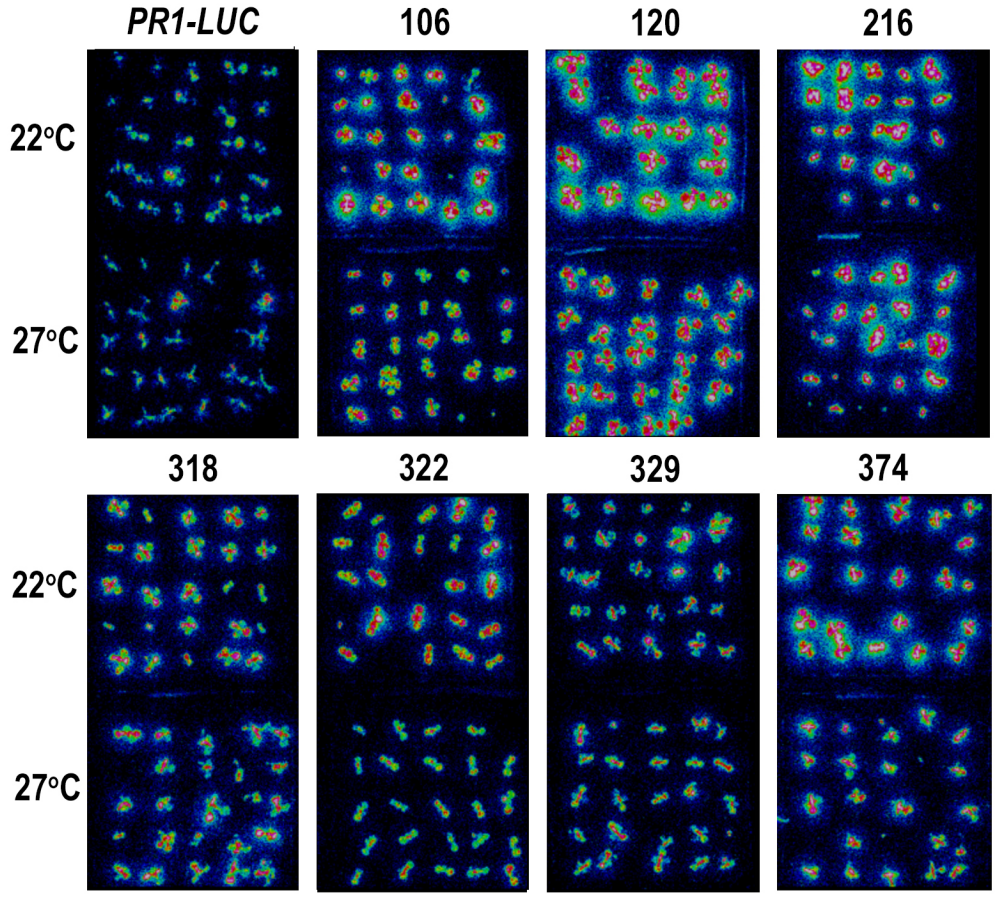

Figure 3-4 Temperature resilient *PR1-LUC* expression in a subset of M4 *resilient* mutants–Seedlings from the fourth generation of *resilient* mutant mother lines were grown at either constant 22°C or shifted to 27°C and induced with 100nM flg22 for 18 hours before *PR1-LUC* expression was quantified with the Photek HRPCS-3 PSU. Numbers represent arbitrary sequential numbers mutant mother lines singled out for their thermosensory resilient expression of this gene. Data adapted with permission from [228].

Earlier, I detailed how thermosensory suppression of flg22-induced *PR1-LUC* expression is abolished in WT plants (Figure 3-2). From this screen, a novel set of

mutants displaying a lack of TSI at 27°C has been identified thus providing a novel toolkit with which to dissect TSI and uncover key molecules governing regulation of this process (Figure 3-4). In addition to their robust *PR1-LUC*, many of these mutants displayed a range of growth and developmental defects, presumably as a direct result of their heightened defences, disturbing the growth-defence balance [20]. This may be a consequence of the inhibitory effects of potentially elevated levels of defence activation, or as a result of perturbing an upstream coordinator of this finely tuned balance. In general, small rosette size, stunting of inflorescences, perturbations of flowering time and fertility defects were some of the key phenotypes observed in these mutants (Figure 3-5) [228,230]. Growth defects such as these indicate disturbance of generalised thermosensory pathways in these plants in addition to TSI.

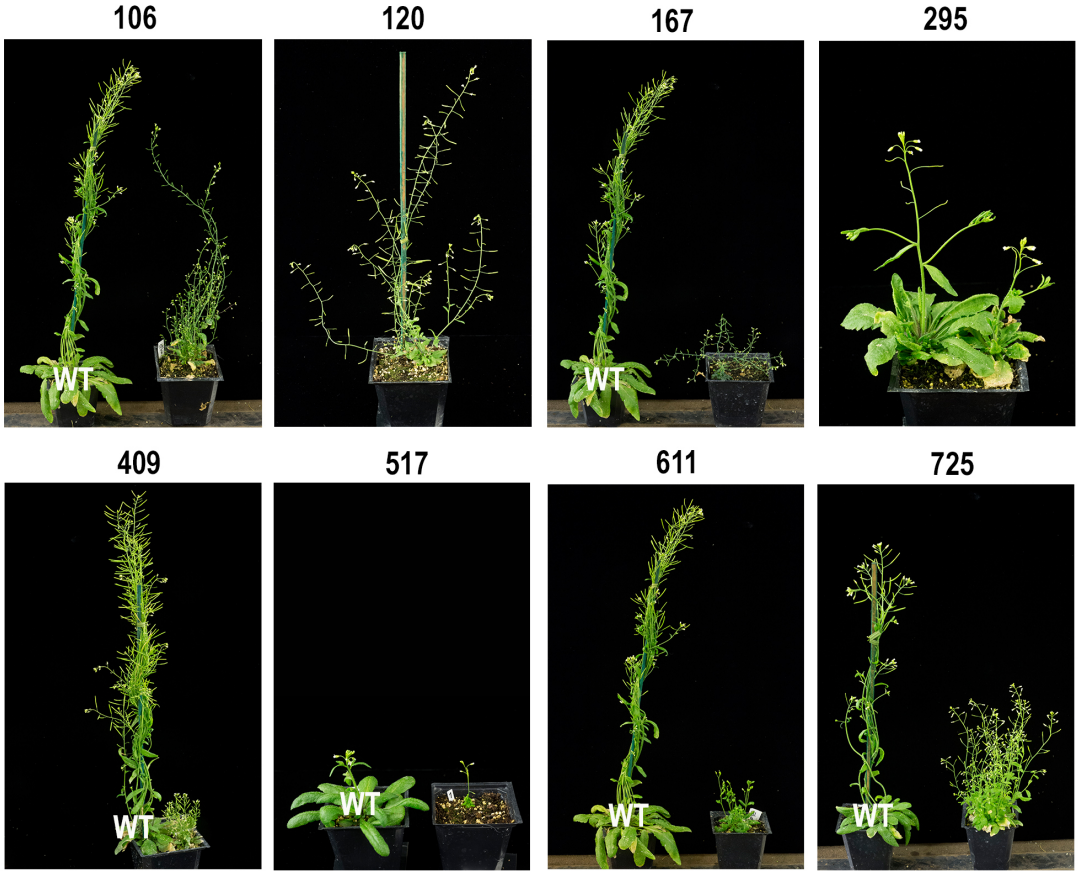

Figure 3-5 Growth and development of *resilient* mutants- Plants were grown under 20°C LD conditions and growth and developmental phenotypes of a representative subset of mutants is displayed. Comparisons with WT (*PR1-LUC*) plants of the same age are indicated. Mutant plants display various degrees of developmental and growth defects in comparison with WT plants grown under the same conditions. Adapted with permission from Kasemthongsri (2012) [228].

Differences in rosette size, leaf size, plant height, flowering time and fertility are all clearly observable here (Figure 3-5). Outputs such as these suggest generally perturbed growth and defence responses in these mutants along with their robust *PR1-LUC* expression. Further study of these mutants and the mutations underlying their phenotypes will thus provide opportunities to identify and characterise key regulatory molecules involved in growth and immunity.

With this chapter, I aimed to take forward one of these mutants for further characterisation, both in terms of its robust immunity and its consequential defects in growth and development. In-depth study of this mutant and underlying mutation furthermore enabled identification of a key player in coordination of TSI and thus thermosensory responses in general.

3.2.3 resilient1

From the initial set of putative mutants screened as described above, mutant #322, hereafter called *resilient1* (*res1*) was initially selected for further study as a result of its very robust *PR1-LUC* expression at 27°C [228]. To further characterise and confirm *PR1-LUC* expression in *res1*, I first investigated expression of this gene under both normal (22°C) and elevated (27°C) temperature conditions. Seedlings were grown according to screen conditions at either 22 or 27°C before being treated with 100 nm flg22 in 0.01% Silwet or mock (0.01% Silwet) solutions for 18 hours. *PR1-LUC* expression was characterised as before through visualisation of luminescence with the Photek HRPCS-3 PSU photon-counting camera.

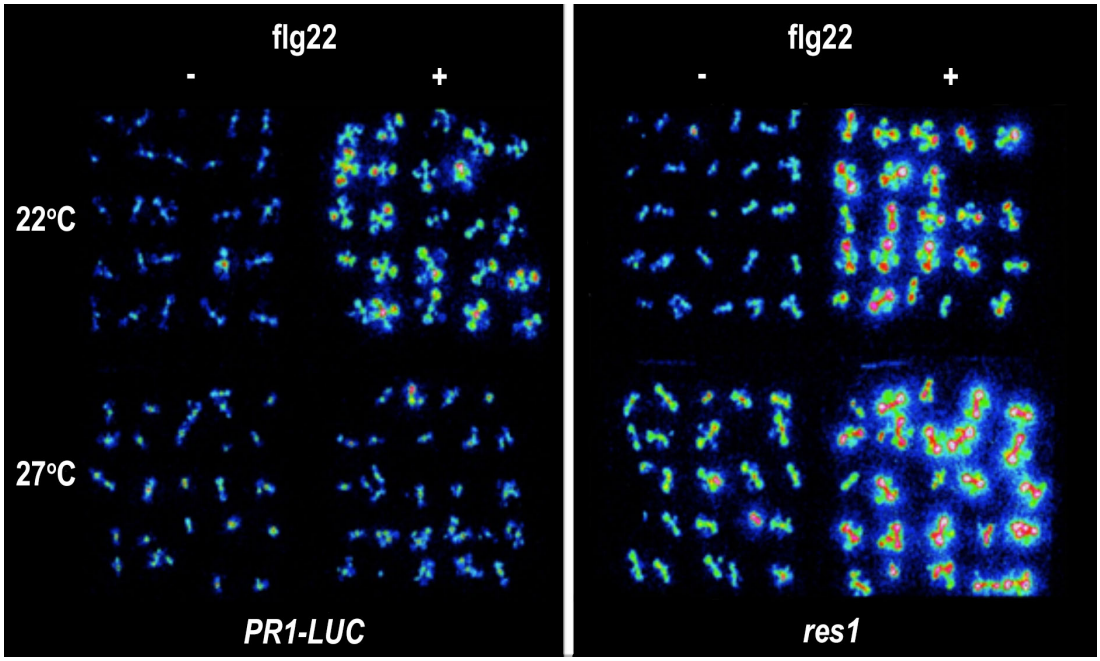

Figure 3-6 flg22 induced (+) or mock treated (-) *PR1-LUC* expression in WT and *res1* seedlings – Seedlings grown according to mutant screen conditions at 22 or 27°C induced with either mock (0.01% Silwet) or flg22 (100 nM flg22 in 0.01% Silwet) solutions for 18 hours before spraying with luciferin substrate (1 μM in 0.01% Triton X-100) and imaging using Photek HRPCS-3 PSU luminometer. Robust induction of *PR1-LUC* can be observed in *res1* compared to WT at both temperatures tested, with remarkable lack of suppression of this gene at 27°C. Data adapted and presented with permission from [228].

It can clearly be seen in Figure 3-6 how *res1* maintains extremely high induction of *PR1-LUC* compared with WT plants at 22°C. Furthermore, in confirmation of what was previously observed during the mutant screen, expression of this gene is not abolished by growth at 27°C where it is strongly attenuated in WT plants (Figure 3-6).

Constitutive *PR1* expression as observed here, along with its consequent effects on growth and development as demonstrated in the *resilient* mutants, has specifically been associated with autoimmune phenotypes such as necrosis [231]. Autoimmune mutants display HR like lesions or premature leaf senescence alongside their dwarf phenotypes [140,232,233] (Figure 3-7). In line with these characteristics, *res1* displays early senescence of leaves alongside its stunted rosette phenotype (Figure 3-7).

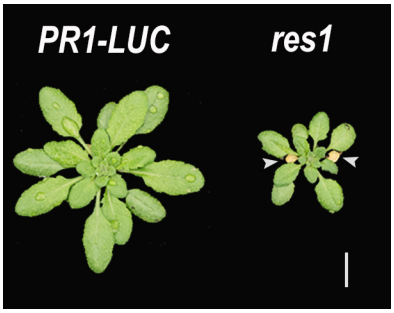

Figure 3-7 Rosette growth and senescence phenotypes of 5-week-old *res1* plants – Plants were grown at continuous 22°C SD conditions for 5 weeks and representative plants displayed to indicate relative size and characteristic senescence in *res1*. In addition to its stunted growth in comparison with WT, *res1* plants show early leaf senescence, as indicated by arrows. Scale bar = 1 cm.

Clearly here, *res1* shows a dwarf phenotype compared to WT plants as well as senescent leaves characteristic of autoimmune mutants. Taken with the observed robust maintenance of *PR1-LUC* expression in these plants at 27°C, these phenotypes indicate generally perturbed immunity and thus consequential impacts on growth and development in *res1*. To determine whether immune responses in general are perturbed in *res1* I next aimed to characterise additional key outputs of SA-mediated immunity in this mutant at both normal and elevated ambient temperature conditions.

3.2.4 *res1* displays thermostable SA-mediated immunity

In order to establish whether *res1* plants display generally elevated levels of SA associated immunity in line with their *PR1-LUC* expression, I first aimed to comprehensively characterise defence phenotypes in this mutant at both 22 and 27°C.

Since the screen was carried out based on reporter-based expression of *PR1*, my first aim was to characterise whether expression of endogenous *PR1* in these plants was likewise robust. In addition to *PR1*, I also looked at two additional genes associated with SA mediated immunity. I selected *PATHOGENESIS-RELATED5* (*PR5*), which like *PR1* is known as a marker of SA-induced and systemic acquired resistance (SAR) [234], along with *SAR-DEFICIENT1* (*SARD1*), a master regulator of defences including the SA biosynthesis pathway [41,235] for further characterisation.

I grew seedlings on soil according to screen conditions for 7 days at 22°C before shifting to 27°C or maintaining at 22°C for a further three days and inducing with 100 nM flg22. At 18 hours post induction (hpi) I collected seedling tissue in order to quantify expression of these three marker genes through qPCR, as before. Expression from a total of 3 biological and 4 technical replicates was measured and normalised to EF1α.

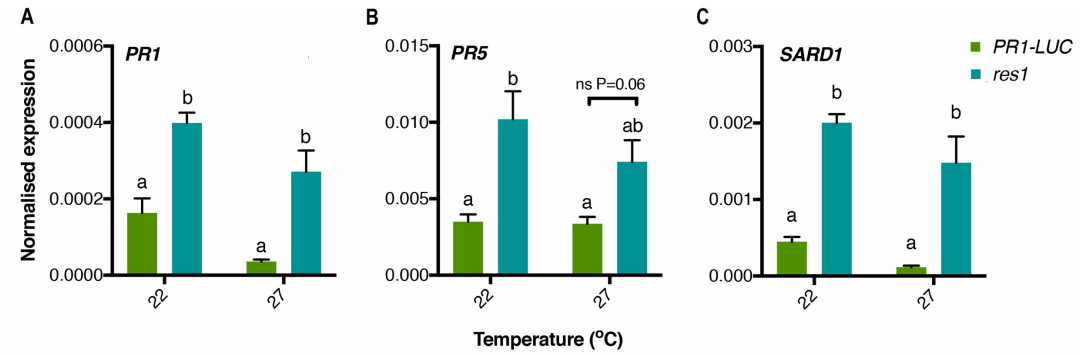

Figure 3-8 Comparative *PR1*, *PR5* and *SARD1* expression in WT and *res1* seedlings at 22 or 27°C – Seedlings grown according to screen conditions followed by 22 or 27°C were induced with flg22 and tissue collected at 18 hours post induction (hpi). Gene expression for each technical replicate was normalized to average levels of the housekeeping gene, *EF1*α in each biological replicate. Statistical analysis conducted – A - ordinary one-way ANOVA followed by Tukey's post-hoc analysis B, C Kruskal-Wallis ANOVA followed by Dunn's multiple comparisons test.

These data clearly reflect what was previously observed through visualisation of *PR1-LUC* expression (Figure 3-8A). Levels of *PR1* expression are very high in *res1* plants at 22°C compared to WT, a response which is strongly maintained at 27°C (Figure 3-8).

In a similar manner to *PR1*, *res1* showed a more robust induction of *PR5* at 22°C than WT which was maintained at 27°C, although the difference between *res1* and WT

was not as strong as for *PR1* (Figure 3-8B). *res1* also shows robust elevation of *SARD1* expression at both normal and elevated ambient temperatures (Figure 3-8C) which suggests broad-scale, upregulation of defences in this mutant [235].

Altogether, it logically follows how the levels of gene expression observed here reflect generalised elevated levels of SA-triggered immunity (SATI) in *res1,* which are strongly resilient to moderate increases in ambient temperature.

3.2.5 *res1* maintains robust resistance at elevated ambient temperatures

I have previously shown how typically, elevated temperatures compromise resistance to the biotrophic pathogen, *Pseudomonas syringae* Pv. Tomato, DC3000 (*Pto* DC3000). As a result of the robust and resilient activation of SA-mediated immunity demonstrated in *res1*, I hypothesised that these mutant plants would maintain elevated levels of resistance to this pathogen. I thus next assayed resistance of *res1* to this pathogen at 22 and 27℃ to determine whether elevated defence gene expression and SATI in this mutant brings about an increase in resistance compared to WT plants and whether they maintain higher resistance at 27℃.

To establish resistance levels of *res1* to *Pto* DC3000, I grew mutant plants at 22℃ for 4 weeks alongside WT plants before either maintaining them at this temperature or shifting them to 27℃ for 3 days before spray inoculating with *Pto* DC3000 (OD_{600}=0.02). Following a further three days at their respective temperatures, I measured bacterial CFU as before.

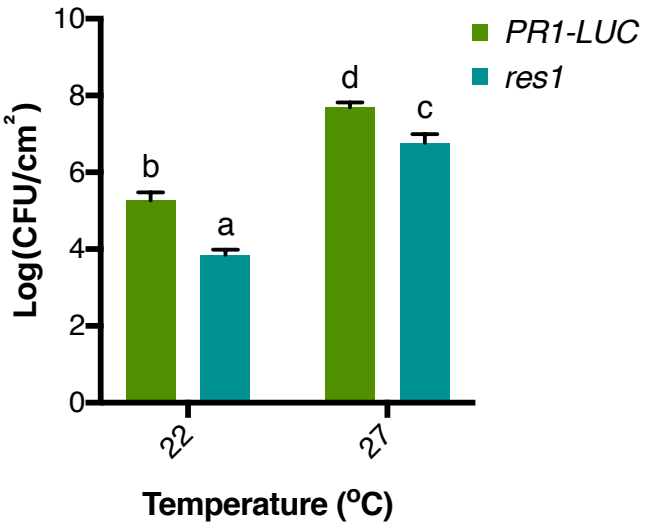

Figure 3-9 Resistance of *PR1-LUC* and *res1* plants to *Pto* DC3000 at 22 and 27°C - Plants grown at 22°C for 4 weeks followed by 3 days growth at either 22 or 27°C were infected with *Pto* DC3000 for 3 days and bacterial CFU on leaf surfaces quantified. Statistical analysis carried out- 2-way ANOVA followed by Tukey's post-hoc test n=5-6. One representative example of 3 biological replicates is shown here.

Just as this mutant shows elevated levels of SA-mediated immunity, *res1* shows increased resistance to this pathogen at 22°C compared to WT. *res1* showed a moderate response to temperature-upshift but stronger resistance than WT plants grown at 27°C is still clearly displayed by this mutant (Figure 3-9). This is in noticeable contrast to other similar mutants which display enhanced resistance at 22°C such as *snc1-1* which revert completely to WT at higher ambient temperatures [236].

Taken together with the gene expression data, it is clear therefore that *res1* lacks a crucial aspect of TSI regulatory mechanisms. This phenotype is significant given the rarity of similarly thermo-insensitive immune phenotypes in similar, autoimmune mutants. A key feature of these mutants in addition to the elevated levels of defence is their consequential dwarfism, which is suppressed by growth at elevated temperature [184]. This response appeared lacking in *res1* from initial characterisations [228]. My next aim was therefore to determine whether *res1* maintains similarly dampened thermosensory growth responses.

3.2.6 Thermosensory elongation growth is perturbed in *res1*

In response to temperature increases, plants undergo thermomorphogenic changes such as elongation-growth of hypocotyl and petioles, hyponastic leaf movement and rosette size increases as well as accelerating initiation of developmental transitions such as flowering [155,172]. Extensive characterisation of these responses at a range of ambient temperatures has recently been carried out in several elegant studies including natural variation of these responses in a number of different *Arabidopsis* accessions [92] and as an output of thermosensory suppression of autoimmunity [184]. To determine whether the loss of *RES1* function leads to a specific lack of thermo-responsiveness of plant immunity or whether it affects temperature responses in general, I aimed to characterise elongation growth and flowering time responses in *res1* mutants at 22 and 27°C.

To begin my investigations, I first set out to quantify seedling hypocotyl elongation, as previously validated as a robust output for thermosensory elongation growth [92,127,165]. I grew plants for 7 days following stratification at 22°C SD before shifting them to 27°C for three days. These seedlings were then removed from soil and aligned on agar plates before imaging, and hypocotyl length measured using ImageJ.

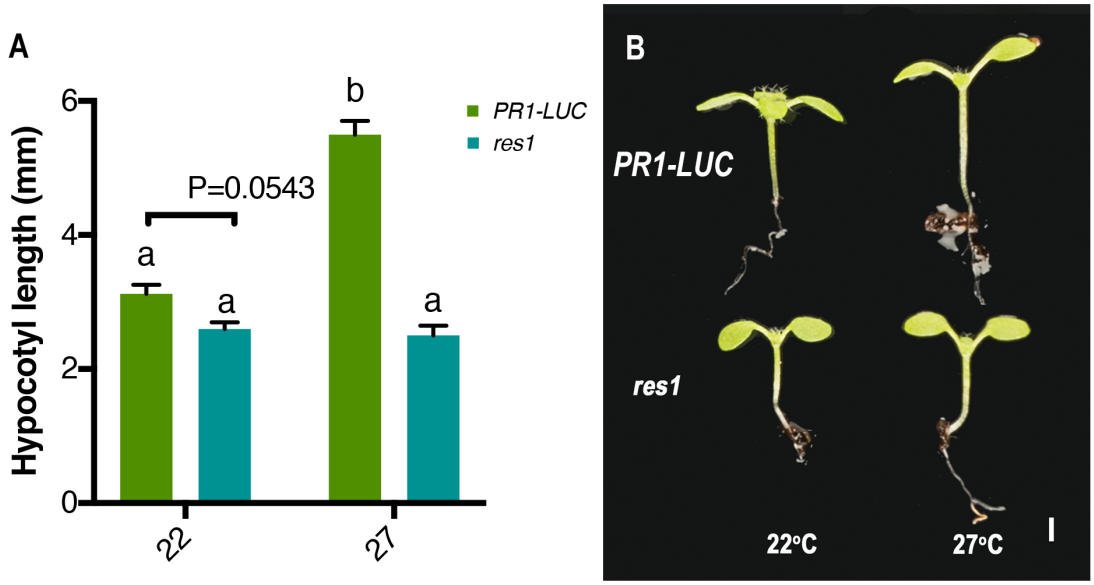

Figure 3-10 *res1* maintains shorter hypocotyls than WT seedlings at 22 and 27°C – Plants grown on soil at constant 22°C for 7 days followed by a further three days growth at 22°C or being shifted to 27°C. (A) Hypocotyls quantified through ImageJ image analysis software. Statistics carried out – 2 Way ANOVA followed by Tukey's

post-hoc analysis (n = 10-23). (B) Representative seedlings displayed for each genotype at each temperature assayed, scale bar = 1 mm.

Here, key phenotypic elongation growth differences can be observed. *res1* plants display signs of short hypocotyls at 22°C in comparison with WT plants. Furthermore, where WT plants show an increase in elongation growth at 27°C, *res1* shows no significant elongation. (Figure 3-10A). From Figure 3-10B it is clear how different *res1* plants are from WT, even at this early growth stage, and that they do not show signs of temperature responsiveness both in terms of hypocotyl length and hyponastic leaf angle changes which are noticeable by this stage in 27°C- grown WT seedlings.

Other key thermosensory growth responses can be observed as plants develop, such as petiole elongation. To assess this response in *res1*, I grew seedlings subjected to the same conditions as above for a further 7 days under their respective temperature regimes. After a total of 10 days growth at divergent temperatures following their initial 7 days together at 22°C, I measured petiole elongation to determine differences in thermosensory growth.

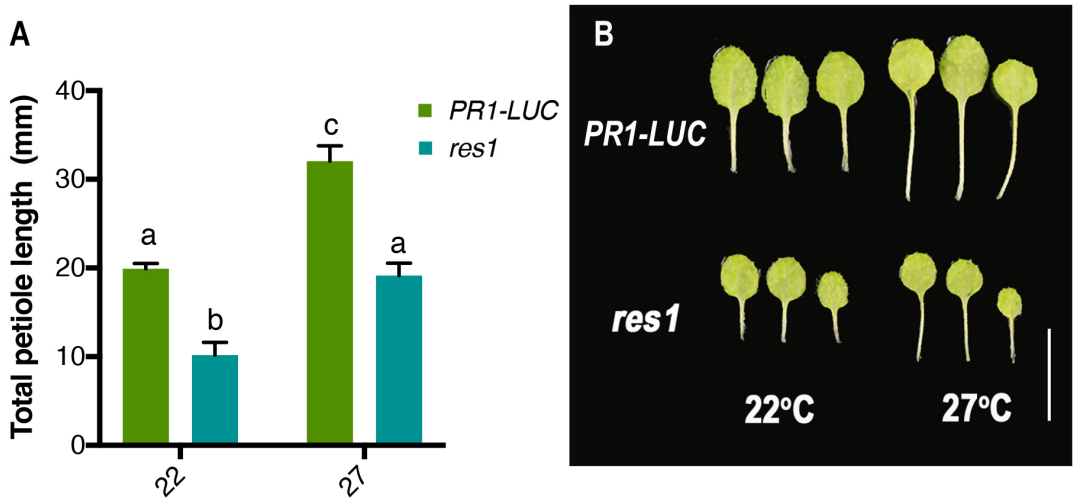

Figure 3-11 Thermosensory petiole elongation growth of young WT and *res1* plants – Seedlings were grown for 7 days at 22°C followed by 10 days at either 22 or 27°C. Petioles from the three most mature leaves were excised and **combined length of three petioles** for each plant quantified using ImageJ analysis software (A). Statistics carried out – 2-way ANOVA followed by Tukey's multiple comparisons test (n = 6). Representative petioles are displayed from both lines at both temperatures tested (B). Scale bar = 1 cm.

In line with what I observed for seedling hypocotyl elongation, petiole elongation in WT plants increases between 22 and 27°C (Figure 3-11A). Although a slight

responsiveness to temperature can be observed here, *res1* maintains shorter petioles than WT at both temperatures tested. In fact, petiole length of *res1* plants at 27°C mimics that of WT at 22°C, highlighting a lack of dwarf phenotype reversion in these mutants by growth at elevated temperature. Interestingly, these plants also seem to maintain smaller leaves regardless of temperature (Figure 3-11B).

Altogether, I have now observed how, in addition to its lack of TSI, *res1* displays compromised thermosensory elongation growth, which seems to suggest a reduction in thermosensory responses in this mutant. In order to further characterise this observation in *res1* plants compared to WT, my next aim was to investigate growth and developmental phenotypes in *res1* over both a broader temporal as well as temperature range.

To gain a better understanding of the growth and development of *res1*, and thus of its potentially compromised thermosensory responses, I grew mutant plants alongside WT plants at constant 17, 22 or 27°C SD for 10 weeks and recorded growth phenotypes at 1-2-week intervals. Representative examples of plants at each time point are displayed in Figure 3-12.

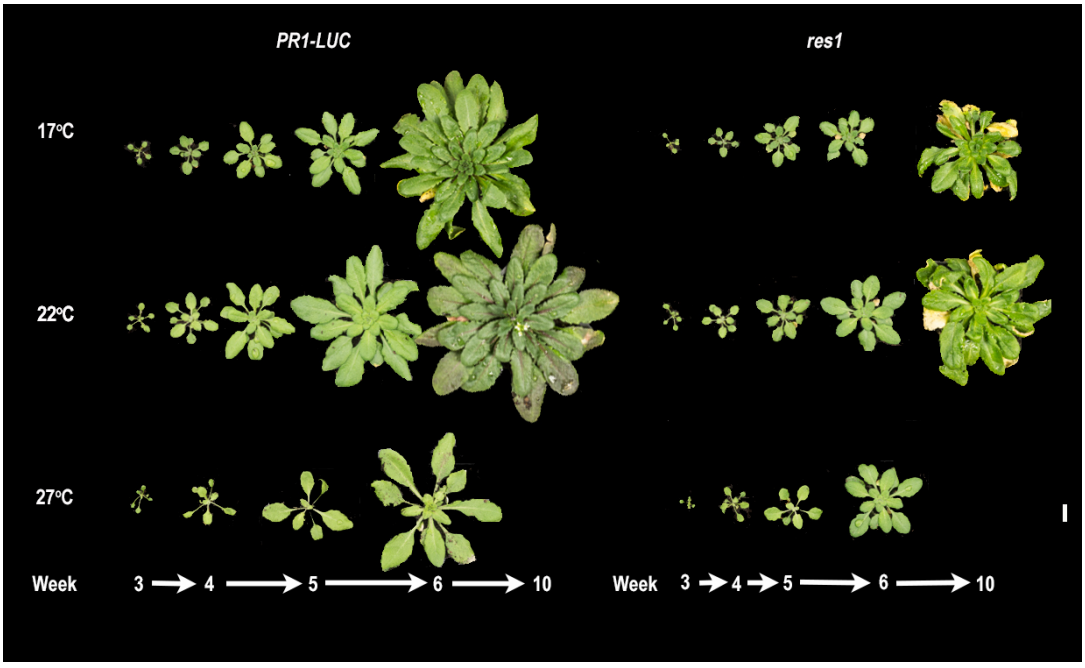

Figure 3-12 Adult rosette development of WT and *res1* plants at 17, 22 or 27°C – 3-10-week-old plants of each genotype were grown under constant (SD) temperature regimes. Four time-points only displayed at 27°C for one biological replicate. Scale bar = 1 cm.

This figure demonstrates how, alongside growth increases, development is generally accelerated in WT plants as temperature increases, a response which appears to be dampened in *res1*. In comparison with *res1*, WT plants show further signs of growth and developmental processes than *res1* at all three temperatures tested (Figure 3-12). A moderate increase in size can be observed with increases in temperature in *res1*, but it is not as obvious as in WT. Rosettes of this mutant maintain a more compact leaf organisation, lag behind WT plants in terms of development and never reach the same size as WT. In addition, the previously observed accelerated senescence of leaves in *res1* is clearly visible (Figure 3-12). This phenotype seems to be further enhanced by growth at 17℃ in comparison with 22℃.

In addition to growth increases, acceleration of flowering transition is typically observed in WT plants grown under elevated ambient temperature conditions [181]. To determine whether this response is compromised in *res1* I next aimed to quantify thermosensory acceleration of flowering in this mutant.

3.2.7 Thermosensory acceleration of flowering is intact in *res1*

To determine whether, like its compromised hypocotyl and petiole elongation phenotypes, *res1* displays perturbations in thermosensory acceleration of flowering, I investigated flowering time of these plants at both 22 and 27℃.

To achieve this, I grew WT and *res1* plants on soil at constant 22 or 27℃ SD and measured total number of days from end of stratification to flowering for 5-9 plants per genotype. In addition, I grew plants from each genotype at 20℃ LD conditions in order to document comparative phenotypes flowering, stature and fertility of *res1* which are not possible under SD conditions.

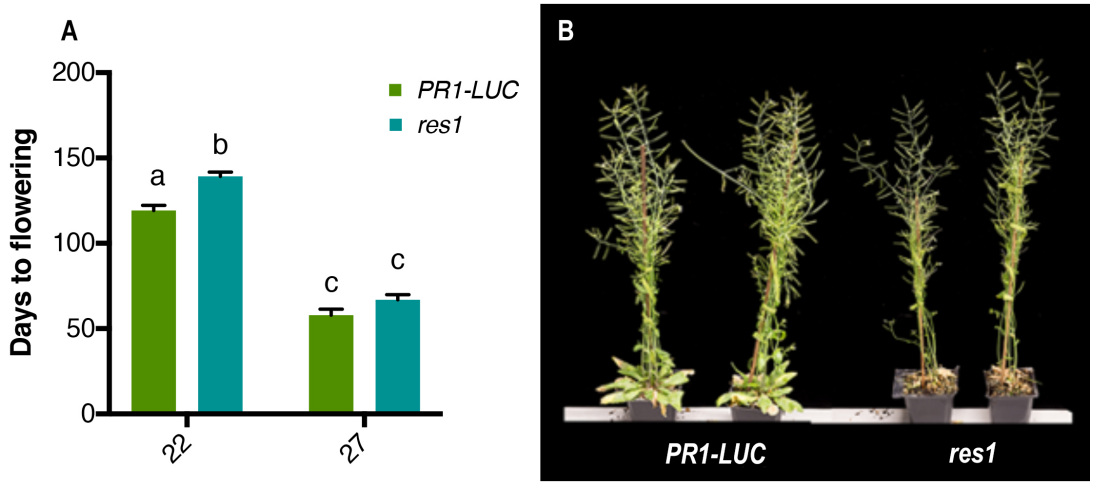

Figure 3-13 Flowering and reproductive phenotype of *res1* in and WT plants – (A) Flowering time measured at first flower opening stage in plants grown constantly at 22 or 27°C SD. Statistics carried out – One-way ANOVA followed by Tukey's multiple comparisons test (n = 5-9). (B) Representative plants from WT and *res1* lines grown constantly at 20°C LD.

Typically, *Arabidopsis* plants show a strong acceleration of flowering when grown at 27°C SD compared to 22°C. This was clearly shown here in the WT plants (Figure 3-13A). *res1* however flowered significantly later at 22°C. Any delay was not detectable at the higher temperature.

In terms of thermosensory responses, this seems to suggest an increase in responsiveness of this mutant to temperature at this later stage of development.

Further to their late flowering under normal temperature conditions, *res1* plants maintain a comparatively stunted phenotype into adulthood. Plants do not appear produce as many branches or seeds under 20°C LD conditions (Figure 3-13B) and show early onset severe leaf senescence which is particularly evident in these plants which are nearing the end of their life cycle (Figure 3-13B). Thus, in spite of the apparent decrease in severity of *res1* on thermosensory responses with time, the effects of this mutation are detectable throughout plant life cycle.

Having been isolated as a mutant lacking TSI, further characterisation has here implicated RES1 as modulating generalised thermosensory responses in plants. In early growth stages, *res1* mutants show strong suppression of thermomorphogenic responses such as hypocotyl and petiole elongation. Later in their life cycle, the phenotypes of this mutant become less severe in terms of growth and flowering but

do not revert back to WT in the same way characterised for autoimmune mutants such as *snc1-1* at elevated ambient temperatures [143,236]. To determine whether thermosensory growth changes in *res1* are underpinned by alterations in regulation of gene expression, I next investigated synthesis levels of key growth genes.

3.2.8 *res1* mutants display compromised expression of key growth genes

Increases in ambient temperature facilitate thermosensory elongation responses such as those documented above through upregulation of key elongation genes such as those involved in auxin biosynthesis and cell proliferation [155]. The transcription factor, PHYTOCHROME-INTERACTING FACTOR4 is known to play a crucial role in regulation of growth gene expression in response to temperature increases [127,155,237]. Both negative regulation of this factor by PhyB and altered expression of this gene have been cemented as crucial to effective growth and defence coordination in plants [81,127,131,238]. To begin to unpick the underlying causes of the reduced elongation growth in *res1,* my first step was therefore to determine whether *PIF4* is misregulated in this mutant.

To investigate expression of *PIF4* in *res1*, I grew plants alongside WT for 7 days at 22℃ before shifting to 27℃ or maintaining at 22℃ for a further four days in line with the growth conditions used for *LUC* characterisation. I collected tissue from plants in order to quantify gene expression via qPCR as before. Gene expression values were normalised to EF1α as previously for a total of 3 biological and 3 technical replicates.

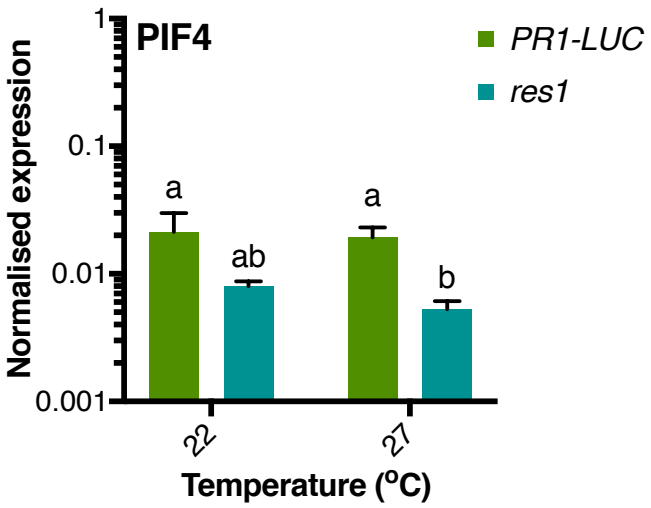

Figure 3-14 *res1* shows compromised *PIF4* induction qt 27°C – Seedlings were grown according to screen conditions at either 22 or 27°C. Tissue was collected at 18hpi and *PIF4* expression normalised to levels of EF1α. Statistics conducted — Kruskal-Wallis ANOVA followed by Dunn's multiple comparisons test.

Where previously, expression of *PIF4* has been shown to increase substantially with increasing temperature [128,136,224], no apparent increase was observable in this dataset (Figure 3-14). This lack of difference may be as a result of the range of temperatures used, since the temperature-dependent increase in *PIF4* expression previously observed was more apparent in the lower temperature regime [128]. In comparison with WT plants however, *res1* shows an apparent reduction in expression of this gene at 27°C, with an intermediate phenotype observable at 22°C (Figure 3-14). This reduction in expression compared to WT plants may underpin the reduction in elongation growth responses at elevated temperature observable in this mutant.

Since *PIF4* is regulated both at transcription [136,224] and post-translational/ functional levels [136,239], many regulatory interactions can affect initiation of downstream responses governed by this transcription factor. To determine the downstream outputs of PIF4 in *res1* and further understand the changes in gene expression responsible for modulating growth in this mutant under different ambient temperature regimes, I selected further key markers associated with different aspects of growth in plants through which to characterise this response.

Downstream to PIF4, auxin biosynthesis is required for increases in elongation growth at elevated temperatures [240] and acts antagonistically with SA-mediated defences [241,242]. Upregulation of auxin biosynthesis genes such as *YUCCA* family members increases elongation growth outputs at higher ambient temperatures [243,244].

In response to auxin increases, real changes in elongation growth are brought about by upregulation of key growth genes such as *XTR7* which encodes a xyloglucan endotransglucosylase required for PIF4-mediated elongation growth [245] through reorganisation and biosynthesis of cell walls.

To investigate whether *res1* has compromised auxin-mediated growth alterations, I looked at expression levels of the *YUCCA* family member *YUC8*, a gene directly regulated by PIF4 and shown to be responsible for elongation growth [224], as well as *XTR7* in *res1*. cDNA previously isolated from seedlings grown at 22°C before being either maintained at this temperature or shifted to 27°C for 3 days was used here.

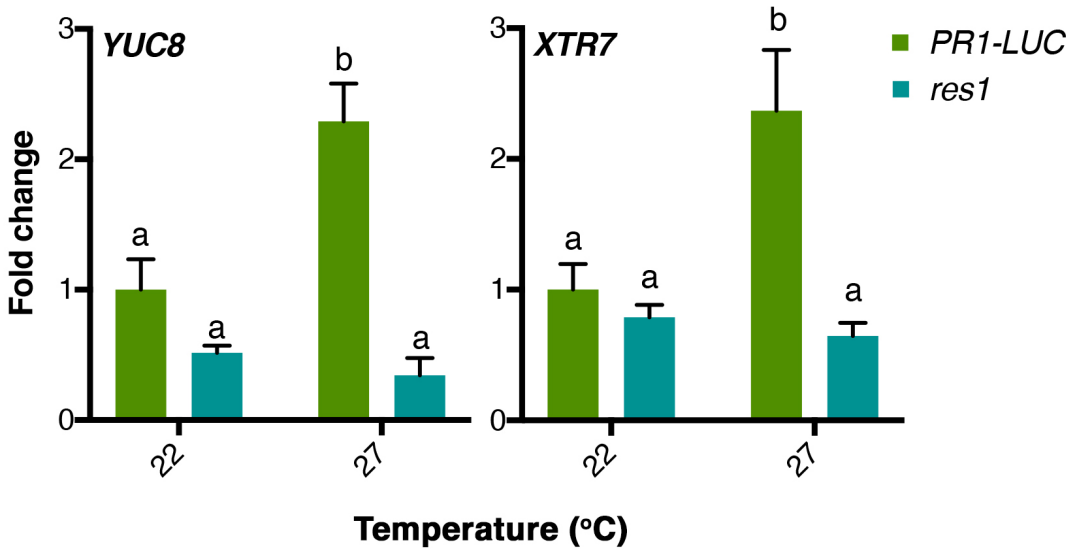

Figure 3-15 Comparative expression of *YUC8* and *XTR7* in WT and *res1* seedlings at 22 and 27°C – Seedlings grown according to screen conditions followed by 22 or 27°C and tissue collected at 18 hours post induction (hpi). Statistical analysis conducted – two-way ANOVA followed by Tukey's post-hoc analysis.

In WT plants, both *YUC8* and *XTR7* are strongly upregulated by growth at 27°C compared to 22°C. This regulation brings about changes in growth mediated by both genes, as a result of increased auxin signaling. In *res1* seedlings however, this

response is completely lost, which may underpin the differences observed in terms of thermosensory elongation growth which I have so far observed in this mutant. This suggests that these plants are compromised in auxin-mediated elongation growth and further supports my hypothesis that *res1* lacks key thermosensory responses (Figure 3-15). Furthermore, the decreased expression I have observed here may be underpinned by the decrease in *PIF4* expression I observed above.

It is possible to conclude therefore that in addition to its lack of TSI as detailed above, *res1* lacks PIF4/ auxin mediated growth responses at elevated ambient temperatures. This suggests that in general, thermosensory responses in *res1* are attenuated, resulting in coordinate perturbations of growth and defence. In order to understand the molecular basis for these alterations in *res1*, I subsequently aimed to characterise the location and nature of the mutated gene(s) underlying these phenotypes.

3.2.9 Molecular mapping of *res1*

Having gained a comprehensive understanding of the effects of the *res1* mutation of growth and defence in response to elevated temperature, I next set out to identify the causative mutation in this mutant and thus which gene *RES1* represents and how it functions in coordination of these processes.

At first, I carried out a series of backcrosses with *res1* to WT(*PR1-LUC*) plants to remove background mutations. I grew F1 plants from these crosses under 20℃ LD conditions in order to obtain F2 seeds. Each F2 line was then grown under elevated ambient temperature screen conditions (22℃ followed by 3 days of growth at 27℃) and seedlings selected for *res1*'s high luciferase phenotype following induction with flg22. Seedlings were validated by a further luciferase assay in the F3 generation to ensure strong *PR1-LUC* reporter gene expression. This process was then repeated to ensure minimal background mutations in the mutant line (Figure 3-16).

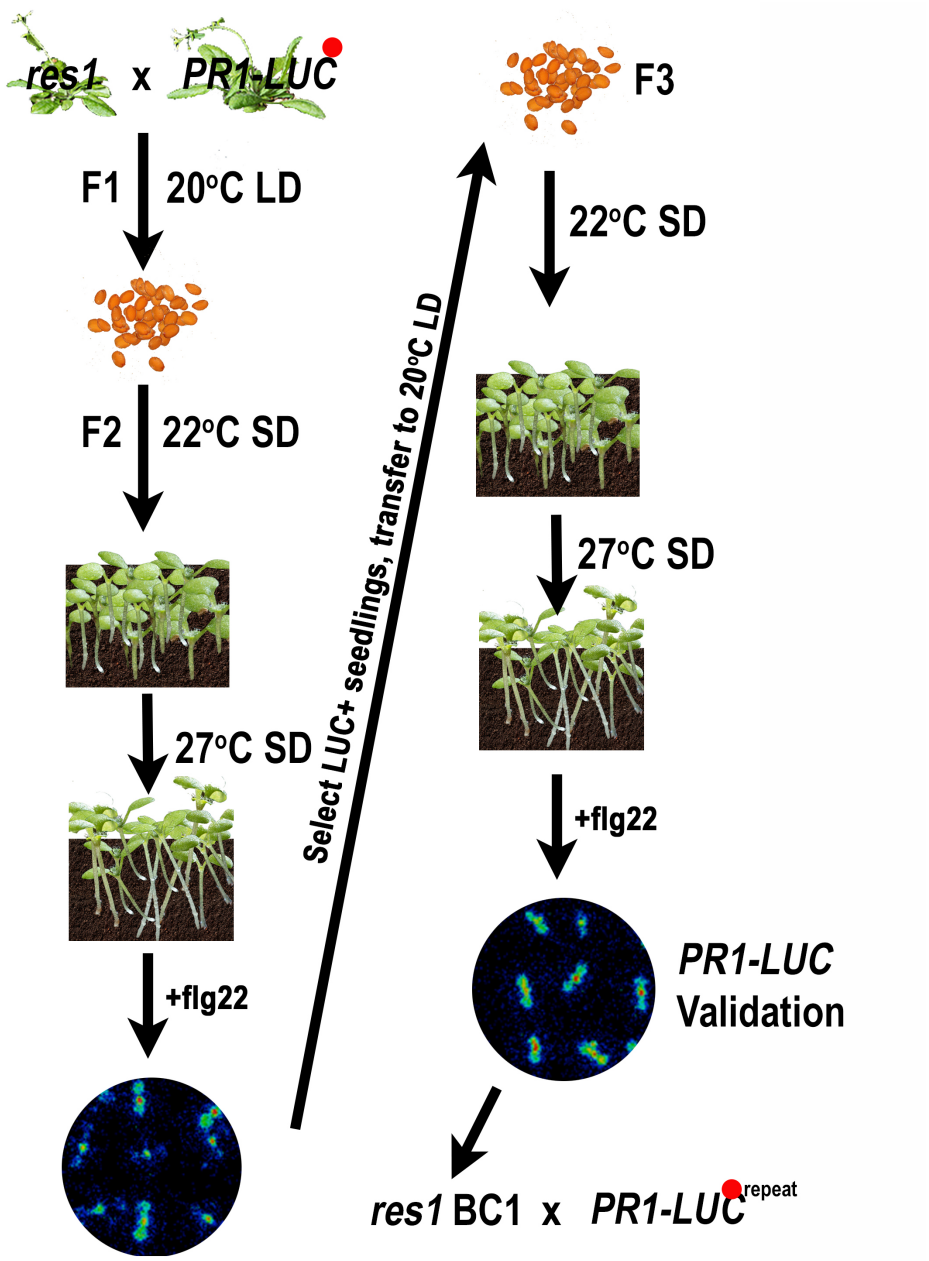

Figure 3-16 Schematic diagram of *res1* backcrosses and selection based on flg22-induced LUC expression at 27°C - F1 seeds from backcrosses were grown at 20°C LD to obtain F2 seeds. These were then grown according to screen conditions and positive seedlings selected and transferred to 20°C LD. Seeds were bulked and F3 seedlings validated for homozygosity through consistency and lack of segregation of *PR1-LUC* expression. F3 plants were grown up at 20°C LD and re-backcrossed to *PR1-LUC* for a total of 3 backcrosses.

Once these backcrosses had been conducted and zygosity validated through characterisation of *LUC* expression, I grew F2 segregating seeds from the second backcross (BC2F2) at the mutant screen conditions (22 followed by 27°C), induced with 100 nM flg22 and visualised *LUC* expression as before to enable isolation of WT and mutant segregants. RNA from these high *LUCIFERASE* (*LUC*+) and low LUCIFERASE (*LUC*-) bulk segregant populations was then extracted and sequenced in

order to identify candidate genes underpinning the *LUC*+ phenotype in *res1* (Figure 3-17).

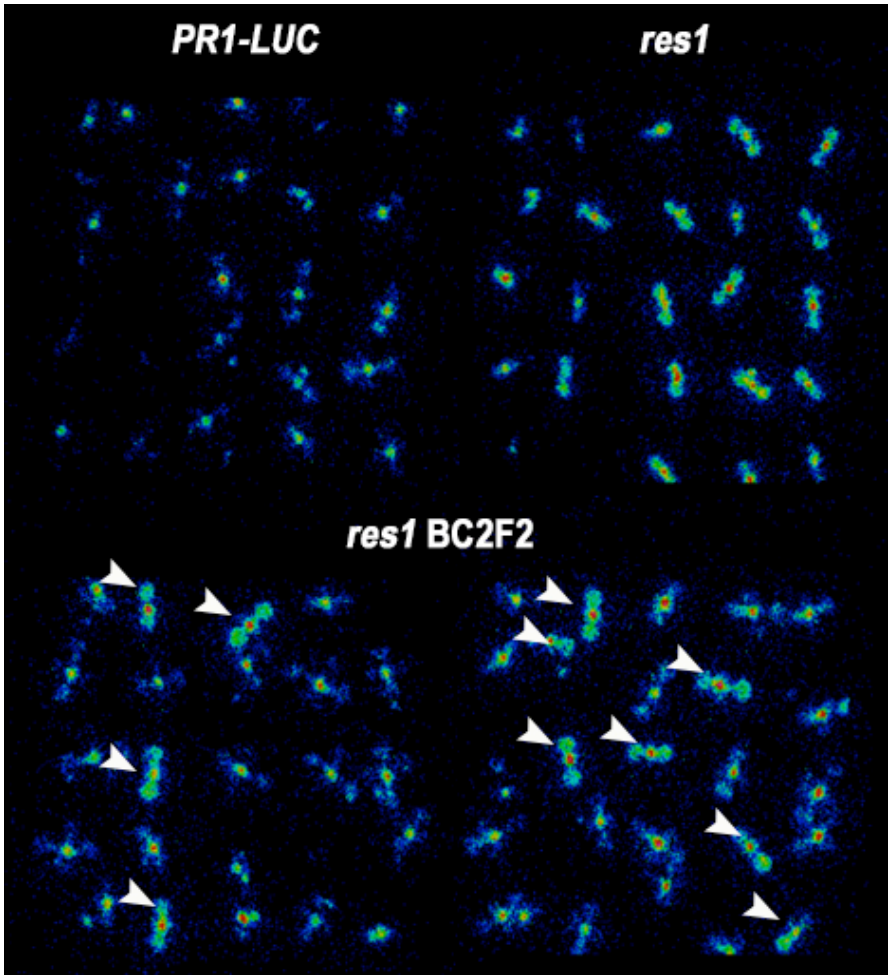

Figure 3-17 Isolation of *res1* bulk segregants for RNA-seq – Seedlings from a segregating backcrossed line (BC2F2) were grown under mutant screen conditions (27°C) and identified based on *PR1-LUC* expression. Seedlings displaying high levels of *PR1* expression in line with *res1* (LUC+) were isolated separately from those displaying low levels of expression in line with WT (*PR1-LUC*) seedlings and sent for RNA sequencing. Arrows indicate representative LUC+ seedlings isolated for analysis.

3.2.10 Identification of *RES1* candidate genes through bulk segregant RNA sequencing

In brief, Illumina Hiseq 2000 sequencing data from both bulk segregant populations were aligned to the WT (Col-0) *Arabidopsis* reference genome and significant non-synonymous SNPs in coding regions identified using Avadis NGS software. Following this, I compiled a comprehensive list of these mutations in both LUC+ and LUC- populations in order to identify differences in mutant allele frequency of non-

synonymous SNPs (ΔMAF) between populations. Using this comparison, I was able to identify a 7.8 Mb region on chromosome 5 containing 21 non-synonymous SNPs which was positively selected for in LUC+ bulk segregants (Figure 3-18). Clearly here, backcrossing has been effective in removal of background.

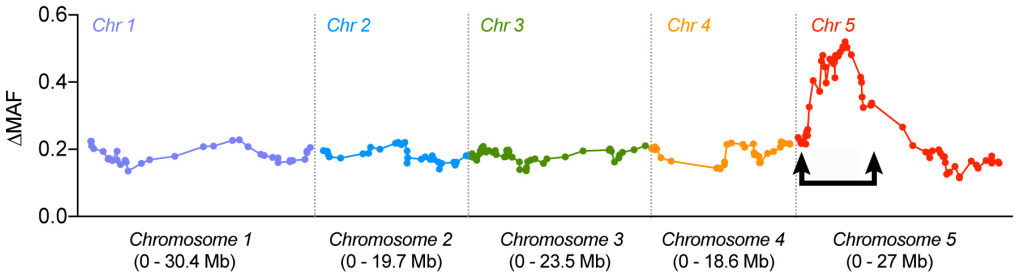

Figure 3-18 Differentially segregating SNPs between *res1* LUC+ and LUC- in comparison with the Col-0 reference genome – Change in mutant allele frequency (ΔMAF, (LUC+) - (LUC-)) of non-synonymous SNPs between bulk segregant high luciferase (LUC+) and low luciferase (LUC-) populations across the genome was filtered in order to remove SNPs with <10% difference in frequency between populations. All non-synonymous SNPS with ΔMAF >0.1 are presented here according to their position in the *Arabidopsis* genome, thus highlighting those enriched in the LUC+ population on chromosome 5 compared with other chromosomes.

Here, a 7.8 Mb region on chromosome 5 shows a group of non-synonymous SNPS preferentially present in a large proportion of LUC+ bulk segregants compared to the rest of the genome (Figure 3-18). Following identification of this region, I investigated gene ontology for each of 21 linked candidate genes which were >25% more highly represented in the LUC+ population (Table 1).

Table 1 Ontology of genes containing non-synonymous SNPs which are differentially enriched between LUC-/+ bulk segregant populations, as identified through RNA-seq analysis.

Gene	SNP category	Gene name (description)	Gene ontology/ function (according to arabidopsis.org)
AT5G07110	Non Synonymous Substitution	PRA1.B6 (Prenylated Rab Acceptor 1.B6)	Vesicle-mediated transport
AT5G09840	Non Synonymous Substitution	MNU2 (Mitochondrial Nuclease2)	Regulation of gene expression
AT5G10350	Non Synonymous Substitution	RRM (RNA Recognition Motif - containing protein)	RNA, poly(A), protein binding, protein self-association
AT5G11610	Non Synonymous Substitution	(exostosin family protein)	Protein glycosylation
AT5G11700	Non Synonymous Substitution	(ephrin type-B receptor)	Unknown
AT5G12050	Non Synonymous Substitution	BG1 (Big grain1)	Rho GTPase activating protein
AT5G13500	Non Synonymous Substitution	HPAT3 (Hydroxyproline O-Arabinosylatransferase 3)	Transferase/ unknown
AT5G15410	Non Synonymous Substitution	DND1/ CNGC2 (Defence, No Death1/ Cyclic Nucleotide Gated Channel 2)	Ca^{2+}/K^{+} permeable cation channel
AT5G15470	Non Synonymous Substitution	GAUT14 (Galacturonosyltransferae 14)	Galacturonosyltransferase activity
AT5G16600	Non Synonymous Substitution	MYB43 (Myb domain protein 43)	Transcription factor
AT5G17290	Deletion - frameshift mutation	APG5 (autophagy 5)	Nutrient recycling and senescence prevention
AT5G18190	Non Synonymous Substitution	MLK1/ PPK2 (MUT9P-Like Kinase 1/ Photoregulatory Protein Kinase 2)	Negative regulation of ABA, other
AT5G18230	Non Synonymous Substitution	Transcription regulator Not2/3/5 family protein	Negative regulation of transcription
AT5G18940	Non Synonymous Substitution	Mo25 family protein	Protein serine/ threonine kinase activity
AT5G20960	Non Synonymous Substitution	AO1 (Amine Oxidase1)	Extracellular amine oxidase
AT5G22290	Non Synonymous Substitution	FSQ6(Fructose-sensing quantitative trait locus 6)	DNA-binding transcription factor
AT5G24350	Non Synonymous Substitution	MIP2 (Mag2-Interacting Protein 2)	Protein transport
AT5G25060	Non Synonymous Substitution	RRC1 (Reduced red light responses in cry1cry2 background)	RNA splicing, mRNA processing
AT5G27290	Non Synonymous Substitution	stress regulated protein	ATP binding, metalloendopeptidase activity
AT5G27540	Non Synonymous Substitution	MIRO1 (Miro-related GTPase-1)	GTP binding, GTPase activity, Calcium ion binding
AT5G27990	Non Synonymous Substitution	PrerRNA processing protein TSR2	Unknown

3.2.11 res1 carries a mutation in CYCLIC NUCLEOTIDE GATED CHANNEL2 (CNGC2)

Candidate genes in the target region from the bulk segregants RNA-seq, were investigated for predicted functions and previously characterised roles and mutant

phenotypes available with an extensive literature search. Based on this initial analysis I selected one candidate for further consideration. This gene - *DEFENCE, NO DEATH1* (*DND1*), encodes CYCLIC NUCLEOTIDE GATED CHANNEL2 (CNGC2), a channel permeable to monovalent and divalent cations, in particular Ca^{2+} and K^{+} [232].

CNGC2 has in fact been previously implicated in the context of heat-shock as a *"primary thermosensor of land plant cells"* [107] as well as being a known regulator of plant immunity [246,247] across species [248]. In addition, *CNGC2* is a known target for *TOPLESS-RELATED1* (*TPR1)*, a transcriptional corepressor associated with SNC1-mediated immunity [236], thus implicating it in a well-known thermosensitive immune pathway. Its effect on growth is also known by the small stature of both *Arabidopsis* and *Physcomitrella patens* knockout mutants [107] and has recently been implicated in regulation of auxin-mediated growth [249]. Function of this protein is thought be through modulation of transient increases in subcellular calcium concentration crucial for low [118,250,251] and high [110] temperature acclimation, as well as many other biotic and abiotic stresses [252,253]. Whilst this gene has separately been implicated in all of the responses seen in *res1* in the context of heat shock, or under constant environmental conditions, its potential for a coordinatory function within ambient thermosensory growth and defence responses has not previously been tested.

Before conducting comparative analyses, I next aimed to confirm the presence of the *CNGC2* polymorphism in *res1* plants. To confirm this, I used a set of Cleaved Amplified Polymorphic Sequence (CAPS) primers to amplify and modify sequences in order to enable specific digestion of the mutant version of this gene by BspHI restriction digestion (Figure 3-19). Following WT and *res1* DNA extraction, I used these primers to amplify *CNGC2* in both lines and digested PCR products with BspHI.

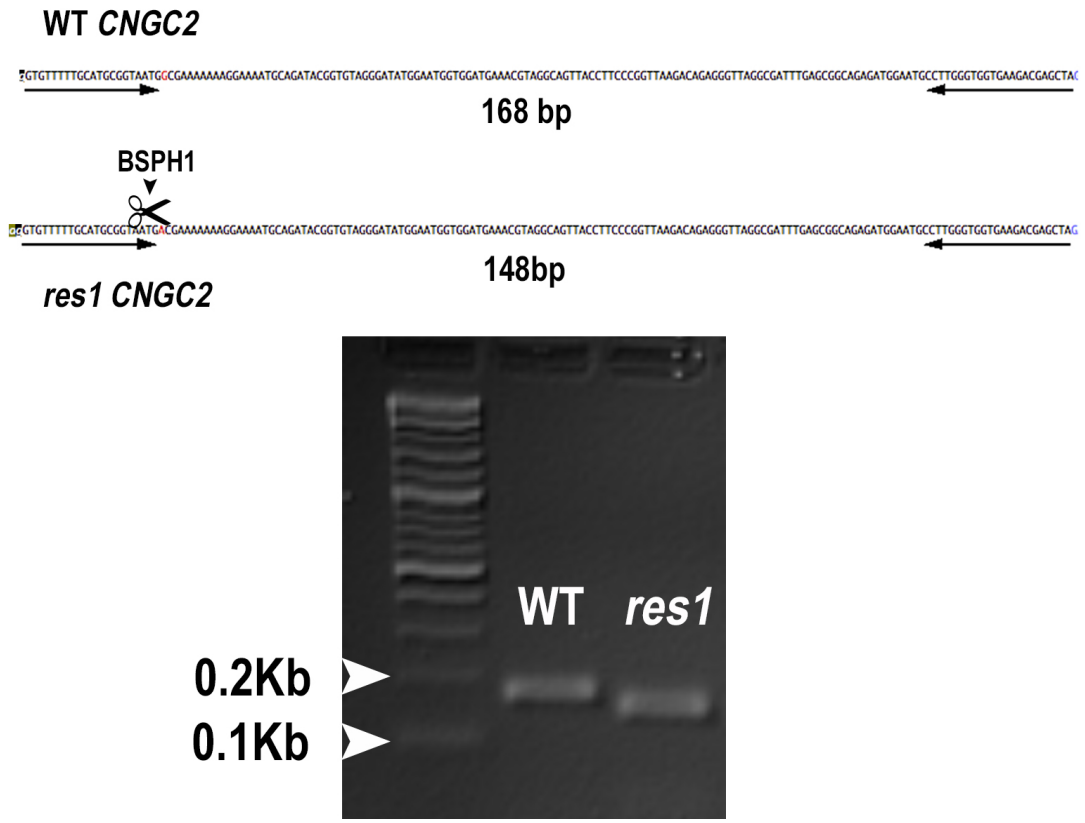

Figure 3-19 CAPS genotyping of WT and *res1 CNGC2* – Primers were designed such that, BspHI would preferentially cut mutant DNA, yielding a fragment 20bp shorter than full length PCR product, as observed through agarose gel electrophoresis on digested WT and *res1* PCR products.

Presence of the mutation in *CNGC2* in *res1* can be observed here through the smaller, successfully digested *CNGC2* PCR product in Figure 3-19.

3.2.12 res1 phenocopies *cngc2* null mutants

As a result of the responses I have observed already in *res1*, I hypothesised that this mutant would phenocopy *CNGC2* null mutants when grown under SD conditions. Confirmation of the shared identity of these two mutants could implicate a role for this channel in ambient temperature responses. In order to test this hypothesis, I obtained seeds from the *cngc2* T-DNA insertional knockout line SALK_019922C, hereafter referred to as *cngc2-T*.

To determine whether *res1* and *cngc2-T* phenocopy each other, I initially grew seedlings from these lines to compare hypocotyl length at a range of ambient temperatures. Whilst *cngc2* null mutants have well-established growth retardation phenotypes, hypocotyl length in this mutant has never specifically been tested

except in etiolated seedlings [254]. Having been established as a mutant with severely compromised growth however, I hypothesised that *cngc2-T* seedlings would display growth retardation as seedlings and thus have short hypocotyls.

To measure hypocotyl length in these mutants, I sterilized seeds from *PR1-LUC*, *res1* and *cngc2-T* lines and grew on GM agar plates. Following 3 days stratification at 4℃, seedlings were germinated at 22℃ before being moved to 17, 19.5, 22, 24.5 or 27℃ for 7 days and hypocotyl measurements carried out using ImageJ.

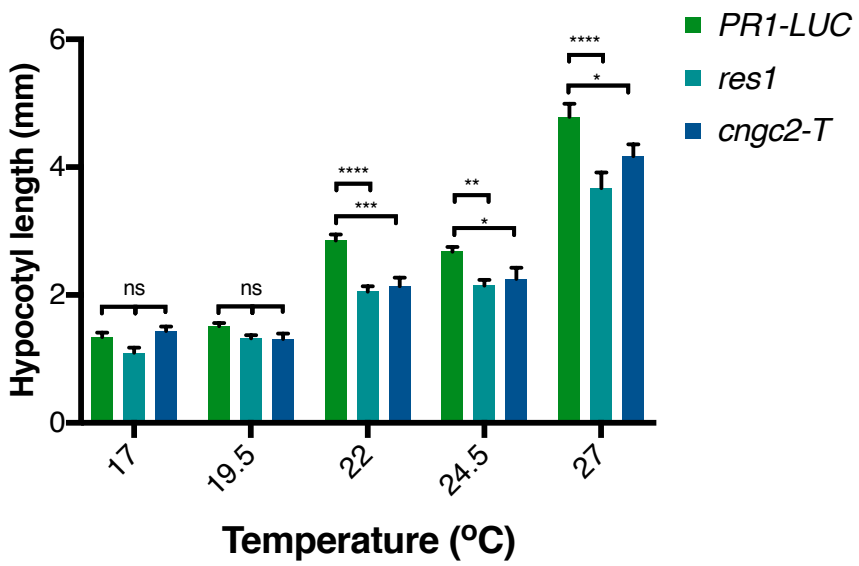

Figure 3-20 Comparative hypocotyl elongation of *res1* and *cngc2-T* seedlings between 17 and 27℃ - Seedlings grown at either constant 22°C for 10 days or shifted to 17, 19.5, 24.5 or 27°C following germination were imaged and hypocotyl length quantified with ImageJ. Statistical analysis – Two-Way ANOVA followed by Tukey's post-hoc multiple comparison test within each temperature tested (n=12-16).

As expected, *cngc2-T* mutants maintained short hypocotyls in comparison with WT plants at 22, 24.5 and 27℃, thus confirming dwarf phenotype in seedlings lacking *CNGC2*. In comparison with *res1*, which likewise showed shorter hypocotyls than WT for ≥22℃, no difference could be observed at any of the temperatures tested (Figure 3-20). No difference could likewise be observed between any genotypes tested at 17 or 19.5℃. This experiment confirmed hypocotyl length as a robust readout for *cngc2-T* stunting phenotype as well as verifying similarity in stature for this mutant with *res1*.

Next, to investigate the comparative phenotypes of adult mutants, I grew plants of each genotype alongside *PR1-LUC* for 6 weeks at constant 17, 22 and 27°C SD and documented rosette phenotypes of representative plants for each line (Figure 3-21).

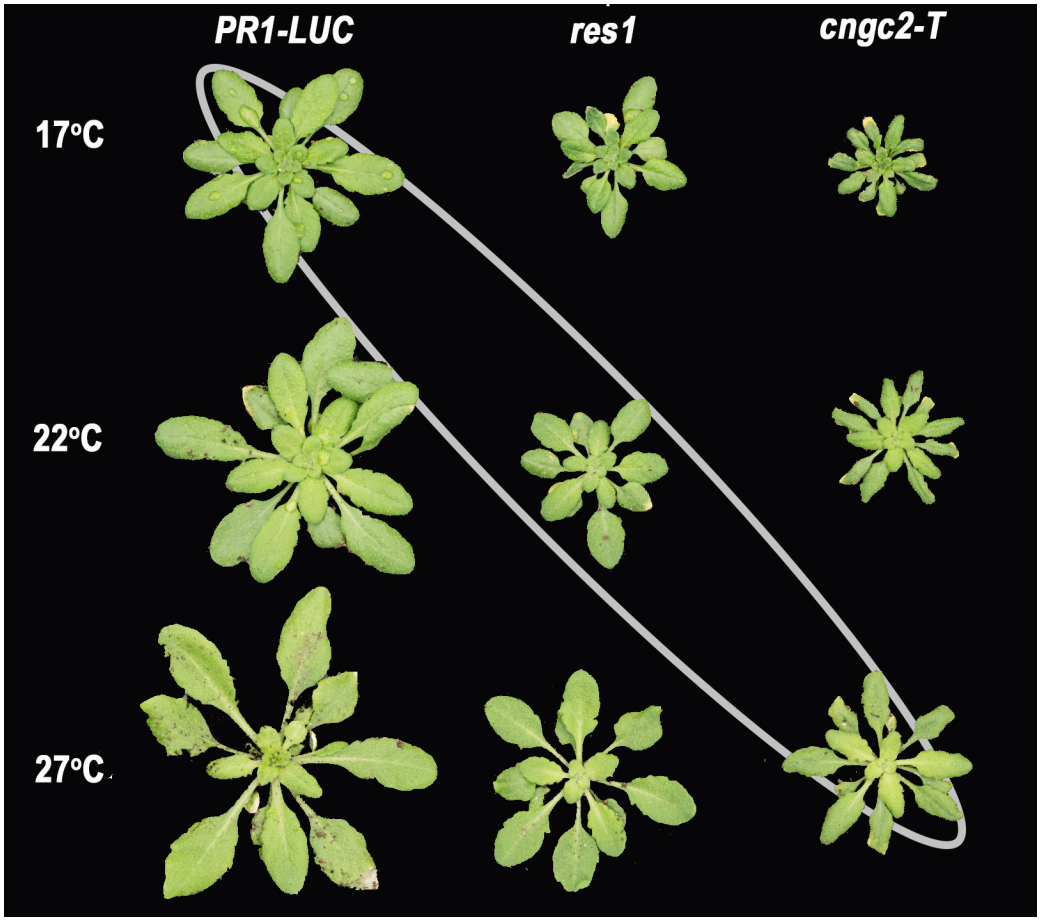

Figure 3-21 6-week-old WT, *res1* and *cngc2-T* plants under three temperature conditions – Plants grown at constant temperature, SD following 3 days stratification at 4°C. *res1* and *cngc2-T* mutants both show compromised growth responses. Grey ellipse is to indicate the comparable sizes of plants grown at each temperature and therefore apparent "perceived" temperature compared to WT at 17°C.

Comparison of *res1* and *cngc2-T* plants as well as with WT plants reveals phenotypic similarities. In terms of size, *res1* maintains a smaller rosette size than WT plants regardless of temperature, and *cngc2-T* appears to display more severe stunting. *res1* plants grown at 22 or 27°C phenocopy WT plants grown at 17°C. *cngc2-T* show further compromised growth to *res1*, where mutants grown at 27°C phenocopy WT plants grown at 17°C. Both *res1* and *cngc2-T* thus show an apparent reduced sensitivity to temperature changes due to their small rosette size compared to WT

plants, with *res1* potentially representing a weaker allele with some residual function compared to null mutants.

From this experiment, I observed the premature senescence previously detailed in young leaves in *res1,* as well as around the edges of newer leaves, particularly at lower temperatures. A similar effect could be seen for *cngc2-T* mutant leaves. This behaviour may be an example of "necrotic lesions" which are a well-documented phenotype of *cngc2* mutants, despite lacking an effective hypersensitive response [246]. In addition to a mutation in *CNGC2*, *res1* plants contain several linked mutations, including *AUTOPHAGY5 (APG5)*. APG5 may play a role in enhancing the senescence phenotypes observed and will therefore be important to consider in the future, following confirmation of allelism of *CNGC2* and *RES1*. In terms of both growth and defence phenotypes, *CNGC2* still remained my primary candidate due to its undeniable similarities to *cngc2-T* null mutants. However, to eliminate other linked mutations from consideration, I conducted a series of segregation analyses of SNPs within the candidate region.

3.2.13 Segregation and characterisation of *CNGC2*-linked polymorphisms

To verify *CNGC2* as the primary candidate for *RES1*, I designed a set of CAPS primers for non-synonymous SNPS flanking *CNGC2* to track segregation of both luciferase and growth phenotypes with these mutations.

I grew BC3F2 seedlings under mutant screen conditions to identify individual plants with high *PR1-LUC* expression following flg22 induction at 27℃. Following luciferase screening, I removed LUC- plants and allowed LUC+ plants to grow on for a week before classifying them as small (i.e. *res1*-like in stature), medium (intermediate in stature) or large (WT in stature). I then extracted gDNA from each plant to determine zygosity for the *res1* SNP in *CNGC2* as well as those up/downstream from this gene at increasing distances. I amplified DNA from each plant using CAPS primers for the SNPs in At5G11610, At5G13500, At5G15410 (*CNGC2*), At5G15470 and At5G20960 followed by digestion and zygosity determination through agarose gel electrophoresis. Cosegregation of mutations with size phenotype and evidence of recombination is presented in Figure 3-22.

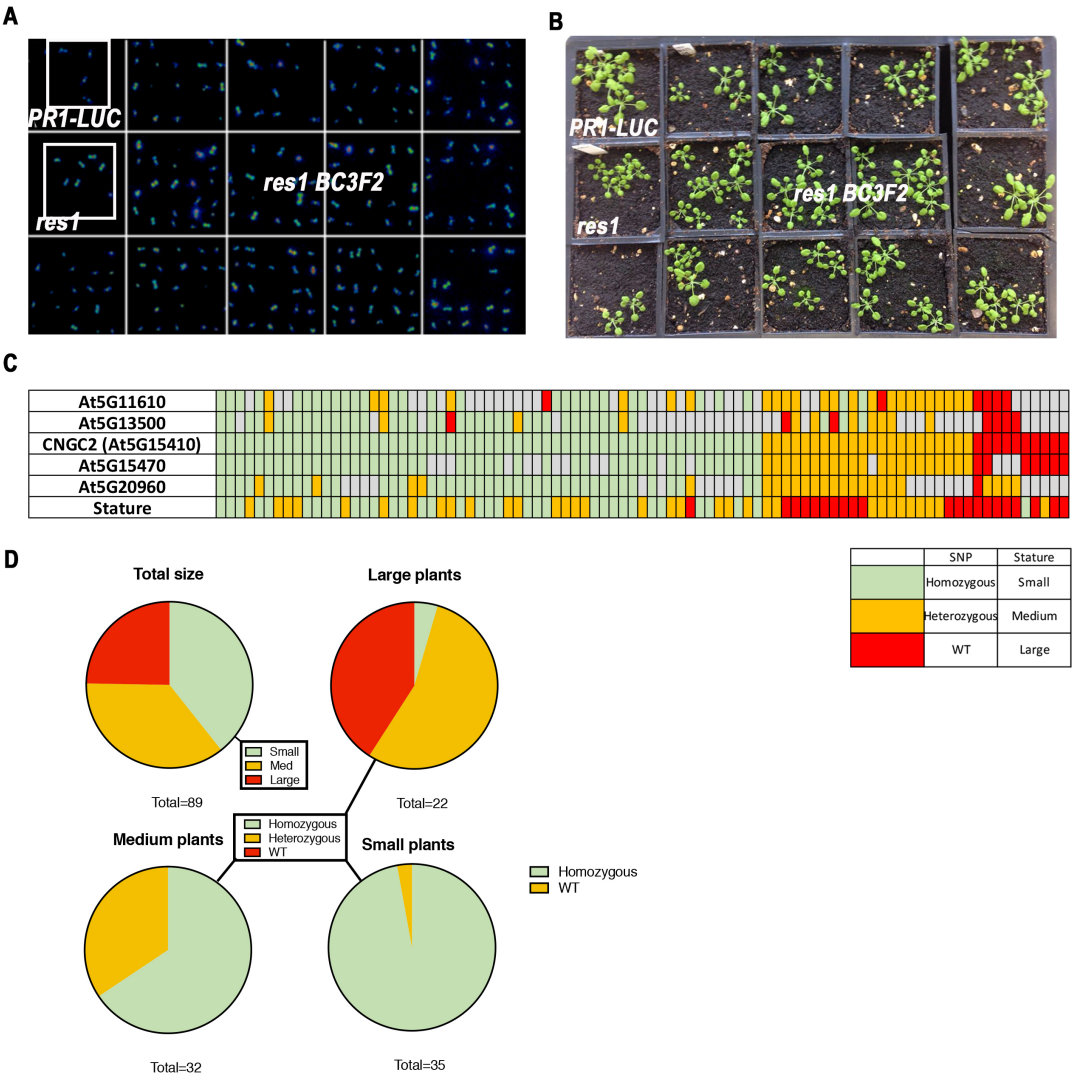

Figure 3-22 Segregation characterisation of *CNGC2*$^{(res1)}$ and linked SNPs through CAPS genotyping – (A) Zygosity of 89 *LUC*+ seedlings screened for SNPs in *CNGC2* and linked genes, sorted by plants homozygous for *CNGC2*$^{(res1)}$ and further characterised for cosegregation of LUC expression (B) and size (C) with SNPs. Seedlings characterised for *LUC* expression and size phenotypes were separated by size and zygosity of *res1* SNP characterised by size (D).

Of the plants categorised as small, most were homozygous for the *res1CNGC2* SNP (Figure 3-22 D). Of the medium plants, all were either homozygous or heterozygous for this SNP and of the large plants all were WT or heterozygous. As expected there is an association of the SNP specific to *CNGC2* in *res1* with size and luciferase phenotype. Proximity of plants to each other and place within the growth tray may have contributed to the overlap in phenotypes of small WT plants and large *res1*.

Further to this, the identification of a large number of heterozygous plants in this study through selection by luciferase phenotype suggests that the mutation is not completely recessive.

Of the 89 LUC+ plants identified, 57 were homozygous for the SNP in *CNGC2*, 22 were heterozygous and 10 were WT. Recombination could be observed between *CNGC2* and all except the closest linked of the SNPs (At5G15470) tested. Within the unrecombined region lies the previously mentioned senescence-associated gene *ATG5* which contains a frame-shift mutation in *res1*.

To eliminate *ATG5* as well as other linked non-synonymous SNPs, including those for which I did not observe recombination *res1*, I obtained T-DNA insertion mutants from NASC to observe any noticeable phenotypes (Table 2).

Table 2 SALK T-DNA insertional mutants obtained for *CNGC2*-linked SNPs in *res1*

Line	Gene	Gene ID
SALK_086227C	At5G11610	Exostosin family protein
SALK_062726	At5G13630	CCH1
SALK_029525C	At5G15470	GAUT14
SALK_030146C	At5G16600	MYB43
atg5-1	At5G17290	APG5 (ATG5)
SALK_018100C	At5G20960	AO1

I grew plants from each line for seven weeks at 22℃ SD alongside *PR1-LUC*, *res1* and *cngc2-T* to monitor and assess growth. Representative plants from each line are displayed in Figure 3-23.

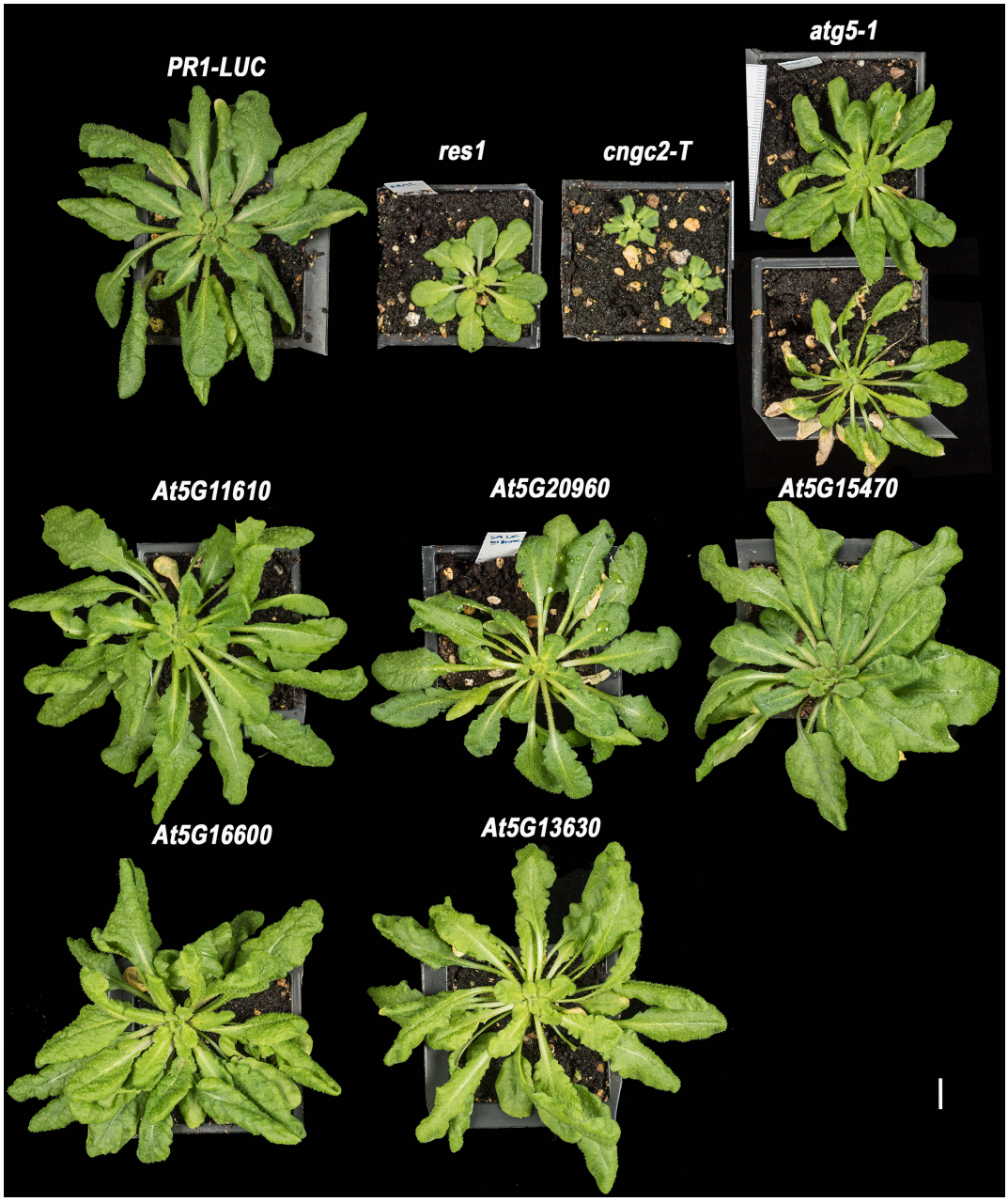

Figure 3-23 Phenotypic comparison of T-DNA mutants in indicated genes with non-synonymous SNPs within the differentially segregating region in the *res1* mapping population – Representative plants shown after 7 weeks growth at 22°C SD. Scale bar = 1 cm.

Of the mutants tested, At5G11610, At5G20960, At5G15470, At5G1660 and At5G13630 showed no noticeable phenotypic difference from WT plants at 22°C SD. *atg5-1* plants showed a modest decrease in growth compared to WT or the other mutants whilst both *res1* and *cngc2-T* plants were noticeably stunted. In addition, some *atg5* plants displayed their characteristic senescence phenotype [255] as pictured in Figure 3-23 (bottom plant as displayed), but this phenotype was only observable in plants inadvertantly challenged with a herbivorous pest. This pattern of

senescence was not observed for either *res1* or *cngc2* mutants exposed to similar challenges and thus clearly not an indication of autoimmunity as described for both mutants. Therefore, so this mutation was removed from consideration.

Whilst these data further support *CNGC2* as a plausible candidate for *RES1*, to confirm identity of these two genes I investigated allelism through complementation assays.

3.2.14 res1 and *cngc2-T* are allelic *CNGC2* mutants

As previously described, *cngc2* mutants show strong growth attenuation, such as small hypocotyls and rosette size, as well as delayed flowering [256]. these mutants also show elevated levels of *PR1* expression, SA accumulation and broad-spectrum resistance to pathogens [113,107]. Because of the observed growth similarities between *res1* and *cngc2-T,* confirmation of the potentially causative SNP in *res1* and previously documented enhanced resistance conferred by lack of *CNGC2* function, I hypothesised that the two mutants were allelic.

To test whether *RES1* is allelic to *CNGC2*, I crossed *res1* with *cngc2-T* and characterised hypocotyl length phenotypes of F1 plants. In addition, I crossed both lines back to WT (*PR1-LUC*) plants as a control.

I grew seedlings from each F1 cross for 10 days at 22°C before quantifying hypocotyl length with ImageJ, as before.

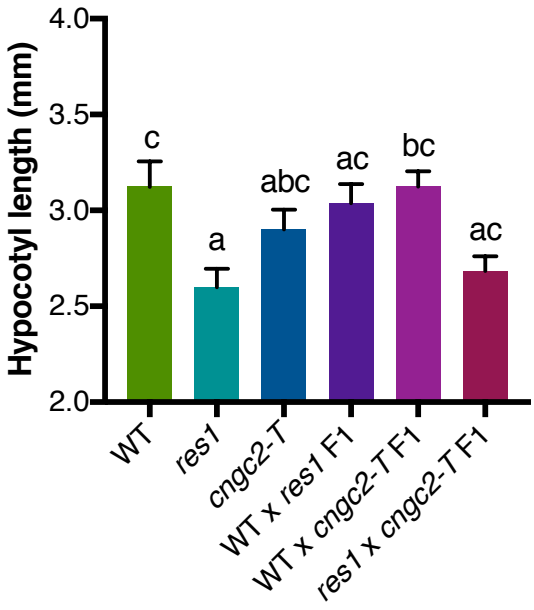

Figure 3-24 Hypocotyl elongation growth of between F1 crosses of *cngc2-T* and *res1* - Ten-day old seedlings grown at 22℃ SD on soil and hypocotyls measured through transfer to plates and analysis using ImageJ. WT represents *PR1-LUC* seedlings here. Statistical analyses carried out – One-way ANOVA followed by Tukey's multiple comparisons test (n = 10-23).

In accordance with what I have shown previously, *res1* maintains shorter hypocotyls than WT at 22℃. *cngc2-T* seedlings show a weaker phenotype than *res1* plants (Figure 3-21). *res1* x *cngc2-T* F1 seedlings maintain short hypocotyls, comparable with either individual mutant line and robustly different from WT plants. Lack of mutual complementation here confirms that the two mutants are allelic. There also appears to be a mild effect of the *res1* mutation in the control (WT x *res1*) F1 cross. Further work is required to test the semi-dominant/dose-dependent effects of this mutation, however this would seem to agree with the previously observed variations in luciferase and size phenotypic segregation.

Following hypocotyl measurement, I grew four representative seedlings from each cross alongside WT or single mutant plants at 22℃ SD to observe rosette sizes as plants matured. I documented phenotypes of these lines at both 4- and 5-weeks post germination to compare rosette growth between lines (Figure 3-25). In addition, I used Feret's diameter (the distance between two perpendicular planes restricting an object's diameter) to quantify observed differences in these non-circular plants. No

statistical analyses were possible as n<6, quantifications are thus only indicative of presented data from 4 plants per genotype.

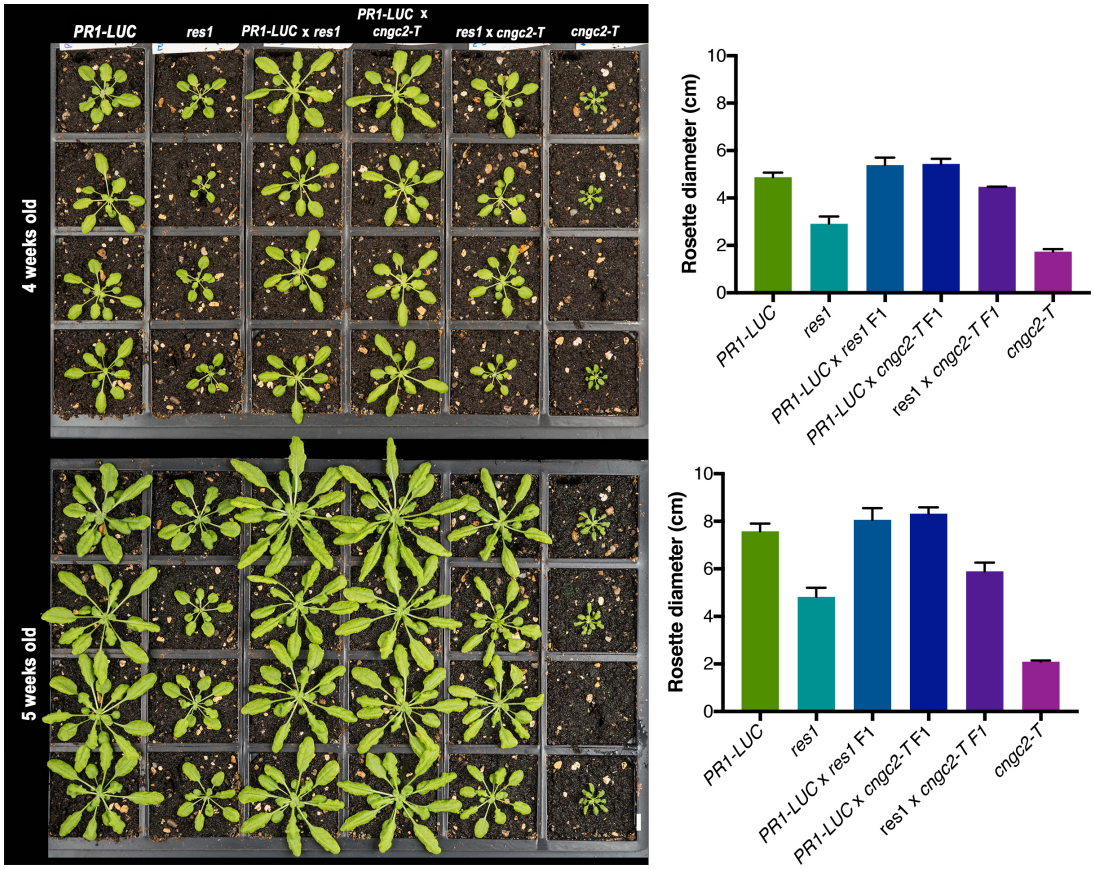

Figure 3-25 Adult rosette phenotype of *res1* x *cngc2-T* F1 plants– 4- and 5-week old plants from F1 allelism crosses are presented, along with quantification of rosette size. No statistical analyses were carried out due to small sample size however graphs are included to show representative size variation between the lines tested (Feret's diameter as measured through ImageJ). Bars represent S.E.M. n=4.

From observation of adult rosettes, both *res1* and *cngc2-T* plants maintain a smaller rosette than WT. *cngc2-T* plants are even more severely dwarfed, as shown previously. In the F1 *cngc2-T* x *res1* cross, plants appear moderately smaller than WT but not as small as either *res1* or *cngc2-T* alleles. Whilst this provided routes for further investigation into genetic interactions, the initial confirmation of allelism led me to conduct a more in-depth analysis of complementation using *Agrobacterium* mediated transformation of *res1* plants with *CNGC2*$^{(WT)}$.

3.2.15 Creation of transgenic lines to assess complementation of *res1* with *CNGC2*

To confirm complementation of *res1* with *CNGC2*, I introduced the WT variant of this gene both under its native promoter as well as under the CaMV 35S constitutive promoter and assessed phenotypic characteristics of the resultant transgenic plants.

Using Col-0 genomic DNA (gDNA), I amplified WT *CNGC2* both with and without a 1.3Kb native promoter by PCR and inserted it into the entry vector, pENTR/D-Topo. Following confirmation of successful insertion of the full-length construct via restriction digest and sequencing, I transferred this construct into the gateway binary vectors, pGWB604 with C-terminal GFP and pB7FWG2, Cauliflower Mosaic Virus (CaMV) 35s promoter and C-terminal FLAG epitope (DYKDDDDK).

In addition to WT gDNA, I cloned *CNGC2* from *res1* in the same manner as above for future phenotypic comparisons. Final complementation constructs are depicted in Figure 3-26. Each binary vector cassette contained the BaR (BASTA resistance) gene as part of their plasmid cassette to enable herbicide-based selection of positive transformants. Successful gateway plasmids were confirmed and transformed into *Agrobacterium tumefaciens* for transformation via floral dip.

Following gateway cloning, I transformed *res1* and *cngc2-T* mutant lines and collected T0 seeds for BASTA selection.

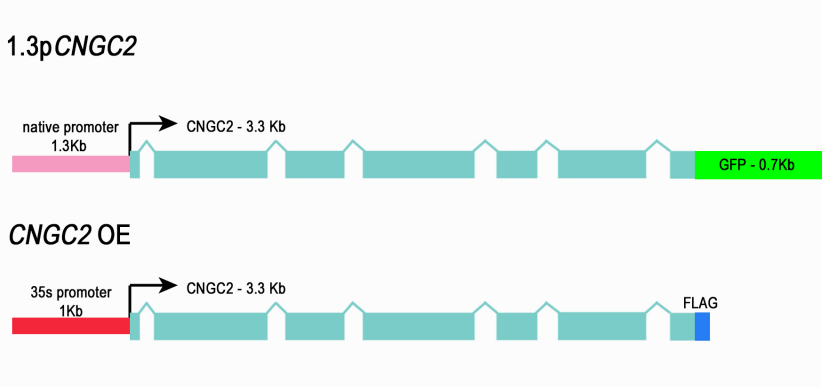

Figure 3-26 Complementation constructs made through gateway cloning – WT CNGC2 was amplified with or without its native promoter and cloned into GWB vectors in order to enable addition of selective marker genes as well as detectable C-terminal labels (GFP/ FLAG).

Following transformation, I germinated first transgenic generation (T_1) seedlings at 20°C LD before spraying with BASTA to identify positively transformed individuals.

These plants were pricked out and transgene copy number determined by qPCR measurement of BaR gene expression [257] in T_1 Transgenics by iDNA genetics. A summary of copy number of transgenic lines generated can be seen in Table 3.

After collection of seeds from positively identified lines with single insertions of the transgene (Single Insertion Lines, SILs), this process was repeated in the next (T_2) generation to determine homozygous lines for each construct using copy number analysis as before and plants grown on to collect T_3 seeds. I characterised phenotypes of identified SIL transgenic plants in T_2 and T_3 generations to assess phenotypic complementation of *res1* with *CNGC2*$^{(WT)}$.

Table 3 Copy number in T_1 transgenic lines created to characterise complementation of *res1*

Background	Construct	# lines generated	# SILs identified
res1	1.3p*CNGC2*	23	9
res1	*CNGC2* OE	24	8
cngc2-T	1.3p*CNGC2*	19	11
cngc2-T	*CNGC2* OE	16	9

3.2.16 Growth and immune phenotypes of *res1* are complemented through overexpression of *CNGC2*

Following identification of several independent SIL transgenic lines, I next aimed to determine whether complementation of *res1* had been achieved through characterisation of both growth and defence phenotypes. Since *res1* was isolated through its high temperature-resilient *PR1-LUC* expression, I began characterisation of transgenic lines in the *res1* background through assessing flg22-induced expression of *PR1-LUC* at both 22 and 27°C.

I grew seeds from five 1.3p *CNGC2* lines and three *CNGC2 OE* lines for 7 days at 22°C before shifting to 27°C or maintaining at 22°C for a further three days and inducing with 100 nM flg22. Following addition of luciferin, I quantified luciferase expression at 18-20 hpi using the Photek HRPCS-3 as before. Luminescence data was normalised

to seedling area in order to compare lines. Normalised *PR1-LUC* expression of two representative 1.3p *CNGC2* lines and three *CNGC2 OE* lines is depicted in Figure 3-27.

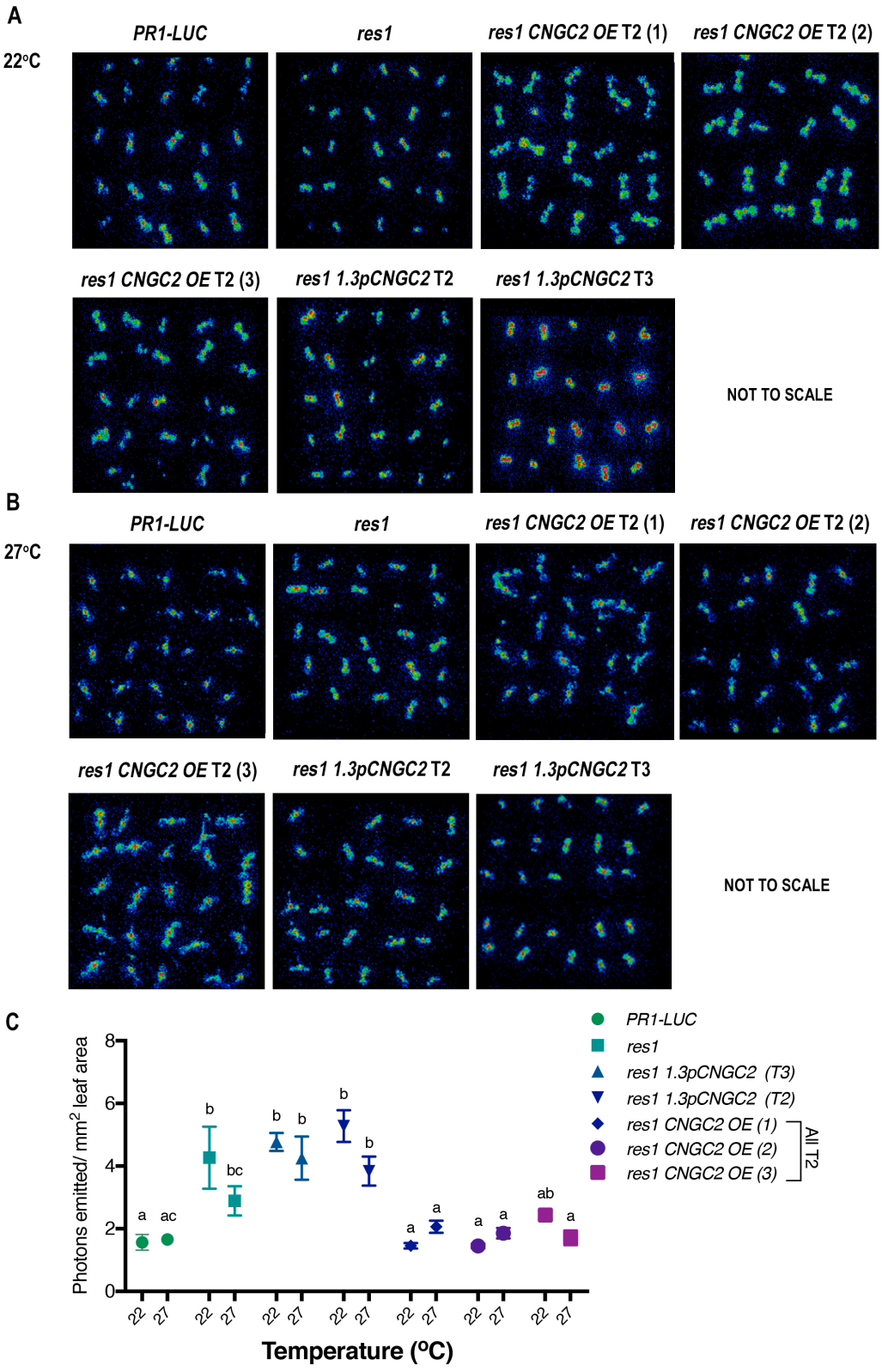

Figure 3-27 *PR1-LUC* expression of transgenic lines – T2/ T3 seedlings were grown under mutant screen conditions at 22 (A) or 27 (B)°C. Pictures are to best estimate of scale. (C) Quantification of *PR1-LUC* expression

per mm^2 per seedling is depicted. Statistical analysis conducted – Two-way ANOVA followed by Tukey's post-hoc test, n=20-50 seedlings per line.

From these data, both native promoter lines (1.3p*CNGC2*) clearly display robust expression of *PR1-LUC* in line with *res1* plants following induction with flg22 at both 22 and 27℃ (Figure 3-27 A-C). Transformation of *res1* with *CNGC2* under its native promoter is not sufficient to complement its high temperature-resilient luciferase expression phenotype.

For each line overexpressing *CNGC2* however, levels of flg22-induced *PR1-LUC* expression returned to WT levels at both temperatures tested (Figure 3-27A-C), showing full complementation. Strong phenotypic rescue by introduction of *CNGC2* OE into *res1* therefore confirms the SNP in *res1CNGC2* as underpinning this mutant's high temperature resilient defence gene expression. The necessity for overexpression in complementation of *res1* is not entirely unexpected given the semi-quantitative behaviour already observed in this mutant. In addition, a similar case has been presented recently in a group IV CNGC mutant, where overexpression was also necessary to complement a hypomorphic *CNGC2* mutant allele [258].

Following confirmation of complementation of *PR1-LUC* expression, I set out to assess reversion of *res1*'s growth defects in transgenic lines. To determine whether the dwarf stature and reduced thermosensory elongation growth of *res1* was complemented by overexpression of *CNGC2*$^{(WT)}$ I grew seedlings from each line as before according to screen conditions at 22 or 27℃ and conducted hypocotyl length measurement with ImageJ. To see if any effect of native promotion of *CNGC2* reintroduction could observed on growth I included 1.3p*CNGC2* lines as before.

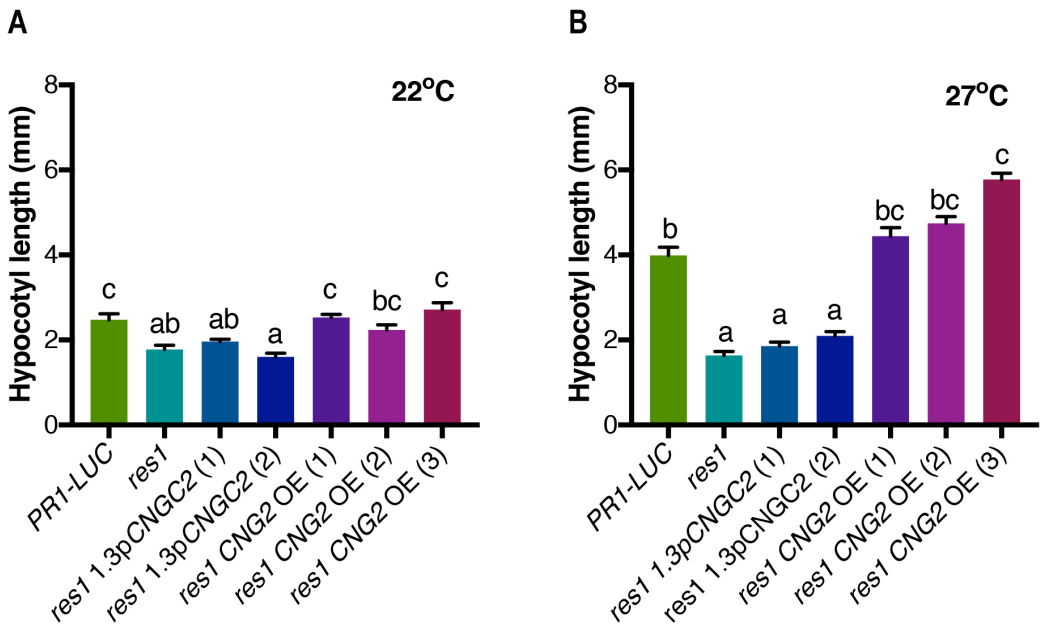

Figure 3-28 Hypocotyl length of *CNGC2,* native promoter or overexpressor lines – T_2/T_3 seedlings were grown constantly at 22°C (A) or shifted to 27°C three days prior to measurement (B). All OE lines presented, plus 1.3p*CNGC* (2) are in the T_2 generation, 1.3 (1) is in the T_3. Statistical analyses carried out: Kruskal-Wallis one-way analysis of variance followed by Dunn's post-hoc multiple comparisons test (n=13-44).

Seedlings from each 1.3p*CNGC2* line tested here showed hypocotyl length akin to that of *res1* at both 22 and 27°C (Figure 3-28 A, B). This suggests that the native promoter *CNGC2* construct failed to complement hypocotyl elongation of *res1* as well as *PR1-LUC* expression. Overexpression of *CNGC2* successfully complemented this mutant however, which is evident through robust hypocotyl elongation at both temperatures tested. There is also a strong thermosensory elongation response following temperature upshift, similar to that of WT plants. In one line (*res1 cngc2* OE (3)), a stronger elongation response than WT could be observed at 27°C, which suggests a hyper-thermoresponsive phenotype. In addition to the ability of *CNGC2* OE to complement *res1,* this implicates CNGC2 as playing a role in thermosensory hypocotyl elongation, and potentially thermosensory responses in general. Increasing expression of this channel may thus increase sensitivity of plants to increases in ambient temperature. Further characterisation of these lines will be necessary in order to confirm this effect and the role of CNGC2 in coordination of thermosensory responses in general.

Growth of both native and overexpression *CNGC2* lines at 20°C LD for seed collection further revealed phenotypic differences between *res1* 1.3p*CNGC2* and *res1 CNGC2* OE lines in terms of growth and development (Figure 3-29).

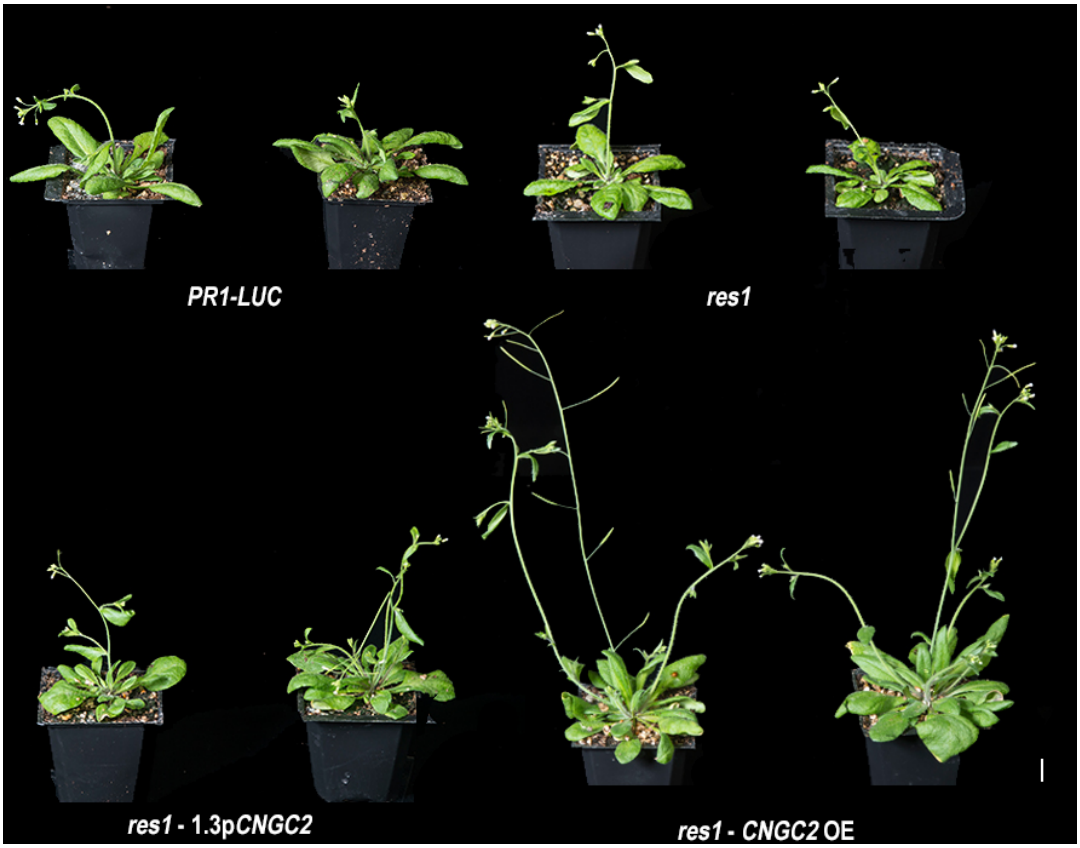

Figure 3-29 Initial characterisation of T2 phenotypic complemented line growth phenotypes – Plants grown at 20°C LD conditions. Two representative plants shown for one line for each construct in comparison with WT (*PR1-LUC*) and *res1* mutant plants grown under the same conditions. Scale bar = 1 cm.

OE lines appear to show accelerated transition to flowering compared to any other line. Phenotypic differences between WT, *res1* and 1.3p*CNGC2* lines are not apparent at this stage, under LD conditions (Figure 3-29).

I have now confirmed how, in terms of *PR1-LUC* expression, hypocotyl length and other growth and developmental phenotypes, overexpression of *CNGC2* robustly complements *res1.*

To validate and expand my observations, I next carried out hypocotyl length quantification in the next generation of *res1 CNGC2* OE lines alongside *cngc2-T* and its complemented line. I also included *snc1-1* seedlings as a representative

thermosensitive autoimmune mutant for comparison with both alleles of *cngc2* and their complemented lines.

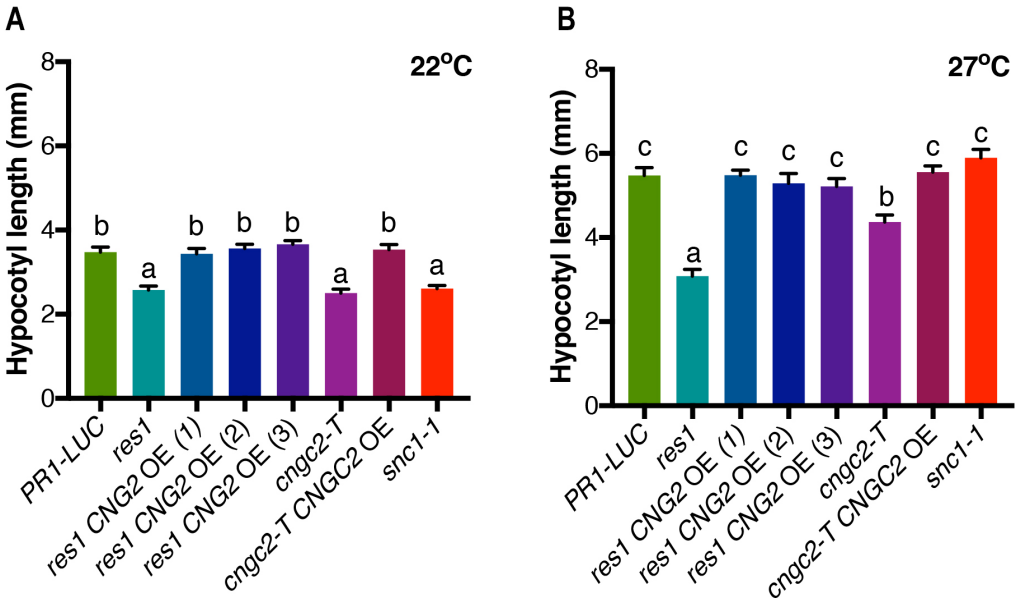

Figure 3-30 Hypocotyl length of transgenic seedling lines grown at 22 or 27°C - Seedlings were grown constantly at 22°C (A) or shifted to 27°C three days prior to measurement (B**)** Statistical analyses carried out - one-way ANOVA carried out for each temperature dataset, followed by Tukey's post-hoc test n= 13-26.

In agreement with what I have previously observed for these lines in the T_2 generation, hypocotyl length of *res1* was successfully complemented by *CNGC2* OE constructs (Figure 3-30A, B). In this experiment, *cngc2-T* seedings showed a thermosensory elongation response of 70% to increase in temperature (Mann-Whitney U test, P<0.0001) but remain short compared to WT plants at both temperatures. In comparison, *res1* shows just a 20 % increase (MWU, P=0.03) , a response which was successfully complemented by the *CNGC2* OE construct. *snc1-1 shows* severely short hypocotyls equivalent to those of *res1* and *cngc2-T* at 22°C (Figure 3-30A) but returned completely to WT at 27°C (Figure 3-30B). Comparison of *snc1-1*with both *cngc2* mutants further establishes the lack of typical thermosensory responses in plants deficient in CNGC2 function.

To complete characterisation of growth phenotypes in transgenic *res1* lines, I grew plants from each line under constant 22 or 27°C SD conditions for 4 weeks to document adult rosette phenotype.

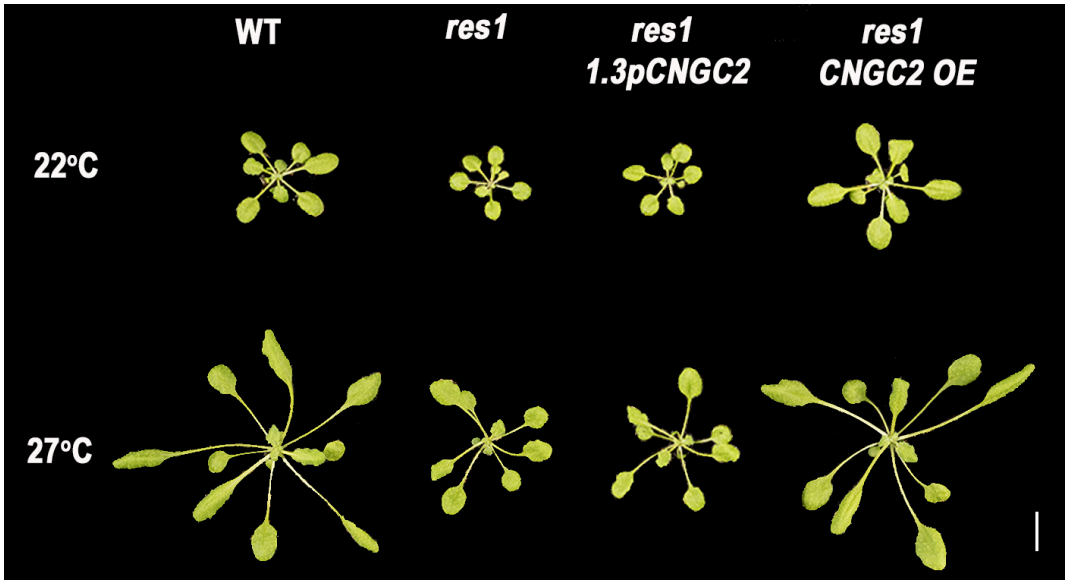

Figure 3-31 Adult rosette phenotypes of complemented *res1* lines – representative plants from each line grown constantly at 22 or 27°C SD. Scale bar = 1 cm.

Figure 3-31 demonstrates the inability of *CNGC2* under its native promoter to complement the adult growth phenotypes of *res1* and overexpression results in a complete reversion of the stunting and thermosensory growth defects.

All the data presented above shows that, when overexpressed, *CNGC2* can fully complement the *res1* phenotypes. To further validate immune responses of complemented adult plants, I characterised resistance to *Pto* DC3000 in one selected line for each of the *1.3pCNGC2* and *cngc2* OE lines. I grew 5-6 plants from each line for 4 weeks at 22°C as before, before either maintaining them at this temperature or shifting them to 27°C and challenging them with *Pto* DC3000 for three days.

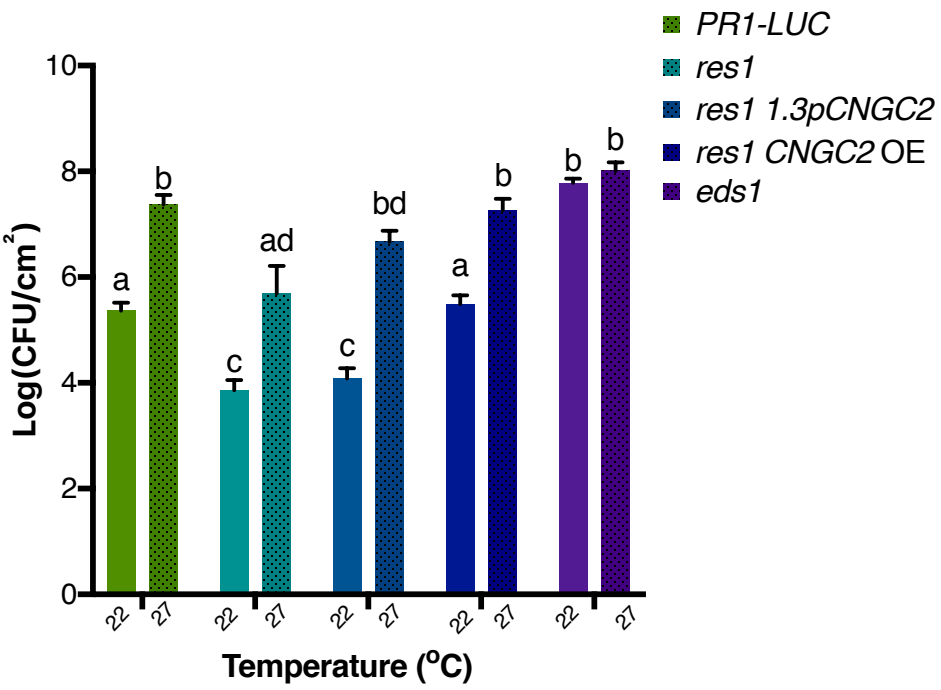

Figure 3-32 Resistance of complemented *res1* plants to *Pto* DC3000 at 22 and 27°C – 4-week old plants grown at 22°C SD and shifted to 27°C or maintained at 22°C for a further three days before being infected with *Pto* DC300 for three days and bacterial CFU measured per cm^2 leaf area. Data presented are overall average values over three experimental repeats, each with n= 5-6 plants per genotype per treatment. Statistics conducted - 2-way ANOVA plus Tukey's post-hoc test.

These data show that *res1* maintains strong resistance to *Pto* DC3000, compared to WT plants, at both 22 and 27°C. Resistance levels of the 1.3p*CNGC2* line were comparable with *res1* at both temperatures, whereas *res1 CNGC2* OE reverted back to WT levels of resistance, confirming the complementation of *res1* adult plant resistance with overexpression of *CNGC2*. In addition to verification of the allelism of *res1* and *cngc2-T,* these data reflect overall confirmation of complementation in OE lines, and confirm pathogen resistance follows both growth and *PR1-LUC* expression.

Whilst *cngc2-T* and *res1* have been shown to be allelic, the precise nature of the mechanism through which RES1 modulates growth and defence for different growth stages and under different environmental conditions remains to be elucidated.

Further study on the role of calcium channel dynamics in thermosensory responses through characterisation of the effects of different allelic variants on protein function will enable a more in depth understanding of the mechanism through which CNGC2 simultaneously influences growth and defence in plants. To begin further characterisation of the interaction of CNGC2 with known aspects of plant

thermosensory growth and defence coordination, I investigated the interaction of this channel with the SNC1-mediated pathway.

3.2.17 SNC1 and CNGC2 additively affect autoimmune phenotypes in deficient mutants

SNC1 has been implicated in the growth-defence trade-off in a highly thermosensitive manner through study of *snc1* autoimmune mutants such as the gain-of-function allele, *snc1-1* [141,143]. I have now identified a distinct pathway which functions in similar processes and is sensitive to temperature changes. In comparison with SNC1, an intracellular NB-LRR protein [194], CNGC2 is known as a trans-membrane calcium channel and thus functions through modulating calcium signalling [113]. These two diverse regulatory pathways have previously been implicated as interacting, where SNC1 protein acts with transcriptional co-repressor TPR1 to suppress *CNGC2* expression and activate R-gene mediated immunity [236]. To investigate the interaction between these SNC1 and CNGC2 I carried out a series of crosses between *snc1-1*, *res1* and *cngc2-T*. If a lack of phenotypic enhancement is observed in these crosses, it could be hypothesised that both molecules act exclusively within the same pathway.

To investigate the ability of alterations in *SNC1* to enhance *res1* or *cngc2-T* mutant phenotypes, I crossed the gain-of-function mutant *snc1-1* to both of these lines. I examined plants in the F2 generation for signs of enhanced phenotypic abnormalities characteristic of autoimmune mutants, such as senescence and stunting of growth.

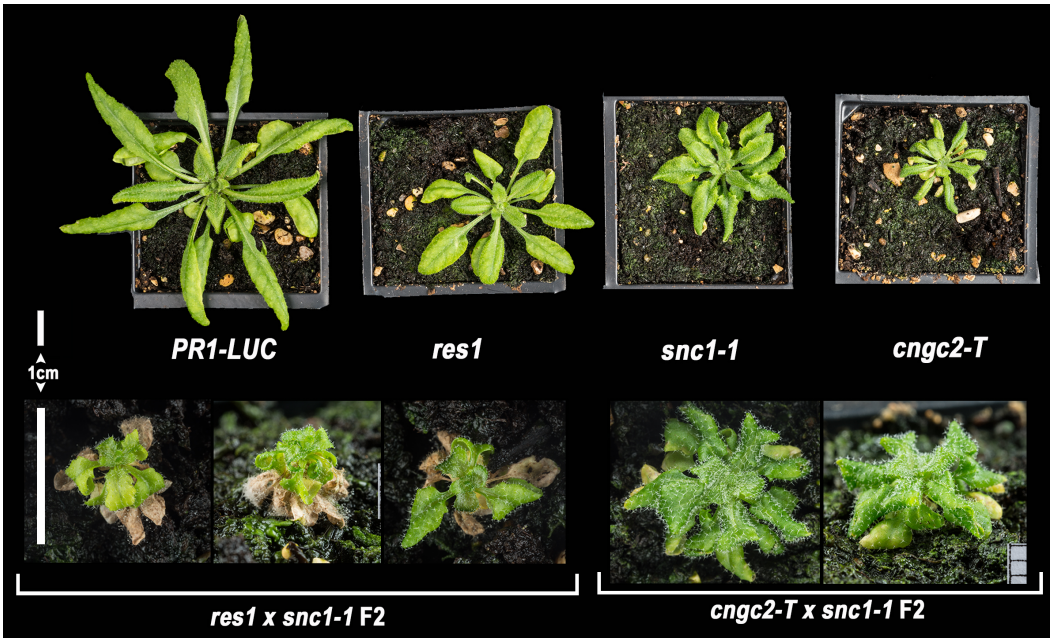

Figure 3-33 Adult phenotypes of *cngc2* x *snc1-1* potential double mutants – 6-week-old WT, *res1, snc1-1* and *cngc2-T* single mutants scale bar = 1cm; possible *res1* x *snc1-1* double mutants and heterozygous double mutants for *cngc2-T* x *snc1-1*, scale bar = 1 mm.

Genotypic confirmation of homozygous double mutants was not possible due to growth and survival rates of putative double mutants. However, I was able to document observed phenotypes of these putative mutants from the segregating F2 lines which displayed signs of enhanced autoimmunity compared to single mutants (Figure 3-33). From these plants, we can see that *res1* and *cngc2-T* very strongly enhance *snc1-1* phenotype, both in terms of stunting and leaf senescence. It appears that plants with enhanced phenotype are less severe in *cngc2-T* x *snc1-1*compared to those observed for *res1* x *snc1-1*. It is likely that, because this allele represents a total loss of *CNGC2* function in comparison to *res1*, the double mutant phenotype may have resulted in lethality at a very early growth stage. Therefore, the identified plants represent heterozygotes for the *snc1-1* mutation. Some residual *CNGC2* function in *res1* may have thus enabled these mutants to survive where *cngc2-T* double mutants did not. This remains to be confirmed, but an enhancing effect of *snc1* gain of function can clearly be seen in both cases. This suggests a role for SNC1 in mediating autoimmunity in both CNGC2 dependent and independent manners. Similar roles for this protein have previously been highlighted in terms of its regulation of SA dependent and independent pathways [142]. Likewise here, a role for

CNGC2 in coordination of SNC1-mediated immunity cannot be ruled out (Figure 3-34).

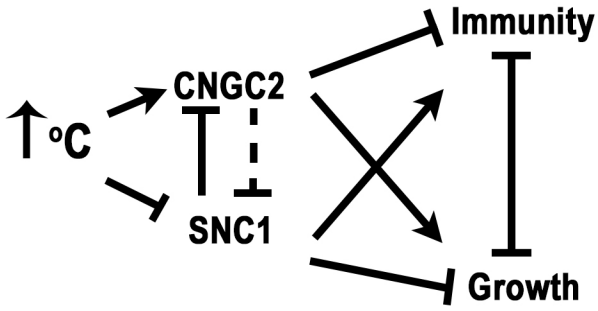

Figure 3-34 Hypothetical model of CNGC2 and SNC1 interaction and distinct methods of growth and immune regulation

Whilst there is known overlap between CNGC2 and SNC1-mediated pathways, I have shown how both play distinct roles in regulation of thermosensory responses including autoimmune suppression (Figure 3-34).

Aside from its potential associations with known regulatory components such as SNC1, the primary mechanism through which CNGC2 coordinates growth and defence is through calcium signalling and thus initiation of global, simultaneous downstream responses to temperature changes.

I have now sufficient evidence to show a lone polymorphism in *CNGC2* affects the function of this gene and results in a lack of thermosensory outputs observed in *resilient1* plants. This novel allele of *CNGC2* may provide an additional tool with which to understand *CNGC2* functions, particularly with respect to its role in coordination of calcium signalling for the ambient temperature responses.

3.2.18 The role of CNGC2 in modulation of environmental responses

The identification of a novel allele of CNGC2, in *res1,* has implicated this channel in managing ambient temperature as well as its previously recognised independent roles in coordination of immunity [246,259,256] and response to heat shock [107]. The precise mechanisms through which this channel receives temperature information and transduces appropriate signalling responses in order to bring about plant phenotypic changes is yet to be determined.

CNGCs were initially identified as membrane-bound transporters of mono or divalent cations such as Na^+, Ca^{2+} and K^+ [260] however their role in coordination of signalling in response to environmental changes or stress is thought to be primarily through calcium signalling [259,261].

Accurate spatial and temporal control of transient increases in cytosolic or organellar calcium concentration by CNGCs and other Ca^{2+} channels enable signalling and initiate appropriate downstream responses to many external environmental cues [67,262-264]. Maintenance of a calcium gradient between cellular compartments is necessary in order to generate these messages. Disruption of calcium transport mechanisms can therefore dampen or alter responses to a vast range of environmental signals. In *cngc2* mutants, calcium signalling is thought to be deregulated, but precisely how this affects downstream responses is not yet understood. The constitutive lesions and necrosis brought about by lack of functional CNGC2 are thought to be due to overaccumulation of calcium in the apoplast [265] resulting from a lack of Ca^{2+} transport into the cytoplasm [113]. CNGC2 is thought to interact with another calcium channel, CNGC4. Consequently, other studies have alluded to a lack of CNGC2 resulting in a hyperaccumulation of calcium due to a "leaky" channel and thus toxicity within cytoplasm [258,266] due to the absence of essential heteromeric interactions with the interacting channel, CNGC4 [256]. Whether specific accumulation in different subcellular compartments underlies the autoimmune phenotypes of *cngc2* mutants is not yet known.

In support of the latter "leaky" calcium hypothesis however, deregulation of calcium homeostasis through heterologous expression studies using *CNGC18* in *E. coli* resulted in cells with a higher cytoplasmic Ca^{2+} concentration [267], and studies on *Arabidopsis* mutants have highlighted hypersensitivity to growth in high exogenous calcium [268]. Other studies showed a role for CNGC2 in calcium uptake of leaf cells near minor veins, thus suggesting phenotypic alterations of plants caused by mutations CNGC2 are rather caused by alterations in signalling than oversensitivity to Ca^{2+} [265].

Whilst CNGC2 therefore plays a role in the regulation of calcium dynamics, the mechanisms of activation in response to environmental changes are unknown. Several hypotheses have previously been put forward as to how temperature might directly influence CNGC2 activity.

Firstly, demonstration of a direct impact of temperature on CNGC2 function has been shown though the effects of altering membrane fluidity [110]. Changes in temperature have been shown to increase membrane fluidity and directly alter microdomain modelling in plasma and thylakoid membranes, thus enabling alterations in membrane component dynamics [269,100,270,110]. In addition, the direct interaction of pathogens with plasma membranes, through their use of effector secretion systems, provides a hypothetical mechanism whereby pathogens directly affect plasma membrane dynamics and thus initiate association of signaling components.

Previous studies on *cngc2* and *cngc4* mutants in *Arabidopsis* have confirmed that loss of function of either gene has similar consequences on plant growth, development and thermotolerance as a result of perturbations in calcium homeostasis and signalling [256,99]. Although no direct biochemical evidence has been shown, CNGC2 and CNGC4 are thought to function non-redundantly, both in homomeric and heteromeric tetramers. A lack of both channels results in a severe, occasionally lethal double mutant, termed "super-*dnd*" [256,271]. Interaction of CNGC2 with CNGC4, or other membrane components, could thus play a crucial role in appropriate cytoplasmic releases of Ca^{2+} in a temperature-dependent manner[107,256,265]. In addition to membrane-associated interactions, activation of CNGCs is brought about by associations with cytoplasmic regulators such as cyclic nucleotides and calmodulin [272,107,247,256]. Alterations in binding of calmodulin or other post-transcriptional modifications [268,273] could therefore represent avenues for intra-cytoplasmic modulation of channel function and therefore are potential mechanisms to modulate calcium signalling in response to environmental changes or biotic interactions.

Since the precise mechanism of CNGC2 regulation is unknown, it is unclear at this stage what the specific effects of the *res1* mutation channel function are. So far however, the indication of *res1* as a novel allele of *CNGC2* suggests changes in

calcium signaling are responsible for alterations in plant architecture as well as suppression of immunity at elevated ambient temperature. Previously, calcium channels such as CNGC2 have been implicated as direct sensors of temperature through plasma membrane alterations [107,274]. Such an interaction would allow influx of calcium in response to temperature and initiate and its downstream effects such as expression of HSP genes alongside growth and defence coordination in plants. Lack of function of CNGC2 therefore may allow unregulated influx of apoplastic calcium, thus preventing effective temperature responses.

3.2.19 Sensitivity of *CNGC2* mutants to exogenous calcium

Previous studies have *cngc2* mutants are hypersensitive to growth in external calcium, due to perturbation of calcium conductance [265]. To determine whether *res1* is similarly hypersensitive to exogenous Ca^{2+} increases, I established a hydroponic system to test the effects of increasing external calcium concentration on growth of *cngc2* mutants.

To achieve this, I sterilised seeds before stratifying and germinating on ½ MS +0.5% sucrose agar. Following germination, I transferred young seedlings to ½ MS +0.5% sucrose media in six-well plates with increasing concentrations of $CaCl_2$(Figure 3-35 B). 10-12 seedlings per genotype were grown in media supplemented with 10, 25, 50 or 100 mM $CaCl_2$ for 10 days, visible phenotypes were documented and average seedling weight per concentration calculated (Figure 3-35 A-C).

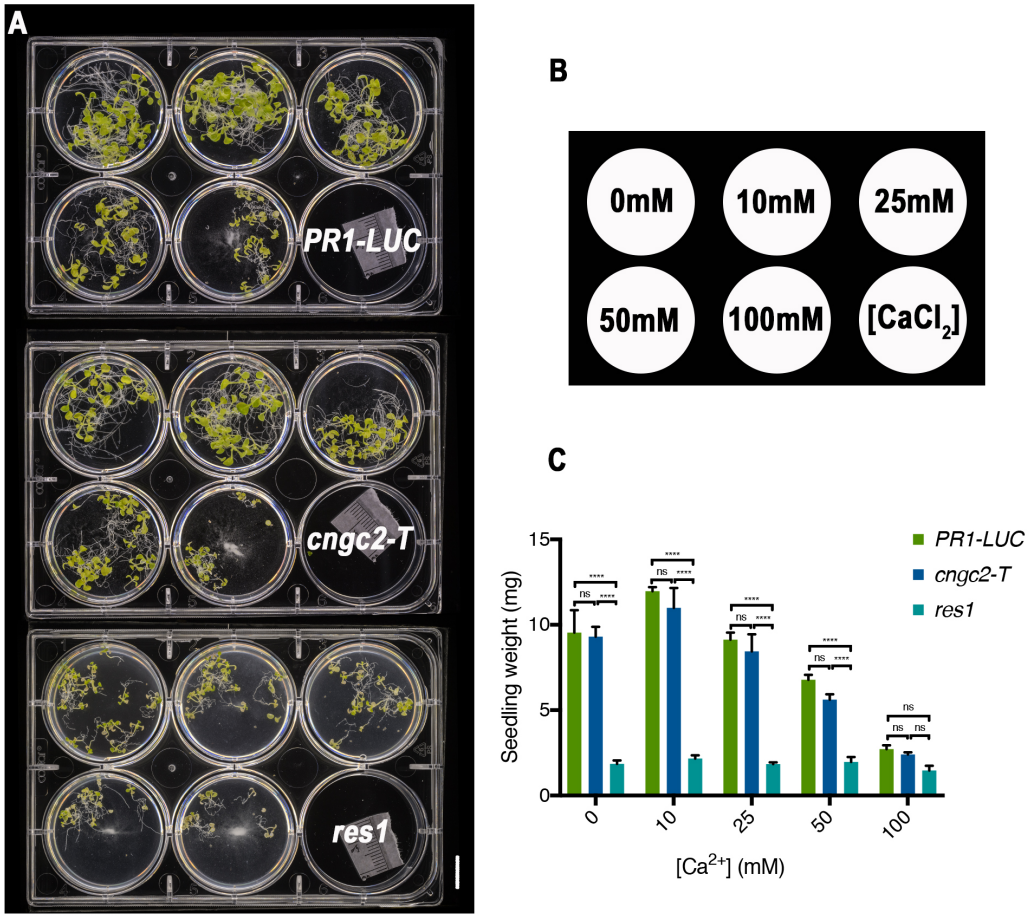

Figure 3-35 Inhibition of growth by exogenous calcium application in *cngc2* mutants – Seedlings grown for 10 days hydroponically in ½ MS = 0.5% sucrose with 0, 10, 25, 50 or 100 mM supplemental calcium chloride. (A) growth phenotypes of seedlings pictured after data collected. (B) layout of plates with increasing calcium concentration (C) quantification of seedling fresh weight. Statistics used – 2-Way anova between genotypes for each concentration followed by Tukey's multiple comparisons test n=4-7 bulk replicates of ~20 seedlings. Bulk weights of seedlings were divivded by number weighed in order to gain multiple readings for averge seedling weight. Comparison between concentrations was not conducted.

Whilst previous studies have shown *cngc2* null mutants to have an increased sensitivity to growth in external calcium, I found no significant effect of exogenous calcium application on growth in *cngc2-T* seedlings. In addition, *res1* seedlings showed severe growth retardation even without exogenous calcium application, suggesting a negative impact of hydroponic growth conditions on *res1*, regardless of calcium. This suggests a necessity for optimisation of the hydroponic experimental conditions used. In their study, Wang et al (2017) [265] showed an apparent alleviation of dwarfing in *CNGC2* mutants grown in hydroponic systems compared to those grown on soil [265], further advocating a need to optimise experimental growth conditions in the future. Future investigations of sensitivity of these mutants to exogenous calcium under both hydroponic and soil-based conditions will enable a

more comprehensive understanding of channel perturbation effects in *cngc2* and *res1* mutants.

Contradictory evidence of the effect of Ca^{2+} conductance in *cngc2* plants [256,265], means it is still not possible to determine the mechanism through which loss of CNGC2 function affects downstream signaling. It can however be concluded that, loss of function of this channel results in dysregulated calcium conductance and thus dampened thermosensory growth and defence responses.

To further understand how *res1* as an allele of *CNGC2* governs thermosensory responses in plants and thus coordinately promotes growth and suppresses defences at high temperature, I subsequently characterised the precise effects of the SNP in *CNGC2*$^{(res1)}$ on channel function.

3.2.20 Consequences of *res1* mutation

From the observations I have made so far, it is likely that the presence of CNGC2$^{(res1)}$ prevents effective thermosensory calcium signalling and downstream responses of thermomorphogenesis and TSI. I therefore aimed to understand the location, nature and potential functional impact of the non-synonymous polymorphism in *CNGC2*$^{(res1)}$.

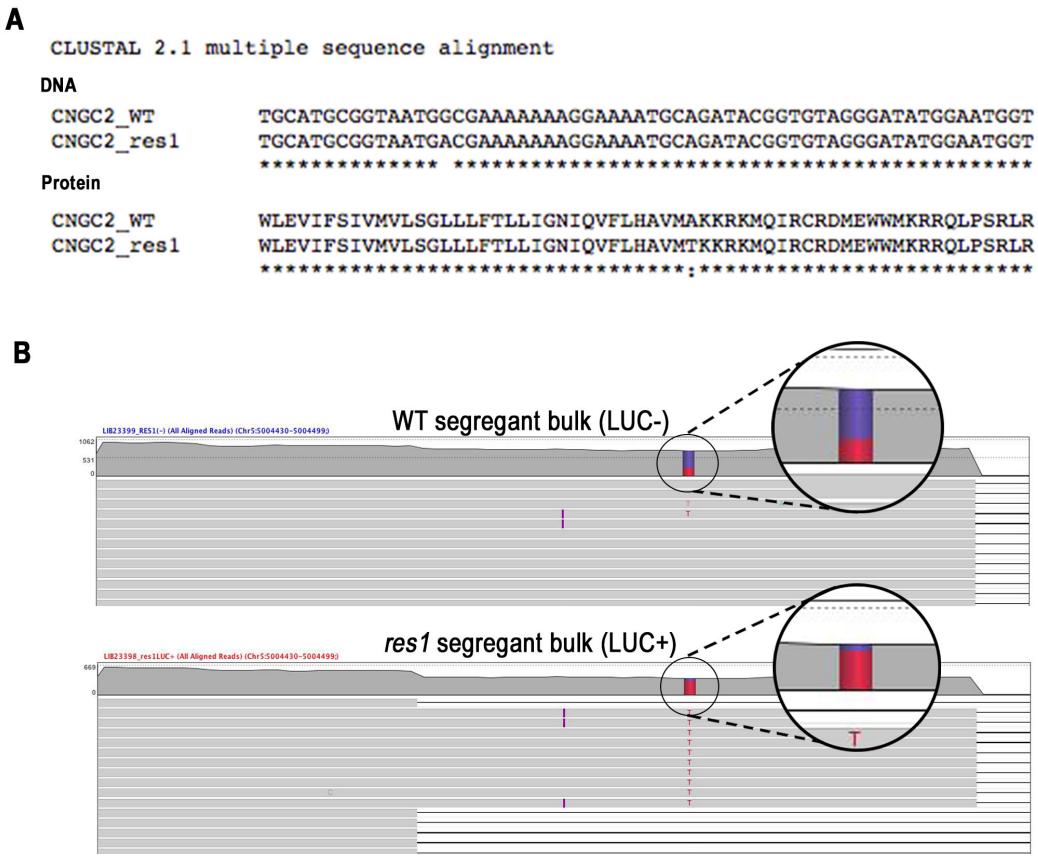

Figure 3-36 DNA and protein sequence alignment and RNA-sequencing of *CNGC2*$^{(WT)}$ and *CNGC2*$^{(res1)}$ – (A) ClustalW multiple sequence alignment of WT and *res1 CNGC2* nucleotide and CNGC2 protein sequences, with * denoting nucleotides or amino acids conserved between alleles (B) screenshot from Avadis NGS of RNA sequencing data from bulk segregant populations, highlighting the frequency of the *res1* G-A (C-T) SNP in WT or *res1* populations. Complementary sequences are shown since CNGC2 is on the Crick strand.

As previously identified, *res1* plants contain a non-synonymous SNP in *CNGC2* resulting in an A457-> T amino acid substitution (Figure 3-36A). This mutation is positively associated with the *res1* bulk segregant population of RNA (Figure 3-36B). The Alanine to Threonine amino acid substitution is significant as it represents the substitution of an amino acid from a non-phosphorylatable residue to a phosphorylatable one. This substitution could affect localisation, turnover, confirmation or interaction of this CNGC2 with other molecules [275], which could significantly influence function.

To test whether 457T represents a novel phosphorylatable residue in *res1*, I inspected the phosphorylation potential using NetPhos[276].

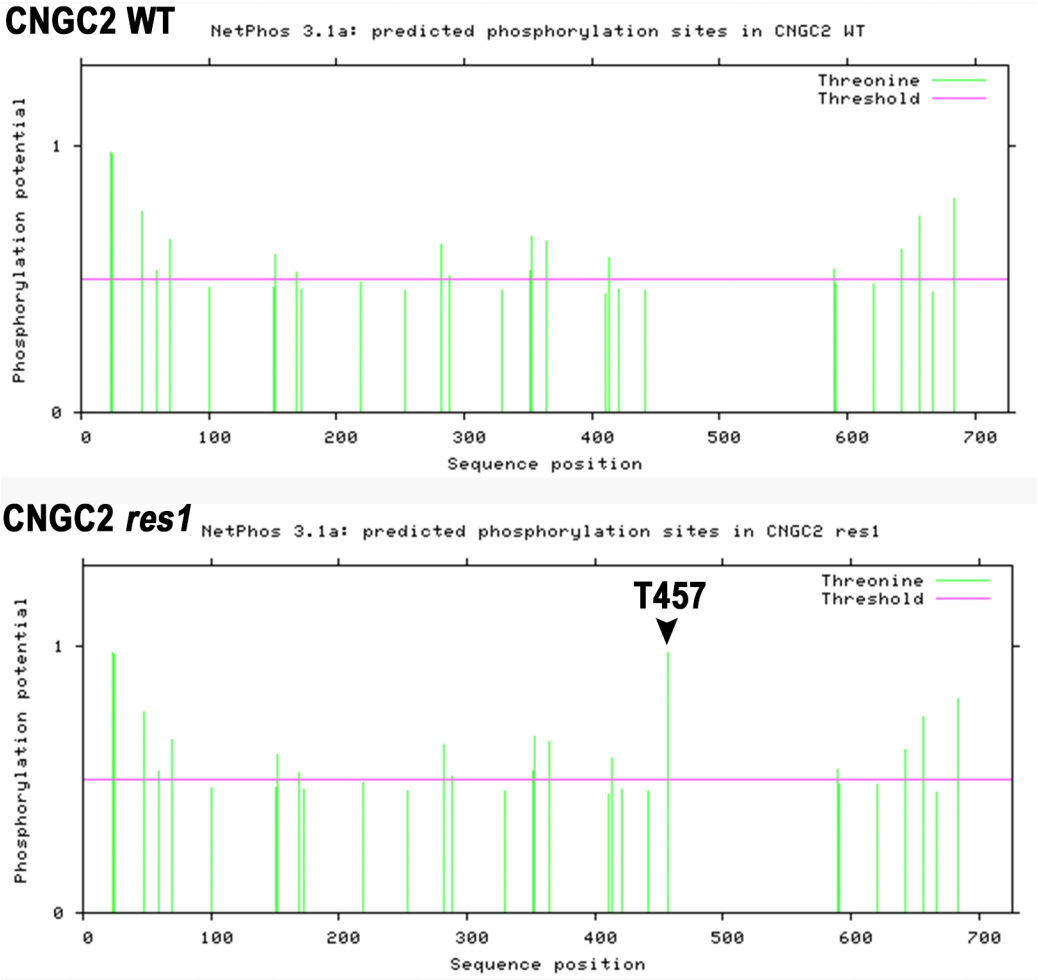

Figure 3-37 NetPhos prediction of threonine phosphorylation potential across CNGC2$^{(WT)}$ and CNGC2$^{(res1)}$ - Phosphorylation potential threshold (pink line) shows a novel phosphorylation site in *res1* (green line, arrowhead) which is absent in CNGC2$^{(WT)}$, (http://www.cbs.dtu.dk/services/NetPhos/).

The *res1* amino acid substitution is predicted to result in a novel potential phosphorylation site in CNGC2 which is absent in WT (Figure 3-37). The altered potential for phosphorylation of this could represent one of the key alterations of CNGC2 causing disruption of function in *res1*. Whether or not CNGC2^{res1} is phosphorylated remains to be experimentally tested.

In addition, the site of this polymorphism could affect the interaction of CNGC2 with other signalling components. The A457T substitution in CNGC2 could also affect association with CNGC4 [256] in addition to affecting binding of regulatory factors such as Calmodulin [273] or cyclic nucleotides [277]. Maintenance of specific residues and motifs in the intracellular region of CNGCs have been shown to be important for effective interaction of CNGC11 and 12 with regulatory factors [278,272]. In order to

understand other potential effects of the SNP on CNGC2(res1), I aimed to determine the topological location of this amino acid substitution.

To understand the mutation in *res1* in its functional context, I used the web-based prediction programme, TOPCONS to predict the topology of CNGC2 and determine the location of the A457T substitution [279](Figure 3-38A).

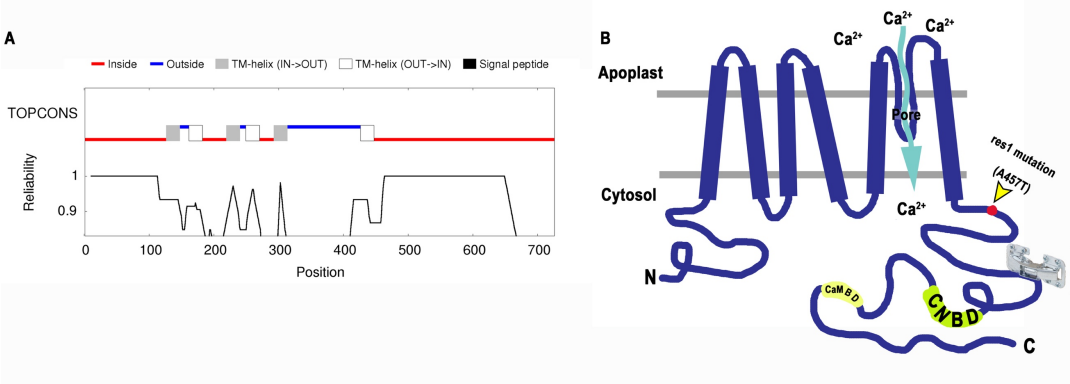

Figure 3-38 AtCNGC2 topology (A) TOPCONS - consensus topological prediction of CNGC2 structure (B) Structural model with Calmodulin binding domain (CaMBD), cyclic nucleotide binding domain (CNBD) and the location of the amino acid substitution in *res1* highlighted.

Like other CNGCs [232], CNGC2 is predicted to have 6 alpha-helical transmembrane domains and a long cytosolic C terminus, containing both the IQ domain responsible for binding calmodulin [272,280] and a phosphate-binding cassette (PBC) which binds cyclic Nucleotide Mono Phosphates (cNMPs), responsible for channel activation, known as the cyclic nucleotide binding domain (CNBD) (Figure 3-38 B). The so called "hinge region" where beta sheets enclose a pocket for cyclic nucleotides (cNMPs) to bind [281] is responsible for modification of binding capability of cNMPs (specifically cAMP and cGMP) [282,283](Figure 3-38B). The "hinge" region is distinct in group IV CNGCs [284], suggesting changes within this region could modulate function of CNGCs between different family members. Changes in the placement of hydrophobic residues have been shown to affect CaM binding within the CaMBD in CNGCs [273]. In particular, perturbing specific regions of the CaMBD of CNGC2 resulted in calcium hypersensitivity similar to that of *cngc2/4* [273], highlighting the potential effects of disruptions within this region on overall channel function.

In a recent study, Chiasson *et al* detailed a *CNGC* allele in *Lotus japonicus* with a SNP in the N-terminal cytosolic domain which conferred quantitative hypomorphic

qualities on this channel subunit. The unusual genetic behaviour of this CNGC allele necessitated overexpression of the WT version of this CNGC to complement plant phenotypes, similar to the observations I have made with regards to *res1*. These findings led them to hypothesise how the interaction ratio of the allele (*BRUSH),* with *CNGC$^{(WT)}$* is responsible for lack of complementation by a native promoter construct in a similar way to how overexpression was necessary to complement *res1* [258]. This led me to hypothesise whether a similar phenomenon could be observed in *res1*. The polymorphism in *res1* falls just inside the cytosolic C terminal region, close to the "hinge" region (Figure 3-38B). This mutation is at the opposing cytosolic end to the *BRUSH* mutation [258], but within the same region known to be important in the chimeric *cpr22 CNGC11/12* mutant [278]. Although the *L. japonicus BRUSH* allele is thought to be most closely related to CNGC11/12, genes which are phylogenetically relatively unrelated to CNGC2 [284], mutations in either of these channels in *Arabidopsis* brings about similar effects on plant phenotype to *cngc2/4* mutants and those in *L. japonicus BRUSH* mutants [247].

Perturbations in the region of the *res1* mutation could therefore affect any aspect of CaM or cyclic nucleotide binding as well as potentially affecting interactions of CNGC2 with other CNGC2 or CNGC4 subunits thus preventing homo or heteromeric channel formation. This remains to be tested in this mutant.

In addition to the potential modifications caused by a mutation in *res1* detailed above, a third mechanism for *res1* modulation of CNGC2 function was brought to light within the protein sequence of CNGC2. Just downstream from the mutation in *res1* a noticeable conserved nuclear localisation motif ((K/R)(K/R)(K/R)X) can be identified (Figure 3-36A). This is particularly notable since CNGCs have been long considered plasma membrane-localised as a result of initial studies of these channels in mammalian rod cells [256,285]. There is accumulating evidence however to show a lack of conservation of localisation of some of these channels between animals and plants. Aside from an initial homology study confirming similarities of mammalian and plant CNGCs in barley aleurone [286] no evidence exists to confirm a maintenance of localisation of CNGCs between kingdoms. It is not therefore surprising how recently a study identified a nuclear localised CNGC15 involved in symbiotic calcium

signalling in *Medicago truncatula.* From further scrutiny of this study, predicted nuclear localisation potential of MtCNGC2 can be observed [287]. The NLS identified in this species can be found in the same region in *Arabidopsis* which, in addition to functional studies of CNGC2 in Solanaceous plants, [248] suggests a high degree of conservation between species and thus potential for nuclear localisation of CNGC2 in *Arabidopsis*. Furthermore, the proximity of the nuclear localisation signal (NLS) to the mutation in *res1* (-7 amino acids) highlights another potential route for modification of this protein in *res1* and thus area for further characterisation in this study.

I therefore set out to characterise localisation of AtCNGC2 using CNGC2-GFP transgenic lines generated in this study.

3.2.21 CNGC2 localises to the plasma membrane as well as nuclear membrane and ER

To characterise the localisation of CNGC2 in Arabidopsis, I next used confocal microscopy to characterise GFP localisation in previously made transgenic lines.

In addition to the GFP-tagged 1.3p*CNGC2* lines, through the same process as before I was able to isolate lines overexpressing *CNGC2*$^{(res1)}$ with C-terminal GFP (*CNGC2*$^{(res1)}$OE). After growth of seedlings on plates at 20℃ LD I mounted seedlings on slides in water and used a Leica SPV confocal microscope to investigate GFP localisation. In native promoter lines, expression of GFP was not sufficient to pinpoint localisation of this protein, possibly due to low expression. Using the *res1CNGC2* OE line however, I was able to observe strong expression and localisation in a number of seedlings (Figure 3-39).

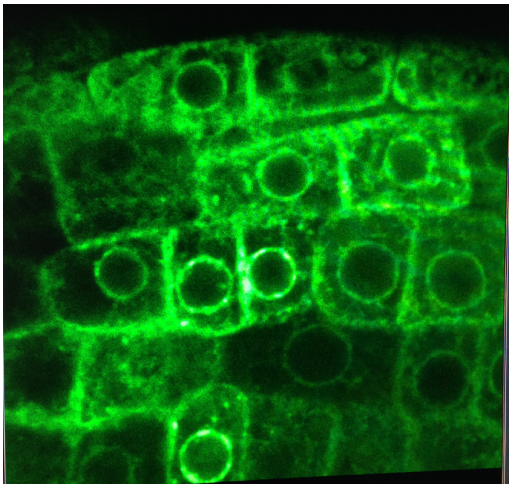

Figure 3-39 Characterisation of *res1*CNGC2-GFP localisation in *Arabidopsis cngc2-T* mutant seedlings – Root cell files imaged using Leica SPV confocal microscope. GFP localisation can be seen at potential NM/ ER locations in addition to PM.

Here, in *Arabidopsis* root cells, GFP can clearly be seen localised on nuclear membrane/ ER in addition to plasma membrane. An extensive search of existing literature also brought to light a study which showed similar localisation. Through characterisation of CNGC2-CaM associations, it is possible to identify possible nuclear/ ER-like structures in the CNGC2-YFP line presented in their study [273]. This is significant as it may mean mobilization of calcium is possible both from apoplastic stores as previously thought, but also between cytoplasm, nuclear membrane lumen or nucleus and thus affect the predicted mechanism of calcium signal generation by this channel. Whether localisation observed in Figure 3-39 is affected by, or as a result of, the *res1* mutation is yet to be determined.

3.2.22 *res1* contains a novel, stably expressed splice variant of *CNGC2*

Following my investigations into alteration in *res1*, I observed a feature of this mutant which led me to moderate the nature of additional transgenic lines I was in the process of making. In addition to the previously identified SNP, the RNA-seq data revealed the presence of an alternative splice form of *CNGC2* in *res1* LUC+ bulk segregants, which was consistently lacking 42bp flanking the region of the *res1* SNP (Figure 3-40 A). This splice variant possesses an in-frame deletion of 14 amino acids, including the putative NLS previously identified. The identification of a potential novel splice variant of this channel caused by the mutation in *res1* thus presents exciting possibility for novel modes of disruption of this channel.

A significant proportion of reads in *res1* segregants were consistent with this splice variant being specific to mutant *CNGC2* RNA (Figure 3-40 A, B). Of the total reads in this population, 75% were for full length *CNGC2* (SV1), and 24% were of the novel splice variant (SV2). Of the full length reads, a small proportion of reads (15%) in *res1* segregants were of the WT *CNGC2* allele, which is most likely as a result of bulk contamination with heterozygous plants which, as previously discussed, show an intermediate phenotype with incomplete penetrance and thus could have been misidentified as homozygotes during selection as *LUC+* (Figure 3-40C, D). Likewise, a small number of heterozygotes identified as WT bulk segregants have led to 30% of *LUC*- segregant mRNA reads containing the *res1* SNP and 9% of total reads as SV2 (Figure 3-40C, D). Considering the level of (unavoidable) cross-contamination (Figure 3-40D), if the *res1* mutation itself is initiating mis-splicing of *CNGC2*, SV2 could thus represent more than 1/4 total *CNGC2* mRNA in homozygous mutants.

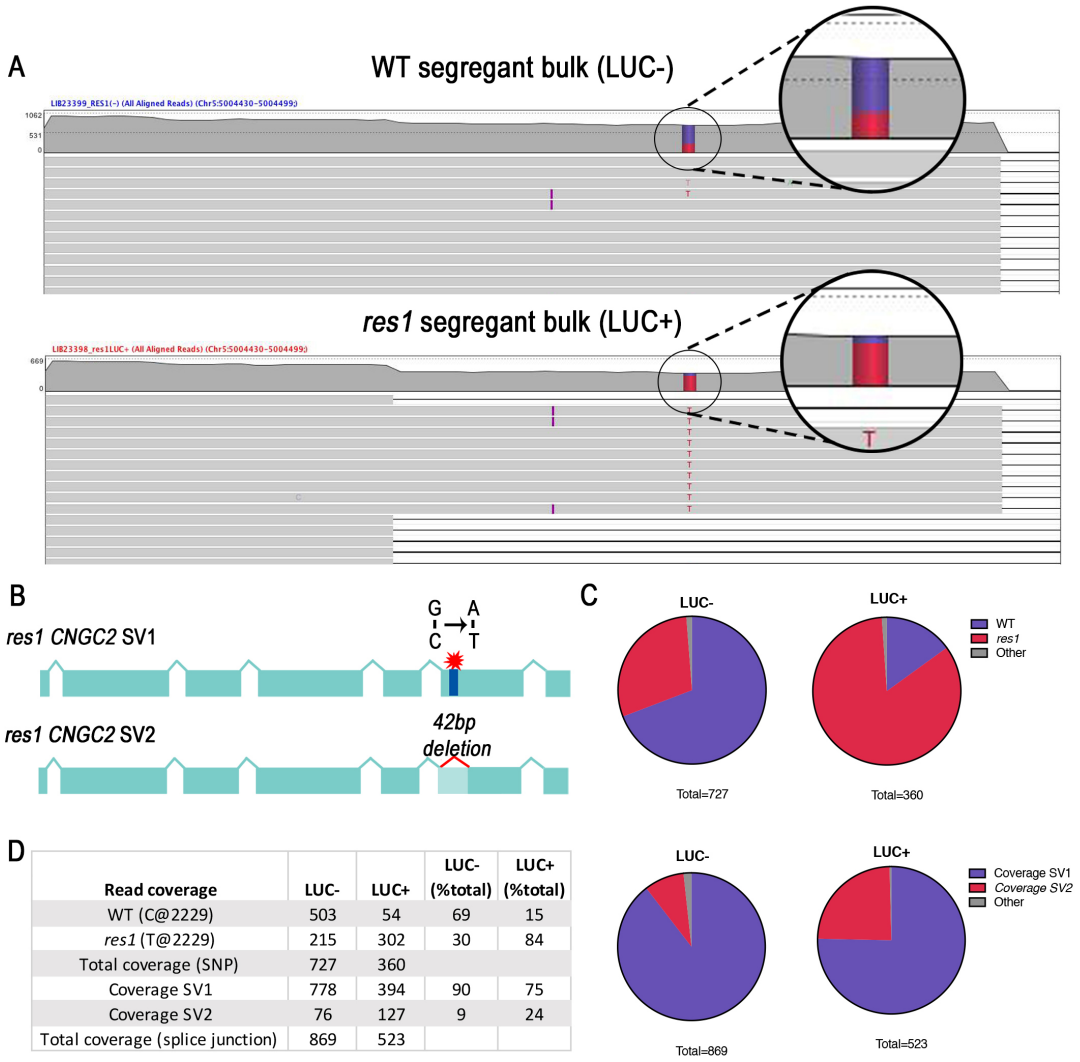

Read coverage	LUC-	LUC+	LUC- (%total)	LUC+ (%total)
WT (C@2229)	503	54	69	15
res1 (T@2229)	215	302	30	84
Total coverage (SNP)	727	360		
Coverage SV1	778	394	90	75
Coverage SV2	76	127	9	24
Total coverage (splice junction)	869	523		

Figure 3-40 SNP and splice variation in *res1* mapping populations –(A) Differential segregation of C->T SNP in LUC-/+ populations, along with pictured 42bp deletion in LUC+ population. (B) schematic diagram of SNP/ Splice variants. (C) Proportion of LUC-/+ populations containing *res1* SNP (top) and coverage of SV1 or SV2 (bottom) (D) read coverage and segregation of *res1* SNP.

Whilst no mutations in CNGCs have previously been described as leading to changes in splicing in *Arabidopsis*, differential splicing of voltage gated calcium channels is known to play a key role in modulating gating properties and sensitivity to calcium channel blockers [288] and in general, alternative splicing is known to play a key role in environmental regulation of gene function [123,289,290], so could equally play a role in modulating CNGC2 function in *res1*.

Detection of the splice variant forms in the RNA-seq could be an artifact arising from degradation products, and might not necessarily be stably present in plant cells.

Therefore, before attempting to dissect any potential mechanisms of SV2 or SV1 function, I first aimed to confirm the presence of stable, poly-adenylated SV2 in *res1*. To achieve this, I used primers to specifically amplify a section of this gene apart from the potential splice junction in *res1* cDNA alongside those spanning the novel putative splice site, and a third set amplifying specifically priming across the region missing in the *res1*-specific splice variant (SV2). A diagram of primer position can be observed in Figure 3-41A. I used WT genomic and cDNA as controls from samples previously isolated for genotyping/ qPCR to test the primers and determine whether *res1* contains a novel splice variant at detectable levels.

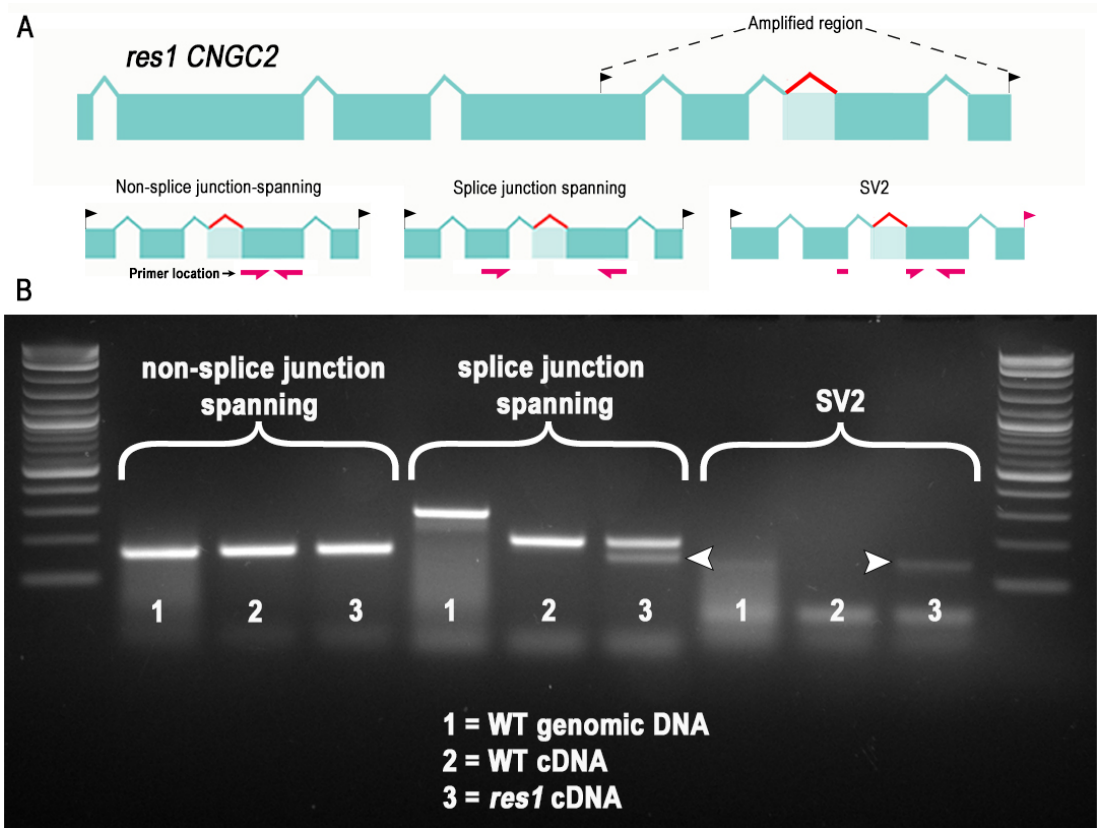

Figure 3-41 Amplification of *CNGC2* SV1 and SV2 – (A) Schematic representation of splice variant amplification specific primer location - 1. non-SV-specific, non splice-junction spanning primers, 2. splice junction spanning and 3. SV2-specific primers. (B) Image of 1% Agarose gel showing amplification of WT genomic and cDNA samples alongside *res1* cDNA Arrows indicate specific amplification of SV2 in *res1* cDNA

Using these three combinations of primers to amplify WT and *res1* cDNA, the presence of SV2 can clearly be detected, exclusively in *res1* (Figure 3-41B). Amplification with both splice junction spanning and SV2-specific primers (Figure 3-41 A) revealed SV2 presence in *res1* cDNA. No detection of this novel splice variant

was observable in WT cDNA (Figure 3-41B). This suggests that SV2 represents a novel, stable, poly-adenylated variant of *CNGC2* in *res1*.

Following this observation, to test whether the alternative splice forms of *CNGC2* are affected by temperature or pathogen signals, I quantified expression of the different splice variants in *res1* using qRT-PCR. I used cDNA previously obtained from mock and 18 h flg22-treated seedlings for this analysis to further detect whether, if SV2 was exclusively expressed in *res1*, levels of this variant or of SV1 were affected by temperature or PAMP-treatment. I therefore designed an additional set of primers to those previously used, to specifically prime within the spliced-out region in SV2 and thus act as a measure for SV1 levels only (Figure 3-42A).

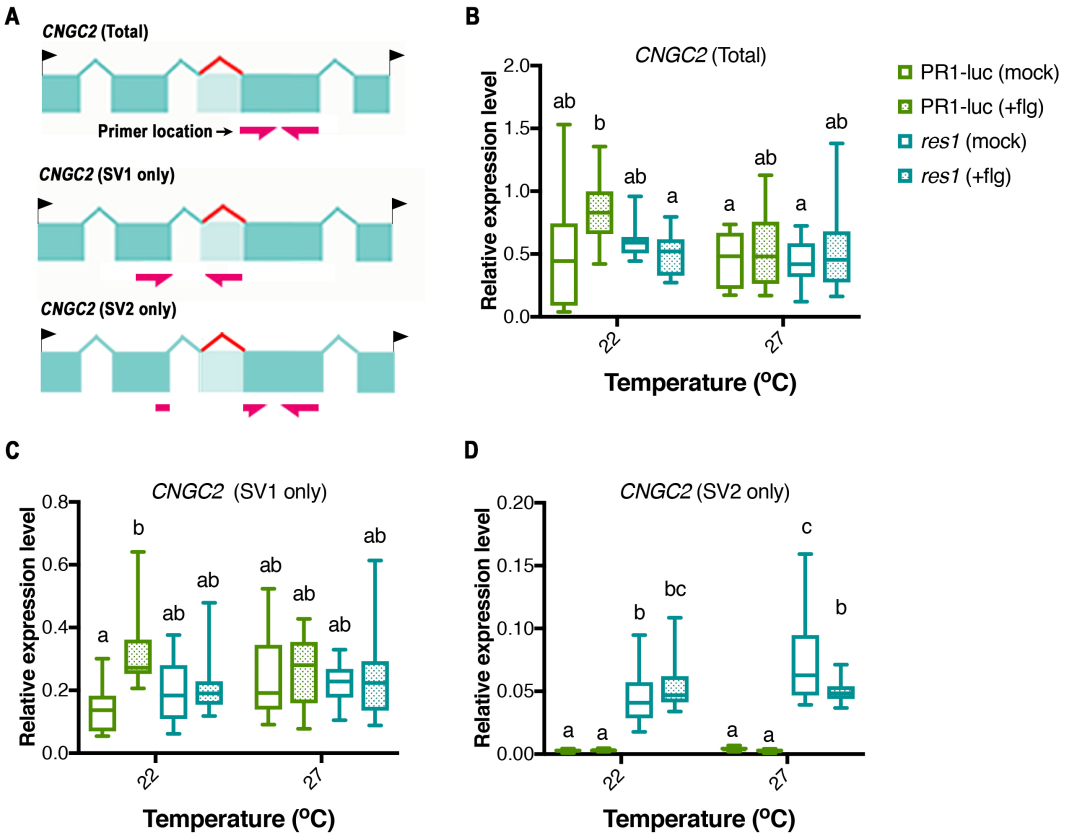

Figure 3-42 Differential *CNGC2* splice variant expression – Three sets of primers were used to amplify mock or flg22 (+flg) treated seedling cDNA. (A) Primer location for total CNGC2, SV1 only and SV2 only (B) Quantification of total *CNGC2* expression in each cDNA sample. (C) specific quantification of CNGC2$^{(SV1)}$ (D) specific quantifiation of SV2. Statistical analysis carried out – 2 way ANOVA followed by Tukey's post-hoc multiple comparison test.

To gain an overall picture of *CNGC2* expression in *res1* vs WT plants and understand whether temperature or flg22-induction influences this, I initially used the *CNGC2* (Total) primers to amplify a section apart from the variant region in cDNA samples created previously (Figure 3-42A). From this, a moderate difference can be observed between *res1* and WT induced plants at 22℃, but otherwise *CNGC2* expression levels remained relatively stable between groups.

Following this, I used primers either specifically priming within the region lost in SV2 (SV1 only), or only when this region is lost (SV2 only) to investigate changes between genotypes/ treatments and confirm lack of SV2 presence in WT cDNA (Figure 3-42A, C, D). This data confirmed a modest effect of flg22 treatment on *CNGC2* expression at 22℃ in WT plants which is absent in *res1* or at 27℃ in either genotype (Figure 3-41C). Most notably, SV2 expression is not present at detectable levels in any of the WT samples assayed. *res1* however shows stable expression of this variant, with a slight decrease apparent at 27℃ in flg22-induced plants. In addition, having observed SV2 expression levels as ~0.05 in *res1* plants (Figure 3-41D) and SV1 levels around ~0.2 (Figure 3-41C), these data would seem to agree with previous predictions of SV2 representing around ¼ total *CNGC2* transcripts in *res1.*

These data further confirm the presence of a novel, stable, poly-adenylated *CNGC2* splice variant in *res1*. It is not yet known whether the gene product of this splice variant underpins any of the phenotypes observed in *res1*. Detection at such levels observed however led me to consider whether this splice variant may alone underpin *res1*'s phenotypic changes in thermosensory growth or defence, act in combination with $SV1^{(res1)}$, or have no contributing effect on *res1* phenotype.

To determine which of these hypotheses was correct, I made overexpression constructs of $SV1^{(WT)}$, $SV1^{(res1)}$ and SV2 of *CNGC2* in order to transform *cngc2-T* mutant plants and observe comparative growth and immune phenotypes. In addition, to enable me to further understand CNGC2 localisation as detailed earlier,

I made each construct with a C-terminal GFP labels to facilitate further confocal microscopy.

As before, I cloned *CNGC2* SV1$^{(res)}$ and SV2 from *res1* cDNA as well as CNGC2$^{(WT)}$ from WT cDNA into the pENTR-D-TOPO entry vector, followed by pB7FWG2 gateway vector with N-terminal CaMV 35s promoter and C-terminal GFP, verifying directionality and sequence in both stages (Figure 3-43).

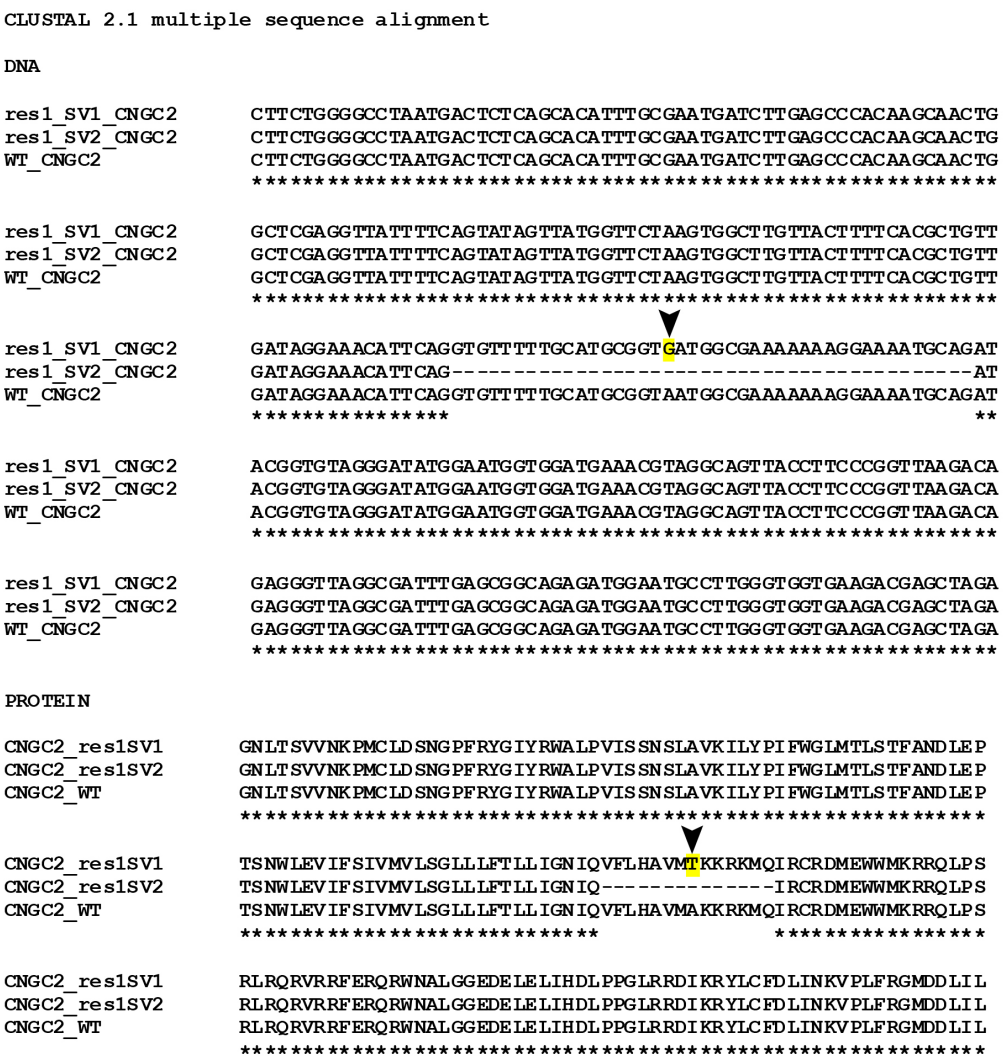

Figure 3-43 ClustalW alignment of DNA and protein sequences from CNGC2 SV1$^{(WT)}$, SV1$^{(res1)}$ and SV2 – Polymorphism highlighted, arrow shows site of polymorphism, dashes indicate missing nucleotides/ amino acids

Sequencing results further confirmed the presence of both splice variants in *res1* cDNA, as highlighted in Figure 3-43.Once I had confirmed identity and successful cloning of each construct, I introduced the binary vectors into *Agrobacterium* in order to transform *cngc2-T* plants via the floral dip method. I collected transformed T0

seeds from each construct/line and germinated them on soil at 20°C LD. I selected 10-day old seedlings with BASTA® and transplanted positive transformants. When plants were large enough, I collected leaf samples in order to conduct copy number analysis as before. Number of positive single or double insertion lines isolated are presented below in Table 4.

Table 4 T1 transgenic lines with copy number – SIL= single insertion line, Brackets = double insertion line

Background	Construct	# lines generated	# SILs identified
cngc2-T	$SV1^{(WT)}$ OE	6	3
cngc2-T	$SV1^{(res1)}$ OE	3	0(2)
cngc2-T	SV2 OE	5	4

Following the identification of stable single or double insertional transgenic lines, I next aimed to collect seeds in order to obtain homozygous T3 lines in the next generation. This was possible for each transformant *cngc2-T* $SV1^{(WT)}$ and $SV1^{(res1)}$ OE line however *cngc2-T* SV2 OE transformants were extremely late flowering and not very fertile until late stages of flowering. This observation is interesting to note, since it demonstrates a potentially enhancive effect of SV2 overexpression on *cngc2-T* single mutant phenotype.

As a result of this phenotype, I carried out characterisation of the phenotypic effects of these constructs on segregating T2 lines. Any differences observed therefore represent a somewhat "diluted" effect of including heterozygous (or WT where no BASTA® selection was possible) plants, and are therefore representative of even stronger underlying effects.

3.2.23 CNGC2 SV1$^{(res1)}$ and SV2 contribute differentially to immune resilience in *res1*

Having confirmed stable presence of SV2 exclusively in *res1* plants, regardless of temperature or PAMP treatment, and now possessing transgenic *cngc2-T* lines constitutively expressing SV1$^{(WT)}$, SV1$^{(res1)}$ and SV2, I next aimed to determine whether these constructs affected TSI in these plants.

I initially investigated resistance to *Pto* DC3000 *cngc2-T* lines overexpressing SV1$^{(WT)}$, SV1$^{(res1)}$ or SV2 to see whether either variant may contribute to *res1*'s elevated defences at high temperature and whether overexpression of either *res1* variant is able to complement *cngc2-T*'s previously identified elevated immunity [113]. To achieve this, I initially grew each transgenic line on GM media at 22°C SD with 15 μg/ml BASTA to eliminate WT seedlings. Following selection, I transplanted seedlings to soil and grew for a further 4 weeks at 22°C before shifting to 27°C for three days, infecting with *Pto*DC3000 and measuring bacterial CFU at 3dpi.

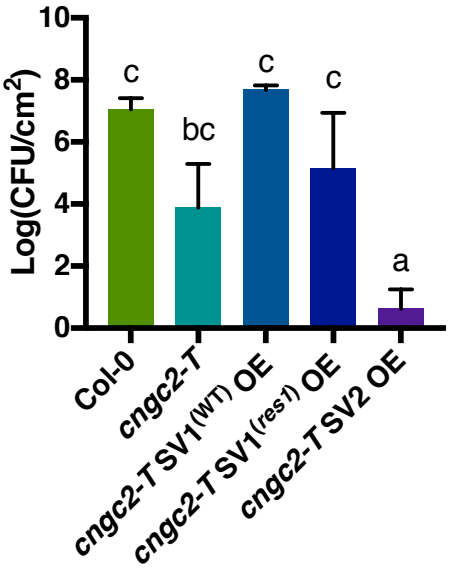

Figure 3-44 *Pto* DC3000 resistance of *cngc2-T* transgenic SV1$^{(WT)}$, SV1$^{(res1)}$ and SV2 OE lines at 27°C –Average CFU per cm^2 of one T2 transgenic line for each of SV1$^{(WT)}$, SV1 $^{(res1)}$ and SV2 overexpressor (OE) lines in the *cngc2-T* mutant background. Statistics carried out – ordinary one-way ANOVA followed by Tukey's post hoc test for multiple comparisons (n=6-18).

Here, it is clear to see how both *SV1*$^{(WT)}$ and *SV1*$^{(res1)}$ complement *cngc2-T* phenotype (Figure 3-44) overexpression of SV2 in comparison with either SV1 clearly does not complement *cngc2-T* and in fact appears to enhance this mutant's phenotype (Figure 3-44). These data are particularly remarkable given the mixture of heterozygous

transgenics and thus show a clear effect even of one transgene copy on plant phenotype.

The ability of the SV2 OE construct to enhance *cngc2-T* immune phenotype confirms my previous observations of the growth and flowering phenotypes of T1 transgenic plants. This observation suggests the potential existence a negative functional interaction of this protein with other factors such as CNGC4. To determine whether either of the *res1* splice variants was able to rescue or enhance *cngc2-T* growth phenotypes similarly, I next characterised thermosensory hypocotyl elongation in these lines.

3.2.24 CNGC2$^{(res1)}$ variants differentially affect thermosensory growth responses

To detect potential effects of different *CNGC2* splice variants in *res1* on plant thermosensory growth responses, I next assessed their ability to complement or enhance *cngc2-T* phenotype. *cngc2-T* transgenic SV1$^{(WT)}$, SV1$^{(res1)}$ and SV2 OE lines were therefore assessed for growth and development phenotypes as before.

To begin these characterisations, I investigated thermosensory hypocotyl elongation in these lines as before. Seedlings were stratified for 3 days at 4℃ on soil before being moved into 22℃ SD conditions for 7 days growth. Following this, half the seedlings were shifted to 27℃ for four days, seedlings were imaged and hypocotyl lengths quantified using ImageJ.

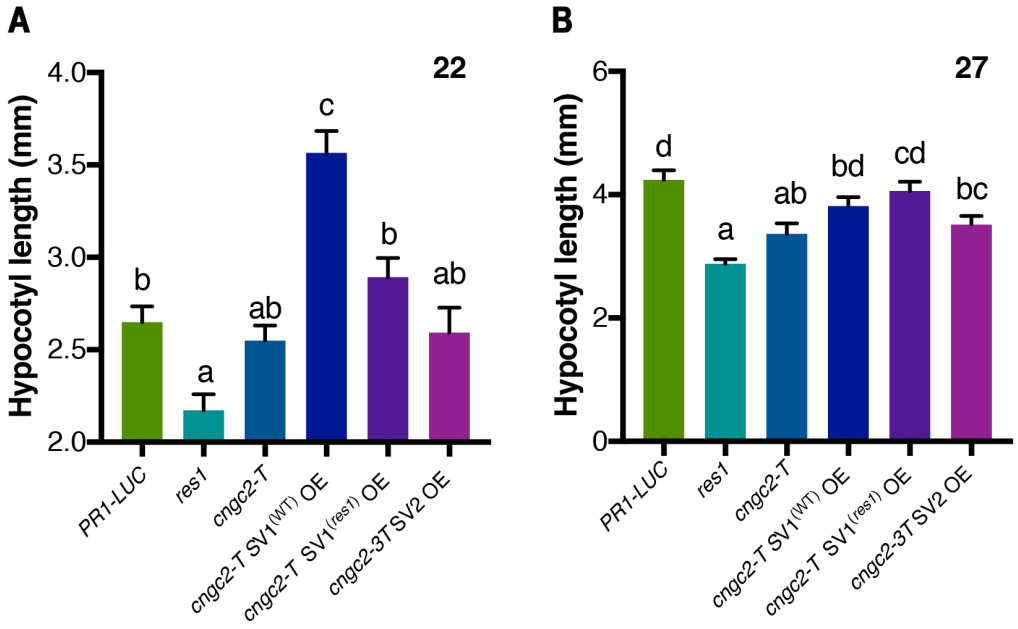

Figure 3-45 – Hypocotyl length phenotype of *CNGC2* splice variant overexpressor lines at 22 and 27℃ –SV1$^{(WT)}$, SV1$^{(res1)}$ or SV2 overexpression lines in the *cngc2-T* background at 22℃ (A) or 27℃ (B). Statistics conducted – Ordinary one-way ANOVA followed by Tukey's Post-hoc analysis (n=13-16).

From these analyses, a clear lack of complementation can be observed with overexpression of SV2 compared to SV1$^{(WT)}$ at 22℃. SV1$^{(res1)}$ OE plants appear to display an intermediate phenotype at this temperature (Figure 3-45 A). At 27℃, an effect of SV2 overexpression only can be observed (Figure 3-45 B). The weaker responses observed here may in part be due to the inclusion of WT plants as a result of necessarily working with segregating T2 lines as previously discussed, thus affecting hypocotyl length more strongly at 27℃ where WT thermosensory elongation responses increase. Altogether, these data suggest that SV2 is not capable of complementing *cngc2-T*, although no enhancive effect similar to that of this construct on immunity can be observed here. In addition, there is a potential weaker effect of SV1$^{(res1)}$ on hypocotyl complementation of *cngc2-T* mutants, observable at 22℃ which may suggest a weak loss of function of this gene variant.

This is an exceptionally descriptive set of information as to the effect of the different splice variants on CNGC2 function in addition to substantiating the role of CNGC2$^{(WT)}$ on governing thermosensory growth and immune responses. What I have observed here suggests a complex mechanism of interactions of these different variants with

each other, and of reducing WT channel or potentially other subcellular component function.

Following quantification of hypocotyl length, I next aimed to characterise the effects of the different splice variants on the adult growth phenotypes of *cngc2-T* mutants. To ensure removal of WT seedlings from T_2 seed stock, I grew seeds on GM media + 15ug/ml BASTA® at 22°C and selected resistant seedlings to transplant onto soil for growth at continuous 22 or 27°C. I documented phenotypes of representative seedlings at 5- and 9-weeks post germination.

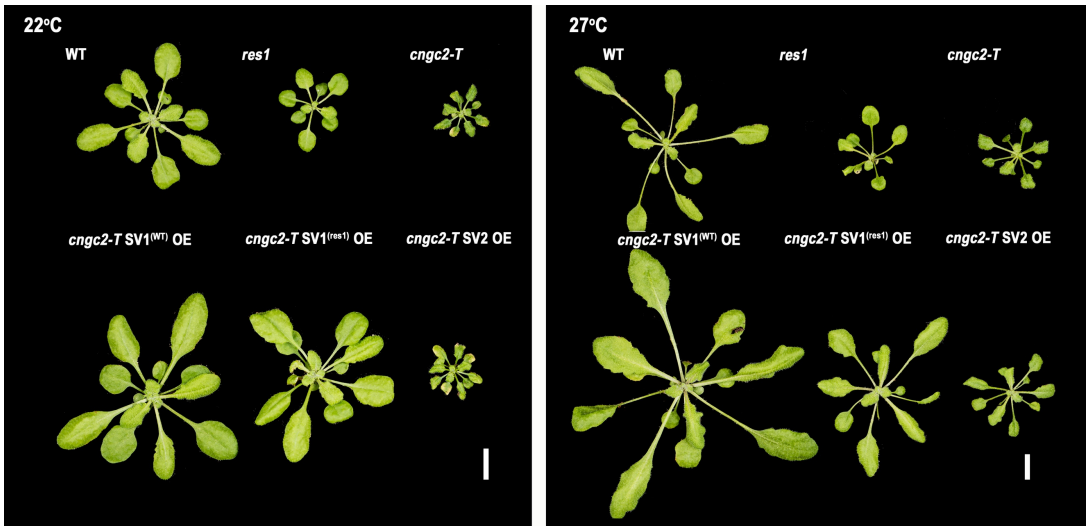

Figure 3-46 Adult rosette phenotypes of representative 5-week old plants for each transgenic line grown constantly at 22 or 27°C - plants selected on GM + 15 μg BASTA agar at 22°C SD before transfer to 22 or 27°C SD on soil. Scale bar = 1 cm

The adult phenotypes here evidently reflect what I have observed in terms of both thermosensory growth and immunity in *cngc2-T* plants expressing the three different variants of *CNGC2* investigated. At 22°C, a moderate decrease in growth can be observed in *cngc2-T* SV1$^{(res1)}$ OE plants compared to their SV1$^{(WT)}$ counterparts and *cngc2-T* SV2 OE plants phenocopy *cngc2-T* mutants both in terms of growth and leaf senescence. These responses are likewise observable at 27°C, with SV2 OE plants strongly phenocopying their untransformed mutant counterparts, and a moderate effect of SV1$^{(res1)}$ OE is observable in comparison with SV1$^{(WT)}$ (Figure 3-46).

These effects are strongly maintained throughout the life cycle of these plants, regardless of temperature treatment, as can be observed in the 9-week-old plants depicted in Figure 3-47.

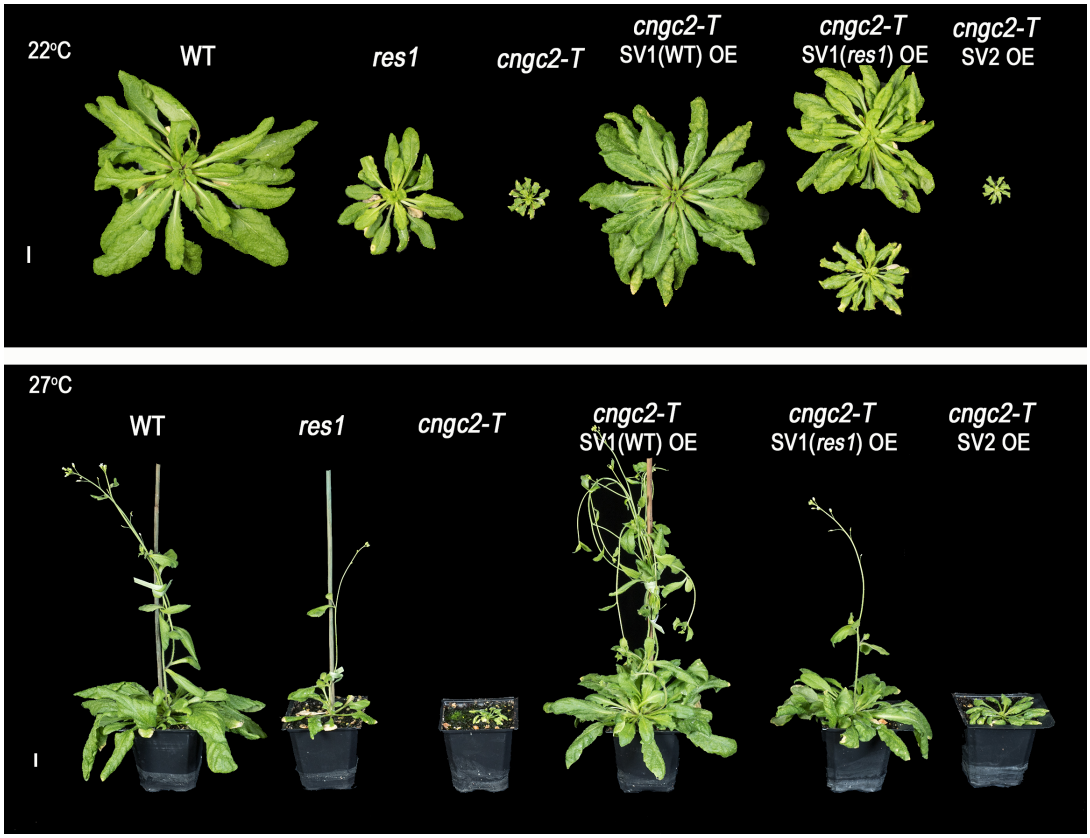

Figure 3-47 Representative 9-week-old plants from each transgenic line grown at constant 22 or 27℃ - Initial selection of seedlings was carried out on GM agar + 15 μg/ml BASTA. *cngc2* SV1(*res1*) OE line contains two copies, and silencing of the transgene can begin to be observed, thus returning plants back to *cngc2* null. Both silenced (bottom)and non-silenced (top) plants are therefore depicted here to represent the set of plants grown from this line. Scale bar = 1 cm.

As with 4-week-old plants, the different phenotypic consequences of overexpressing *CNGC2* SV1$^{(WT)}$, SV1$^{(res1)}$ and SV2 can clearly be seen here (Figure 3-47). AT 22°C, SV2 OE plants maintain a highly dwarfed stature at both temperatures and at 27°C, whilst all other lines have begun flowering, this line remains in the rosette stage, in line with *cngc2-T* mutants.

It was not possible to quantify flowering time for SV2 OE lines within the scope of this project, suggesting a potentially enhancive effect of this transgene on *cngc2-T* phenotype but which remains to be verified.

The severe dwarfing observed in the SV2OE lines, particularly at 22°C seems to comply with previous observations of the apparent enhanced phenotypes of *cngc2/cngc4* ("super-dnd") mutants [256,271] and may thus suggest a potential negative affect of SV2 on CNGC4 or other regulatory components, however this remains to be directly tested.

Altogether, it is now possible to get an idea as to the genetic basis for the observed defects in thermosensory responses in *res1*. The polymorphism itself appears to result in a weak loss of gene function in comparison with WT *CNGC2* when overexpressed, however a much stronger effect of this mutation can be seen through its consequences on splicing, resulting in a novel genetic variant which lacks 14 amino acids in translated form. This variant fails to complement immunity in *cngc2* null plants at both 22 and 27°C, and similarly lacks effective function in terms of thermosensory growth. The specific mechanism of functional alteration of CNGC2 in *res1* remains to be determined.

Further examination of the effect of the *res1* mutation on protein function, topology and localisation of different splice variants will enable elucidation of the precise mechanisms by which the polymorphism and associated novel splice variant in this mutant affect calcium signalling and therefore downstream thermosensory pathways.

3.3 Summary and discussion

A novel, reporter-based forward genetic screen here identified *res1* as a mutant with robust defence activation at elevated temperature, that is otherwise inhibited. This mutant shows high ambient temperature-resilient defence gene expression underpinning robust SA-mediated resistance to biotrophic pathogens such as *Pto* DC3000. Further phenotypic characterisation here conducted further revealed that *res1* is compromised in general thermosensory growth responses such as elongation growth, underpinned by changes in gene expression. Taken with the lack of immune suppression in this mutant I therefore implicated RES1 as a central coordinator of thermosensory regulation. This mutant allowed me to attempt to dissect a previously unknown feature of ambient temperature responses in plants. Using bulk segregant RNA-seq as I was able to confirm a novel polymorphism in *AtCNGC2* underpinning the phenotypes observed in *res1*. This mutation resulted in an A457T amino acid substitution in a region of this gene known to be crucial for modulating its function. Complementation of this mutant was achieved through reintroduction of $CNGC2^{(WT)}$ under constitutive CaMV 35s promotion. Further characterisation identified an additional splice variant of this gene present exclusively in *res1* cDNA displaying a 42bp in-frame deletion, including a putative NLS. Through creation and study of novel transgenic lines overexpressing this novel splice variant alongside those with $CNGC2^{(res1)}$ I was able to understand the differential contribution of these variants to the phenotypes observed in *res1*.

The lack of the ability of SV2 to complement *cngc2* null mutant phenotypes, in addition to conditional enhancement of this mutant's phenotypes points towards a mechanism of function whereby this channel variant possibly inhibits function of both WT CNGC2 molecules, where present, in addition to other interacting factors, most likely with CNGC4. The effects of *res1* on CNGC2 function could therefore be multiple and complex. Alterations in the localisation of this channel as well as its ability to interact with other CNGCs or regulatory factors could all result in the observed modulation of thermosensory responses in this mutant due to perturbed calcium signalling (Figure 3-48). When considered as a whole, the number of possible alterations in interactions with other factors may explain the complexity of observed

phenotypes in both mutant and overexpressor lines. CNGC2$^{(WT)}$, CNGC2$^{(res1)}$ CNGC2$^{(SV2)}$, CNGC4, CaM, cNMPs and interaction with protein kinases represent just a fraction of potential factors playing a role in this process (Figure 3-48). Clearly, further work will be needed to precisely characterise the effects of the different splice variants identified on these functions. Identification of a novel localisation of one of these factors provides an interesting route to explore these effects. Both nucleus/ER and apoplast are known storage compartments with roles in calcium signalling [291,67]. Disruption of localisation or ability to efficiently conduct calcium from these stores in response to cellular signals could all affect the thermosensory responses which it governs.

Regardless of the mechanism however, this study has identified a novel signal transduction node of plant ambient temperature responses. Moreover, I have now implicated calcium signalling as important in response to biotic challenges under normal temperature conditions as well as in suppression of these responses in favour of growth at higher ambient temperatures. Previously, mutants within components of the pathway regulating SNC1 such as *snc1-4* and *siz1* are the only examples where immunity is not completely suppressed by elevated temperature [139,236]. The identification of a completely distinct pathway thus shows the potential for existence of many as yet unknown factors in governing thermosensory responses. Additional study will enable dissection of the precise mechanism through which SV2 affects calcium signalling and thus how WT CNGC2 governs thermosensory coordination of growth and defence. In particular, investigating the nature of calcium signalling in response to pathogen perception at elevated ambient temperatures as well as investigating interaction of CNGC2 variants with each other as well as other molecules will enable further understanding of this putative thermosensor.

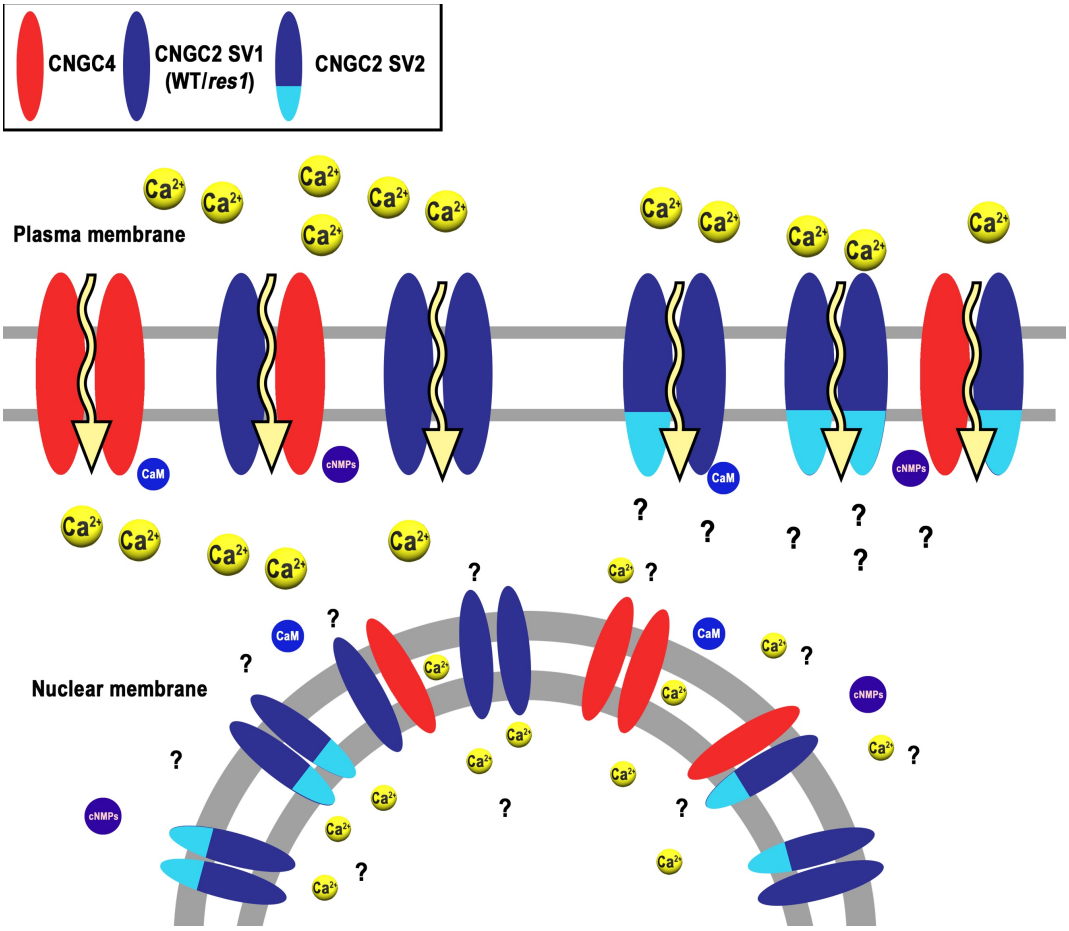

Figure 3-48 Functional model of effect of different splice variants on calcium transport in *res1* – Combinatorial predicted interaction changes between CNGC2 and CNGC4 as well as CNGC2$^{(res1)}$ and SV2 and their potential effect on downstream signalling. Presence of these components on both plasma membrane as well as nuclear membrane/ER highlights the large range of possibility for alterations of calcium dynamics by these channels. The precise effect of alterations of CNGC2 on calcium signalling are yet to be unraveled.

4 Early Pattern-Triggered Immunity Outputs are Compromised in *res1*

4.1 Introduction

4.1.1 Thermosensory suppression of immunity in *res1*

In my previous chapters, I have so far detailed how elevated ambient temperature simultaneously compromises PTI and ETI, resulting in attenuated SA-triggered immunity (SATI). In addition, I have characterised *res1* as a new mutant with compromised thermosensory suppression of (SA-triggered) immunity (SATI), underlain by alterations in a key calcium channel.

res1 shows robust defences at high ambient temperature where typically multiple defence outputs are compromised. This mutant was isolated based on *PR1-LUC* expression, with *PR1* used as an output of SA production, and SA-triggered systemic immunity as a shared output of several immune signalling pathways including PTI. *PR1* induction is a delayed output compared to PTI, and given the fact that *res1* shows robust flg22-induced *PR1* expression at elevated ambient temperatures, it raises the possibility that *res1* may likewise display temperature resilient PTI responses. Both PTI and ETI have common outputs such as HR, upregulation of defence genes and SAR [43] but are distinguishable through their early signalling mechanisms [41]. Similarly, both processes result in elevated SATI [44] when initiated by perception of a biotrophic pathogen.

The res1 mutant shows enhanced, constitutive SATI phenotype as shown above. This could be a consequence of a robust or amplified PTI responses. My next aim therefore was to characterise responses further upstream to SATI in *res1* to understand whether PTI is reinforced in *res1* and whether this layer of immunity underpins its robust downstream defense responses. As a result of existing paradigms, I hypothesised that *res1* would maintain robust PTI responses, regardless of temperature.

4.2 Results

4.2.1 Early PTI gene induction is compromised in *res1*

To determine whether the elevated levels of defence observed in *res1* extend as far as PTI activation, and whether they may underpin the high levels of SA-mediated defence activation in this mutant, I quantified induction of *FRK1* in addition to *VACUOLELESS GAMETOPHYTES* (*VLG*, At2G17740), a second marker which is known to be strongly induced in response to PAMP treatment under normal ambient temperature conditions[292,293].

I grew seedlings for 7 days at 22°C before shifting them to 27°C or maintaining at 22°C for a further 3 days and including with 100 nm flg22 or mock (0.01 % Silwet) solutions. I collected seedling tissue at 3 hpi in order to measure expression levels of these early PTI marker genes through qPCR as previously carried out. Data from two to three biological replicates and four technical replicates was combined in order to conduct statistical analyses.

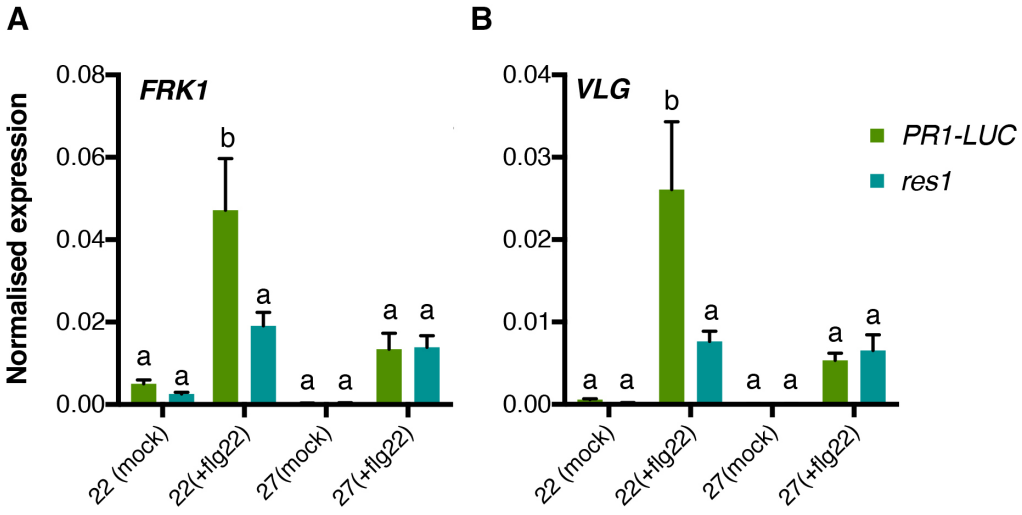

Figure 4-1 Induction of *FRK1* and *VLG* in *res1* at 22 and 27°C - Expression of (A) *FRK1* and (B) *VLG* measured in 10 day-old seedlings, 3 hours post-induction with 100nm flg22 or mock solutions. Levels were normalised to EF1α. Statistical analyses conducted – 2-way ANOVA followed by Tukey's multiple comparison's test. n=8-12 biological/technical replicates (4 technical + 2-3 biological).

As I have observed in WT plants, expression of early PTI marker gene *FRK1* is strongly induced at 22°C, its expression is lost at 27°C. This is likewise true for *VLG* expression

here. In comparison, It is clear to see here how *res1* does not show robust induction of either of these genes, in contrast to what I had expected given elevated levels of SATI I have already observed in this mutant. *res1* seedlings show a lack of robust induction of *FRK1* at 22℃ compared to WT (Figure 4-1) and no difference can be observed at 27℃ (Figure 4-1A). A similar pattern can be observed for *VLG*, with levels of this gene in *res1* comparable to those of the PTI-compromised WT plants at 27℃, regardless of temperature (Figure 4-1B).

The observed lack of induction of these genes in *res1* is particularly interesting since this result is in contrast to what I expected, given earlier studies in autoimmune mutants of other PTI outputs [294,295]. To verify the lack of PTI gene induction in *res1*, I next looked at signal reinforcement by increased expression of recognition receptors as a robust output of PTI, which I described in Chapter 2. I hypothesised how, if PTI responses in *res1* were generally dampened, induction of PAMP receptor components would be similarly attenuated with early defence genes.

Using cDNA isolated as above, I quantified induction of *FLS2* and *BAK1*, two crucial components of the surface-bound receptor complex responsible for perception of flagellin and initiation of downstream signalling at 3 hpi. Fold change from mock-treated seedlings following normalisation to *EF1*α was measured for each gene through qPCR analysis as before.

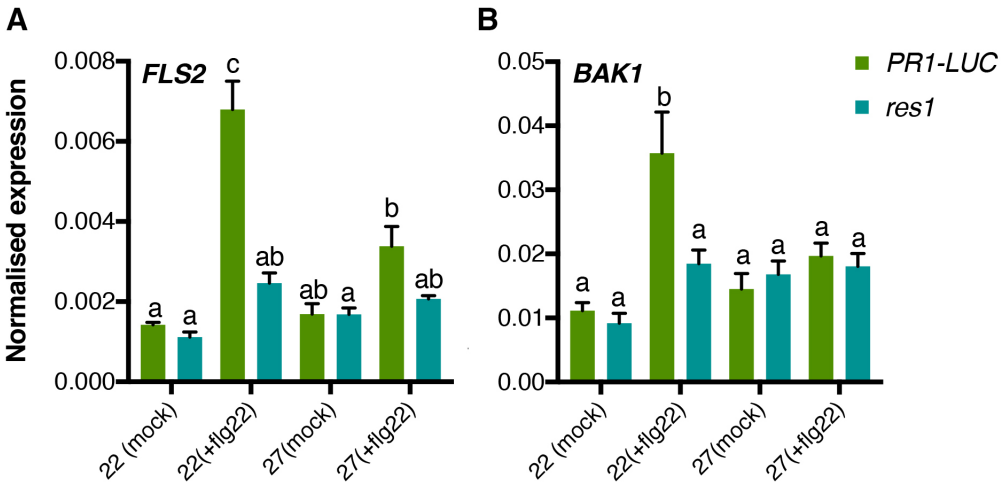

Figure 4-2 Expression of membrane-bound flg22 receptor complex components *FLS2* and *BAK1* – Gene expression analysis of (A) *FLS2* and (B) *BAK1* on 10 day old seedlings induced with 100 nm flg22 or mock solutions for three hours following 22°C or 27°C acclimation. Expression of each gene was normalised to EF1α. Statistical analyses conducted – 2-way ANOVA followed by Tukey's multiple comparisons test. n=8-12 biological/technical replicates (4 technical + 2-3 biological)

In strong agreement with what I observed for *FRK1* and *VLG* induction, the reinforcement of expression of these components which is present In WT plants at 22°C but attenuated at 27°C is not observable in *res1* at either temperature tested. Upregulation of the flagellin receptor, *FLS2* has been validated in response to pathogen challenge or elevated levels of SA[295-297], but is absent in *res1* (Figure 4-2A). Similar responses can be seen for its coreceptor BAK1 (Figure 4-2B).

Here, *res1* plants phenocopy WT plants in which PTI has been attenuated by growth at high temperature. This observation is unexpected, given that I have now confirmed how *res1* lacks generalised thermosensory responses including SATI and phenocopies colder grown plants with respect to all other aspects of its physiology. A lack of robust expression of either *FLS2* or *BAK1* suggests that elevated SATI in this plant is not as a result of robust PTI responses.

To determine whether PTI as a whole is dampened in *res1*, resulting in the observed gene expression, I next investigated further stages of early PTI signalling.

4.2.2 Early PTI signalling is dampened in *res1*

Following perception of PAMPs by pattern recognition receptors on cell surfaces, a series of signalling mechanisms are initiated in order to upregulate expression of

early PTI genes such as *FRK1* or *VLG*. As I have already described, different aspects of PTI signalling mechanisms such as ROS burst and MAPK activation act in parallel to bring about changes and, in the case of ROS burst, are attenuated by growth under elevated ambient temperature conditions (see section 2.2.6).

The importance of ROS burst in PTI signalling and immunity has previously been demonstrated. For example, in mutants lacking robust ROS production, a lack of robust resistance can be observed [298]. Conversely, mutants lacking functional SA signalling lack adequate ROS burst responses and autoimmune mutant lines with known elevated levels of SA such as *cim6* have demonstrated how elevated levels of ROS production follow PTI activation [294,295]. Furthermore, in mutants such as *fatty acid biosynthesis2* (*fab2*) which show severe dwarf phenotypes and very high levels of both ROS and SA can be observed, an enhancive effect of ROS on attenuation of plant growth as a result of further enhanced defence activation can be inferred [299,300]. In addition, *accellerated cell death 6* (*acd6*) shows similar dwarfing phenotypes and has been implicated in both PTI and SATI [301-303].

I hypothesised earlier how constraints on all aspects of immunity such as in *fab2* and *acd6* mutants may similarly exist in *res1,* resulting in the growth, senescence and immune responses I have observed. However, my observation of low PTI gene expression in *res1* may indicate this is not in fact the case. To determine whether early PTI signalling is deregulated in *res1*, I next aimed to assess PTI-induced ROS burst in this mutant at 22 and 27℃.

To achieve this, I grew plants from WT and *res1* lines alongside the flg22-insensitive mutant, *fls2* at 22℃ SD for 4 weeks. Plants were subsequently maintained at 22℃ or shifted to 27℃ for three days. Three leaves of a similar age per plant were excised, 3mm leaf discs cut and suspended in 200 μl sterile dH_2O in 96-well opaque plates at their relative temperatures overnight. Water from plates was then removed and 100 nm flg22 added with 10 μl luminol (17 mg/ml) and 10 μl peroxidase (10 mg/ml) in 100 μl sterile dH_2O and ROS burst over a 40-minute period was measured using a Varioskan Flash luminometer.

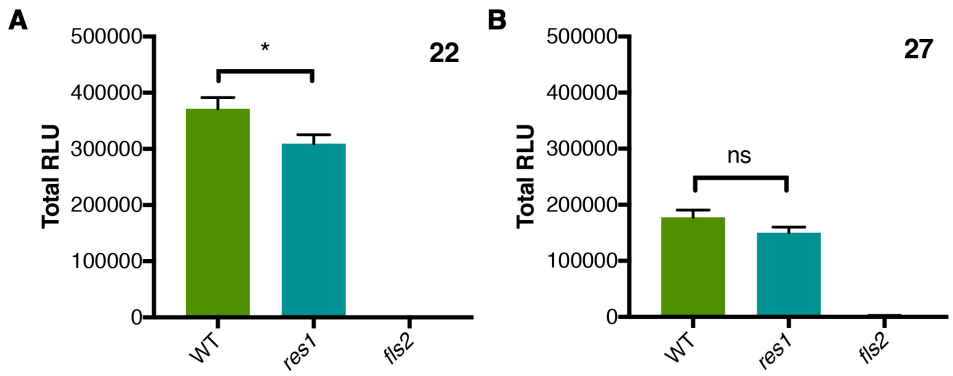

Figure 4-3 flg22-induced ROS burst in *res1* at 22 and 27℃ - Average relative light units (RLU) per plant for *res1* and WT plants at 22 (A) or 27℃ (B). Average total ROS per plant, three discs/ leaves per plant quantified for 40 minutes post-flg22 addition. Statistical analysis conducted – Unpaired t-test, (n=18). One repeseative example of 3 biological replicates is displayed here.

Here, in agreement with the attenuated gene expression I observed, following flg22-induction, *res1* shows a moderate reduction in ROS burst compared to WT plants at 22℃ (Figure 4-3A). Additionally, no difference between WT and *res1* plants at 27℃ can be observed (Figure 4-3B). *res1* also displays a temperature-dependent reduction of ROS between temperatures of around 50% from ~300000 to ~150000, suggesting an increased sensitivity of flg22-induced ROS burst to temperature than SATI in *res1*. Thus, robust PTI responses do not appear to underlie the high *PR1* expression levels or resistance observed in *res1* and that high levels of immunity are possible in spite of compromised PTI.

Following this, to confirm whether the unexpected outputs observed here are caused by the mutation in CNGC2 in *res1,* I repeated this flg22-induced ROS burst assay using the transgenic lines I generated in Chapter 2 which demonstrated complementation of both growth and immunity in *res1*'s when WT *CNGC2* is overexpressed. I grew WT, *res1*, *res1 1.3pCNGC2* and *res1 CNGC2* OE lines alongside each other and the control line *fls2* for 4 weeks at 22℃ before shifting one set of plants to 27℃ for three days. Leaf discs were incubated in plates overnight and ROS quantification was carried out as before following induction with 100 nm flg22.

4.2.3 Functional CNGC2 is necessary for early PTI signalling

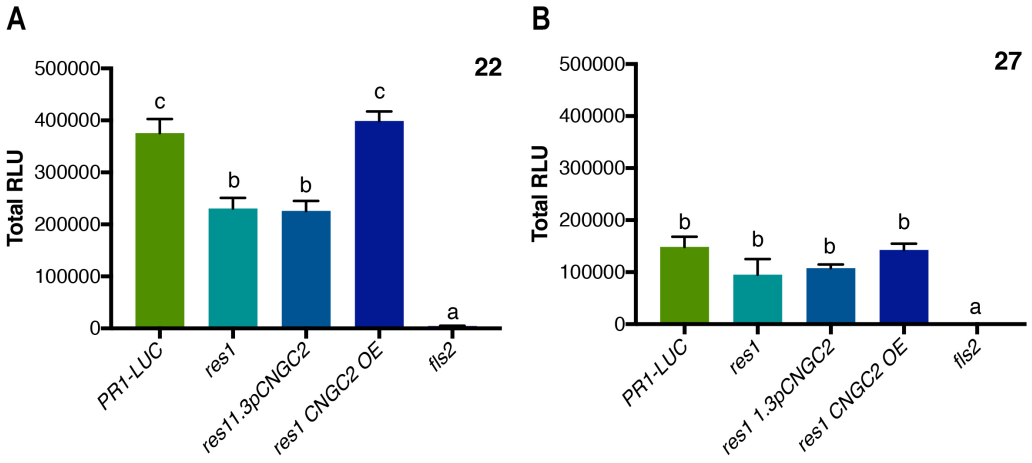

Figure 4-4 PAMP-induced ROS burst in *res1* complemented lines, at 22 and 27°C - Average relative light units (RLU) per plant for *res1* and WT plants alongside transgenic *CNGC2* overexpressor or native promoter lines in the *res1* background at 22 (A) or 27°C (B). Average total ROS per plant, three discs/ leaves per plant quantified for 40 minutes post-flg22 addition. Statistical analysis conducted – 2-way ANOVA followed by Tukey's multiple comparisons test (n=18). One repesative example of 2 biological replicates is shown here.

In a manner precisely mimicking that of other phenotypic responses of these transgenic lines, overexpression of *CNGC2*$^{(WT)}$ complements the attenuated PAMP-induced ROS burst of *res1*, where native promotion of this gene does not (Figure 4-4). At 22°C, both *res1* and its native promoter transgenic line show attenuated ROS production compared to both WT and *CNGC2 OE* lines (Figure 4-4A). At 27°C, no difference can be observed between any of the lines (Figure 4-4B). This further supports the lack of robust induction I have observed as a notable phenotype of *res1*, underpinned by its mutation in *CNGC2*, in spite of its notably high *PR*-mediated immunity.

All these results together suggest that although *res1* is able to sense and respond to bacterial PAMPs, its responses to these signals are attenuated. In spite of this, *res1* is able to maintain inducible and constitutive SA-mediated defences against pathogens at both moderate and high ambient temperatures. *res1* therefore highlights a potential alternative route for maintenance of elevated immunity when PTI responses are dampened.

To test whether dampened PTI responses are specific to the complex effects of the mutation I have previously shown on *res1* immune responses, I next aimed to characterise whether this response was exclusive to *res1* or whether it could be similarly observed in the loss of function *CNGC2* mutant, *cngc2-T*.

As before, I grew five-week-old plants from each line alongside *fls2* at 22℃ and quantified ROS burst over a 40-minute period in 3 mm leaf discs excised from 6 plants per genotype using a Varioskan flash luminometer. Since no difference in response between any genotypes can be observed at 27℃, moving forward, all PTI-ROS burst activation comparisons between genotypes were conducted at 22℃.

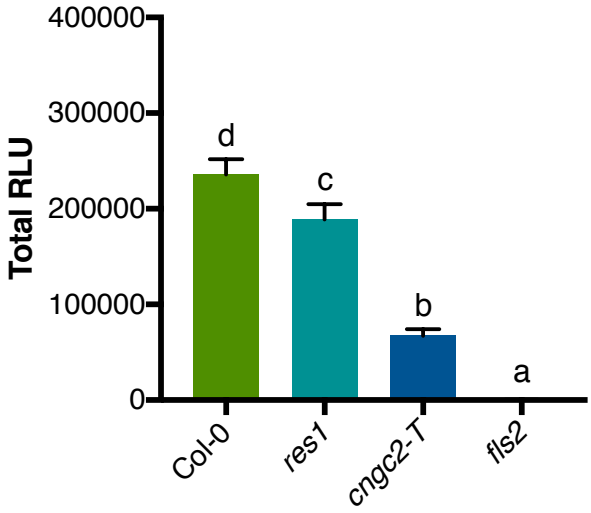

Figure 4-5 PAMP-induced ROS burst in two mutant *CNGC2* alleles at 22 and 27℃ - Average total relative light units (RLU) per plant for each mutant alongside WT and *fls2* plants at 22℃ SD. Statistical analysis conducted – one-way ANOVA followed by Tukey's multiple comparisons test, (n=12-18). One repesative example of 3 biological replicates is shown here.

Here, the loss of function *CNGC2* mutant, *cngc2-T* shows a similarly reduced PTI response to *res1* (Figure 4-5), suggesting the attenuated ROS burst in these mutants occurs as a result of loss of CNGC2. Contrary to my earlier hypothesis, resilient resistance in *res1* is therefore not due to enhanced PTI.

When PTI is activated, a biphasic ROS burst brought about through activation of RBOHD [205,304], is accompanied by a transient calcium influx into the cytosol [305] and activation of early defence genes such as *FRK1* follows shortly after [212,213]. Since Ca^{2+} signalling is a known component both of PTI signalling and of SATI as I have shown,

the observation I have made here led me to hypothesise whether a lack of functional CNGC2 could differentially affect these processes.

In spite of their temporal separation, early PTI signalling and SATI are strongly linked. Under elevated ambient temperature conditions, as I have now shown, both PTI and ETI/SATI are simultaneously negatively influenced. Furthermore, I have confirmed regulation of PTI by H2A.Z which is known to play similar roles in regulation of other distinct immune pathways [158] implicating a central regulatory system governing overall immune responses. Activation of SATI has also previously been shown to enhance amplification of early PTI responses such as ROS burst in [306], since accumulation of peroxide has been shown following exogenous SA application [307]. As a result of my observations for *res1* however, I questioned whether the differential immune responses of *cngc2* mutants could be as a result of the derepression of SATI, therefore pre-empting the requirement for a strong PTI response.

To determine whether a lack of PTI in *cngc2* mutants is specifically a consequence of perturbed calcium responses or as result of deregulated SA-mediated immunity on PTI, I next looked at this response in an array of different mutants with known perturbations in SATI.

4.2.4 SATI activation negatively influences PTI strength

Alongside *cngc2-T,* I included a range of mutants with notably high levels of SATI at 22℃, as well as those with constitutively low levels of this immunity, to determine the effect of perturbing SA levels on PTI activation (Table 5). I obtained mutants from known components of SA-mediated immune regulatory pathways such as *det1* and *cop1* which modulate PIF4[81] in addition to *pif* and *phyB* mutants [127]. To determine the effects of increasing *PIF4* and *PHYB* dosage, I further looked at ROS burst in transgenic overexpression lines (PIF4 OE/ PHYB OE) of these genes [127]. I also included *snc1-1* as a key thermosensitive autoimmune mutant with constitutively high levels of SA associated defences, *pad4* as a mutant with low SA signalling[308] and *NahG*, a

transgenic line constitutively expressing the bacterial salicylate hydroxylase resulting in depleted levels of SA [168].

Table 5 Shortlist of mutants or transgenic lines displaying constitutively high of low levels of SATI [59,81,113,127,128,138,143,168,194,308-313]

Mutant allele/ transgene	SATI-associated Resistance level	WT Gene Function	Key References
cngc2-T	High	Cyclic nucleotide gated calcium channel	Clough *et al* (2000), Moeder *et al* (2011)
snc1-1	High	TIR-NB-LRR (gain of function)	Yang *et al.* (2004), Gou and Hua (2014)
det1	High	Photomorphogenesis regulator, chromatin remodelling, PIF4 regulation	Dong *et al.* (2014), Gangappa *et al.* (2018)
cop1	High	Coordinates photo and skotomorphogenesis, PIF4 + Phyb regulation	Hoffman *et al.* (2015), Gangappa *et al.* (2018)
pif4/pifq	High	bHLH transcription factor, flowering and growth promotion, negative regulator of SA-mediated defences	Kumar *et al* . (2012), Gangappa *et al.* (2017)
snc1-11	Low	TIR-NB-LRR (loss of function)	Yang *et al.* (2004), Li *et al.* (2007)
phyb-9	Low	Red/far red photoreceptor, negative regulator of PIF4 protein abundance	Franklin and Quail (2009), Gangappa *et al* . (2017)
pad4-1	Low	Salicylic acid signalling, interaction with EDS1	Zhou *et al.* (1998), Feys *et al.* (2001)
NahG	Low	Transgenic line expressing bacterial hydroxylase suppressing SA accumulation	Gaffney *et al* . (1993), Bowling *et al* . (1997)
PIF4 OE	Low	bHLH transcription factor	Gangappa *et al.* (2017)
PHYB OE	High	Red/far red photoreceptor, negative regulator of PIF4 protein abundance	Gangappa *et al.* (2017)

To determine whether alterations in SA affect early PTI signalling, I carried out PAMP-induced ROS burst measurements as before in the mutants detailed in Table 5.

I grew plants from each line for 5 weeks at 22℃ SD, before making leaf discs as before and measuring total ROS production following 100 nm flg22 treatment for each mutant over a 40-minute period.

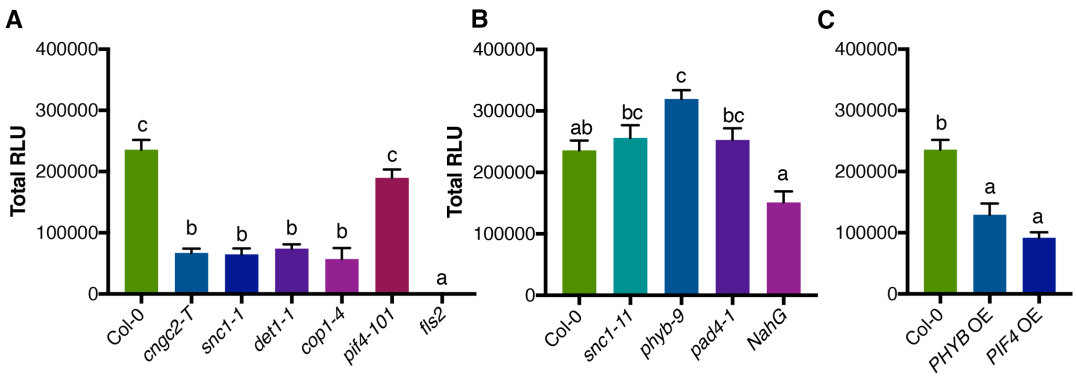

Figure 4-6 PAMP-induced ROS burst in mutants with perturbed SATI - Average relative light units (RLU) per plant for each mutant alongside WT and *fls2* plants at 22°C SD. (A) mutants lines with constitutive activation of SATI (B) mutant lines with low levels of SA. (C) Transgenic *PHYB* and *PIF4* OE lines with contrasting levels of SATI. Statistical analysis conducted – one-way Kruskal-Wallis ANOVA followed by Dunn's multiple comparisons test, (n=12-18). One repesative example of 2 biological replicates is shown here.

An apparent, almost universal lack of effective ROS production can be observed here in mutants with known constitutive immune activation and high SA levels (Figure 4-6A). *cngc2-T*, *snc1-1, det1-1, cop1-4* all show reduced levels of ROS compared to WT plants. *pif4* mutants showed no difference from WT here. It is possible to conclude therefore that elevated SA-mediated immunity may negatively affect PTI responses (Figure 4-6A). Conversely, mutants with depleted basal SA levels indicate either elevated, unchanged or low ROS production. *snc1-11*, *phyb-9* and *pad4-1* all showed opposing responses to mutants displaying elevated SATI as would be expected given a direct effect of SA on PTI (Figure 4-6B).

Interestingly for the transgenic overexpression lines, *PIF4 OE* displayed a similar phenotype to *PHYB OE,* in spite of their known contrasting effects on plant immunity [127] (Figure 4-6C). *PIF4* is known to play complex roles in coordination of plant growth and defence, and is regulated both at the transcriptional and posttranscriptional level by a variety of different factors including PhyB[136,239]. It may be possible that PhyB does not play a role in regulation of PIF4 in the context of PTI, since both in mutant and OE lines, responses mimic those of *PIF4* rather than opposing them as I would have expected (Figure 4-6A,C), given the typically negative regulatory influence of PhyB on *PIF4*[127]. Important to note also is the response observed in *NahG* plants which constitutively break down SA and accordingly lack its associated immune responses. Lower levels of ROS production can be observed in *NahG* plants

(Figure 4-6B), which suggests that whilst SA may be important in negative regulation of PTI, the mechanisms leading to enhanced ROS production in some of the low SA mutants tested may not be as a direct result of SA. Some level of SA production may be necessary for any reinforcement of PTI. This is not unexpected given the complex regulatory mechanisms surrounding SA accumulation and its associated downstream responses [78].

ROS production in response to PAMP detection has now been established as a signalling mechanism rather than a suppressive toxic mechanism, since accumulation of ROS can have unintended fitness costs for plants[300].This observation would indicate PTI as a weaker response than SATI so mutants with constitutively high SATI may therefore lack the need to initiate strong PTI as their immunity is already robust.

Following observations of perturbed flg22-induced ROS burst in these mutants as above, I next decided to take a more detailed look at the effects of increased or depleted SATI on early vs late immune gene expression.

4.2.5 Alterations in SATI differentially affect PTI output

Going forward, since it is not possible to determine whether the PTI outputs observed are as a result of constitutive (or equally externally triggered) high or low levels of SATI are specifically as a result of elevated levels of SA [199], I will use this term to encompass both SA-dependent and independent pathways associated with longstanding immune responses following upstream activation of PTI, ETI or equally other preceding biotic stress response induction.

I have previously shown how PTI-associated genes such as *FRK1* are strongly detectable at 3hpi. In contrast, following activation of SATI, *PR1* expression is expressed later[62,227,314], and strongly detectable at 18 hpi as I have already shown. These two sectors of immunity are therefore possible to differentiate by the timing as well as nature of the response measured.

To investigate the novel negative association between SATI and early PTI, I conducted a large-scale gene expression quantification assay in a refined range of defence mutants. To differentiate between levels of SATI and PTI strength I decided to

investigate both basal *PR1* expression and induced *FRK1* expression in seedlings from mutant lines as before.

I selected a subset of the mutants tested above, as well as including *nonexpresser of PR1* (*npr1*) to assess the role of *PR1* in particular in regulation of PTI, as a marker for SATI[229]. In addition, I substituted *pif4-101* for the mutant lacking PIFs 1, 3, 4 and 5 (*pifq)* [315]to investigate the overall role of PIF transcription factors in PTI and gain a wider picture of its feedback inhibition by SATI.

I grew seedlings from each line at 22℃ SD for 10 days before treating with PAMP (200 nm flg22 in 0.01% Silwet) solution for 3 h or leaving untreated (T_0). A higher concentration was used in this case to ensure strong initiation of defences. I collected tissue from each batch of seedlings for RNA extraction, cDNA synthesis and qPCR. To quantify basal *PR1* expression, following normalisation to the housekeeping gene, EF1α, I investigated levels of *PR1* in the T_0 seedlings and compared them to the levels in Col-0 plants to obtain fold-change in expression levels from WT. To quantify induced *FRK1* expression, following normalisation as before, I measured induction of *FRK1* as fold-change from T_0 seedlings from each line at 3 hpi.

Both datasets are compared side-by-side in to allow for mutual comparison of expression pattern between mutants.

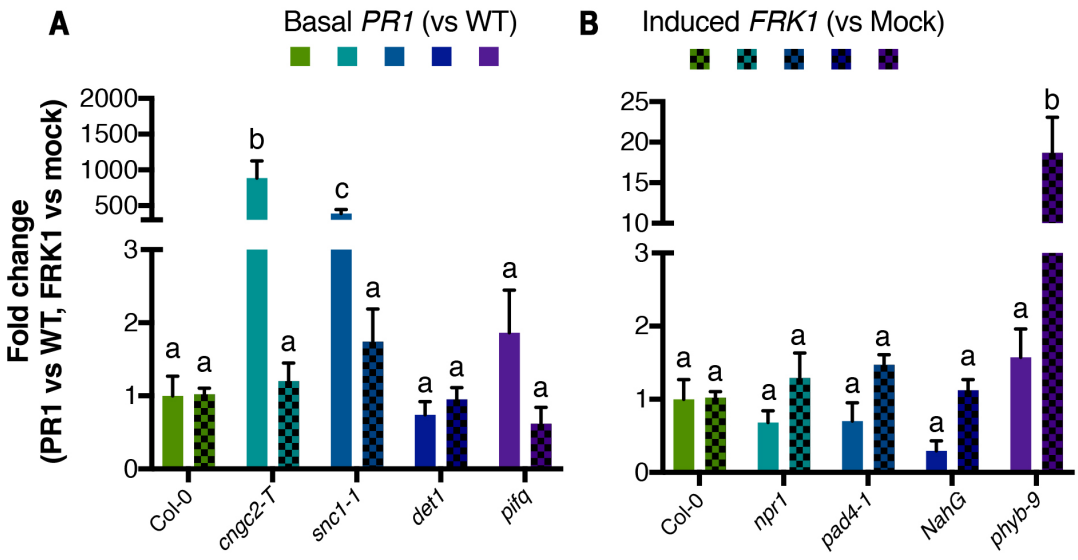

Figure 4-7 Basal *PR1* and induced *FRK1* expression in mutants with altered SATI levels - Expression of each gene measured in 10 day-old mutant seedlings with high (A) or low (B) SATI 3 hours post flg22 induction or mock

treatment. Levels were normalised to EF1α followed by fold change compared to WT (basal *PR1*) or mock, per genotype (induced *FRK1*). Statistical analyses conducted – 2-way ANOVA followed by Šidak's (A) or Tukey's (B) multiple comparison's test. Šidak's rather than Tukey's test was used for (A) to increase statistical power (n=6-9 biological/ technical replicates (3 technical + 2-3 biological).

In Figure 4-7A, *cngc2-T* and *snc1-1* mutants both show constitutively high levels of *PR1* whilst maintaining levels of *FRK1* induction in line with WT plants. In contrast to what I had expected, neither *det1* nor *pifq* showed any observable difference from WT for either gene. Conversely, in Figure 4-7B, *phyb* mutants showed an opposite effect to that of *cngc2* and *snc1-1*, with no difference in *PR1* expression levels compared to WT and vastly increased expression of *FRK1*. *npr1*, *pad4* and *NahG* plants did not show any noticeable difference in expression of either gene in spite of their known low levels of SATI. This seems to suggest a weak reciprocal effect of basal *PR1* on induced *FRK1* level, as evidenced through *cngc2-T*, *snc1-1* and *phyb-9,* however further work is needed here to confirm this effect, given the lack of phenotype observed in several mutants with known perturbations of SATI.

For future characterisations, it would be preferable to measure induced *PR1* expression at 18 hpi in comparison to induced *FRK1*, to deduce the parallel effects of each mutation on SATI and PTI. In addition, treatment of WT with SA or antagonists of SA will enable a stronger link specifically between SA and PTI to be drawn.

In general, here however, it is possible to conclude that the effects of elevated SATI in *cngc2* mutants such as *res1* and *cngc2-T* are not as a direct result of altered Ca^{2+} signalling, but rather as a result of perturbations in their downstream SA triggered immunity or associated responses. In the future, it will be possible to test a direct involvement of SA in this process through exogenous treatment with this hormone.

4.3 Discussion

4.3.1 Negative regulation of PTI

Overall, having initially set out to characterise PTI in *res1,* I have now identified how in contrast to earlier observations, a feedback mechanism exists between SA and early PTI.

In addition to central regulation, it would seem that both PTI and SATI are closely linked and mutually influence each other. Evidence in favour of a positive feedback between early PTI and SA such as an increase in *FLS2* expression induced by SA treatment has previously been shown [297]. Treatment with JA also identified contrasting effects on PTI ROS burst to SA, consistent with their known mutual inhibitory roles [316]. These observations of the involvement of SA in amplification of PTI led me to hypothesise that *res1* would maintain robust PTI in addition to its demonstrated levels of SATI. I have now shown how *res1* in fact lacks robust *PTI* responses such as induction of early PTI-associated genes, in addition to compromised aspects of signalling such as ROS burst. Furthermore, I have shown how, in other mutants with perturbed SATI, alterations in PTI responses can also be observed, suggesting the existence of a negative feedback interaction between these two sectors in addition to the positive feedback previously documented.

Contrary to the existing evidence of a reciprocal positive influence of these two sectors, negative feedback between SA and ROS has in fact already been demonstrated in mutants with constitutive defences[317]. Leading with the original *cngc2* loss-of-function mutant line, *dnd1,* Xu and Brosche (2014) [317] showed a reduction of apoplastic ROS induction in *dnd1* which was underpinned by both SA-dependent and independent mechanisms, since elimination of SA only partially reverted its reduced ROS burst [317]. This would support my extension of SATI definition to encompass similar, SA-independent immunity. My results also did not show a direct link between SA accumulation and PTI, but rather implied a role of SATI and its associated response in PTI attenuation.

mRNA profiling and network modelling in another study has further revealed a negative regulatory relationship between early PTI signalling and SATI in mutant and WT plants inoculated with *Pto* AvrRPT2 [318]. Even upon looking back at early studies investigating SA and peroxide accumulation, decreases in ROS can be observed as correlating with increases in salicylate production [304], indicating a direct influence of one on the other. A reduction in early PTI may therefore be a general effect of heightened SATI, whether triggered by previous pathogen exposure or constitutively activated in mutants lacking pathway regulation.

To try to understand the mechanisms underpinning the apparent antagonism between SA and PTI, I investigated this phenomenon from several angles. In terms of a physiological mechanism of inhibition, both SA and its synthetic analogue INA have been shown to inhibit catalase and ascorbate peroxidase, two enzymes which facilitate ROS production[205]. This may suggest a direct mechanism for accumulation of SA to inhibit ROS production and its associated early PTI signalling. Such a direct biochemical effect may be advantageous for a plant to exploit, since uncontrolled activation of ROS production is well known to lead to autoimmunity as a result of growth trade-offs [299]. Although continuous, robust maintenance of resistance would be a preferable method of existence in the absence of any other fitness costs caused by this activation, as I have clearly shown by now, braking systems on immunity have evolved as a result of the growth-defence trade off and allow plants to grow and reproduce rapidly when pathogen pressure is low. Further support for this link can be seen in plants grown under LD conditions, where increases in SATI can be observed, presumably as a result of a lesser need for resource rationing, along with decreases in ROS production [78, 366].

There must therefore exist feedback control mechanisms to enable plants to maintain growth and prevent inhibitory accumulation of ROS or hormone- associated defences under conditions where plants must balance immunity and growth [235]. Already, SA is known to be regulated both positively and negatively[78,303], so it may follow how PTI does the same, depending on the nature of the biotic environment in which it exists. It may be possible how, given the complexity of plant immunity, both

reinforcement and braking mechanisms could exist between these two sectors, which are active under different circumstances and pathogen pressures.

Important early studies such as[295] and[306] which previously showed the existence of positive feedback between these two sectors predominantly used a 1 μM concentration of flg22 to elicit PTI responses. Similarly, in[318], pretreatment with SA was shown to increase ROS production in plants in an *NPR1*-dependent manner using the same concentration of elicitor. As a result, they concluded that a complicated relationship between early microbial perception and SA signalling must exist since they also showed an increase in flg22-induced callose deposition in mutants lacking effective SA production [318]. This 5-10-fold higher concentration of flg22 is significant given the implications of elicitor concentration in terms of perceived pathogen pressure, leading me to hypothesise how the concentration of flg22 used is crucial to the specific response observed. In some cases, concentration of flg22 used in experiments was not reported so it is not possible to confirm whether lower concentrations of flg22 underpin the differences in responses I observed [317].

In addition to the necessity to ensure appropriate regulation of plant immunity, there are features of plant-pathogen interactions which necessitate direct deactivation of PTI by the plant such as targeting of this pathway by effectors.

Effector targeting of PTI signalling is a well-documented and relatively common mechanism of pathogenicity [35]. ROS signalling itself has been shown as a key target of pathogen effectors[319], in addition to Calmodulin and its associated Ca^{2+} signal targeting by bacterial HopE1[320] and MAPK signalling by the widely conserved effector HopA1[321]. As an example, in the case of HopA1, disruption of MAP kinase activation by this effector within the MEKK1-MKK1/MKK2-MPK4 cascade leads to activation of ETI by NB-LRR protein SUMM2[322,323]. Thus, loss-of-function mutants within the MAPK pathway display severe dwarf phenotypes and enhanced pathogen resistance similar to that of autoimmune mutants[322]. In cases such as these, preferential deactivation of PTI in favour of robust SATI would be highly advantageous for a plant and facilitate the selection of SA-inhibition of PTI in this context.

4.3.2 Hypothetical model of feedback regulation of early PTI by SATI

Typically, PTI is a weak immune response to initial perception of a potentially pathogenic microorganism [222]. Activation of PTI results in a signal transduction cascade, which includes MAP Kinase activation, ROS burst, calcium dynamics and early gene expression amongst other responses previously detailed, but ultimately leads to the later stages of immune activation such as SA accumulation, expression of SA-inducible *PR* genes and systemic resistance [42]. Where previously it was thought that SA induction leads to upregulation of early PTI responses in preparation for further challenge, I have now shown how in fact, PTI responses are dampened in mutants with elevated SA. Additionally, in some cases, mutants lacking SATI show elevated PTI responses, highlighting a conditional reciprocal influence of low SATI on increasing PTI.

In reality, plants exist in an environment where total lack of biotic interactions is an unusual circumstance. Constant interaction with microorganisms means that plants detect fluctuating low levels of elicitors throughout their lifecycles. As a result, plants must maintain an equilibrium between activation of different sectors of defence, in order to maintain inducibility and activate immunity only as necessary, to avoid the consequential negative impacts on growth. When elicitor levels indicate a potential pathogenic challenge, plants initiate PTI responses, ultimately resulting in SATI (Figure 4-8). Where PTI is suppressed by pathogenic elicitor, and a relevant R gene is possessed by the plant, ETI is initiated, similarly resulting in SATI (Figure 4-8). Furthermore, as I have observed, PTI responses include reinforcement of pattern receptor machinery. This could act as a mechanism to amplify PTI responses when effectors target this pathway. In a case where SATI is already activated as a result of PTI or ETI, further PTI activation would not be beneficial however, since effective immune systems had already been employed. Challenge by additional pathogens and recognition of effectors would remain a preferable method of immune modulation, with alteration of responses specific to the pathogen which a plant is subsequently exposed to. Since activation of both PTI and SATI simultaneously have been shown as causing severe growth defects [299,300], resetting PTI once SATI had been activated

would also ensure minimal deleterious effects of defence activation on plant growth and development.

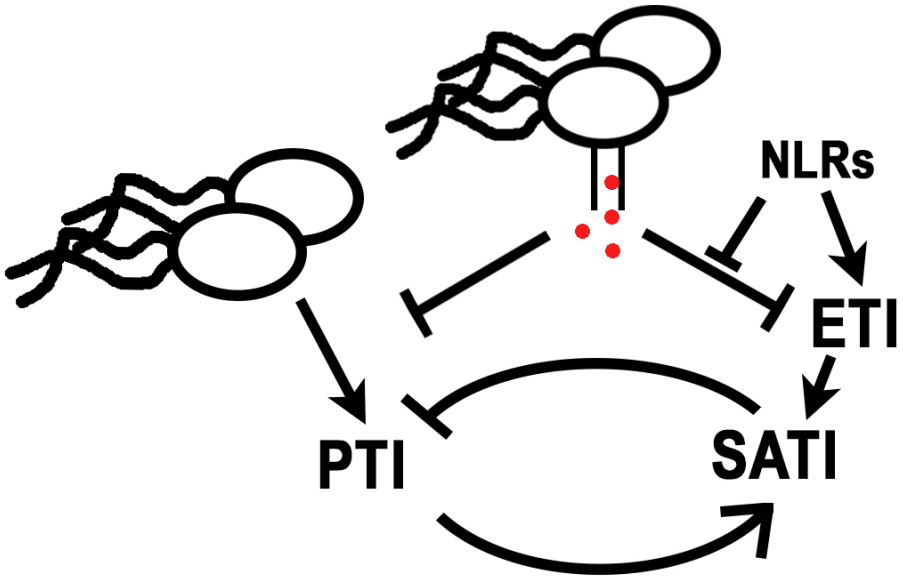

Figure 4-8 Feedback regulation of PTI by SATI – Activation of SATI by effector or pattern recognition activation negatively impacts early PTI signalling and gene expression. In some cases, lack of SATI activation reinforces PTI signalling.

As for a specific role of CNGC2 in these processes, it is currently not known which plasma membrane bound channel(s) are responsible for calcium influxes during PTI or ETI [324]. It may be possible for CNGC2 to play an additional role in immune coordination through government of Ca^{2+} release and therefore regulation of downstream signals such as RBOHD activation [325], but this remains to be tested. Currently however, it would appear that the primary mechanism of PTI attenuation in *res1* as well as similar mutants with enhanced SATI is through a direct regulatory feedback mechanism between this sector of immunity and early PTI responses (Figure 4-8).

4.4 Summary

In this chapter, earlier work showing detailing positive feedback between later stages of immunity and early PTI signalling led me to hypothesise how *res1* would maintain robust PTI signalling as a result of its constitutively elevated SATI. Following measurement of early PTI marker gene expression and ROS burst in *res1* however, I identified the presence of a negative regulatory relationship between these outputs and SATI. Furthermore, the lack of robust PTI was not specific to just *res1* or directly linked to lack of CNGC2 function. Constitutively elevating or depleting levels of SA by affecting regulators of this sector of immunity revealed feedback inhibition of PTI as a feature of resistance mechanisms and highlighted an antagonistic, negative feedback relationship between SA and early PTI. Previous work has both supported [317,318] and contradicted [295,297] what I have found here, suggesting an existence of both positive and negative regulatory mechanisms, depending on specific pathogen challenge. There is a possibility that the negative feedback mechanism I have observed has evolved as a result of pathogen effector targeting of PTI signalling. Further investigations into the attenuation of PTI by artificially inducing or inhibiting SA or its associated immune pathways in WT and high/low SATI mutants will enable deeper understanding of this pathway and the specific contribution of SA or other factors. In addition, characterisation of other aspects of PTI signalling in *res1* and other SATI mutants will enable further dissection of the extent of the novel association I have here characterised.

In conclusion, this study has further substantiated the SA-mediated signalling sector as a robust sector from which to study TSI, given how PTI is strongly influenced by SATI and ultimately alone is not sufficient to suppress pathogen growth[222]. In addition, I have established a novel relationship between two temporally and functionally distinct immune pathways which are in themselves both susceptible to environmental changes, further highlighting the complexity and highly coordinated nature of plant immune systems.

5 General discussion

5.1 Key findings

5.1.1 Moderate increases in ambient temperature suppress immunity

Temperature is one of the most influential environmental cues governing plant growth and development. In line with thermosensory growth changes such as hypocotyl and petiole elongation, a reduction in immunity to a wide range of pathogenic organisms can be observed with increases in ambient temperature [1].

Plant immunity exists as a multi-layered, antagonistic network of hormone mediated signalling and responses. Up to this point, the effects of temperature on SA or R gene-mediated immunity for upshifts of ≥ 5℃ were extensively characterised [1,20,27,82,136,147] however, increases in temperature used previously were not sufficient to understand the nature of this process. In addition, the effects of increases in ambient temperature on PTI were not well understood.

Initially, I detailed how thermosensory suppression of immunity exists for PTI in addition to ETI, with certain aspects of this immune signalling pathway particularly thermosensitive and overall outputs decreased, resulting in decreased resistance to biotrophic pathogens such as *Pseudomonas syringae pv.* tomato, DC3000. In addition, with these studies I have begun to unpick the physiological fine tuning of plant defence responses upon perception of moderate temperature increases. Overall, I found an increase in temperature of 2.5℃ proved sufficient to initiate this process, highlighting the degree of sensitivity to temperature plants possess and the tight control over growth and defence processes employed under normal ambient temperatures. The existence of 24.5℃ or thereabouts as a potentially "critical" temperature, beyond which the effects of TSI can begin to be observed in *Arabidopsis* is interesting, having previously been implicated as a critical threshold both for plant [176,184] and pathogen [326] growth. However, experiments carried out here in seedlings seem to suggest relative, rather than absolute temperature changes are the primary stimulus.

Following establishment of the thermosensory suppression of PTI and the degree of sensitivity of this process, I further implicated H2A.Z/SWR1 in coordination of this process alongside their established roles in ETI and thermosensory growth [157,158]. This further underpinned previous evidence of mechanisms of universal regulation of these processes by elevated temperature and the existence of thermosensory molecules responsible for regulating these processes.

In addition to showing the degree of sensitivity and coordination of both PTI and ETI processes to elevated temperature, I observed how TSI is independent of developmental growth stage, with decreases in immunity following increases in temperature in both seedling and adult plants. A moderate increase in susceptibility in *eds1* seedlings further highlighted to me the potential contribution of EDS1-independent mechanisms in seedlings which are lost in adult plants

In the future, it would be advantageous to study TSI responses in plants at different developmental stages further to establish the molecular mechanisms underpinning these differences. In addition, it would be interesting to study these processes for *Arabidopsis* accessions adapted to different climates, to expand the understanding of what I have observed here. Comparisons of temperature responses between plants adapted to different temperature differentials or ranges would enable further understanding of the nature of a potential plant "thermostat" system.

Altogether, the investigations undertaken here have expanded and enriched knowledge as to TSI as a thermosensory output as well as providing scope for future research into the effect of environmental changes on plant immunity.

5.1.2 Identification of a novel mutant with resilient immunity

As an output of both PTI and ETI/SATI in plants, *PR1* has been firmly established as a marker [225,226,327] whose expression is attenuated by elevated temperatures [82,139]. Through usage of the luminescent *PR1-LUC* reporter line, a set of mutants was able to be identified with high temperature resilient immunity, of which I took forward *resilient1* for characterisation and further study. Upon characterising this mutant further, I found it to have robust resistance at 27℃ compared to 22℃, alongside with

having compromised thermosensory growth responses. Through bulk segregant RNA-seq analysis, I was able to map *RES1* to *CNGC2*. The implication of CNGC2 through this study highlighted the importance of this channel in coordination of temperature responses. Furthermore, this discovery implicated the crucial role of calcium signalling in mediating the thermosensory growth/ defence trade-off. Following identification of this channel, I set out to understand the effects of a SNP in this channel in *res1* on function and downstream output of this channel. From this, I identified this single mutation as resulting in differential splicing of CNGC2, with the novel splice variant attenuating function of this channel and thermosensory growth and (SA-mediated) defence responses in this mutant.

5.1.3 SA-triggered immunity negatively regulates early PTI responses

In addition to its implication of calcium in ambient temperature responses, characterisation of PTI responses in *res1* enabled identification of potential feedback between SA and PTI. I identified a deficiency of this important layer of immunity in *res1* which was common to PAMP-induced ROS burst as well as downstream gene expression outputs and signalling reinforcement mechanisms.

The phenotypes I observed in *res1* were strengthened in the *cngc2-T* loss of function mutant, leading me to consider whether a direct impact of SATI on PTI existed as a result of negative feedback between the two. I found that mutants within other regulatory divisions of defence, displaying constitutively elevated or decreased levels of SA revealed a general association of elevated SA with dampened PTI and a weaker reciprocal effect of low SA on maintaining or increasing PTI output. Whilst it was not possible to directly implicate a role for SA in governing these processes, there still exists a strong association of this hormone with the observed phenotypes, leading me to consider SA and its associated responses as potential direct modulators of PTI. Moreover, I identified how the suppression of PTI in this manner is not specific to *res1,* but rather a general feature of enhanced SATI.

These data also highlighted mutants deficient or abundant in PIF4 levels as an exception to this process, given its opposing phenotypes to its known levels of SATI. This molecule is known to be regulated by various environmental cues, at both the

transcriptional and post-translational level in order to coordinate growth and defence [86,128,136,155,169,237]. Further studies of PTI in mutant or transgenic overexpressor lines will further elucidate the complex role of this factor in immune processes, and whether it may act independently to PhyB in this context.

Overall, I have now identified an important aspect of feedback between different defence sectors which has opened up possibilities for further research as to pattern-triggered immune activation in the context of its existing SA-mediated immunity status.

5.1.4 Elevated temperatures affect bacterial pathogenicity

In addition to the clear effects of temperature on plant immunity, this thesis has also highlighted the effects of temperature on pathogen lifestyle. I have observed how an increase in disease symptoms can be observed with increases in temperature, even when bacterial load on leaf surfaces are quantifiably similar. Previously, it was thought that effector production by pathogens decreases with elevated temperature [328,329]. An increase in wilting and chlorosis in *eds1* plants could be observed in Chapter 2, particularly between 22 and 27°C, even where no detectable difference in colony forming units was present. This study highlighted the dual effects of temperature on plant immunity and bacterial pathogenicity. This observation is supported by a recent study, which demonstrated an increase in bacterial effector secretion with increasing temperature [27]. Further work will therefore be necessary to determine the combined effects of increasing temperature on both plant immunity and bacterial pathogenicity, to determine their contribution to the predicted northwards shift and increase in severity of crop diseases as a result of climate change [22,23].

5.2 Research implications and future directions

5.2.1 The quest for the thermosensor

Over the past decades, research regarding the existence of crucial thermosensory nodes responsible for coordination of ambient temperature responses in plants has become increasingly important, particularly in the light of anthropogenic climate change and its wide-ranging effects on every aspect of human existence. As evidenced by the work I have conducted in this thesis, whilst not stressful to the plant, more modest changes in temperature, are still influential on plant phenology. Given the impact of temperature on important plant processes such as growth and immunity, further understanding of plant thermosensory mechanisms is necessary in order to understand and mitigate potential effects of climate change on food security.

To this end, many important contributing factors to temperature sensing and responses have been identified [97,126] leading to Important fundamental discoveries towards understanding the underlying molecular mechanisms governing ambient temperature responses across plant species. Known components of plant ambient temperature responses such as DET1/COP1-PIF4, PhyB and SNC1 have already been identified and interact with each other [81,131,132,136,127] as well as being modified through components such as SIZ1, a SUMO-E3 ligase [139]. In the case of PhyB, natural variation within this molecule and its coordination of this process has been shown to underlie adaptation of *Arabidopsis* [127]. In addition, the importance of H2A.Z and SWR1 components in governing global transcriptomic responses to these processes has been characterised [157,158]. These components must all act synergistically in order to transmit information about the plant in its environmental context.

When considered in the evolutionary context of plants life history, individual thermosensory molecules are unlikely to exist in isolation from each other and from other internal physiological processes without numerous interactions or buffering by parallel mechanisms, since temperature evidently affects all subcellular components simultaneously. For example, plasma membrane composition and fluidity, metabolic

changes and alterations in protein-protein interaction are all directly affected by temperature [103,330-332].

To this end, I think it is important to consider a network of thermosensory modules which interact in order to coordinate a diverse set of responses and allowing plants to adapt to moderate or tolerate stressful environmental changes over the course of their life time and evolutionary time. Precisely how signalling in response to ambient temperature changes was not known previously, but with *res1,* I have enabled implication of a crucial sensory and signal transduction mechanism which could act as a key initiation and modulation mechanism within this network.

5.2.2 CNGC2 as a signal integrator

With my studies, the implication of calcium in particular has contributed towards understanding of thermosensory mechanisms by providing a common mechanism of regulation of both growth and defence processes in response to temperature changes.

In general, CNGC2 is known to coordinate calcium signalling in response to external environmental cues and I have now implicated it in coordination of ambient temperature signalling. Precisely how this channel functions to modulate calcium dynamics in response to temperature however is not yet known. In spite of this, the work I have conducted highlights the potential for modification of this channel on conferring advantageous immune traits in crop species. Existing studies on this CNGC in distantly related crops such as potato and tomato would seem to suggest conservation of function of this channel across species [248] and the potential for minor modifications to alter temperature and immune responsiveness in crop plants over evolutionary time. Silencing of *CNGC2* in these Solanaceous plants has been shown to increase resistance to several commercially important diseases with little or no fitness cost in terms of size and yield [252,333]. Furthermore, in their study, Sun *et al* (2015) observed how the resistance conferred to tomato and potato plants was not influenced by changes in environmental conditions [248] which would seem to support what I have observed under controlled experimental conditions in *Arabidopsis* and its potential for translation and impact of the research conducted here in the future.

It will also be necessary to further understand the precise nature of alterations in calcium signalling initiated by these changes in order to understand TSI as an output of thermosensory responses.

So far, my work has implicated the importance of calcium signalling, mediated via CNGC2, in ambient temperature responses, where previously it was implicated separately in high temperature stress [107], immune and growth [113] processes. Furthermore, a direct route for changes in temperature to affect operation of this channel such as this has previously been highlighted, and a mechanistic hypothesis proposed whereby direct effects of changes in plasma membrane fluidity affect channel function and/or interaction [99,110], but this has yet to be shown under ambient temperature conditions. Alteration of temperature causes transient influx of calcium into the cytosol [274,334] in specific patterns according to the precise nature of the stimulus encountered [335], so modulation of CNGC2 could directly attenuate downstream responses in plants though its reduced capability to react to environmental stimuli.

Dissection of the particular mechanism of downregulation of this channel or other Ca^{2+}-dependent processes involved in plant thermosensory growth and defence responses in *res1* would be an important area to investigate further in the future. In particular, greater understanding of the effect of combined temperature and immune challenges on calcium signatures may enable a more in-depth mechanistic understanding of this process possible. In addition, to verify the role of CNGC2 as a central coordinator of temperature information in this way, it would be important to investigate the interaction of calcium-mediated pathways with known thermosensory components in the future, in particular with PhyB and PIF4, as well as further study into the interaction of CNGC2-mediated pathways with SNC1.

Further investigation of the localisation and molecular associations of this channel will also enable determination of the contributions of differential subcellular calcium stores and channels in this process.

5.2.3 Calcium signalling regulates ambient temperature responses

In light of the well-known contribution of calcium signalling to environmental and stress responses [107,108,250,335-338], the identification of its importance in ambient temperature signalling with this study has not been unexpected, despite no known direct role for this important secondary messenger in ambient temperature responses. Furthermore, given the range and diversity of calcium channels as well as calcium-modulated plant processes [111], no direct mechanism of upstream initiation of these responses could have been predicted. The implication of CNGC2 in particular in this study has extended the role of this channel and linked the previously separate growth and defence processes it had been implicated in. Along with its partner, CNGC4, these cyclic nucleotide-gated channels are particularly interesting since they are both distinct from the rest of their family at key residues and highly conserved in others [232]. This observation shows the potential effects minor alterations may have on channel function and how modifying CNGC2 could enable adaptations to temperature changes over evolutionary time. Previous work has also identified CNGC2 as a key candidate for initiation of calcium signalling in plant innate immunity [339] so future study may enable extension of the role of this crucial channel even further. Calcium signalling in response to PAMP perception can act directly via phosphorylation by RLCKs such as BIK1 [340], so future studies into posttranslational modification of both WT and mutant versions of this channel and the roles PTI components in this process would also prove highly informative.

In addition to its novel role, the identification of localisation of CNGC2 on nuclear or ER membranes in addition to the plasma membrane implicates apoplastic-cytoplasmic as well as cytoplasmic-nuclear calcium gradients as generating necessary signals for ambient temperature responses. Various studies have highlighted the importance of the nuclear or ER membrane lumen in facilitating calcium oscillations both within the nucleus and propagating from the nucleus to cytoplasm as well as highlighting the potential for many nuclear localised channels [287,291,341,342]. Furthermore, the importance of the ER in propagation of calcium signals known as calcium-induced calcium release (CICR) [324] may highlight a direct role for this channel with regards to its demonstrated position on nuclear/ER membranes.

Next steps for this research would therefore be to elucidate the precise downstream effects modifying this channel brings about and how it functions normally. Whilst many of the intermediate signalling effects of calcium are known, any direct mechanisms of calcium signal propagation and translation into gene expression and plant-wide changes are yet to be determined. In general, intracellular calcium changes are thought to bring about stress responses through activation of genes encoding proteins which confer tolerance [343]. The potential for environmental signal perception through direct effects of calcium changes on genes and transcription factors in the nucleus has recently been shown [338] and if identified in its new context, this process could exist as the crucial link between what I have observed for CNGC2 and downstream effects of ambient temperature changes.

Whilst many specific signatures of calcium are known [344], the precise signal generated by plants to pathogen challenge when at elevated ambient temperature conditions is not yet known[345]. To this end, in recent years a number of highly useful and versatile calcium reporter lines allowing subcellular calcium fluxes to be visualised have been generated.

Previously, the use of calcium sensitive aequorins or Förster resonance energy transfer (FRET) based Camelion probes have enabled characterisation of subcellular calcium dynamics [346,347] in response to environmental signals [250,348,349]. In addition, novel dual fluorescent protein-based sensors [350] have recently enabled simultaneous, multiparameter changes in calcium flux to be imaged [348]. Usage of these resources will enable much greater understanding of the simultaneous effects of elevated ambient temperature increase and pathogen challenge on plant signalling in the future. If this precise response were to be characterised and modelled, it would then open the door to further understanding of how changes in this process directly or indirectly affect plant gene expression and accordingly phenotypic adaptations.

5.2.4 The growth-defence trade-off

Through my work conducted in this thesis, I have identified a novel mechanism of coordination of growth and defence at elevated ambient temperatures. The

existence of components such as CNGC2 as part of a thermoregulatory system governing growth and immune responses is thought to be instigated by the growth-defence tradeoff in plants.

Throughout this thesis, I have demonstrated how the effects of this trade-off could negatively affect plant life in the future, particularly if unusually high temperatures are perceived during spring when day lengths are shorter [351,352].

Whilst I have established the potential consequences of this trade-off on plant immunity at elevated temperatures, there remain several questions open as to the nature and selection pressures existing for this process. Classically, this trade-off has been implicated as a result of the high energetic cost of both growth and defence [2], requiring plants to prioritise the use of the resources according to their environmental conditions, but establishing such a direct link has been difficult [175]. Direct costs of defence activation such as autotoxicity or antagonistic compromising of other defence processes can occur in addition to the physical costs of energetic consumption and resource allocation [175]. The availability of photosynthate and other nutrients are known to fluctuate under different environmental conditions [330,353,354]. Recent evidence however would suggest a lack of direct connection with photosynthate availability and resistance, since increasing day length has been shown to increase resistance of plants independently of growth stage or light intensity [81]. In the future, it would be important to verify the role photosynthate levels and photoperiod play in modulation of the thermosensory growth-defence trade-off to further establish the extent of this phenomenon and therefore the consequences of temperature perturbations on plant immunity under different seasonal conditions.

5.2.5 SA-triggered immunity

The involvement of SA-mediated pathways in control of responses to biotrophic pathogens has been long established [56]. This phenolic regulatory molecule has also been implicated in modulation of the trade-off between growth and defence given the wide range of roles this hormone plays in growth and development in plants [355].

Many antagonistic and complementary pathways are thought to exist alongside SA to modulate specific pathogen responses. but both SA-dependent and independent mechanisms contribute to the heightened resistance in autoimmune mutants such as *snc1-1* [140].

The existence of these complementary pathways has been demonstrated throughout my studies. Firstly, by the identification of EDS1-independent defence mechanisms in seedlings, I showed the contribution of parallel pathways to EDS1/ SA to immunity. In addition, I showed how PTI regulation is associated constitutively elevated or low levels of SATI, however I was not able to implicate SA directly, suggesting potential direct influence of SA along with associated pathways in modulating this process. In support of this, transgenic *NahG* plants constitutively expressing salicylate hydroxylase and thus unable to mount SA-mediated immunity likewise lacked robust PTI unlike other mutants with similarly low known levels of SATI. In addition, *pif4* mutant or overexpressor plants, with constitutively high/ low levels of SATI [127] displayed levels of PTI opposite to other mutants with similar phenotypes, which suggests differential function of this transcription factor in terms of PTI coordination. The mechanisms by which PIF4 coordinates PTI responses has yet to be determined.

There exists a large body of evidence to suggest that other pathways act alongside SA in governing responses such as ETI. No genes can be identified as regulated by the SA-sector alone [62]. Likewise, SA does not always confer resistance [356] and has been shown as sufficient but not necessary for ETI [302].

Further work as to the direct effect of SA on modulation of immunity will be necessary to distinguish this process from other, parallel immunity. Studies into the effects of exogenous SA addition on modulation of processes such as PTI will enable further understanding of this important immune layer.

5.2.6 CNGC2 modulates SA-triggered immunity

The identification of *res1* as a mutant with implicitly high endogenous SA levels in parallel with *cngc2* null mutants would seem to suggest modulation of phenotypes

in this mutant may act via this pathway, however *cngc2* mutants are known to display pleiotropic, SA-independent phenotypes such as late flowering [357] and sporophytic defects underpinning a reduction in fertility in this mutant [358], showing a parallel role of this channel in modulation of growth and development to that governed by SA. Furthermore, CNGC2 has also been implicated as directly regulation of auxin signalling [249], a phenomenon which I have observed through the downstream effects on YUC8 and XTR7 expression in *res1* mutants resulting in their attenuated growth. It is likely that CNGC2 regulates both SA-dependent and independent pathways upstream, with downstream hormones then governing growth and defences in their own right. *cngc2* mutants clearly hold the key to understanding some of the most important developmental and immune "decisions" in plants and the implications of this channel on higher regulation of growth and defence components which are in themselves regulatory further highlights the complex and robust nature of TSI. There remain many unanswered questions with regard to ambient temperature responses and the role of SA and calcium therein.

5.3 Further work

Over the course of this thesis, I have built upon existing knowledge of thermosensory suppression of immunity at elevated ambient temperatures as well as identifying a key novel component of its regulation. Initially, I showed how both PTI and ETI are suppressed by elevated ambient temperature. Following this, I used *PR1-LUC* as the basis for a mutant screen in order to identify potential components of the regulatory system governing TSI. Identification and characterisation of *res1* highlighted the importance of CNGC2, a cyclic nucleotide-gated calcium channel in modulation of thermosensory growth and immune responses, likely through alteration of key calcium signals. Furthermore, I identified a novel negative regulatory link between SATI and PTI activation.

These studies have highlighted key areas for future research in order to understand these processes are brought about at a fundamental level as well as in their

environmental context. Below I have highlighted some of the potential scope for future directions of the research conducted in order to progress this research further.

5.3.1 Consequences of modulating CNGC2 on ambient temperature responses

The data I have generated as well as observations I have made so far would seem to suggest a mechanism of inhibition of CNGC2 function by interactions of the alternative splice variant of this channel with other versions as well as a moderate effect of the version containing the non-synonymous SNP in *res1* in a number of potential ways. Investigating the interaction of these splice variants with other subcellular components such as CNGC4 would enable determination of their effect and potential for perturbing calcium signalling [256]. Initially, looking at protein-protein interactions between $CNGC2^{(SV2)}$ with $CNGC2^{(res1)}$ or $CNGC2^{(WT)}$ as well as with CNGC4 through split luciferase assays such as those developed by Paulmurugan and Gambhir (2003) [359] would be informative to this end. In addition, co-immunoprecipitation followed by mass spectrometry to identify a complete list of physically interacting proteins with the different splice variants of CNGC2 would provide further targets to investigate in terms of interaction with this channel.

5.3.2 Subcellular quantification of calcium dynamics in response to temperature changes

I have now identified a calcium channel as an important player in governance of plant thermosensory responses and implicated calcium dynamics in these processes. Characterisation of precise calcium dynamics in WT plants subjected to changes in ambient temperature and exposed to pathogens would be a beneficial first step here, using bioluminescent calcium sensors such as aequorin or the ratiometric cameleon/GECO sensors [347,348,360]. In addition, further analyses of these signals in *res1* or stronger *cngc2* mutant alleles such as *cngc2-T* will allow the precise effects of perturbations of these channels on calcium signalling in response to temperature changes, PTI elicitation and SA-mediated defence to be determined.

A study recently published highlighted the extent to which PTI-induced calcium influx inhibition is a key mechanism of pathogen colonisation [361]. Studies such as those

proposed above would also enable solving whether "leaky" hyper-responsive phenotype in *res1* facilitates higher resistance via this mechanism or if a lack of calcium signalling in this mutant phenocopies persistent targeting of this mechanism by effectors. Usage of exogenous calcium or calcium agonists such as mastoparan [362] may further enable dissection of different aspects of TSI and allow determination of the precise effects of CNGC2 on calcium signalling.

5.3.3 Interaction of CNGC2-mediated calcium and known thermosensory pathways

Following investigations into ambient temperature-mediated calcium dynamics in mutant and WT lines, further detail as to thermosensory networks and levels of regulation could be gained through genetic and proteomic interaction studies. Associations of CNGC2 with Phytochromes, PIFs and SNC1-mediated pathways as well as known regulators such as BON1, which have recently been implicated in calcium signalling in its own right [349] would provide crucial information in this respect.

To enable further understanding as to the direct mechanism of temperature regulation of CNGC2, it will also be possible to determine whether this channel is directly affected by membrane fluidity or other aspects of composition as previously hypothesised, through use of artificial membrane fluidisers such as benzyl alcohol [110].

5.3.4 Towards applications of research conducted

With this research I have shown how calcium and modulation of calcium signals by CNGC2 are crucial for thermosensory responses and may represent one of the key nodes underpinning environmental adaptation. Whilst clearly positive effects of the *res1* mutation can be observed with regards to immunity, these effects come with an apparent yield cost to the plant. In the future, it will be important to balance potential negative impact of modifying plant resistance on productivity and fitness through processes such as modifying CNGC2 as demonstrated with this thesis. In areas where pathogen pressure is highest an overall benefit of increasing crop immunity may be visible of enhancing the thermostability of plant immunity, in spite of the yield cost. To this end, modifications in CNGC2 activity such as downregulation

with RNA interference (RNAi) as previously carried out [248,252] or through introduction of *CNGC2*$^{(SV2)}$ may provide mechanisms to improve immunity in crops. Understanding the molecular mechanisms underpinning plant thermosensing as governed by CNGC2 and the downstream effects of perturbing this channel on all aspects of immunity will further unpick the potential applications of this research.

5.4 Final comments

With this thesis, my primary aims were to understand and dissect the suppression of immunity in *Arabidopsis* as an output of plant thermosensory responses. Initially, I investigated the effects of temperature on PTI and ETI in order to characterise TSI as a whole, before using this process as an output of thermosensory mechanisms to recognise CNGC2 as a crucial calcium channel regulating ambient temperature responses. In addition, I identified and characterised a negative feedback relationship between two key sectors of plant immunity. Overall, with this thesis I have expanded knowledge of the nature as well as the underlying mechanisms governing TSI in plants.

6 Materials and methods

6.1 Seed sterilisation

Seedlings were sterilised in 70% ethanol + 0.5% Triton X-100 for 1 minute followed by 100% ethanol for 1 minute before being plated on GM media and stratified for 3 days at 4℃ in the dark (media recipes can be found at the end of this chapter).

6.2 Plant material and growth conditions

All seed material and mutants used in this study were in the Columbia (Col-0) background. For assays conducted on adult plants, seeds were surface sterilised as per method 6.1 and germinated at 22℃ under short day photoperiod conditions (SD, 8 h light/16 h dark) for 7-10 days before being transplanted into 24-well solid compost trays at 22℃, 70% humidity in Sanyo environmental test chambers MLR352-H (Sanyo, Osaka, Japan) unless otherwise stated. Compost used for all experiments was F2 peat in a 6:1 ratio with 4mm grit and Exemptor (Chloronicotinyl Insecticide (0.28 g/litre), Bayer, Leverkusen, Germany) added.

For assays conducted on seedlings, seeds were spread evenly across 15-well soil trays and stratified at 4℃ in the dark for three days. Seedlings were then germinated at 22℃ SD for 3 days, then either kept on at this temperature or shifted to a range of other temperature conditions as required.

For general plant growth purposes for multiplication, genetic crosses and genotyping, plants were grown at 20℃ under long day (LD, 16 h light, 8 h dark) conditions.

6.3 Backcrossing and generation of double mutants

Following stratification as detailed in 6.2, plants were grown for crossing under constant 20℃ LD conditions in a non-humidity-controlled chamber until flowering and production of fertile siliques. Developing meristems and siliques were removed from inflorescence and 3-5 buds maintained and developing anther removed. Two

days following emasculation, buds were pollinated and siliques isolated. Seeds were collected once ready and used for F1 characterisation, or taken forward for *LUC* quantification in F2 segregant populations, selection of double mutants or homozygous lines based on phenotype and genotyping for the respective marker/ mutation.

6.4 Hypocotyl measurement (plate)

Seeds were sterilised as per 6.1 and regularly spaced on 10 x 10 cm square GM agar plates using a sterile toothpick, plates sealed with microporous tape and seeds stratified for 4 days at 4℃. Seedlings were grown at 22℃ for 2 days then transferred to 17, 19.5, 22, 24.5 or 27℃. Images were taken at 8-days post – germination and hypocotyl length from apical meristem to beginning of root using ImageJ (Ver. 1.51H) was measured using the segmented line tool to account for changes in hypocotyl direction.

6.5 Hypocotyl measurement (soil)

Seeds were dispensed in 5 x 5 rows on soil in 15 well soil trays as per *LUCIFERASE* assay and stratified at 4℃ for 4 days before being at 22℃ SD for 7 days. Seedlings were either maintained at this temperature or shifted to 27℃ for three days. Individual plants were removed from soil and arranged on plates so that the full length of their hypocotyl was visible, imaged and measured with ImageJ as per 6.5.

6.6 Petiole measurement

Seedlings were grown on soil as per hypocotyl measurement, and maintained at their respective temperatures for a further 7 days. The three longest petioles from each seedling were dissected and total length quantified using ImageJ as above.

6.7 Flowering time measurement

Seeds were stratified and germinated on GM agar at 22℃ SD before being transplanted to 24-well soil trays with forceps at 22 or 27℃. Plant growth was monitored and days to opening of first flower bud quantified and rosette leaf number measured from 5-9 plants per genotype.

6.8 Growth characterisation and phenotypic comparison of adult rosette size

Seeds were sterilised and germinated on GM agar plates as above (6.7) at 22℃ for 7 days and transferred one plant per well into 24-well soil trays at constant 17, 22 or 27℃ SD as appropriate in large controlled environment rooms (CERs). Growth and senescence phenotypes were monitored and documented at one-week intervals unless otherwise stated. Rosette diameter was measured with ImageJ, using Feret's diameter to quantify differences in diameter of these non-circular objects.

6.9 *Arabidopsis* transformation and generation of transgenics

Floral dip procedure detailed by Clough and Bent (1998) [363] was performed. In brief, *Agrobacterium* strains were cultured in 10 ml LB media + antibiotics overnight. The following day, bacterial culture was transferred to 100 ml LB (no antibiotics) and incubated with agitation at 28℃ for 4 hours. Cells were spun down at 3000 rpm for 5 minutes and supernatant discarded. Cells were resuspended in Trato media (see below) and used to dip flowering *Arabidopsis* plants, ensuring emerging buds were completely submerged. Plants were dried overnight in the dark and transferred to 20℃ LD for seed collection.

6.10 Flg22-induced resistance

Five plants each of Col-0 and *fls2* lines were grown for four weeks at 22℃ SD before being shifted to 27℃ SD for three days or maintained at 22℃ and sprayed with 100 nM flg22 in 0.01% Silwet or Mock (0.01% Silwet) solution 24 hours before the seedlings were spray-inoculated with *Pto* DC3000 as above (OD_{600}=0.02). Plants were grown for a further 3 days at their respective temperatures following infection, after which bacterial CFU/cm^2 was measured as above.

6.11 Oxidative burst assay

Eight to sixteen plants per genotype were stratified at 4℃ for 3 days then grown at 22℃ SD for 5 weeks, or until leaves are big enough for leaf discs but well ahead of initiation of start flowering. If necessary, half the plants were shifted to 27℃ SD three days before the start of the experiment. On the evening of the day before ROS measurement, leaf discs were made using a 3 mm sterile tissue borer and 3 leaves

per plant and placed right side up into 100 μl water in 96 well white opaque plates. Plates were incubated overnight at their respective temperatures. The following day, water was removed from each well using a multichannel pipette, making sure no residual water remained. 100 μL assay solution (100 μM Luminol, 100 μM peroxidase and 100 nM flg22 in water) was added to each well and the luminescence immediately measured 2x per minute over a 40-minute period using a Varioskan Flash microplate reader.

6.12 Calcium sensitivity assay

Seeds were sterilised as per 6.1 and plated on ½ MS +0.5% sucrose. Plates were stratified at 4℃ for three days and seeds grown until germination at 22℃ SD Following germination, I transferred 10-12 seedlings per genotype to ½ MS +0.5% sucrose liquid media in six-well plates under a laminar flow hood (Bassaire, Southampton, UK) with 10, 20, 500 or 100 mM $CaCl_2$ for ten days. Seedlings from each well were separated into groups and average weight per seedling measured for each concentration.

6.13 Confocal microscopy

Seedlings were sterilised as per 6.1 and grown for 8 days at 20℃ LD (16 h light/8 h dark) conditions on GM plates, +BASTA (15 μg/ml (BASF, Ludwigshafen, Germany)) as necessary. Seedlings were transferred to microscope slides, immersed in water and imaged using a Leica SPVIII confocal microscope (Leic, Wetzlar, Germany). In the case of *N. benthamiana,* 0.5 mm^2 leaf sections were dissected from around infiltration sites and placed on microscope slides in distilled water. Cover slips were added and tapped to ensure removal of air bubbles. Slides were imaged as above. GFP imaging was conducted with an argon ion (488 nm) laser, with output collected at 495-530 nm. Image analysis and Z-stack amalgamation was conducted using ImageJ.

6.14 Bacterial strains

One Shot™ TOP10 chemically competent *E. coli* was used for cloning (ThermoFischer, Massachussets, USA). *Agrobacterium tumefasciens* GV3101 was used for

transformation of *Arabidopsis thaliana* plants and *Nicotiana benthamiana* leaves. *Pseudomonas syringae* Pv. Tomato, DC3000 (*Pto* DC3000) strains were used for pathogen- based immunity assays. *Pto DC3000* expressing luminescent *Photorhabdus luminescens* luxCDABE operon [192] (*Pto* DC3000-lux) was used for luminescence and CFU-based infection quantification. *Pto* DC3000 strains expressing the non-native avrRps4 effector (*Pto* DC3000 AvrRPS4) was used for quantification of RPS4-dependent immunity in *Arabidopsis* as an output of ETI [195].

6.15 Culture of *Pseudomonas syringae* Pto DC3000 strains

Pseudomonas syringae Pto DC3000 was streaked from glycerol stock or from previous bacterial culture on selective NYGA media (+Rifampicin (50 μg/ml) for DC3000 strains or +Rifampicin (50 μg/ml) + Kanamycin (50 μg/ml) for DC3000 lux, DC3000 AvrRPS4 strains) for two days at 28℃. Bacteria were re-streaked on the same media for one day before being used for infection assays.

6.16 Assaying of resistance to *Pseudomonas syringae* pv. DC3000 (adult rosette stage)

Eight to sixteen plants per genotype were stratified at 4℃ for 3 days then grown at 22℃ SD for 4 weeks, or until leaves are big enough for leaf discs but well ahead of initiation of flowering. Unless otherwise stated, half of the plants were shifted to 27℃ SD three days before infection with *Pto* DC3000. On day of infection, plants were covered for 2 h with clear propagator lids to increase humidity and ensure open stomata. Bacteria were harvested from plates cultivated as per 6.15 and suspended in 10 mM $MgCL_2$ in 0.04% Silwet L-77 adjuvant (Silwet) and bacterial optical density at 600 nm (OD_{600}) was adjusted to 0.02. Solution was sprayed onto plants until runoff from leaves (around 15-20 ml per ~770 cm^2 tray) and infected plants were covered with clear propagator lids for 4 h.

Three days after infection, bacterial titre was measured as follows. Three leaf discs per plant of intermediate, similar aged leaves were cut with an 4mm sterile tissue borer. Discs were incubated in 2 ml microtubes with 500 μL 10 mM MgCl2 in 0.01 % Silwet at 28℃ for 1 hour. After this time, serial 10-fold dilutions were made of the bacterial suspension up to $1x10^{-5}$ with the suspension being carefully mixed between dilutions. 20 μL of each concentration was pipetted onto square NYGA plates with appropriate antibiotics and allowed to dry. Plates were incubated at 28℃ and bacterial colony forming units (CFU) counted and normalised to leaf area. In all experiments, *eds1-2* plants were used as a susceptible control for infection.

6.17 Assaying of resistance to *Pseudomonas syringae* pv. DC3000 (seedling stage)

Seeds from each line tested were stratified on soil in 15-well trays for 3 days and transferred to 22℃ SD conditions unless otherwise stated for one week's growth. Following this, seedlings were either maintained at this temperature or shifted for three days and infected as per 6.16.

At 3 days post inoculation (dpi), 6 biological replicates of 8-10 seedlings per genotype/ condition were collected in 2 ml tubes, and weight documented. 500 μl $MgCl_2$ in 0.01% Silwet was added and tubes incubated for 1 hour at 28℃. Following this, serial dilutions were made as above and 20 μl of each concentration plated on NYGA plates with appropriate antibiotics which were then incubated at 28℃ for 2 days. Bacterial CFU were then counted and normalised to the previously documented fresh weight (FW, mg) of seedlings measured to gain CFU/mg FW for each replicate.

6.18 Quantification of *LUCIFERASE* expression by luminescence

Seeds from the *LUCIFERASE* (*LUC*) expressing lines *PR1-LUC* and *FRK1-LUC* were placed on soil in 5 x 5 rows by suspending in 0.01% agar and pipetting onto F2 soil in 15 well solid trays and stratified at 4℃. Seedlings were grown at 22℃ SD unless otherwise specified. If a temperature shift was used, 7-day-old seedlings were shifted to their new temperature for three days before induction, otherwise 10-day old seedlings were induced with 100 nm or 1 μM flg22 in 0.01 % Silwet, or mock (0.01%

Silwet) solutions and imaged at 3 hpi for *FRK1-LUC* and 18 hpi for *PR1-LUC* expression. Seedlings were sprayed with 1 mM luciferin in 0.01%Triton X-100 before being kept in the dark until measurement. Four pots at a time were then imaged using the Photek HRPCS-3 photon counting camera for 30 s -10 min, depending on observed luminescence levels. All measurements from the same experiment were measured at the same time point. Odd area profile (OAP) measurement was quantified as stated, per individual seedling. In cases where large differences in growth or cotyledon size could be observed, OAP values per second of quantification were normalised to leaf area, as quantified through area analysis of photographical images with ImageJ.

6.19 RNA extraction

RNA was extracted from frozen plant tissue after grinding using Qiagen RNeasy® Plant Mini Kit (Qiagen, Hilden, Germany) following the manufacturer's instructions. An additional DNase treatment step was used before elution using Qiagen RNase-free DNase kit as per instructions. RNA purity and concentration were quantified using a Nanodrop™ 1000 spectrophotometer (ThermoFischer scientific, Massachusetts, USA).

6.20 Bulk segregant RNA-sequencing

RNA from 11-day-old bulk segregant seedlings was isolated as per 6.19 and sequenced with an Illumina Hiseq 200 sequencer with 8x multiplexing. Single nucleotide polymorphism (SNP) detection analysis on sequencing data was performed using Avadis NGS software. Significant SNPs between bulk segregant and reference genome sequences were isolated and synonymous or heterozygous mutations were filtered out. Segregation of significant non-synonymous SNPs within each bulk segregant population was examined to identify differentially segregating, homozygous SNPs enriched in seedlings with high *LUC* expression compared to those with low expression. Non-synonymous SNPs were isolated and compared between populations. Changes in mutant allele frequency (ΔMAF) were calculated, and mutations with a ΔMAF cut-off of 25% (0.25) were taken for further consideration.

6.21 Flg22- induced MAPK phosphorylation detection via Western Blot

Seeds were sterilised as per 6.1 and grown on ½ MS agar plates for 7 days at 22℃ before being either maintained at this temperature or shifted to 27℃ for three days. Following this, 100 nM flg22 in 0.01% Silwet or mock (0.01% Silwet) solutions were added to sufficiently cover seedlings and tissue collected and frozen at 15 minutes post treatment. Protein was extracted from each sample as follows: Tissue was ground to a fine powder in liquid nitrogen and 100 µl extraction buffer + 1x PhosSTOP (Merck KGAA, Darmstadt, Germany) phosphatase inhibitor added (Extraction Buffer – 150 mM Tris-HCl, 150 mM NaCl, 5 mM EDTA, 2 mM EGTA, 1 % NP40/ IGEPAL, 1 x cOmplete Protease Inhibitor (Roche, Basel, Switzerland)). Tissue was sonicated for 5 minutes and centrifuged for 15 minutes at 13000 rpm, 4℃ and protein concentration measured as follows: 10 µl of each sample was added to 150 µl Pierce 600 reagent (ThermoFisher, Massachusetts, USA), mixed and incubated at room temperature for 5 minutes and protein concentration extrapolated by using a standard curve of serially diluted BSA using the Nanodrop1000 spectrophotometer. Protein samples were then adjusted to have equal concentration before SDS PAGE was carried out followed by Western Blot. Samples were denatured by incubating at 70˚C for 10 min in TruPage®LDS sample loading buffer. Samples were run on TruPage® pre-cast gels (Sigma, Welwyn garden city, UK) at 140 V for 60-90 min until adequate protein separation detected. Following this, PVDF membrane was charged in methanol for 10 seconds and equilibrated in TruPage® transfer buffer (Sigma). Transfer sandwich (Sponge, filter paper, gel, PVDF, filter paper, pad) was assembled and membrane transferred for 1 h at 100V at 4℃. Membrane was blocked for 2 h at room temperature with 5% BSA in TBST (Tris-buffered saline + 0.01% Tween-20). Membrane was then incubated HRP Conjugated anti phospho-p44/42 MAPK (Erk1/2; Thr202/Tyr204) rabbit monoclonal antibodies (Cell Signaling technology, Massachusetts, USA) (1:5000 dilution) overnight at 4℃. Antibody was discarded and membrane washed 6 x at RT with TBST for 5 minutes followed by 5 minutes with TBS. Immobilon Chemiluminescent HRP substrate (Millipore, Massachusetts, USA) was added and membrane incubated with it for 5 minutes in the dark. Films were exposed in order to visualize the levels of MAPK phosphorylation.

6.22 Gene expression analysis through quantitative Reverse-Transcription Polymerase Chain Reaction (qRT-PCR)

RNA from frozen and ground tissue samples was extracted as per 6.19 using Qiagen RNeasy® Plant Mini Kit (Qiagen, Hilden, Germany) including a DNase step. Complementary DNA (cDNA) was then synthesized as follows. 1-2 μg RNA was added to 1 μl oligodT and 1 μl dNTPs and nuclease free water added up to 13 μl. This mixture was incubated at 65℃ for 15 minutes, chilled quickly on ice and spun down. To this mix, 4 μl 5 x first strand buffer, 1 μl DTT, 1 μl RNase inhibitor and 1 μl Superscript III (Invitrogen, California, USA) was added and mixture incubated at 50℃ for 1 hour followed by 70℃ for 15 minutes. cDNA samples were diluted 10-fold and 2 μl used for each qPCR reaction alongside 5 μl 2x SYBR™ green master mix (Roche, Basel, Switzerland) 1 μM oligo mix and 2 μl nuclease free water. Relative transcript levels were quantified as fluorescence cycle threshold (Ct) with light cycler® 480 (Roche life science) and normalised to Ct of the housekeeping gene, *EF1α*. From each set of tissue analysed, three biological samples were taken and from each experiment, three to four technical replicates were taken from cDNA samples. Statistical analyses combined both biological and technical values to obtain comparisons.

6.22.1 Genomic DNA extraction

Plant material was collected in individual tubes, frozen and ground with pestle or Geno grinder (Spex, Stanmore, UK). 300 μl extraction buffer (0.14 M d-Sorbitol, 0.22 M Tris-HCl (pH8), 0.022 M EDTA (pH8), 0.8 M NaCl, 0.8 % CTAB, 1 % n-Lauroylsarcosine in distilled water) was added and samples were mixed by inversion, followed by incubation at 60℃ for 15 min. 300 μl chloroform was added and samples mixed by inversion, followed by 2 min centrifugation at 5000 rpm. Upper phase was transferred to a new tube and 300 μl isopropanol added and mixed by inversion. Samples were left at -20℃ for 10 min and DNA spun down for 10-15 min. Supernatant was removed and pellet washed with 70% EtOH before being re-spun, supernatant removed and allowed to air dry. DNA was resuspended in 100 μl water, quality and quantity measured using a Nanodrop™ 1000 spectrophotometer and samples stored at -20 until used for PCR.

6.22.2 PCR (Phusion)

Phusion® high fidelity DNA polymerase (New England Biolabs, Massachusetts, USA) was used for all PCR amplification reactions for cloning, as per the manufacturer's instructions.

For each PCR reaction, 2 μl template DNA was used with 1 μM forward primer and 1 μM reverse primer alongside 200 μM dNTPs, and 0.2 μM Phusion DNA polymerase, up to a total of 10 μL per reaction, made up to volume with dH_2O.

Table 6 PCR conditions

Step	Temperature	Time
Initial denaturation	98 ℃	30 sec
25-35 cycles	98 ℃	5-10 sec
	45-72 ℃	10-30 sec
	72 ℃	15-30 sec per Kb
Final extension	72 ℃	5-10 minutes
Hold	4 ℃	

PCR reactions were carried out using an Eppendorf Master cycler Pro (Eppendorf, Stevenage, UK). Genomic or cDNA *CNGC2* sequences were amplified with or without promoter and without stop codons for introduction into entry and gateway vector plasmids.

6.23 DNA extraction for genotyping

One flower bud per plant or small piece of leaf tissue was isolated and kept on dry ice in 0.2 ml Eppendorf tube. 20 μl 0.25 N NaOH added to each tube and sample incubated at 96℃ for 10 minutes and centrifuged briefly. 20 μl 0.25 N HCl added to each tube followed by 20 μl Neutralisation buffer (0.5 M Tris-HCl pH8, 0.25 % NP40). Samples were vortexed briefly and incubated at 96℃ for 3 min, spun down for 30 s. 50 μl distilled water was added and samples spun at max speed for 2 min. 2 μl of the supernatant containing DNA was used for each PCR reaction. GoTaq® DNA polymerase (Promega, Wisconsin, USA) was used as per manufacturer's instructions.

6.24 Cloning

6.24.1 Gateway® Cloning and Transformation of *Arabidopsis*

Gateway® Cloning was performed as described by the manufacturer (ThermoFischer) as follows. DNA fragments for cloning were amplified by PCR and cloned into the pENTR^{TM}-D-TOPO^{TM} entry vector (ThermoFischer scientific, Massachusetts, USA) and successful insertion of DNA was confirmed through restriction digest and Sanger sequencing. Gateway reactions were then conducted to introduce successful entry clones into the gateway binary vectors pGWB 604 (pPZP backbone, Spectinomycin/ BASTA resistance for bacterial/ plant selection, no promoter, C-terminal GFP), pGWB 611 (pPZP backbone, CaMV 35S promoter, C-terminal FLAG) or pB7FWG2 (pPZP backbone, CaMV 35s promoter, C-terminal GFP) [364,365]. Full length insertion and direction of DNA sequence was reconfirmed through restriction enzymatic digest and Sanger sequencing. Positive clones were used to transform *Agrobacterium tumefaciens* GV3101 cells by electroporation and bacteria cultured in 10 ml LB+ antibiotics, to be used for Floral dip.

6.25 Analysing copy number and zygosity of transgenic lines

First or second generation (T_1/T_2) transgenic seeds were germinated on soil and sprayed with BASTA (15 μg/ml) to select transgenics. Successful transformants were transferred to 24-well soil trays and 0.5 cm^2 leaf samples were harvested for genotyping to assess copy number and zygosity. Lines containing single or double insertions of constructs were isolated using a qPCR-based assay to determine number and zygosity of BaR (Basta resistance) as a measure of transgene number insertion in a method adapted for *Arabidopsis* [257] and performed by iDNA genetics (Norwich, UK).

6.26 Statistical analyses

For comparisons of two datasets, data were assessed for normality using the D'Agostino-Pearson omnibus normality test followed by the F test to determine normality and equality of variances. For data which fit these parametric requirements, I used unpaired t-tests to assess differences between datasets with a

95% confidence interval. If data deviated from normality or equal variances, I used a Mann-Whitney test to compare unpaired groups with a confidence level of 95%. For comparisons of multiple groups, I assessed normality as before using the D'Agostino-Pearson omnibus test, followed by the Brown-Forsythe test for equal variances. If data were normally distributed with equal variances, I used the parametric one-way analysis of variance (ANOVA), or 2-way ANOVA for multiple variables, with a 95% confidence interval. I used Tukey's or Šidak's (2-way ANOVA) post-hoc test for multiple comparisons between data. If data deviated from normality and equal variances I conducted a Kruskall-Wallis one-way ANOVA followed by Dunn's multiple comparisons test with the same level of confidence. All statistical analyses were carried out using GraphPad Prism. Specific tests carried out for each dataset are detailed in figure legends or body text.

7 Appendix

7.1 Media and buffers

GM (1 L): 4.41 g Murashige and Skoog (MS) medium (Duchefa, Haarlem, Netherlands), 10 g Glucose, 0.498 g MES hydrate (Sigma, Missouri, USA) (pH 5.7), 10 g Bacto agar (Difco (ThermoFischer), Massachussets, USA).

½ MS (1 L): 2.2 g MS salts including vitamins (Duchefa, Haarlem, Netherlands), 0.5 g MES hydrate (Sigma, Missouri, USA), 5 g Sucrose (pH5.7)

Trato (250 ml): 0.545 g MS (Duchefa Haarlem, Netherlands), 12.5 g Sucrose, 125 µl Silwet L-77 (pH5.7)

MMA (100 ml): 10 ml of 0.1 M MES (Sigma, Missouri, USA) pH5.6, 1 ml of 1 M MgCl2, 100 µl Acetosyringone

NYGA (1 L): 20 ml glycerin (Invitrogen), 5 g Bacto-peptone (Difco (ThermoFischer), Massachussets, USA), 3 g yeast extract (Sigma, Missouri, USA), 15 g Bacto-agar (Difco (ThermoFischer), Massachussets, USA)

7.2 Primer sequences

7.2.1 Primers for cloning and genotyping

Target	Direction	Function	Sequence
CNGC2	Sense	CNGC2 genomic fragment with native 1.3 Kb promoter for cloning into pENTR	CACCAGCTCGAAACAGCATC
CNGC2	Antisense	CNGC2 for gateway cloning, no STOP	TTCGAGATGATCATGCGGTC
CNGC2 (cds)	Sense	sense oligo for amplifying CNGC2 cds for TOPO cloning	CACCATGCCCTCTCACCCCAAC
CNGC2	Sense	Sequencing oligo for C-terminal fusion	ACTCTCATGGTGCCTACGTC
CNGC2-GFP	Sense	Amplifying Into GFP from CNGC2 for confirmation of homozygosity in transgenic lines	GAAAAGAACCCGTGGTGAAA
CNGC2 cDNA	Sense	Forward primer for amplifying CNGC2 cDNA. Amplifies both SV1 and SV2 with same product size of 80bp	ACGGTGTAGGGATATGGAATGG
CNGC2 cDNA	Antisense	Reverse primer for amplifying CNGC2 cDNA. Amplifies both SV1 and SV2 with same product size of 80bp	GCTCAAATCGCCTAACCCTCT
CNGC2	Sense	Sense oligo for amplifying SV1 of CNGC2. Primes within the spliced-out region in SV2 so cannot amplify SV2	GTGTTTTTGCATGCGGTAATG
CNGC2	Antisense	Common antisense oligo for CNGC2 cDNA SV1 and SV2.	TCTAGCTCGTCTTCACCACC
CNGC2	Sense	Sense oligo specific for SV2 of CNGC2. Primes at the exon junction.	GATAGGAAACATTCAGATACGGTG
CNGC2	Sense	Common sense oligo for CNGC2 cDNA SV1 and SV2.	ACTTTTCACGCTGTTGATAGGA
GFP	Antisense	Sequencing oligo for C-terminal fusions. reads into gene of interest in pGWB vectors	TCCTTGAAGTCGATGCCCTT
35SPromoter	Sense	Sequencing oligo for inserts downstream of 35S promoter	ACGCACAATCCCACTATCCT
CNGC2 (*res1*)	Sense	CAPS genotyping, mutant sequence will cut with BSPH1	TTGAAGGTGTTTTTGCATGCGGTCATG
CNGC2 (*res1*)	Antisense	CAPS genotyping, mutant sequence will cut with BSPH1	TAGCTCGTCTTCACCACCCAAGG
AT5G11700	Sense	CAPS genotyping, mutant sequence will cut with ASUI	CAGCATAACTAGATACGAAGTGGAC
At5G11700	Antisense	CAPS genotyping, mutant sequence will cut with ASUI	CCTCCGATTTGATGCTTGCG
AT5G11610	Sense	CAPS genotyping, mutant sequence will cut with TAQ I	TGGGTCTAACGTAACCGTGC
AT5G11610	Antisense	CAPS genotyping, mutant sequence will cut with TAQ I	CGCTTGCCATGACTGGGTAT

AT5G13500	Sense	CAPS genotyping, mutant sequence will cut with RSA I	ATGCATCTCTGGAGCTTTACC
AT5G13500	Antisense	CAPS genotyping, mutant sequence will cut with RSA I	GAGTTGCCAATGGGGTCGAT
AT5G20960	Sense	CAPS genotyping, mutant sequence will cut with ESP3I	TTTAGCCTTTTCGAGGTCCCTCCG
AT5G20960	Antisense	CAPS genotyping, mutant sequence will cut with ESP3I	CTCCTTGTATTCCCTTCGGCA
MYB43	Sense	CAPS genotyping, mutant sequence will cut with HINDIII	ATGAGATCTTGATCGAAAGCT
MYB43	Antisense	CAPS genotyping, mutant sequence will cut with HINDIII	TCCACTAAACTGCAACACCA
GAUT14	Sense	CAPS genotyping, mutant sequence will cut with AHA III	GTCCAGAATGGCCGCAGAT
GAUT14	Antisense	CAPS genotyping, mutant sequence will cut with AHA III	TCCCCTAGTTTGAACTTGCAATAGA

7.2.2 qPCR primers

Target	Direction	Function	Sequence
FRK1	Sense	qPCR	CGGTCAGATTTCAACAGTTGTC
FRK1	Antisense	qPCR	AATAGCAGGTTGGCCTGTAATC
VLG	Sense	qPCR	TGCTCCATCTCTCTTTGTGC
VLG	Antisense	qPCR	ATGCGTTGCTGAAGAAGAGG
YUC8	sense	qPCR	CGATGAGACCAGTGGCTTGT
YUC8	antisense	qPCR	TTTTCTCCCGTAGCCACCAC
EF1α	sense	qPCR	TACGCCCCAGTTCTCGATTG
EF1α	antisense	qPCR	GGCTTGGTTGGGGTCATCTT
PR1	Sense	qPCR	ACCAGGCACGAGGAGCGGTA
PR1	Antisense	qPCR	TCCCCGTAAGGCCCACCAGA
PR5	Sense	qPCR	ACCCACAGCACAGAGACACACA
PR5	Antisense	qPCR	TGGCCATAACAGCAATGCCGC
RBOHD	Sense	qPCR	TGGGTGACTAGGGAACAAGG
RBOHD	Antisense	qPCR	GATGTTGTGTCGGGTACACG
PBS3	sense	qPCR	TGAGTCAAGCGAAGCTCGTA
PBS3	antisense	qPCR	ATCGATCCGTCTTTGAATCG
PIF4	sense	qPCR	GTTTGCCAAAACCCGGTACA
PIF4	antisense	qPCR	ACATCTCCATCGGCTGAGTC
XTR7	Sense	qPCR	CGGCTTGCACAGCCTCTT
XTR7	Antisense	qPCR	TCGGTTGCCACTTGCAATT
BAK1	Sense	qPCR	TGTCCTGACGCTACAAGTTCTGG
BAK1	Antisense	qPCR	AGCAACTCCTCCCGCAATCG
FLS2	Sense	qPCR	GCGAAACAGAGCTTTGAACC
FLS2	Antisense	qPCR	GTGTCGTAACGAACCGATGA
BIK1	Sense	qPCR	TTTGGCAGGCACCTTGTGTA
BIK1	Antisense	qPCR	GAACCGCATTCAATCCGTCG

Bibliography

1. Hua, J. Modulation of plant immunity by light, circadian rhythm, and temperature. *Current Opinion in Plant Biology* **16,** 406–413 (2013).
2. Huot, B., Yao, J., Montgomery, B. L. & He, S. Y. Growth defense tradeoffs in plants a balancing act to optimize fitness. *Molecular Plant* **7,** 1267–1287 (2014).
3. Fujita, M. *et al.* Crosstalk between abiotic and biotic stress responses: a current view from the points of convergence in the stress signaling networks. *Current Opinion in Plant Biology* **9,** 436–442 (2006).
4. Gamir, J., Sánchez-Bel, P. & Flors, V. Molecular and physiological stages of priming: how plants prepare for environmental challenges. *Plant Cell Rep* **33,** 1935–1949 (2014).
5. Mittler, R. Abiotic stress, the field environment and stress combination. *Trends in Plant Science* **11,** 15–19 (2006).
6. Cramer, G. R., Urano, K., Delrot, S., Pezzotti, M. & Shinozaki, K. Effects of abiotic stress on plants: a systems biology perspective. *BMC Plant Biology* **11,** 163 (2011).
7. Anderson, J. T., Willis, J. H. & Mitchell-Olds, T. Evolutionary genetics of plant adaptation. *Trends in Genetics* **27,** 258–266 (2011).
8. Kissoudis, C., van de Wiel, C., Visser, R. G. F. & van der Linden, G. Enhancing crop resilience to combined abiotic and biotic stress through the dissection of physiological and molecular crosstalk. *Frontiers in Plant Science* **5,** (2014).
9. McClung, C. R. & Davis, S. J. Ambient thermometers in plants: from physiological outputs towards mechanisms of thermal sensing. *Current Biology* **20,** 1086–1092 (2010).
10. Flowers, T. J. & Colmer, T. D. Plant salt tolerance: adaptations in halophytes. *Annals of Botany* **115,** 327–331 (2015).

11. Reichman, S. M. *The responses of plants to metal toxicity: a review forusing on copper, manganese & zinc*. (Australian Minerals and Energy Environment Foundation, 2002).
12. Schirawski, J. & Perlin, M. Plant–microbe interaction 2017—the good, the bad and the diverse. *International Journal of Molecular Sciences* **19,** 1374–6 (2018).
13. Jump, A. S. & Penuelas, J. Running to stand still: adaptation and the response of plants to rapid climate change. *Ecology Letters* **8,** 1010–1020 (2005).
14. Huntley, B. How plants respond to climate change - migration rates, individualism and the consequences for plant-communities. *Annals of Botany* **67,** 15–22 (1991).
15. Shaw, R. G. & Etterson, J. R. Rapid climate change and the rate of adaptation: insight from experimental quantitative genetics. *New Phytologist* **195,** 752–765 (2012).
16. Keneni, G., Bekele, E., Imtiaz, M. & Dagne, K. Genetic vulnerability of modern crop cultivars: causes, mechanism and remedies. *PLANT* **2,** 69–79 (2012).
17. Todesco, M. *et al.* Natural allelic variation underlying a major fitness trade-off in Arabidopsis thaliana. *Nature* **465,** 632–636 (2010).
18. Craufurd, P. Q. & Wheeler, T. R. Climate change and the flowering time of annual crops. *Journal of Experimental Botany* **60,** 2529–2539 (2009).
19. Parmesan, C. & Hanley, M. E. Plants and climate change: complexities and surprises. *Annals of Botany* **116,** 849–864 (2015).
20. Alcázar, R. & Parker, J. E. The impact of temperature on balancing immune responsiveness and growth in Arabidopsis. *Trends in Plant Science* **16,** 666–675 (2011).
21. Ghini, R., Hamada, E. & Bettiol, W. Climate change and plant diseases. *Scientia Agricola* **65,** 98–107 (2008).
22. Milus, E. A., Kristensen, K. & Hovmøller, M. S. Evidence for increased aggressiveness in a recent widespread strain of Puccinia striiformis f.

sp. tritici causing stripe rust of wheat. *Phytopathology* **99,** 89–94 (2009).

23. Evans, N., Baierl, A., Semenov, M. A., Gladders, P. & Fitt, B. D. L. Range and severity of a plant disease increased by global warming. *Journal of The Royal Society Interface* **5,** 525–531 (2008).
24. Bebber, D. P. Range-expanding pests and pathogens in a warming world. *Annual Review of Phytopathology* **53,** 335–356 (2015).
25. Evans, N. *et al.* The impact of climate change on disease constraints on production of oilseed rape. *Food Security* **2,** 143–156 (2010).
26. Butterworth, M. H. *et al.* North-South divide: contrasting impacts of climate change on crop yields in Scotland and England. *Journal of The Royal Society Interface* **7,** 123–130 (2009).
27. Huot, B. *et al.* Dual impact of elevated temperature on plant defence and bacterial virulence in Arabidopsis. *Nature Communications* **8,** 1–11 (2017).
28. Paris agreement. *United nations framework convention on climate change*. (2015).
29. Dhankher, O. P. & Foyer, C. H. Climate resilient crops for improving global food security and safety. *Plant, Cell & Environment* **41,** 877–884 (2018).
30. Chisholm, S. T., Coaker, G., Day, B. & Staskawicz, B. J. Host-microbe interactions: shaping the evolution of the plant immune response. *Cell* **124,** 803–814 (2006).
31. Wheat, C. W. *et al.* The genetic basis of a plant–insect coevolutionary key innovation. *Proceedings of the National Academy of Sciences* **104,** 20427–20431 (2007).
32. Becklin, K. M. A Coevolutionary arms race: understanding plant-herbivore interactions. *The American Biology Teacher* **70,** 288–292 (2008).
33. Jones, J. D. G. & Dangl, J. L. The plant immune system. *Nature* **444,** 323–329 (2006).

34. Kunze, G. *et al.* The N terminus of bacterial elongation factor Tu elicits innate immunity in Arabidopsis plants. *Plant Cell* **16,** 3496–3507 (2004).
35. Anderson, J. P. *et al.* Plants versus pathogens: an evolutionary arms race. *Functional Plant Biology* **37,** 499 (2010).
36. Zipfel, C. & Felix, G. Plants and animals: a different taste for microbes? *Current Opinion in Plant Biology* **8,** 353–360 (2005).
37. Bigeard, J., Colcombet, J. & plant, H. H. M. Signaling mechanisms in pattern-triggered immunity (PTI). *Elsevier* (2015).
38. Faulkner, C. *et al.* LYM2-dependent chitin perception limits molecular flux via plasmodesmata. *Proceedings of the National Academy of Sciences* **110,** 9166–9170 (2013).
39. Cui, H., Tsuda, K. & Parker, J. E. Effector-triggered immunity: from pathogen perception to robust defense. *Annual Review of Plant Biology* **66,** 6.1–6.25 (2014).
40. Stael, S. *et al.* Plant innate immunity – sunny side up? *Trends in Plant Science* **20,** 3–11 (2015).
41. Peng, Y., van Wersch, R. & Zhang, Y. Convergent and divergent signaling in PAMP-triggered immunity and effector-triggered immunity. *Molecular Plant-Microbe Interactions* **31,** 403–409 (2018).
42. Peng, Y., van Wersch, R. & Zhang, Y. Convergent and Divergent Signaling in PAMP-Triggered Immunity and Effector-Triggered Immunity. *Molecular Plant-Microbe Interactions* **31,** 403–409 (2018).
43. Thomma, B. P. H. J., Nürnberger, T. & Joosten, M. H. A. J. Of PAMPs and effectors: the blurred PTI-ETI dichotomy. *Plant Cell* **23,** 4–15 (2011).
44. Mishina, T. E. & Zeier, J. Pathogen-associated molecular pattern recognition rather than development of tissue necrosis contributes to bacterial induction of systemic acquired resistance in Arabidopsis. *The Plant Journal* **50,** 500–513 (2007).
45. Oliver, R. P. & Ipcho, S. V. S. Arabidopsis pathology breathes new life into the necrotrophs-vs.-biotrophs classification of fungal pathogens. *Molecular Plant Pathology* **5,** 347–352 (2004).

46. Perfect, S. E. & Green, J. R. Infection structures of biotrophic and hemibiotrophic fungal plant pathogens. *Molecular Plant Pathology* **2,** 101–108 (2001).

47. de Wit, P. J. G. M. How plants recognize pathogens and defend themselves. *Cellular and Molecular Life Sciences* **64,** 2726–2732 (2007).

48. Pieterse, C. M. J., Van der Does, D., Zamioudis, C., Leon-Reyes, A. & Van Wees, S. C. M. Hormonal modulation of plant immunity. *Annual Review of Cell and Developmental Biology* **28,** 489–521 (2012).

49. Vlot, A. C., Dempsey, D. A. & Klessig, D. F. Salicylic acid, a multifaceted hormone to combat disease. *Annual Review of Phytopathology* **47,** 177–206 (2009).

50. Rivas-San Vicente, M. & Plasencia, J. Salicylic acid beyond defence: its role in plant growth and development. *Journal of Experimental Botany* **62,** 3321–3338 (2011).

51. Broekgaarden, C., Caarls, L., Vos, I. A., Pieterse, C. M. J. & Van Wees, S. C. M. Ethylene: traffic controller on hormonal crossroads to defense. *Plant Physiology* **169,** 2371–2379 (2015).

52. Thaler, J. S., Humphrey, P. T. & Whiteman, N. K. Evolution of jasmonate and salicylate signal crosstalk. *Trends in Plant Science* **17,** 260–270 (2012).

53. Denancé, N., Sánchez-Vallet, A., Goffner, D. & Molina, A. Disease resistance or growth: the role of plant hormones in balancing immune responses and fitness costs. *Frontiers in Plant Science* **4,** 1–12 (2013).

54. Pieterse, C. M. J., Leon-Reyes, A., Van der Ent, S. & Van Wees, S. C. M. Networking by small-molecule hormones in plant immunity. *Nature Chemical Biology* **5,** 308–316 (2009).

55. Ryals, J. A. *et al.* Systemic acquired resistance. *Plant Cell* **8,** 1809–1819 (1996).

56. Delaney, T. P. *et al.* A central role of salicylic-acid in plant-disease resistance. *Science* **266,** 1247–1250 (1994).

57. Ali, A. *et al.* Plant defense mechanism and current understanding of salicylic acid and NPRs in activating SAR. *Physiological and Molecular Plant Pathology* **104,** 15–22 (2018).

58. Dodds, P. N. & Rathjen, J. P. Plant immunity: towards an integrated view of plant–pathogen interactions. *Nature Publishing Group* **11,** 539–548 (2010).

59. Feys, B. J., Moisan, L. J., Newman, M.-A. & Parker, J. E. Direct interaction between the Arabidopsis disease resistance signaling proteins, EDS1 and PAD4. *The European Molecular Biology Organisation Journal* **20,** 5400–5411 (2001).

60. Bartsch, M. *et al.* Salicylic acid-independent ENHANCED DISEASE SUSCEPTIBILITY1 signaling in Arabidopsis immunity and cell death is regulated by the monooxygenase FMO1 and the Nudix hydrolase NUDT7. *Plant Cell* **18,** 1038–1051 (2006).

61. Cui, H. *et al.* A core function of EDS1 with PAD4 is to protect the salicylic acid defense sector in Arabidopsis immunity. *New Phytologist* **213,** 1802–1817 (2016).

62. Hillmer, R. A. *et al.* The highly buffered Arabidopsis immune signaling network conceals the functions of its components. *Public Library of Science Genetics* **13,** e1006639 (2017).

63. Tikhonovich, I. A. & Provorov, N. A. From plant-microbe interactions to symbiogenetics: a universal paradigm for the interspecies genetic integration. *Annals of Applied Biology* **154,** 341–350 (2009).

64. Motion, G. B., Amaro, T. M. M. M., Kulagina, N. & Huitema, E. Nuclear processes associated with plant immunity and pathogen susceptibility. *Briefings in Functional Genomics* **14,** 243–252 (2015).

65. Jung, H.-S. & Chory, J. Signaling between chloroplasts and the nucleus: can a systems biology approach bring clarity to a complex and highly regulated pathway? *Plant Physiology* **152,** 453–459 (2010).

66. Serrano, I., Audran, C. & Rivas, S. Chloroplasts at work during plant innate immunity. *Journal of Experimental Botany* **67,** 3845–3854 (2016).

67. Costa, A., Navazio, L. & Szabo, I. The contribution of organelles to plant intracellular calcium signalling. *Journal of Experimental Botany* **69,** 4175–4193 (2018).

68. Sperschneider, J. *et al.* LOCALIZER: subcellular localization prediction of both plant and effector proteins in the plant cell. *Scientific Reports* **7,** 1–14 (2017).

69. Bonza, M. C. *et al.* Analyses of Ca2+ accumulation and dynamics in the endoplasmic reticulum of Arabidopsis root cells using a genetically encoded Cameleon sensor. *Plant Physiology* **163,** 1230–1241 (2013).

70. van Hulten, M., Pelser, M., van Loon, L. C., Pieterse, C. M. J. & Ton, J. Costs and benefits of priming for defense in Arabidopsis. *Proceedings of the National Academy of Sciences* **103,** 5602–5607 (2006).

71. Fürstenberg-Hägg, J., Zagrobelny, M. & Bak, S. Plant defense against insect herbivores. *International Journal of Molecular Sciences* **14,** 10242–10297 (2013).

72. Herms, D. A. & Mattson, W. The dilemma of plants: to grow or defend. *The Quarterly Review of Biology* 1–53 (1992).

73. Abreu, M. E. & Munne-Bosch, S. Salicylic acid deficiency in NahG transgenic lines and sid2 mutants increases seed yield in the annual plant Arabidopsis thaliana. *Journal of Experimental Botany* **60,** 1261–1271 (2009).

74. Strauss, S. Y., Rudgers, J. A., Lau, J. A. & Irwin, R. E. Direct and ecological costs of resistance to herbivory. *Trends in Ecology & Evolution* **17,** 278–285 (2002).

75. Hagenbucher, S. *et al.* Pest trade-offs in technology: reduced damage by caterpillars in Bt cotton benefits aphids. *Proceedings of the Royal Society B: Biological Sciences* **280,** 20130042 (2013).

76. Ning, Y., Liu, W. & Wang, G.-L. Balancing immunity and yield in crop plants. *Trends in Plant Science* **22,** 1069–1079 (2017).

77. zar, R. N. A., Reymond, M., Schmitz, G. & de Meaux, J. Genetic and evolutionary perspectives on the interplay between plant immunity and development. *Current Opinion in Plant Biology* **14,** 378–384 (2011).

78. An, C. & Mou, Z. Salicylic acid and its function in plant immunity. *Journal of Integrative Plant Biology* **53,** 412–428 (2011).

79. Melotto, M., Underwood, W. & He, S. Y. Role of stomata in plant innate immunity and foliar bacterial diseases. *Annual Review of Phytopathology* **46,** 101–122 (2008).

80. Zhou, Z. *et al.* An Arabidopsis plasma membrane proton ATPase modulates JA signaling and is exploited by the Pseudomonas syringae effector protein AvrB for stomatal invasion. *Plant Cell* **27,** 2032–2041 (2015).

81. Gangappa, S. N. & Kumar, S. V. DET1 and COP1 modulate the coordination of growth and immunity in response to key seasonal signals in Arabidopsis. *Elsevier* 29-37 (2018).

82. Cheng, C. *et al.* Plant immune response to pathogens differs with changing temperatures. *Nature Communications* **4,** 1–9 (2013).

83. Bowling, S. A. *et al.* A mutation in Arabidopsis that leads to constitutive expression of systemic acquired-resistance. *Plant Cell* **6,** 1845–1857 (1994).

84. Naseem, M., Kaltdorf, M. & Dandekar, T. The nexus between growth and defence signalling: auxin and cytokinin modulate plant immune response pathways. *Journal of Experimental Botany* **66,** 4885–4896 (2015).

85. Pajerowska-Mukhtar, K. M. *et al.* The HSF-like transcription factor TBF1 is a major molecular switch for plant growth-to-defense transition. *Current Biology* **22,** 103–112 (2012).

86. Paik, I., Kathare, P. K., Kim, J.-I. & Huq, E. Expanding roles of PIFs in signal integration from multiple processes. *Molecular Plant* **10,** 1035–1046 (2017).

87. Albrecht, T. & Argueso, C. T. Should I fight or should I grow now? The role of cytokinins in plant growth and immunity and in the growth–defence trade-off. *Annals of Botany* **119,** 725–735 (2016).

88. Lu, H. Dissection of salicylic acid-mediated defense signaling networks. *Plant Signaling & Behavior* **4,** 713–717 (2009).

89. Kus, J. V., Zaton, K., Sarkar, R. & Cameron, R. K. Age-related resistance in Arabidopsis is a developmentally regulated defense response to Pseudomonas syringae. *Plant Cell* **14,** 479–490 (2002).

90. Carella, P., Wilson, D. C. & Cameron, R. K. Some things get better with age: differences in salicylic acid accumulation and defense signaling in young and mature Arabidopsis. *Frontiers in Plant Science* **5,** (2015).

91. Du, L. *et al.* Ca2+ /calmodulin regulates salicylic-acid-mediated plant immunity. *Nature* **457,** 1154–1158 (2009).

92. Ibañez, C. *et al.* Ambient temperature and genotype differentially affect developmental and phenotypic plasticity in Arabidopsis thaliana. *BMC Plant Biology* **17,** (2017).

93. Gummadi, S. N. What is the role of thermodynamics on protein stability? *Biotechnology and Bioprocess Engineering* **8,** 9–18 (2003).

94. Rosa, M., Roberts, C. J. & Rodrigues, M. A. Connecting high-temperature and low-temperature protein stability and aggregation. *Public Library of Science ONE* **12,** (2017).

95. Wiedersich, J., Koehler, S., Skerra, A. & Friedrich, J. Temperature and pressure dependence of protein stability: The engineered fluorescein-binding lipocalin FluA shows an elliptic phase diagram. *Proceedings of the National Academy of Sciences* **105,** 5756–5761 (2008).

96. Nawkar, G. M. *et al.* Activation of the transducers of unfolded protein response in plants. *Frontiers in Plant Science* **9,** 671–10 (2018).

97. Bahuguna, R. & Jagadish, K. Temperature regulation of plant phenological development. *Environmental and Experimental Botany* **111,** 83–90 (2015).

98. Horvath, I. *et al.* Membrane physical state controls the signaling mechanism of the heat shock response in Synechocystis PCC 6803: Identification of hsp17 as a 'fluidity gene'. *Proceedings of the National Academy of Sciences* **95,** 3513–3518 (1998).

99. Saidi, Y. *et al.* The heat shock response in moss plants is regulated by specific calcium-permeable channels in the plasma membrane. *Plant Cell* **21,** 2829–2843 (2009).

100. Bokszczanin, K. L., Fragkostefanakis, S. & Thermotolerance, S. P. Perspectives on deciphering mechanisms underlying plant heat stress response and thermotolerance. *Frontiers in Plant Science* **4,** (2013).

101. Niu, Y. & Xiang, Y. An overview of biomembrane functions in plant responses to high-temperature stress. *Frontiers in Plant Science* **9,** 1449–18 (2018).

102. Harayama, T. & Riezman, H. Understanding the diversity of membrane lipid composition. *Nature Publishing Group* **19,** 281–296 (2018).

103. N Murata, D. A. L. Membrane fluidity and temperature perception. *Plant Physiology* **115,** 875–879 (1997).

104. Zheng, G., Tian, B. O., Zhang, F., Tao, F. & Li, W. Plant adaptation to frequent alterations between high and low temperatures: remodelling of membrane lipids and maintenance of unsaturation levels. *Plant, Cell & Environment* **34,** 1431–1442 (2011).

105. Almeida, P. F. F., Pokorny, A. & Hinderliter, A. Thermodynamics of membrane domains. *Biochimica et Biophysica Acta - Biomembranes* **1720,** 1–13 (2005).

106. Horváth, I. *et al.* Heat shock response in photosynthetic organisms: membrane and lipid connections. *Progress in Lipid Research* **51,** 208–220 (2012).

107. Finka, A., Cuendet, A. F. H., Maathuis, F. J. M., Saidi, Y. & Goloubinoff, P. Plasma membrane cyclic nucleotide gated calcium channels control land plant thermal sensing and acquired thermotolerance. *Plant Cell* **24,** 3333–3348 (2012).

108. Evans, M. J., Choi, W.-G., Gilroy, S. & Morris, R. J. A ROS-assisted calcium wave dependent on the AtRBOHD NADPH oxidase and TPC1 cation channel propagates the systemic response to salt stress. *Plant Physiology* **171,** 1771–1784 (2016).

109. Choi, W.-G. *et al.* Orchestrating rapid long-distance signaling in plants with Ca 2+, ROS and electrical signals. *The Plant Journal* **90,** 698–707 (2017).

110. Finka, A. & Goloubinoff, P. The CNGCb and CNGCd genes from Physcomitrella patens moss encode for thermosensory calcium channels responding to fluidity changes in the plasma membrane. *Cell Stress and Chaperones* **19,** 83–90 (2014).

111. Medvedev, S. S. Principles of calcium signal generation and transduction in plant cells. *Russian Journal of Plant Physiology* **65,** 771–783 (2018).

112. Feijó, J. A. & Wudick, M. M. 'Calcium is life'. *Journal of Experimental Botany* **69,** 4147–4150 (2018).

113. Clough, S. J. *et al.* The Arabidopsis dnd1 'defense, no death' gene encodes a mutated cyclic nucleotide-gated ion channel. *Proceedings of the National Academy of Sciences* **97,** 9323–9328 (2000).

114. Mittler, R., Finka, A. & Goloubinoff, P. How do plants feel the heat? *Trends in Biochemical Sciences* **37,** 118–125 (2012).

115. Fanata, W. I. D., Lee, S. Y. & Lee, K. O. The unfolded protein response in plants: a fundamental adaptive cellular response to internal and external stresses. *Journal of Proteomics* **93,** 356–368 (2013).

116. Walter, P. & Ron, D. The unfolded protein response: from stress pathway to homeostatic regulation. *Science* **334,** 1081–1086 (2011).

117. Li, X.-M. *et al.* Natural alleles of a proteasome alpha2 subunit. *Nature Genetics* **47,** 827–833 (2015).

118. Gardener, C. & Kumar, S. V. Hot n' cold: molecular signatures of domestication bring fresh insights into environmental adaptation. *Molecular Plant* **8,** 1439–1441 (2015).

119. Deng, W. *et al.* FLOWERING LOCUS C (FLC) regulates development pathways throughout the life cycle of Arabidopsis. *Proceedings of the National Academy of Sciences* **108,** 6680–6685 (2011).

120. Antoniou-Kourounioti, R. L. *et al.* Temperature sensing is distributed throughout the regulatory network that controls FLC epigenetic silencing in vernalization. *Cell Systems* **7,** 643–655 (2018).

121. Hepworth, J. *et al.* Absence of warmth permits epigenetic memory of winter in Arabidopsis. *Nature Communications* **9,** 1–8 (2018).

122. Swiezewski, S., Liu, F., Magusin, A. & Dean, C. Cold-induced silencing by long antisense transcripts of an Arabidopsis polycomb target. *Nature* **462,** 799–802 (2009).

123. Sureshkumar, S., Dent, C., Seleznev, A., Tasset, C. & Balasubramanian, S. Nonsense-mediated mRNA decay modulates FLM-dependent thermosensory flowering response in Arabidopsis. *Nature Plants* **2,** (2016).

124. Lorrain, S., Allen, T., Duek, P. D., Whitelam, G. C. & Fankhauser, C. Phytochrome-mediated inhibition of shade avoidance involves degradation of growth-promoting bHLH transcription factors. *The Plant Journal* **53,** 312–323 (2007).

125. Ballaré, C. L. & Pierik, R. The shade-avoidance syndrome: multiple signals and ecological consequences. *Plant, Cell & Environment* **40,** 2530–2543 (2017).

126. Delker, C., van Zanten, M. & Quint, M. Thermosensing enlightened. *Trends in Plant Science* **22,** 185–187 (2017).

127. Gangappa, S. N., Berriri, S. & Kumar, S. V. PIF4 coordinates thermosensory growth and immunity in Arabidopsis. *Current biology* **27,** 243–249 (2017).

128. Kumar, S. V. *et al.* Transcription factor PIF4 controls the thermosensory activation of flowering. *Nature* **484,** 242–245 (2012).

129. Sakamoto, T. & Kimura, S. Plant temperature sensors. *Sensors* **18,** 4365–11 (2018).

130. Franklin, K. A. Light signals, phytochromes and cross-talk with other environmental cues. *Journal of Experimental Botany* **55,** 271–276 (2003).

131. Jung, J.-H. *et al.* Phytochromes function as thermosensors in Arabidopsis. *Science* **354,** 886–889 (2016).

132. Legris, M. *et al.* Phytochrome B integrates light and temperature signals in Arabidopsis. *Science* **354,** 897–900 (2016).

133. Wang, W. *et al.* Timing of plant immune responses by a central circadian regulator. *Nature* **469,** 110–114 (2011).

134. Lau, O. S. *et al.* Interaction of Arabidopsis DET1 with CCA1 and LHY in mediating transcriptional repression in the plant circadian clock. *Molecular cell* **43,** 703–712 (2011).

135. Schwechheimer, C. & Deng, X. W. The COP/DET/FUS proteins—regulators of eukaryotic growth and development. *Seminars in Cell & Developmental Biology* **11,** 495–503 (2000).

136. Gangappa, S. N. & Kumar, S. V. DET1 and HY5 control PIF4-mediated thermosensory elongation growth through distinct mechanisms. *Cell Reports* **18,** 344–351 (2017).

137. Cheong, M. S. *et al.* Specific domain structures control abscisic acid-, salicylic acid-, and stress-mediated SIZ1 phenotypes. *Plant Physiology* **151,** 1930–1942 (2009).

138. Gou, M. & Hua, J. Complex regulation of an R gene SNC1 revealed by autoimmune mutants. *Plant Signaling & Behavior* **7,** 213–216 (2014).

139. Hammoudi, V. *et al.* The Arabidopsis SUMO E3 ligase SIZ1 mediates the temperature dependent trade-off between plant immunity and growth. *Public Library of Science Genetics* **14,** e1007157 (2018).

140. van Wersch, R., Li, X. & Zhang, Y. Mighty Dwarfs: Arabidopsis autoimmune mutants and their usages in genetic dissection of plant immunity. *Frontiers in Plant Science* **7,** 369–8 (2016).

141. Li, X., Clarke, J. D., Zhang, Y. & Dong, X. Activation of an EDS1-mediated R-gene pathway in the snc1 mutant leads to constitutive, NPR1-independent pathogen resistance. *Molecular Plant-Microbe Interactions***14,** 1131–1139 (2001).

142. Zhang, Y. A gain-of-function mutation in a plant disease resistance gene leads to constitutive activation of downstream signal transduction pathways in suppressor of npr1-1, constitutive 1. *Plant Cell* **15,** 2636–2646 (2003).

143. Yang, S. A haplotype-specific resistance gene regulated by BONZAI1 mediates temperature-dependent growth control in Arabidopsis. *Plant Cell* **16,** 1060–1071 (2004).

144. Xu, G. *et al.* uORF-mediated translation allows engineered plant disease resistance without fitness costs. *Nature* **545,** 491–494 (2017).

145. Whitham, S., McCormick, S. & Baker, B. The N gene of tobacco confers resistance to tobacco mosaic virus in transgenic tomato. *Proceedings of the National Academy of Sciences* **93,** 8776–8781 (1996).

146. Holt, B. F., Belkhadir, Y. & Dangl, J. L. Antagonistic control of disease resistance protein stability in the plant immune system. *Science* **309,** 929–932 (2005).

147. Wang, Y., Bao, Z., Zhu, Y. & Hua, J. Analysis of temperature modulation of plant defense against biotrophic microbes. *Molecular Plant-Microbe Interactions***22,** 498–506 (2009).

148. Huang, X., Li, J., Bao, F., Zhang, X. & Yang, S. A gain-of-function mutation in the Arabidopsis disease resistance gene RPP4 confers sensitivity to low temperature. *Plant Physiology* **154,** 796–809 (2010).

149. Fu, D. *et al.* A kinase-START gene confers temperature-dependent resistance to wheat stripe rust. *Science* **323,** 1357–1360 (2009).

150. Wang, Z.-X., Yamanouchi, U., Katayose, Y., Sasaki, T. & Yano, M. Expression of the Pib rice-blast-resistance gene family is up-regulated by environmental conditions favouring infection and by chemical signals that trigger secondary plant defences. *Plant Molecular Biology* **47,** 653–661 (2001).

151. Chellappan, P. Effect of temperature on geminivirus-induced RNA silencing in plants. *Plant Physiology* **138,** 1828–1841 (2005).

152. Szittya, G. *et al.* Low temperature inhibits RNA silencing-mediated defence by the control of siRNA generation. *European Molecular Biology Organisation Journal* **22,** 633–640 (2003).

153. Velázquez, K. *et al.* Effect of temperature on RNA silencing of a negative-stranded RNA plant virus: Citrus psorosis virus. *Plant Pathology* **59,** 982–990 (2010).

154. Zhang, X., Singh, J., Li, D. & Qu, F. Temperature-dependent survival of turnip crinkle virus-infected Arabidopsis plants relies on an RNA

silencing-based defense that requires DCL2, AGO2, and HEN1. *Journal of Virology* **86,** 6847–6854 (2012).

155. Quint, M. *et al.* Molecular and genetic control of plant thermomorphogenesis. *Nature Plants* **2,** (2016).

156. Park, J. H. & Shin, C. The role of plant small RNAs in NB-LRR regulation. *Briefings in Functional Genomics* **14,** 268–274 (2015).

157. Kumar, S. V. & Wigge, P. A. H2A.Z-containing nucleosomes mediate the thermosensory response in Arabidopsis. *Cell* **140,** 136–147 (2010).

158. Berriri, S., Gangappa, S. N. & Kumar, S. V. SWR1 chromatin-remodeling complex subunits and H2A.Z have non-overlapping functions in immunity and gene regulation in Arabidopsis. *Molecular Plant* **9,** 1051–1065 (2016).

159. Park, C.-J. & Seo, Y.-S. Heat shock proteins: a review of the molecular chaperones for plant immunity. *The Plant Pathology Journal* **31,** 323–333 (2015).

160. Kumar, S. V. H2A.Z at the core of transcriptional regulation in plants. *Molecular Plant* **11,** 1112–1114 (2018).

161. March-Diaz, R. *et al.* Histone H2A.Z and homologues of components of the SWR1 complex are required to control immunity in Arabidopsis. *The Plant Journal* **53,** 475–487 (2008).

162. Li, B., Carey, M. & Workman, J. L. The role of chromatin during transcription. *Cell* **128,** 707–719 (2007).

163. Cortijo, S. *et al.* Transcriptional regulation of the ambient temperature response by H2A.Z nucleosomes and HSF1 transcription factors in Arabidopsis. *Molecular Plant* **10,** 1258–1273 (2017).

164. Mizuguchi, G. *et al.* ATP-Driven exchange of histone H2AZ variant catalyzed by SWR1 chromatin remodeling complex. *Science* **303,** 343–348 (2004).

165. Koini, M. A. *et al.* High temperature-mediated adaptations in plant architecture require the bHLH transcription factor PIF4. *Current Biology* **19,** 408–413 (2009).

166. Zhu, Y., Qian, W. & Hua, J. Temperature modulates plant defense responses through NB-LRR proteins. *Public Library of Science Pathogens* **6,** (2010).

167. Murray, S. L., Adams, N., Kliebenstein, D. J., Loake, G. J. & Denby, K. J. A constitutive PR-1::luciferase expression screen identifies Arabidopsis mutants with differential disease resistance to both biotrophic and necrotrophic pathogens. *Molecular Plant Pathology* **6,** 31–41 (2005).

168. Bowling, S. A., Clarke, J. D., Liu, Y., Klessig, D. F. & Dong, X. The cpr5 mutant of Arabidopsis expresses both NPR1-dependent and NPR1-independent resistance. *Plant Cell* **9,** 1573–1584 (1997).

169. Zhu, J.-Y., Oh, E., Wang, T. & Wang, Z.-Y. TOC1–PIF4 interaction mediates the circadian gating of thermoresponsive growth in Arabidopsis. *Nature Communications* **7,** 13692 (2016).

170. Feng, B., Liu, C., Shan, L. & He, P. Protein ADP-ribosylation takes control in plant–bacterium interactions. *Public Library of Science Pathogens* **12,** e1005941–6 (2016).

171. Lin, W. *et al.* Inverse modulation of plant immune and brassinosteroid signaling pathways by the receptor-like cytoplasmic kinase BIK1. *Proceedings of the National Academy of Sciences* **110,** 12114–12119 (2013).

172. Capovilla, G., Schmid, M. & Pose, D. Control of flowering by ambient temperature. *Journal of Experimental Botany* **66,** 59–69 (2014).

173. Paul-Victor, C., Züst, T., Rees, M., Kliebenstein, D. J. & Turnbull, L. A. A new method for measuring relative growth rate can uncover the costs of defensive compounds in Arabidopsis thaliana. *New Phytologist* **187,** 1102–1111 (2010).

174. Vos, I. A., Pieterse, C. M. J. & van Wees, S. C. M. Costs and benefits of hormone-regulated plant defences. *Plant Pathology* **62,** 43–55 (2013).

175. Heil, M. & Baldwin, I. T. Fitness costs of induced resistance: emerging experimental support for a slippery concept. *Trends in Plant Science* **7,** 61–67 (2002).

176. Ibañez, C. *et al.* Ambient temperature and genotype differentially affect developmental and phenotypic plasticity in Arabidopsis thaliana. *BMC Plant Biology* 1–14 (2017).

177. Segonzac, C. C. & Zipfel, C. Activation of plant pattern-recognition receptors by bacteria. *Current Opinion in Microbiology* **14,** 54–61 (2011).

178. Li, B., Meng, X., Shan, L. & He, P. Transcriptional regulation of pattern-triggered immunity in plants. *Cell Host and Microbe* **19,** 641–650 (2016).

179. Howard, B. E. *et al.* High-throughput RNA sequencing of Pseudomonas-infected Arabidopsis reveals hidden transcriptome complexity and novel splice variants. *Public Library of Science ONE* **8,** e74183–18 (2013).

180. Iakovidis, M. *et al.* Effector-triggered immune response in Arabidopsis thaliana is a quantitative trait. *Genetics* **204,** 337–353 (2016).

181. Balasubramanian, S., Sureshkumar, S., Lempe, J. & Weigel, D. Potent induction of arabidopsis thaliana flowering by elevated growth temperature. *Public Library of Science Genetics* **2,** e106 (2006).

182. Peng, S. *et al.* Rice yields decline with higher night temperature from global warming. *Proceedings of the National Academy of Sciences* **101,** 9971–9975 (2004).

183. Thuiller, W., Lavorel, S., Araújo, M. B., Sykes, M. T. & Prentice, I. C. Climate change threats to plant diversity in Europe. *Proceedings of the National Academy of Sciences* **102,** 8245–8250 (2005).

184. Muralidharan, S. *et al.* Different mechanisms for Arabidopsis thaliana hybrid necrosis cases inferred from temperature responses. *Plant Biology* **16,** 1033–1041 (2014).

185. Wann, F. B. Circular No. 85-Chlorosis yellowing of plants: cause and control. *UAES Circulars* **77** (1930).

186. Smirnova, A. *et al.* Thermoregulated expression of virulence factors in plant-associated bacteria. *Archives of Microbiology* **176,** 393–399 (2001).

187. Develey-Rivière, M.-P. & Galiana, E. Resistance to pathogens and host developmental stage: a multifaceted relationship within the plant kingdom. *New Phytologist* **175,** 405–416 (2007).

188. Whalen, M. C. Host defence in a developmental context. *Molecular Plant Pathology* **6,** 347–360 (2005).

189. Goyeau, H. & Lannou, C. Specific resistance to leaf rust expressed at the seedling stage in cultivars grown in France from 1983 to 2007. *Euphytica* **178,** 45–62 (2010).

190. Hovmøller, M. S. Sources of seedling and adult plant resistance to Puccinia striiformis f.sp. tritici in European wheats. *Plant Breeding* **126,** 225–233 (2007).

191. Tao, F. *et al.* Transcriptomic analysis reveal the molecular mechanisms of wheat higher-temperature seedling-plant resistance to Puccinia striiformis f. sp. tritici. *Frontiers in Plant Science* **9,** 1314–19 (2018).

192. Fan, J., Crooks, C. & Lamb, C. High-throughput quantitative luminescence assay of the growth in planta of Pseudomonas syringae chromosomally tagged with Photorhabdus luminescens luxCDABE. *The Plant Journal* **53,** 393–399 (2007).

193. Wu, Z. *et al.* Regulation of plant immune receptor accumulation through translational repression by a glycine-tyrosine-phenylalanine (GYF) domain protein. *Elife* **6,** (2017).

194. Li, Y., Yang, S., Yang, H., plant-microbe, J. H. M.2007. The TIR-NB-LRR gene SNC1 is regulated at the transcript level by multiple factors. *American Phytopathological Society Society* **20,** 1449–1456 (2007).

195. Sohn, K. H., Zhang, Y. & Jones, J. D. G. The Pseudomonas syringae effector protein, AvrRPS4, requires in planta processing and the KRVY domain to function. *The Plant Journal* **57,** 1079–1091 (2009).

196. Narusaka, M. *et al.* RRS1and RPS4provide a dual Resistance-gene system against fungal and bacterial pathogens. *The Plant Journal* **60,** 218–226 (2009).

197. Huh, S. U. *et al.* Protein-protein interactions in the RPS4/RRS1 immune receptor complex. *Public Library of Science Pathogens* **13,** e1006376–22 (2017).

198. Menna, A., Nguyen, D., Guttman, D. S. & Desveaux, D. Elevated temperature differentially influences effector-triggered immunity outputs in Arabidopsis. *Frontiers in Plant Science* **6,** 533 (2015).

199. Zipfel, C. *et al.* Bacterial disease resistance in Arabidopsis through flagellin perception. *Nature* **428,** 764–767 (2004).

200. Halliwell, B. Reactive species and antioxidants. Redox biology is a fundamental theme of aerobic life. *Plant Physiology* **141,** 312–322 (2006).

201. O'Brien, J. A., Daudi, A., Butt, V. S. & Paul Bolwell, G. Reactive oxygen species and their role in plant defence and cell wall metabolism. *Planta* **236,** 765–779 (2012).

202. Gilroy, S. *et al.* A tidal wave of signals: calcium and ROS at the forefront of rapid systemic signaling. *Trends in Plant Science* **19,** 623–630 (2014).

203. Baxter, A., Mittler, R. & Suzuki, N. ROS as key players in plant stress signalling. *Journal of Experimental Botany* **65,** 1229–1240 (2014).

204. Li, L. *et al.* The FLS2-associated kinase BIK1 directly phosphorylates the NADPH oxidase RbohD to control plant immunity. *Cell Host and Microbe* **15,** 329–338 (2014).

205. Wojtaszek, P. Oxidative burst: an early plant response to pathogen infection. *Biochemical Journal* **322,** 681–692 (1997).

206. Malinovsky, F. G., Fangel, J. U. & Willats, W. G. T. The role of the cell wall in plant immunity. *Frontiers in Plant Science* **5,** (2014).

207. Bi, G. *et al.* Receptor-like cytoplasmic kinases directly link diverse pattern recognition receptors to the activation of mitogen-activated protein kinase cascades in Arabidopsis. *Plant Cell* **30**, 1543-1561 (2018).

208. Cristina, M., Petersen, M. & Mundy, J. Mitogen-activated protein kinase signaling in plants. *Annual Review of Plant Biology* **61,** 621–649 (2010).

209. Berriri, S. *et al.* Constitutively active mitogen-activated protein kinase versions reveal functions of Arabidopsis MPK4 in pathogen defense signaling. *Plant Cell* **24,** 4281–4293 (2012).

210. Adachi, H. *et al.* WRKY transcription factors phosphorylated by MAPK regulate a plant immune NADPH oxidase in Nicotiana benthamiana. *Plant Cell* **27,** 2645–2663 (2015).

211. Gómez-Gómez, L. & Boller, T. FLS2: an LRR receptor-like kinase involved in the perception of the bacterial elicitor flagellin in Arabidopsis. *Molecular cell* **5,** 1003–1011 (2000).

212. Asai, T. *et al.* MAP kinase signalling cascade in Arabidopsis innate immunity. *Nature* **415,** 977–983 (2002).

213. de Torres, M., Sanchez, P., Fernandez-Delmond, I. & Grant, M. Expression profiling of the host response to bacterial infection: the transition from basal to induced defence responses in RPM1-mediated resistance. *The Plant Journal* **33,** 665–676 (2003).

214. Kozera, B. & Rapacz, M. Reference genes in real-time PCR. *Journal of Applied Genetics* **54,** 391–406 (2013).

215. Scott, I. M., Clarke, S. M., Wood, J. E. & Mur, L. A. J. Salicylate accumulation inhibits growth at chilling temperature in Arabidopsis. *Plant Physiology* **135,** 1040–1049 (2004).

216. Lewis, L. A. *et al.* Transcriptional dynamics driving MAMP-triggered immunity and pathogen effector-mediated immunosuppression in Arabidopsis leaves following infection with Pseudomonas syringae pv tomato DC3000. *Plant Cell* **27,** 3038–3064 (2015).

217. Tyagi, M., Imam, N., Verma, K. & Patel, A. K. Chromatin remodelers: we are the drivers!! *Nucleus* **7,** 388–404 (2016).

218. Li, G. & Reinberg, D. Chromatin higher-order structures and gene regulation. *Current Opinion in Genetics & Development* **21,** 175–186 (2011).

219. Coleman-Derr, D. & Zilberman, D. Deposition of histone variant H2A. Z within gene bodies regulates responsive genes. *Public Library of Science Genetics* **8**(10) e1002988 (2012).

220. Rosana, M.-D. A. & C, R. J. The beauty of being a variant: H2A.Z and the SWR1 complex in plants. *Molecular Plant* **2,** 565–577 (2009).

221. Deal, R. B., Topp, C. N., McKinney, E. C. & Meagher, R. B. Repression of flowering in Arabidopsis requires activation of FLOWERING LOCUS C expression by the histone variant H2A.Z. *Plant Cell* **19,** 74–83 (2007).

222. Katagiri, F. Review: Plant immune signaling from a network perspective. *Plant Science* **276,** 14–21 (2018).

223. Aikawa, S., Kobayashi, M. J., Satake, A., Shimizu, K. K. & Kudoh, H. Robust control of the seasonal expression of the Arabidopsis FLC gene in a fluctuating environment. *Proceedings of the National Academy of Sciences* **107,** 11632–11637 (2010).

224. Sun, J., Qi, L., Li, Y., Chu, J. & Li, C. PIF4–mediated activation of YUCCA8 expression integrates temperature into the auxin pathway in regulating Arabidopsis hypocotyl growth. *Public Library of Science Genetics* **8,** e1002594 (2012).

225. Ward, E. R. *et al.* Coordinate gene activity in response to agents that induce systemic acquired resistance. *Plant Cell* **3,** 1085–1094 (1991).

226. Schommer, C. *et al.* Control of jasmonate biosynthesis and senescence by miR319 targets. *Public Library of Science Biology* **6,** e230–11 (2008).

227. Murray, S. L., Thomson, C., Chini, A., Read, N. D. & Loake, G. J. Characterization of a novel, defense-related Arabidopsis mutant, cir1, isolated by luciferase Imaging. *Molecular Plant-Microbe Interactions* **15,** 557–566 (2002).

228. Kasemthongsri, P. *Molecular dissection of temperature influence on plant defense responses.* Dissertation. University of East Anglia (2012).

229. CAO, H., Bowling, S. A., GORDON, A. S. & DONG, X. N. Characterization of an Arabidopsis mutant that is nonresponsive to inducers of systemic acquired-resistance. *Plant Cell* **6,** 1583–1592 (1994).

230. Burrowes, C. *Characterisation of temperature responses in Arabidopsis thaliana mutant resilient-2 (res2)*. Dissertation. University of East Anglia (2014).

231. Bomblies, K. & Weigel, D. Hybrid necrosis: autoimmunity as a potential gene-flow barrier in plant species. *Nature Reviews Genetics* **8,** 382–393 (2007).

232. Abdel-Hamid, H. *Structural - functional analysis of plant cyclic nucleotide gated ion channels.* Dissertation. University of Toronto (2013).

233. Heidrich, K. *et al.* Arabidopsis TNL-WRKY domain receptor RRS1 contributes to temperature-conditioned RPS4 auto-immunity. *Frontiers in Plant Science* **4,** (2013).

234. Uknes, S. *et al.* Acquired resistance in Arabidopsis. *Plant Cell* **4,** 645–656 (1992).

235. Sun, T. *et al.* ChIP-seq reveals broad roles of SARD1 and CBP60g in regulating plant immunity. *Nature Communications* **6,** 1–12 (2015).

236. Zhu, Z. *et al.* Arabidopsis resistance protein SNC1 activates immune responses through association with a transcriptional corepressor. *Proceedings of the National Academy of Sciences* **107,** 13960–13965 (2010).

237. Proveniers, M. C. G. & van Zanten, M. High temperature acclimation through PIF4 signaling. *Trends in Plant Science* **18,** 59–64 (2013).

238. Ibañez, C. *et al.* Brassinosteroids dominate hormonal regulation of plant thermomorphogenesis via BZR1. *Current Biology* **28,** 303–310 (2018).

239. Choi, H. & Oh, E. pif4 integrates multiple environmental and hormonal signals for plant growth regulation in Arabidopsis. *Molecules and Cells* **39,** 587–593 (2016).

240. Franklin, K. A. *et al.* Phytochrome-interacting factor 4 (PIF4) regulates auxin biosynthesis at high temperature. *Proceedings of the National Academy of Sciences* **108,** 20231–20235 (2011).

241. Iglesias, M. J., Terrile, M. C. & Casalongué, C. A. Auxin and salicylic acid signalings counteract the regulation of adaptive responses to stress. *Plant Signaling & Behavior* **6,** 452–454 (2011).

242. Weijers, D., Nemhauser, J. & Yang, Z. Auxin: small molecule, big impact. *Journal of Experimental Botany* **69,** 133–136 (2018).

243. Zhao, Y. Auxin Biosynthesis: a simple two-step pathway converts tryptophan to indole-3-acetic acid in plants. *Molecular Plant* **5,** 334–338 (2012).

244. Gray, W. M., Ostin, A., Sandberg, G., Romano, C. P. & Estelle, M. High temperature promotes auxin-mediated hypocotyl elongation in Arabidopsis. *Proceedings of the National Academy of Sciences* **95,** 7197–7202 (1998).

245. Hornitschek, P., Lorrain, S. E. V., Zoete, V., Michielin, O. & Fankhauser, C. Inhibition of the shade avoidance response by formation of non-DNA binding bHLH heterodimers. *The European Molecular Biology Organisation Journal* **28,** 3893–3902 (2009).

246. Yu, I. C., Parker, J. & Bent, A. F. Gene-for-gene disease resistance without the hypersensitive response in Arabidopsis dnd1 mutant. *Proceedings of the National Academy of Sciences* **95,** 7819–7824 (1998).

247. Balague, C. HLM1, an essential signaling component in the hypersensitive response, is a member of the cyclic nucleotide-gated channel ion channel family. *Plant Cell* **15,** 365–379 (2003).

248. Sun, K. *et al.* Down-regulation of Arabidopsis DND1 orthologs in potato and tomato leads to broad-spectrum resistance to late blight and powdery mildew. *Transgenic Research* **25,** 123–138 (2015).

249. Chakraborty, S. *et al.* A novel role for cyclic nucleotide-gated ion channel 2 (DND1) in auxin signaling. *bioRxiv* 1–30 (2018).

250. Knight, H. & Knight, M. R. Imaging spatial and cellular characteristics of low temperature calcium signature after cold acclimation in Arabidopsis. *Journal of Experimental Botany* **51,** 1679–1686 (2000).

251. Ma, Y. *et al.* COLD1 confers chilling tolerance in rice. *Cell* **160,** 1209–1221 (2015).

252. Sun, K. *et al.* Silencing of DND1 in potato and tomato impedes conidial germination, attachment and hyphal growth of Botrytis cinerea. *BMC Plant Biology* **17,** (2017).

253. Vincent, T. R. *et al.* Interplay of plasma membrane and vacuolar ion channels, together with BAK1, elicits rapid cytosolic calcium elevations in Arabidopsis during aphid feeding. *Plant Cell* **29,** 1460–1479 (2017).

254. Zhao, Y., Qi, Z. & Berkowitz, G. A. Teaching an old hormone new tricks: cytosolic Ca2+ elevation involvement in plant brassinosteroid signal transduction cascades. *Plant Physiology* **163,** 555–565 (2013).

255. Thompson, A. R., Doelling, J. H., Suttangkakul, A. & Vierstra, R. D. Autophagic nutrient recycling in Arabidopsis directed by the ATG8 and ATG12 conjugation pathways. *Plant Physiology* **138,** 2097–2110 (2005).

256. Chin, K., DeFalco, T. A., Moeder, W. & Yoshioka, K. The Arabidopsis cyclic nucleotide-gated ion channels AtCNGC2 and AtCNGC4 work in the same signaling pathway to regulate pathogen defense and floral transition. *Plant Physiology* **163,** 611–624 (2013).

257. Bartlett, J. G., Alves, S. C., Smedley, M., Snape, J. W. & Harwood, W. A. High-throughput Agrobacterium-mediated barley transformation. *Plant Methods* **4,** 22–12 (2008).

258. Chiasson, D. M. *et al.* A quantitative hypermorphic CNGC allele confers ectopic calcium flux and impairs cellular development. *Elife* **6,** (2017).

259. Ali, R. *et al.* Death don't have no mercy and neither does calcium: Arabidopsis CYCLIC NUCLEOTIDE GATED CHANNEL2 and innate immunity. *Plant Cell* **19,** 1081–1095 (2007).

260. Hua, B. G., Mercier, R. W., Zielinski, R. E. & Berkowitz, G. A. Functional interaction of calmodulin with a plant cyclic nucleotide gated cation channel. *Plant Physiology and Biochemistry* **41,** 945–954 (2003).

261. Demidchik, V., Shabala, S., Isayenkov, S., Cuin, T. A. & Pottosin, I. Calcium transport across plant membranes: mechanisms and functions. *New Phytologist* **220,** 49–69 (2018).

262. Kudla, J. *et al.* Advances and current challenges in calcium signaling. *New Phytologist* **218,** 414–431 (2018).

263. Liu, J. Ca2+ channels and Ca2+ signals involved in abiotic stress responses in plant cells: recent advances. *Plant Cell, Tissue and Organ Culture (PCTOC)* **132,** 413–424 (2018).

264. Charpentier, M. & Oldroyd, G. E. D. Nuclear calcium signaling in plants. *Plant Physiology* **163,** 496–503 (2013).

265. Wang, Y. *et al.* CNGC2 Is a Ca2+ influx channel that prevents accumulation of apoplastic Ca2+ in the leaf. *Plant Physiology* **173,** 1342–1354 (2017).

266. Katano, K., Kataoka, R., Fujii, M. & Suzuki, N. Differences between seedlings and flowers in anti-ROS based heat responses of Arabidopsis plants deficient in cyclic nucleotide gated channel 2. *Plant Physiology et Biochemistry* **123,** 288–296 (2018).

267. Frietsch, S. *et al.* A cyclic nucleotide-gated channel is essential for polarized tip growth of pollen. *Proceedings of the National Academy of Sciences* **104,** 14531–14536 (2007).

268. Chan, C. W. M., Wohlbach, D. J., Rodesch, M. J. & Sussman, M. R. Transcriptional changes in response to growth of Arabidopsis in high external calcium. *Federation of European Biochemical Sciences Letters* **582,** 967–976 (2008).

269. Horváth, I. *et al.* Heat shock response in photosynthetic organisms: Membrane and lipid connections. *Progress in Lipid Research* **51,** 208–220 (2012).

270. Niu, Y. & Xiang, Y. An overview of biomembrane functions in plant responses to high-temperature stress. *Frontiers in Plant Science* **9,** 1449–18 (2018).

271. Jurkowski, G. I. *et al.* Arabidopsis DND2, a second cyclic nucleotide-gated ion channel gene for which mutation causes the 'defense, no death' phenotype. *Molecular Plant-Microbe Interactions***17,** 511–520 (2004).

272. DeFalco, T. A. *et al.* Multiple calmodulin-binding sites positively and negatively regulate Arabidopsis CYCLIC NUCLEOTIDE-GATED CHANNEL12. *Plant Cell* **28,** 1738–1751 (2016).

273. Fischer, C. *et al.* Calmodulin as a Ca2+-sensing subunit of Arabidopsis cyclic nucleotide-gated channel complexes. *Plant and Cell Physiology* **58,** 1208–1221 (2017).

274. Gao, F. *et al.* A heat-activated calcium-permeable channel - Arabidopsis cyclic nucleotide-gated ion channel 6 - is involved in heat shock responses. *The Plant Journal* **70,** 1056–1069 (2012).

275. Humphrey, S. J., James, D. E. & Mann, M. Protein phosphorylation: a major switch mechanism for metabolic regulation. *Trends in Endocrinology & Metabolism* **26,** 676–687 (2015).

276. Blom, N., Sicheritz-Pontén, T., Gupta, R., Gammeltoft, S. & Brunak, S. Prediction of post-translational glycosylation and phosphorylation of proteins from the amino acid sequence. *Proteomics* **4,** 1633–1649 (2004).

277. Abdel-Hamid, H. *et al.* A suppressor screen of the chimeric AtCNGC11/12 reveals residues important for intersubunit interactions of cyclic nucleotide-gated ion channels. *Plant Physiology* **162,** 1681–1693 (2013).

278. Baxter, J. *et al.* Identification of a functionally essential amino acid for Arabidopsis cyclic nucleotide gated ion channels using the chimeric AtCNGC11/12 gene. *The Plant Journal* **56,** 457–469 (2008).

279. Tsirigos, K. D., Peters, C., Shu, N., Käll, L. & Elofsson, A. The TOPCONS web server for consensus prediction of membrane protein topology and signal peptides. *Nucleic Acids Research* **43,** 401–407 (2015).

280. Kaplan, B., Sherman, T. & Fromm, H. Cyclic nucleotide-gated channels in plants. *Federation of European Biochemical Sciences Letters* **581,** 2237–2246 (2007).

281. Rehmann, H., Wittinghofer, A. & Bos, J. L. Capturing cyclic nucleotides in action: snapshots from crystallographic studies. *Nature Reviews Molecular Cell Biology* **8,** 63–73 (2007).

282. Young, E. C. & Krougliak, N. Distinct structural determinants of efficacy and sensitivity in the ligand-binding domain of cyclic nucleotide-gated channels. *The Journal of Biological Chemistry* **279,** 3553–3562 (2004).

283. Cukkemane, A., Seifert, R. & Kaupp, U. B. Cooperative and uncooperative cyclic-nucleotide-gated ion channels. *Trends in Biochemical Sciences* **36,** 55–64 (2011).

284. Saand, M. A. *et al.* Phylogeny and evolution of plant cyclic nucleotide-gated ion channel (CNGC) gene family and functional analyses of tomato CNGCs. *DNA Research* **22,** 471–483 (2015).

285. Kaupp, U. B. & Seifert, R. Cyclic nucleotide-gated ion channels. *Physiological Reviews* **82,** 769–824 (2002).

286. Spalding, E. P. & Harper, J. F. The ins and outs of cellular Ca2+ transport. *Current Opinion in Plant Biology* **14,** 715–720 (2011).

287. Charpentier, M. *et al.* Nuclear-localized cyclic nucleotide-gated channels mediate symbiotic calcium oscillations. *Science* **352,** 1102–1105 (2016).

288. Liao, P. & Soong, T. W. Understanding alternative splicing of Cav 1.2 calcium channels for a new approach towards individualized medicine. *Elsevier* (2010).

289. Hartmann, L. *et al.* Alternative splicing substantially diversifies the transcriptome during early photomorphogenesis and correlates with the energy availability in Arabidopsis. *Plant Cell* **28,** 2715–2734 (2016).

290. James, A. B. *et al.* Alternative splicing mediates responses of the Arabidopsis circadian clock to temperature changes. *Plant Cell* **24,** 961–981 (2012).

291. Charpentier, M. Calcium signals in the plant nucleus: origin and function. *Journal of Experimental Botany* **303,** 1364–9 (2018).

292. Thilmony, R., Underwood, W. & He, S. Y. Genome-wide transcriptional analysis of the Arabidopsis thaliana interaction with the plant pathogen Pseudomonas syringae pv. tomato DC3000 and the human pathogen Escherichia coli O157 : H7. *The Plant Journal* **46,** 34–53 (2006).

293. Fan, M. *et al.* The bHLH transcription factor HBI1 mediates the trade-off between growth and pathogen-associated molecular pattern-triggered immunity in Arabidopsis. *Plant Cell* **26,** 828–841 (2014).

294. Maleck, K. *et al.* Isolation and characterization of broad-spectrum disease-resistant Arabidopsis mutants. *Genetics* **160,** 1661–1671 (2002).

295. Yi, S. Y., Shirasu, K., Moon, J. S., Lee, S.-G. & Kwon, S.-Y. The activated SA and JA signaling pathways have an influence on flg22-triggered oxidative burst and callose deposition. *Public Library of Science ONE* **9,** e88951–10 (2014).

296. Beck, M. *et al.* Expression patterns of FLAGELLIN SENSING 2 map to bacterial entry sites in plant shoots and roots. *Journal of Experimental Botany* **65,** 6487–6498 (2014).

297. Yi, S. Y. & Kwon, S.-Y. How does SA signaling link the Flg22 responses? *Plant Signaling & Behavior* **9,** e972806–3 (2014).

298. Chinchilla, D. *et al.* A flagellin-induced complex of the receptor FLS2 and BAK1 initiates plant defence. *Nature* **448,** 497–500 (2007).

299. Kachroo, A. *et al.* Oleic acid levels regulated by glycerolipid metabolism modulate defense gene expression in Arabidopsis. *Proceedings of the National Academy of Sciences* **101,** 5152–5157 (2004).

300. Penfield, S. Temperature perception and signal transduction in plants. *New Phytologist* **179,** 615–628 (2008).

301. Ryan, C. A., Huffaker, A. & Yamaguchi, Y. New insights into innate immunity in Arabidopsis. *Cellular Microbiology* **9,** 1902–1908 (2007).

302. Tsuda, K. *et al.* Dual regulation of gene expression mediated by extended MAPK activation and salicylic acid contributes to robust innate immunity in Arabidopsis thaliana. *Public Library of Science Genetics* **9,** e1004015–14 (2013).

303. Zhu, W. *et al.* Modulation of ACD6 dependent hyperimmunity by natural alleles of an Arabidopsis thaliana NLR resistance gene. *Public Library of Science Genetics* **14,** e1007628–20 (2018).

304. Draper, J. Salicylate, superoxide synthesis and cell suicide in plant defence. *Trends in Plant Science* **2,** 162–165 (1997).

305. Jeworutzki, E. *et al.* Early signaling through the Arabidopsis pattern recognition receptors FLS2 and EFR involves Ca2+-associated opening

of plasma membrane anion channels. *The Plant Journal* **62,** 367–378 (2010).

306. Torres, M. A., Jones, J. D. G. & Dangl, J. L. Reactive oxygen species signaling in response to pathogens. *Plant Physiology* **141,** 373–378 (2006).

307. Guo, P. *et al.* A tripartite amplification loop involving the transcription factor WRKY75, salicylic acid, and reactive oxygen species accelerates leaf senescence. *Plant Cell* **29,** 2854–2870 (2017).

308. Zhou, N., Tootle, T. L., Tsui, F., Klessig, D. F. & Glazebrook, J. PAD4 functions upstream from salicylic acid to control defense responses in Arabidopsis. *Plant Cell* **10,** 1021–1030 (1998).

309. Moeder, W., Urquhart, W., Ung, H. & Yoshioka, K. The role of cyclic nucleotide-gated ion channels in plant immunity. *Molecular Plant* **4,** 442–452 (2011).

310. Dong, J. *et al.* Arabidopsis DE-ETIOLATED1 represses photomorphogenesis by positively regulating phytochrome-interacting factors in the dark. *Plant Cell* **26,** 3630–3645 (2014).

311. Hofmann, N. R. A mechanism for inhibition of COP1 in photomorphogenesis: direct interactions of phytochromes with SPA proteins. *Plant Cell* **27,** 8 (2015).

312. Franklin, K. A. & Quail, P. H. Phytochrome functions in Arabidopsis development. *Journal of Experimental Botany* **61,** 11–24 (2009).

313. Gaffney, T. *et al.* Requirement of salicylic acid for the induction of systemic acquired resistance. *Science* **261,** 754–756 (1993).

314. Spoel, S. H. & Dong, X. Making sense of hormone crosstalk during plant immune responses. *Cell Host and Microbe* **3,** 348–351 (2008).

315. Leivar, P. *et al.* Multiple phytochrome-interacting bHLH transcription factors repress premature seedling photomorphogenesis in darkness. *Current Biology* **18,** 1815–1823 (2008).

316. Thaler, J. S., Fidantsef, A. L. & Bostock, R. M. Antagonism between jasmonate- and salicylate-mediated induced plant resistance: Effects of concentration and timing of elicitation on defense-related proteins,

herbivore, and pathogen performance in tomato. *Journal of Chemical Ecology* **28,** 1131–1159 (2002).

317. Xu, E. & Brosche, M. Salicylic acid signaling inhibits apoplastic reactive oxygen species signaling. *BMC Plant Biology* **14,** 1–17 (2014).

318. Sato, M. *et al.* Network modeling reveals prevalent negative regulatory relationships between signaling sectors in Arabidopsis immune signaling. *Public Library of Science Pathogens* **6,** e1001011 (2010).

319. Jwa, N.-S. & Hwang, B. K. Convergent evolution of pathogen effectors toward reactive oxygen species signaling networks in plants. *Frontiers in Plant Science* **8,** 1687 (2017).

320. Guo, M., Kim, P., Li, G., Elowsky, C. G. & Alfano, J. R. A bacterial effector co-opts calmodulin to target the plant microtubule network. *Cell Host and Microbe* **19,** 67–78 (2016).

321. Zhang, J. *et al.* A Pseudomonas syringae effector inactivates MAPKs to suppress PAMP-induced immunity in plants. *Cell Host and Microbe* **1,** 175–185 (2007).

322. Zhang, Z. *et al.* Disruption of PAMP-induced MAP kinase cascade by a Pseudomonas syringae effector activates plant immunity mediated by the NB-LRR protein SUMM2. *Cell Host and Microbe* **11,** 253–263 (2012).

323. Bi, G. *et al.* Receptor-like cytoplasmic kinases directly link diverse pattern recognition receptors to the activation of mitogen-activated protein kinase cascades in Arabidopsis. *The Plant Cell* **30**(7) 1543-1561 (2018).

324. Seybold, H. *et al.* Ca 2+signalling in plant immune response: from pattern recognition receptors to Ca 2+decoding mechanisms. *New Phytologist* **204,** 782–790 (2014).

325. Kadota, Y., Shirasu, K. & Zipfel, C. Regulation of the NADPH oxidase RBOHD during plant immunity. *Plant and Cell Physiology* **56,** 1472–1480 (2015).

326. Wawrzyniak, J., Waśkiewicz, A. & Ryniecki, A. Evaluation of critical points of mould growth and mycotoxin production in the stored barley

ecosystem with a hazardous initial microbiological state of grain. *Journal of Stored Products Research* **77,** 166–176 (2018).

327. Murray, S. L., Adams, N., Kliebenstein, D. J., LOAKE, G. J. & Denby, K. J. A constitutive PR-1::luciferase expression screen identifies Arabidopsis mutants with differential disease resistance to both biotrophic and necrotrophic pathogens. *Molecular Plant Pathology* **6,** 31–41 (2005).

328. van Dijk, K. *et al.* The Avr (effector) proteins HrmA (HopPsyA) and AvrPto are secreted in culture from Pseudomonas syringae pathovars via the Hrp (Type III) protein secretion system in a temperature- and pH-sensitive manner. *Journal of Bacteriology* **181,** 4790–4797 (1999).

329. Smirnova, A. V. *et al.* Control of temperature-responsive synthesis of the phytotoxin coronatine in Pseudomonas syringae by the unconventional two-component system CorRPS. *Journal of Molecular Microbiology and Biotechnology* **4,** 191–196 (2002).

330. Hansen, L. D. *et al.* The relation between plant-growth and respiration - a thermodynamic model. *Planta* **194,** 77–85 (1994).

331. Wolfe, J. Cellular thermodynamics: the molecular and macroscopic views. *eLS Wiley & Sons* (2015).

332. Kim, D., Kwak, Y.-G. & Kang, S. H. Real-time observation of temperature-dependent protein–protein interactions using real-time dual-color detection system. *Analytica Chimica Acta* **577,** 163–170 (2006).

333. Sun, J. *et al.* Activation of symbiosis signaling by arbuscular mycorrhizal fungi in legumes and rice. *Plant Cell* **27,** 823–838 (2015).

334. Ruelland, E. & Zachowski, A. How plants sense temperature. *Environmental and Experimental Botany* **69,** 225–232 (2010).

335. Dodd, A. N., Kudla, J. & Sanders, D. the language of calcium signaling. *Annual Review of Plant Biology* **61,** 593–620 (2010).

336. Behera, S. *et al.* Two spatially and temporally distinct Ca 2+signals convey Arabidopsis thaliana responses to K +deficiency. *New Phytologist* **213,** 739–750 (2016).

337. Chen, J., Gutjahr, C., Bleckmann, A. & Dresselhaus, T. Calcium signaling during reproduction and biotrophic fungal interactions in plants. *Molecular Plant* **8,** 595–611 (2015).

338. Whalley, H. J. & Knight, M. R. Calcium signatures are decoded by plants to give specific gene responses. *The New Phytologist* **197,** 690–693 (2013).

339. Ma, W. & Berkowitz, G. A. Ca2+ conduction by plant cyclic nucleotide gated channels and associated signaling components in pathogen defense signal transduction cascades. *New Phytologist* **190,** 566–572 (2010).

340. Ranf, S. *et al.* Microbe-associated molecular pattern-induced calcium signaling requires the receptor-like cytoplasmic kinases, PBL1 and BIK1. *BMC Plant Biology* **14,** 379–15 (2014).

341. Gerasimenko, J. V., Sherwood, M., Tepikin, A. V., Petersen, O. H. & Gerasimenko, O. V. NAADP, cADPR and IP3 all release Ca2+ from the endoplasmic reticulum and an acidic store in the secretory granule area. *Journal of Cell Science* **119,** 226–238 (2006).

342. Navazio, L. *et al.* Calcium release from the endoplasmic reticulum of higher plants elicited by the NADP metabolite nicotinic acid adenine dinucleotide phosphate. *Proceedings of the National Academy of Sciences* **97,** 8693–8698 (2000).

343. Whalley, H. J. *et al.* Transcriptomic analysis reveals calcium regulation of specific promoter motifs in Arabidopsis. *Plant Cell* **23,** 4079–4095 (2012).

344. Dodd, A. N., Kudla, J. & Sanders, D. The language of calcium signaling. *Annual Review of Plant Biology* **61,** 593–620 (2010).

345. Grant, M. *et al.* The RPM1 plant disease resistance gene facilitates a rapid and sustained increase in cytosolic calcium that is necessary for the oxidative burst and hypersensitive cell death. *The Plant Journal* **23,** 441–450 (2000).

346. Mehlmer, N. *et al.* A toolset of aequorin expression vectors for in planta studies of subcellular calcium concentrations in Arabidopsis thaliana. *Journal of Experimental Botany* **63,** 1751–1761 (2012).

347. Krebs, M. *et al.* FRET-based genetically encoded sensors allow high-resolution live cell imaging of Ca2+ dynamics. *The Plant Journal* **69,** 181–192 (2011).

348. Kelner, A., Leitão, N., Chabaud, M., Charpentier, M. & de Carvalho-Niebel, F. dual color sensors for simultaneous analysis of calcium signal dynamics in the nuclear and cytoplasmic compartments of plant cells. *Frontiers in Plant Science* **9,** 735–14 (2018).

349. Yang, D.-L. *et al.* Calcium pumps and interacting BON1 protein modulate calcium signature, stomatal closure, and plant immunity. *Plant Physiology* **175,** 424–437 (2017).

350. Zhao, Y. *et al.* An expanded palette of genetically encoded Ca2+ indicators. *Science* **333,** 1888–1891 (2011).

351. Ferris, R. E. A. Effect of high temperature stress at anthesis on grain yield and biomass of field-grown crops of wheat. *Annals of Botany* 631–639 (1998).

352. Hatfield, J. L. & Prueger, J. H. Temperature extremes: Effect on plant growth and development. *Elsevier* (2015).

353. Baerenfaller, K., Massonnet, C. & Plant, L. H. C. A long photoperiod relaxes energy management in Arabidopsis leaf six. *Elsevier* (2015).

354. Demmig-Adams, B., Cohu, C. M., Muller, O. & Adams, W. W. Modulation of photosynthetic energy conversion efficiency in nature: from seconds to seasons. *Photosynthesis Research* **113,** 75–88 (2012).

355. Rivas-San Vicente, M. & Plasencia, J. Salicylic acid beyond defence: its role in plant growth and development. *Journal of Experimental Botany* **62,** 3321–3338 (2011).

356. Greenberg, J. T., Silverman, F. P. & Liang, H. Uncoupling salicylic acid-dependent cell death and defense-related responses from disease resistance in the Arabidopsis mutant acd5. *Genetics* **156,** 341–350 (2000).

357. Fortuna, A. *et al.* Crossroads of stress responses, development and flowering regulation—the multiple roles of cyclic nucleotide gated ion channel 2. *Plant Signaling & Behavior* **10,** e989758 (2015).

358. Chaiwongsar, S., Strohm, A. K., Roe, J. R., Godiwalla, R. Y. & Chan, C. W. M. A cyclic nucleotide-gated channel is necessary for optimum fertility in high-calcium environments. *New Phytologist* **183,** 76–87 (2009).

359. Paulmurugan, R. & Gambhir, S. S. Monitoring protein-protein interactions using split synthetic Renilla luciferase protein-fragment-assisted complementation. *Analytical Chemistry* **75,** 1584–1589 (2003).

360. Mithöfer, A. & Mazars, C. Aequorin-based measurements of intracellular Ca2+-signatures in plant cells. *Biological Procedures Online* **4,** 105–118 (2002).

361. Lammertz, M. *et al.* Widely-conserved attenuation of plant MAMP-induced calcium influx by bacteria depends on multiple virulence factors and may involve desensitization of host pattern recognition receptors. *Molecular Plant-Microbe Interactions* **32**(5) 608-621 (2019).

362. Sun, J., Miwa, H., Downie, J. A. & Oldroyd, G. E. D. Mastoparan activates calcium spiking analogous to Nod factor-induced responses in Medicago truncatula root hair cells. *Plant Physiology* **144,** 695–702 (2007).

363. Clough, S. J. & Bent, A. F. Floral dip: a simplified method for Agrobacterium-mediated transformation of Arabidopsis thaliana. *The Plant Journal* **16,** 735–743 (1998).

364. Karimi, M., Inze, D. & Depicker, A. GATEWAY((TM)) vectors for Agrobacterium-mediated plant transformation. *Trends in Plant Science* **7,** 193–195 (2002).

365. Nakagawa, T. *et al.* Development of series of gateway binary vectors, pGWBs, for realizing efficient construction of fusion genes for plant transformation. *Journal of Bioscience and Bioengineering* **104,** 34–41 (2007).

366. Krasensky-Wrzaczek, J. & Kangasjärvi, J. The role of reactive oxygen species in the integration of temperature and light signals. *Journal of Experimental Botany* **69,** 3347–3358 (2018).

367. Lee, S. J. & Rose, J. K. C. Mediation of the transition from biotrophy to necrotrophy in hemibiotrophic plant pathogens by secreted effector proteins. *Plant Signaling & Behavior* **5**, 769–772 (2010).